Deciphering the Role of LRH-1 in Liver Intermediary Metabolism and Cancer

THÈSE N^{O} 7369 (2016)

PRÉSENTÉE LE 9 DÉCEMBRE 2016

À LA FACULTÉ DES SCIENCES DE LA VIE

UNITÉ DE LA PROF. SCHOONJANS

PROGRAMME DOCTORAL EN BIOTECHNOLOGIE ET GÉNIE BIOLOGIQUE

ÉCOLE POLYTECHNIQUE FÉDÉRALE DE LAUSANNE

POUR L'OBTENTION DU GRADE DE DOCTEUR ÈS SCIENCES

PAR

Pan XU

acceptée sur proposition du jury:

Prof. F. Radtke, président du jury
Prof. K. Schoonjans, directrice de thèse
Prof. L. Fajas, rapporteur
Prof. D. Moradpour, rapporteur
Prof. K. Sakamoto, rapporteur

ÉCOLE POLYTECHNIQUE
FÉDÉRALE DE LAUSANNE

Suisse
2016

Acknowledgements

In 2012, I started the first year of my PhD program in EPFL with a chemistry degree and minimal knowledge of biology that I mainly learned during secondary school. It was quite a dramatic switch of my research focus, and of course the transition had never been easy at the early beginning, especially when I gradually realized that my previous training in chemistry did not seem to offer much beneficial route to progress the biology project. I needed to get into the nitty-gritty details of this field on a cellular or molecular level. However, after four years of struggling, I feel more comfortable and more interested, with a determined spirit to walk further in the avenue of biology.

To this end, I am greatly thankful to Professor Kristina Schoonjans, my PhD supervisor, for providing me the opportunity to embark on this project. I am so grateful to her for putting her faith in me, for providing valuable guidance, persistent encouragement and inspiration at various stages of my PhD period. Without her supervision, this thesis would never have taken shape.

Many deep thanks to my beloved family whose value to me only grows with age. Their unconditional love and constant support make me stronger. My appreciation goes to my parents, Dong, Miao and Keke for providing moral support and for encouraging me to stay in Switzerland. Thanks to Susanne and Frans for continuously supporting and taking care of me, I am just so lucky to be their daughter-in-law. My special thanks to Jef, the pillar of my life, for his endless support, for believing so much in me, and for bringing me a life of happiness in the hours when the lab lights were off.

I would like to thank Professor Johan Auwerx whose constructive suggestions have truly contributed to the evolution of my project. Thanks to Dr. Carolina Hagberg. She had a short stay in the lab, but she was so frank in guiding and helping me during this period, and her enthusiasm in science had a long lasting effect on me. Many thanks go to Dr. Sokrates Stein and Vera Lemos. We worked very closely and harmoniously as a team. It impresses me a lot, and I am very grateful to both of them for their encouragement and participation in carrying out the project. Our friendship grows stronger out of all the arguments and discussions within those years.

I also wish to express my gratitude to Dr. Dongryeol Ryu for teaching me so many things and for providing his scholarly advice to my project. My sincere appreciation goes to Dr. Norman Moullan who rendered his

help with many mice arrangements and experiments. My gratitude goes to Dr. Hadrien Demagny for his experimental contribution to the thesis. I am also very thankful to my friend Rachana Pradhan for her support and motivating words when PhD life is dark.

I would also like to expand my sense of gratitude to my colleagues whose name may not all enumerated. I thank them for their inspiration and timely suggestions during the development of the project. My special thanks to Sabrina Bichet, Thibaud Clerc, Soline Odouard and Roxane Pasquettaz for providing me necessary technical help during my research pursuit. My great appreciation goes to Valerie Stengel for organizing all the administrative work and making everything much easier. Many thanks also to the managers and caretakers in animal facility, including Dr. Roy Combe, Dr. Raphaël Doenlen, Gisèle Ferrand and Christine Pehm for their support and assistance of the mice work. I also would like to expand my thanks to the collaborators inside and outside the EPFL. In particular, thanks to Professor Arnaud Comment, Professor Nicola Zamboni, Dr. Maaike Oosterveer, Dr. Emine Can for being so kind to show interest in my project and for providing indispensable contribution to rich and promote my research.

07.09. 2016

Lausanne

Summary

Hepatocellular carcinoma (HCC) is one of the leading causes of cancer death worldwide. Gaining insight into the molecular pathways involved in the development of HCC is hence a prerequisite to design and develop novel and effective therapeutic strategies. Metabolic reprogramming is a universal feature of tumor cells and is characterized by increased glycolysis and diminished oxidative phosphorylation, a phenomenon known as the Warburg effect. More recently, it has become evident that tumor cells heavily rely on glutamine metabolism to compensate for the Warburg effect and to replenish the tricarboxylic acid (TCA) cycle. However, the molecular mechanisms by which glutamine supports tumor cell metabolism remain largely unexplored.

In this thesis, I have established the role of the nuclear receptor LRH-1 as a key regulator in the process of hepatic tumorigenesis. I observed that LRH-1 promotes DEN-induced hepatocellular carcinogenesis (HCC). I demonstrated that LRH-1 facilitates the production of NADPH from glutamine by favoring a non-canonical glutamine pathway that optimizes reductive biosynthesis. Importantly, chronic and acute disruption of LRH-1 also impaired glutamine-induced anaplerosis and α-KG availability, ultimately leading to impaired mTORC1 signaling to block cell proliferation.

Moreover, LRH-1 also coordinates glutamine-dependent asparagine synthesis to protect tumor cell from apoptosis induced by glutamine depletion itself. As a result, gain-of-function of LRH-1 sustained asparagine homeostasis upon glutamine-deprivation to promote cell survival. Collectively, these studies unveiled an unexpected role of LRH-1 in cancer intermediary metabolism, and warranted further studies on pharmacological inhibition of LRH-1 to interfere with hepatocellular carcinogenesis.

Keywords: cancer metabolism; nuclear receptor; glutamine; mTORC1; NADPH; asparagine; apoptosis; hepatocellular carcinoma

Résumé

Le carcinome hépatocellulaire (CHC) est l'une des principales causes de décès à la suite de cancer, dans le monde entier. Mieux comprendre les voies moléculaires impliquées dans le développement du CHC est donc une condition préalable pour concevoir et développer des stratégies thérapeutiques novatrices et efficaces. La reprogrammation métabolique est une caractéristique universelle des cellules tumorales et se concrétise par une augmentation de la glycolyse et une diminution de la phosphorylation oxydative, un phénomène connu sous le nom d'effet Warburg. Récemment, il est apparu évident que les cellules tumorales dépendent fortement du métabolisme de la glutamine afin de compenser les conséquences de l'effet Warburg et de reconstituer le cycle de Krebs, appelé aussi cycle de l'acide citrique (CAC). Cependant, les mécanismes moléculaires par lesquels la glutamine favorise le métabolisme des cellules tumorales restent largement inexplorés.

Dans cette thèse, j'ai établi le rôle du récepteur nucléaire LRH-1 en tant que régulateur clé dans le processus de tumorigenèse hépatique. Nous avons observé que LRH-1 favorise la carcinogenèse hépatocellulaire (HCC) induite par le DEN. Nous avons démontré que LRH-1 facilite la production de NADPH à partir de la glutamine en favorisant une voie non canonique de la glutamine optimisant la biosynthèse réductrice. De plus, la disruption chronique de LRH-1, aussi bien qu' aiguë, altère également l'anaplérose induite par la glutamine ainsi que la disponibilité du α-KG, menant finalement à l'altération de la voie de signalisation mTOR pour bloquer la prolifération cellulaire.

En outre, LRH-1 coordonne aussi la synthèse asparagino-dépendante de la glutamine pour protéger les cellules tumorales contre l'apoptose induite par l'appauvrissement en glutamine. Par conséquent, le gain de fonction de LRH-1 alimente l'homéostase de l'asparagine, grâce à une privation de glutamine, pour favoriser la survie des cellules. Collectivement, ces études ont dévoilé un rôle inattendu de LRH-1 dans le métabolisme intermédiaire du cancer, et justifient de futures recherches sur l'inhibition pharmacologique de LRH-1 dans le but de contrer la carcinogenèse hépatocellulaire.

Mots-clés: métabolisme du cancer; récepteur nucléaire; glutamine; mTOR; NADPH; asparagine; apoptose; carcinome hépatocellulaire

Contents

Figures

Chapter 1 Introduction

1.1 Hepatocellular Carcinoma

1.1.1 Introduction

Hepatocellular carcinoma is the fifth most common malignancy worldwide, and is the third leading cause of cancer death, after lung and stomach[1, 2]. The annual incidence of HCC is similar to the death that it generates, due to its high aggressiveness and mortality[3]. The geographical distribution of HCC is disproportionate. As shown in Figure 1.1, the highest HCC incidence occurs in resource-poor or developing countries such as sub-Saharan African, East Asia and Melanesia, which covers 85% of the total global cases[1, 4]. In developed countries the incidence of HCC is much lower, except in the south of Europe. Globally there is a growing incidence of HCC, even in United States and Europe. Moreover, the risk of developing HCC increases progressively with advancing age in the population, with a peak at the age of 70-year-old[4]. In spite of well-established surveillance programs in patients with chronic liver disease, most tumors are diagnosed in intermediate-advanced stage, and only palliative cares can be applied.

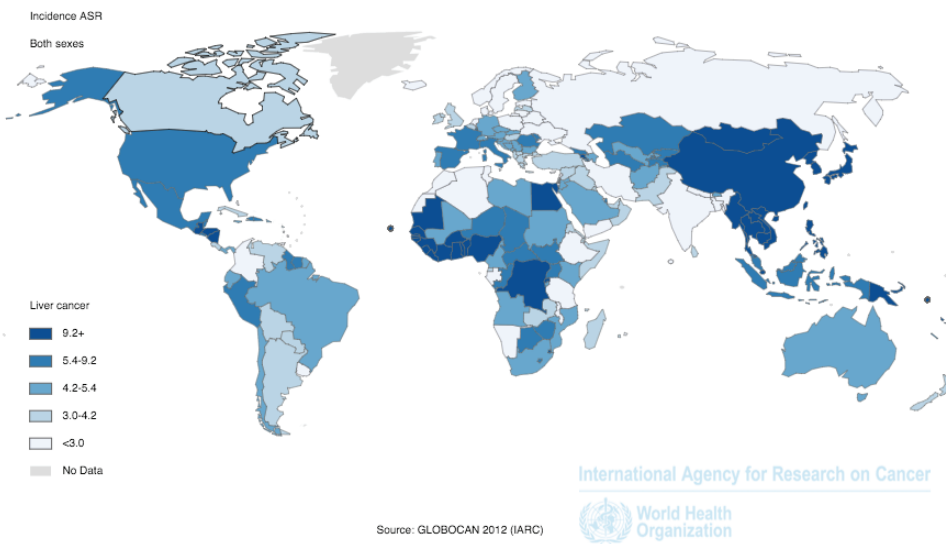

Figure 1. 1 Global Incidence of Hepatocellular Carcinoma

(Sourced from GLOBOCAN 2012)

1.1.2 Etiology

The most frequent risk factors contributing to the development of HCC include chronic viral hepatitis (type B and C infection), alcoholic hepatitis and exposure to aflatoxin-contaminated food. Half of all cases of HCC

are associated with hepatitis B virus (HBV) infection, with approximately a further 30% associated with hepatitis C virus (HCV) infection[4] (Figure 1.2). Geographically, in poor and developing countries, the most frequent risk factor associated with HCC is chronic HBV infection, while in western countries, HCV infection appears to be the main risk factor[4]. Most patients with HCC have liver cirrhosis, which is characterized by a decrease in hepatocyte proliferation, indicating a damage of the regenerative capacity of the liver, and results in an increase in fibrous tissue and a destruction of liver cells, ultimately leads to the development of cancerous nodules. Cirrhosis may develop from chronic viral hepatitis, alcohol abuse, inherited metabolic disorders such as hemochromatosis, and nonalcoholic fatty liver disease (NAFLD). Other metabolic syndromes, such as diabetes and obesity, have also been recognized as emerging causes of HCC[5-7]. Moreover, patients with HIV infection have higher incidence of developing HCC compared to controls, and recent evidence supports that HIV acts as an addictive co-factor enhancing the risk of HCC in patients with chronic viral hepatitis[8]. All of these factors involved in the etiology of HCC have a direct impact on patient characteristics and disease course. Although a causative agent can often be identified, HCC remains an extremely complex condition associated with a poor prognosis. Unfortunately, there are still many gaps in our current understanding, and further research efforts are needed to fully elucidate the diverse mechanisms involved in the pathogenesis of HCC and offer optimal prevention strategies for those at risk.

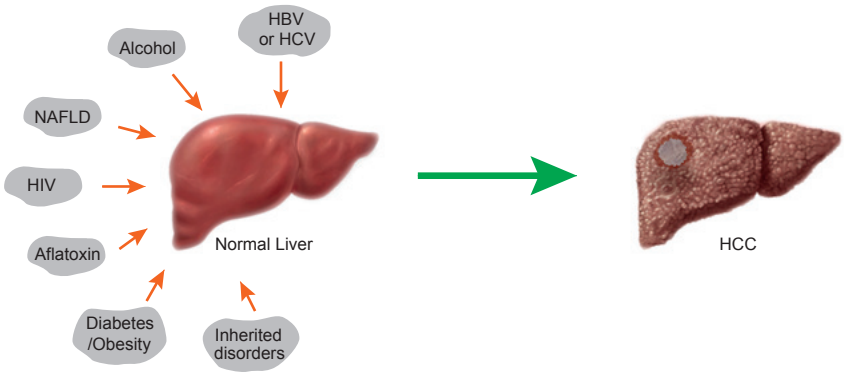

Figure 1. 2 Etiologic Events Contribute to Hepatocellular Carcinoma (HCC)

1.1.3 Prevention and Treatment

Prevention

The prevention of HCC can be conducted through strategies aiming to avoid viral infection, chronic liver damage and carcinogenesis process, to have early diagnosis of the disease, and to reduce the risk of recurrence. Universal vaccination against HBV infection reduces HCC incidence and HCC-related mortality[9, 10]. Hepatitis B vaccination to all newborns and high-risk groups as routine immunization is recommended by the World Health Organization[11].

For subjects at risk of developing HCC, diagnostic test-based surveillance is applied, aiming to reduce disease-related mortality. Ultrasound examination is recommended as the primary surveillance due to its higher sensitivity and specificity[12, 13]. Computed axial tomography (CT) and magnetic resonance imaging (MR) scans present an increased detection of HCC than ultrasound, but also a higher false-positive rate[14]. In addition, the high costs, potential harm related to radiation exposure, and contrast-related injury associated with these tests make them poor candidates for HCC surveillance. Alpha-fetoprotein (AFP) measurement is also commonly used for HCC surveillance because it is relatively inexpensive, simple to perform, and is widely available[15]. However, AFP alone is not recommended due to its low sensitivity and specificity for detecting HCC.

Treatment

The treatment of HCC is dependent on several factors including liver function, tumor size and number, macrovascular invasion, extrahepatic spread. The recommendations for different therapeutic strategies must be concluded from evidence-based data[16].

Curative treatment, such as hepatic resection and liver transplant (LT), offer good prognosis, but are limited to early stage of HCC, while most tumors are diagnosed in intermediate-advanced stage[17, 18]. Local ablation with radiofrequency or percutaneous ethanol injection is considered the standard treatment for patients with early-stage HCC who are not suitable for resection or LT[19]. Chemoembolization is widely used for patients with un-resectable HCC or progression after curative treatment[20, 21]. It is also the first recommendation for patients with intermediate-stage disease having well-preserved liver function and asymptomatic multinodular tumors without vascular invasion or extrahepatic spread. Radioembolization, involving infusion of Iodine-131 or Yttrium-90 into hepatic artery, has been shown to exhibit antitumor results, but it is not recommended as a standard therapy as further research trials are needed to evaluate the efficacy[22-24]. Finally, in patients with advanced HCC but preserved liver function, sorafenib, a multi-tyrosine kinase inhibitor that suppresses cancer cell proliferation and tumor angiogenesis, is the only approved systemic drug that has demonstrated a survival benefit and is the standard of care in advanced HCC patients[25-27].

Moreover, in the past few years, advances have been made in exploring the mechanisms underlying the onset and development of HCC. Liver cancer is a remarkably complex and heterogeneous collection of diseases. Nonetheless, a series of hallmarks that encompass the biological capacities of tumor cells to grow and survive have been proposed and recently revisited[28]. Although initially described nearly a century ago, an increasing list of novel cancer metabolism targets has been emerging[29, 30]. Researchers are actively pursuing predictive biomarkers as well as novel therapeutic targets for the treatment of HCC. Many compounds targeting pathways in intermediary metabolism are currently tested in clinical trials and yet to show promising results.

1.2 Emerging Hallmarks of Cancer Metabolism

Tumorigenesis is dependent on the reprogramming of cellular metabolism as both direct and indirect consequences of oncogenic mutations. In comparison to non-transformed cells, a common feature of cancer cell metabolism is the ability to take up necessary nutrients from a frequently nutrient-deprived microenvironment and metabolize them to support uncontrolled cell growth and proliferation[31].

1.2.1 Understanding the Warburg Effect

Cancer cells usually display a markedly increased consumption of glucose, and metabolize them by aerobic glycolysis rather than through the more energetically efficient oxidative phosphorylation that is used by normal resting cells in the presence of oxygen[32]. This rewired process, termed the Warburg effect, has been confirmed in a variety of tumor contexts and shown to correlate with poor tumor prognosis[33]. Following this phenomenon, positron emission tomography (PET)-based imaging technique using a radioactive fluorine-labeled glucose analog tracer, 18F-fluorodeoxyglucose (18F-FDG), has been successfully and widely applied in the clinic for tumor diagnosis and staging, as well as for monitoring responsiveness to treatment (Figure 1.3)[34]. For many cancers, the specificity and sensitivity of 18-FDG PET to identify primary and metastatic lesions is near 90%[35].

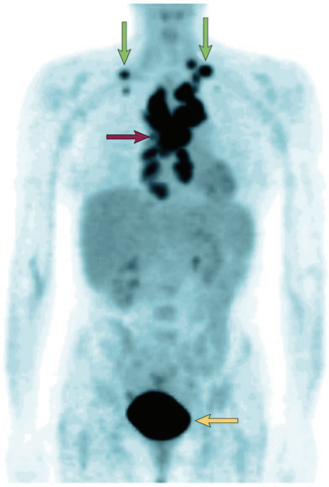

Figure 1. 3 PET-based Imaging with 18F-fluorodeoxyglucose (18F-FDG) of a Patient with Lymphoma

The mediastinal nodes (purple arrow) and supraclavicular nodes (green arrows) show that tumors in these nodes have high levels of 18F-FDG uptake. The bladder (yellow arrow) also has high activity, because of excretion of the radionuclide. PET, positron-emission tomography. Adapted from[36].

An initially proposed misconception was that proliferating cells harbored defective mitochondria that inhibited their ability to carry out oxidative phosphorylation, and thus relied on fermentative glucose metabolism to meet their energetic demands. However, evidence over the last decade demonstrated that

mitochondrial respiration persists in most proliferating cells, and in turn retains its role as the primary source of adenosine 5'-triphosphate (ATP) generation[30, 37]. Instead, the increased uptake and subsequent preferential metabolization of glucose to lactate even in aerobic conditions have been proposed to be an adaption to intermittent hypoxia in pre-malignant lesions, and serve more predominantly towards supporting biomass accumulation and redox maintenance in proliferating cells (Figure 1.4).

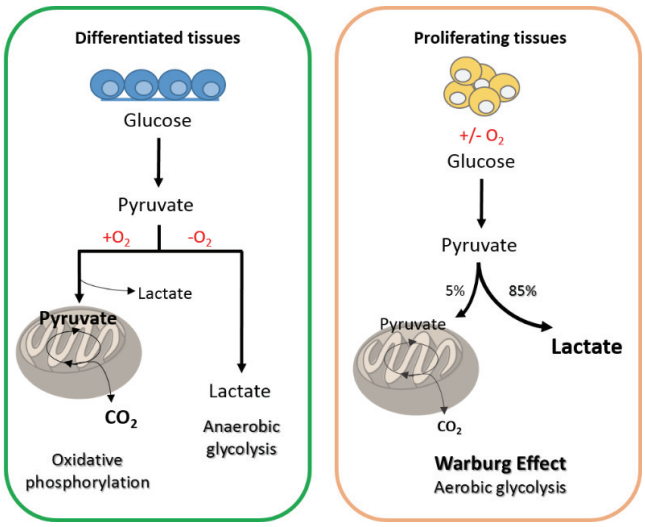

Figure 1. 4 Scheme of Metabolic Differences Between Differentiated Tissues and Proliferating Tissues

In the presence of oxygen, non-proliferating tissues metabolize glucose to pyruvate and oxidize it in mitochondria through oxidative phosphorylation. When oxygen is limiting, cells can redirect the pyruvate generated by glycolysis away from mitochondrial oxidative phosphorylation by generating lactate (anaerobic glycolysis). In proliferative tissues, like tumor cells, glucose is metabolized to lactate regardless of whether oxygen is present, a phenomenon denominated aerobic glycolysis or Warburg effect. Adapted from[38]

Why, then, do tumor cells convert excess pyruvate to lactate rather than entering the mitochondria for oxidative phosphorylation? Interestingly, tumor cells have only a modest increase of ATP consumption relative to their need for biosynthetic precursors and reducing equivalents in the form of NADPH. Glucose catabolism is a robust supplier of these precursors and of reducing power. In contrast, NADH and ATP generated through tricarboxylic acid (TCA) cycle act as the major negative regulator of glucose metabolism. By converting excess pyruvate to lactate, cancer cells prevent accumulation of cytosolic NADH and excessive ATP production, facilitating the continuation of cytosolic glucose metabolism free from feedback repression by excess mitochondrial ATP generation. This notion has stimulated further investigations on advantages of the uncoupling of glycolysis from oxidative phosphorylation in cancer cells. More importantly, although glycolysis is classically depicted as a single chain of metabolic events that leads to the final conversion of pyruvate, it doesn't lie within a metabolic process in which one single metabolite contributes to one single output. As a central source of carbons, glycolysis is highly interconnected with a number of other branching metabolic pathways. Various glycolytic intermediates can serve as substrates for *de novo* synthesis of cellu-

lar building blocks (Figure 1.5). It has been noted that under conditions of high glucose uptake, the flux of glycolytic intermediates into these branching biosynthetic pathways could be substantially increased[39].

For example, one of those sub-pathways is the pentose phosphate pathway (PPP), in which glucose-6-phosphate can feed into the non-oxidative arm of the PPP to yield ribose-5-phosphate, which is a critical intermediate in nucleotide biosynthesis. Glucose-6-phosphate can also shunt into the oxidative arm of the PPP to generate ribose-5-phosphate as well as NADPH that is required for scavenging the reactive oxygen species (ROS) and fatty acid synthesis[40]. Alternatively, fructose-6-phosphate and glyceraldehyde-3-phosphate can be branched into the non-oxidative arm of the PPP, resulting in the generation of ribose-5-phosphate.

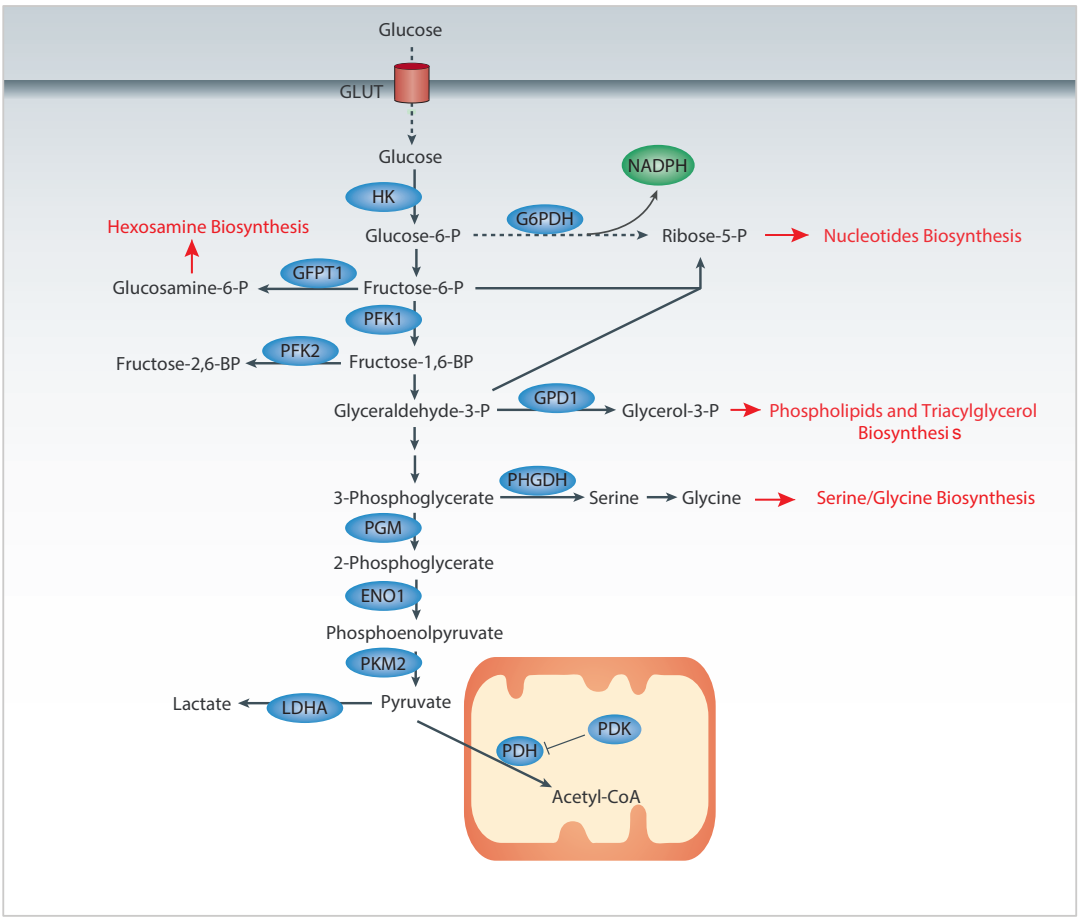

Figure 1. 5 Use of Glycolytic Intermediates for Biosynthesis and NADPH Production

As a central source of carbons, glycolysis is highly interconnected with a number of other branching metabolic pathways. Various glycolytic intermediates can serve as substrates for *de novo* synthesis of cellular building blocks. Enzymes that control critical steps are highlighted. Abbreviations: GLUT, glucose transporter; HK, hexokinase; G6PDH, glucose-6-phosphate dehydrogenase; GFPT1, glutamine fructose-6-phospate transaminase 1; PFK, phosphofructokinase; GPD1, glycerol-3-phosphate dehydrogenase 1; PHGDH, 3-phosphoglycerate dehydrogenase; PGM, phosphoglycerate mutase; ENO1, enolase 1; PKM, pyruvate kinase muscle isozyme; PDH, pyruvate dehydrogenase; PDK, pyruvate dehydrogenase kinase; LDH, lactate dehydrogenase. Adapted from[37]

In addition, fructose-6-phosphate can also be utilized as a substrate for hexosamine biosynthesis (Figure 1.5). Driven by the enzyme glutamine fructose-6-phosphate aminotransferase 1 (GFPT1), fructose-6-phosphate and glutamine can be converted into glucosamine-6-phosphate. Through the generation of N-acetylglucosamine (GlcNAc), a substrate for N- and O-linked glycosylation, the hexosamine pathway provides substrates for cellular glycosylation reactions[41-43].

Another important glycolytic intermediate is 3-phosphoglycerate, which serves as a precursor for the biosynthesis of the amino acids serine and glycine. Metabolic flux studies demonstrated that cancer cells may metabolize up to 50% of glucose-derived carbon in serine biosynthesis and its subsequent catabolism[39]. The rate-limiting enzyme of serine biosynthesis, 3-phosphoglycerate dehydrogenase (PHGDH), is required for the growth of PHGDH-amplified cells, and is frequently overexpressed in breast cancer and melanoma[39, 44] (Figure 1.5). Furthermore, reduction of dihydroxyacetone phosphate to glycerol-3-phosphate by glycerol-3-phosphate dehydrogenase 1 (GPD1) effectively provides cells with a critical substrate for the biosynthesis of macromolecules including phospholipids and triacylglycerol, while 3-phosphoglycerate-derived serine can further feed into phospholipid synthesis as well[45] (Figure 1.5).

Advances over the past decade have shown that altered glucose metabolism lies directly downstream of various oncogenes, tumor suppressors and signaling cascades[46]. In particularly, rewired cellular glucose metabolism in cancer cells can be regulated in large part by key factors, such as MYC, p53, hypoxia-inducible factor 1 (HIF-1) and the PI3K/Akt/mTORC1 pathway.

For example, tumor suppressor p53 regulates aerobic glycolytic pathways through transcriptional activating its downstream targets TP53-induced glycolysis regulator (TIGAR) and cytochrome c oxidase 2 assembly protein (SCO2). TIGAR is a negative regulator of the glycolytic enzyme phosphofructokinase-1 (PFK1). Activation of TIGAR redirects glycolytic flux towards the oxidative PPP shunt and leads to an increase in the production of NADPH, which acts as a intracellular defense against ROS-induced damage[47]. SCO2 is critical for regulating the cytochrome c oxidase (COX) complex in the mitochondrial electron transport chain. By regulating the transcription of SCO2, p53 positively up-regulates oxidative phosphorylation[48]. P53 also remarkably affect glucose metabolism through its regulation of glucose transporters GLUT1 and GLUT2[49], the glycolytic enzyme phosphoglycerate mutase (PGM)[50], pyruvate dehydrogenase kinase-2 (PDK-2)[51], as well as glucose-6-phosphate dehydrogenase (G6PDH), the rate-limiting enzyme of PPP[52].

During cancer development, hypoxia typically occurs in the center of solid tumors where vascularization is abnormal or limiting. As a master regulator of the cancer hypoxic response, HIF-1 plays an important role in the regulation of cancer cell metabolism. HIF-1 promotes Warburg effect through transcriptional regulation of several genes that support glucose fermentation including glucose transporters, hexokinase 2 (HK2), lactate dehydrogenase A (LDHA)[53-55]. Notably, activation of HIF-1 displays additional effects on the inhibition of mitochondrial glucose metabolism, by promoting the expression of PDK1 to suppress PDH activity[56,

[57]. By stimulating the conversion of pyruvate into lactate, HIF-1 subsequently blocks glucose carbon incorporation into mitochondrial citrate and in turn inhibits fatty acid synthesis[58]. This block correlates with the anti-proliferative effect of HIF-1 observed in hematopoietic and renal cells[58], and fits with recent genetic evidence of HIF-1 acting as a tumor suppressor in some cancers [59], indicating that the function of HIF-1 in tumorigenesis is complex and context-dependent.

Proto-oncogene MYC supports glucose metabolism through the direct stimulation of many genes involved in glucose uptake and glycolysis, ultimately contributing to cancer cell growth and proliferation. Glucose transporter GLUT1[60], HK2[61], PFK[62], enolase 1 (ENO1)[63], and LDHA[64, 65] have been identified as MYC-responsive genes. In addition to the direct induction ability of glycolytic genes, MYC has also been implicated in promoting RNA splicing for the expression of pyruvate kinase M2 (PKM2), which has been associated with proliferating cells, versus the alternative form, PKM1[66].

The PI3K/Akt /mTORC1 pathway plays an important role in the regulation of metabolic adaptations required for cell growth[67-69]. One downstream effect of PI3K/Akt pathway activation is the promotion of glycolytic metabolism through Akt-mediated membrane translocation of glucose transporters, and Akt-dependent activation of hexokinase and phosphofructokinase[70-72]. Perhaps the most dramatic metabolic consequence of PI3K/Akt stimulation, however, is the downstream activation of the cell growth regulator mammalian target of rapamycin complex 1 (mTORC1)[73]. While mTORC1 can regulate many cellular processes, it remains best known for elevating protein synthesis through direct phosphorylation of the translational regulators 4E-binding protein 1 (4EBP-1) and S6 kinase 1 (S6K1)[73]. Among the downstream targets of mTORC1 are a number of transcription factors that coordinate metabolic gene expression, including HIF-1α, c-Myc, and sterol regulatory element-binding protein 1 (SREBP-1). mTOR increases surface expression of glucose transporters, allowing cells to boost import of the major lipogenic precursor[74, 75]. It has been shown that SREBP-mediated de novo lipogenesis is a critical component of mTORC1-driven proliferation[76]. mTORC1 also has direct effects on promoting mitochondrial biogenesis, in part via a transcriptional complex that promotes the function of peroxisome proliferator-activated receptor gamma coactivator 1-alpha (PGC-1α)[77-80].

1.2.2 Glutamine Metabolism in Cancer

Although glucose metabolism through aerobic glycolysis has been designated as an important hallmark of cancer metabolism, it cannot explain all the metabolic alterations that are required to support cell growth and proliferation. In the last decade, the importance of glutamine as an additional nutrient in fueling tumor cell proliferation has been established[81, 82].

While glucose is predominantly metabolized into lactate rather than entering the TCA cycle, cancer cells particularly rely on glutamine to replenish TCA cycle intermediates. This process, termed anaplerosis is ac-

complished through the conversion of glutamine to α-ketoglutarate (α-KG) via a two-step deamination reaction catalyzed by glutaminases and then by glutamate dehydrogenase 1 (GLUD1) or transaminases[37, 83-85]. Cancer cells critically depend on glutamine as a fuel for proliferation, and its addition to glutamine is considered another hallmark of tumor cell metabolism. Abrogation of glutamine metabolism blocks tumorigenesis, indicating an accessible therapeutic window for cancer treatment[86]

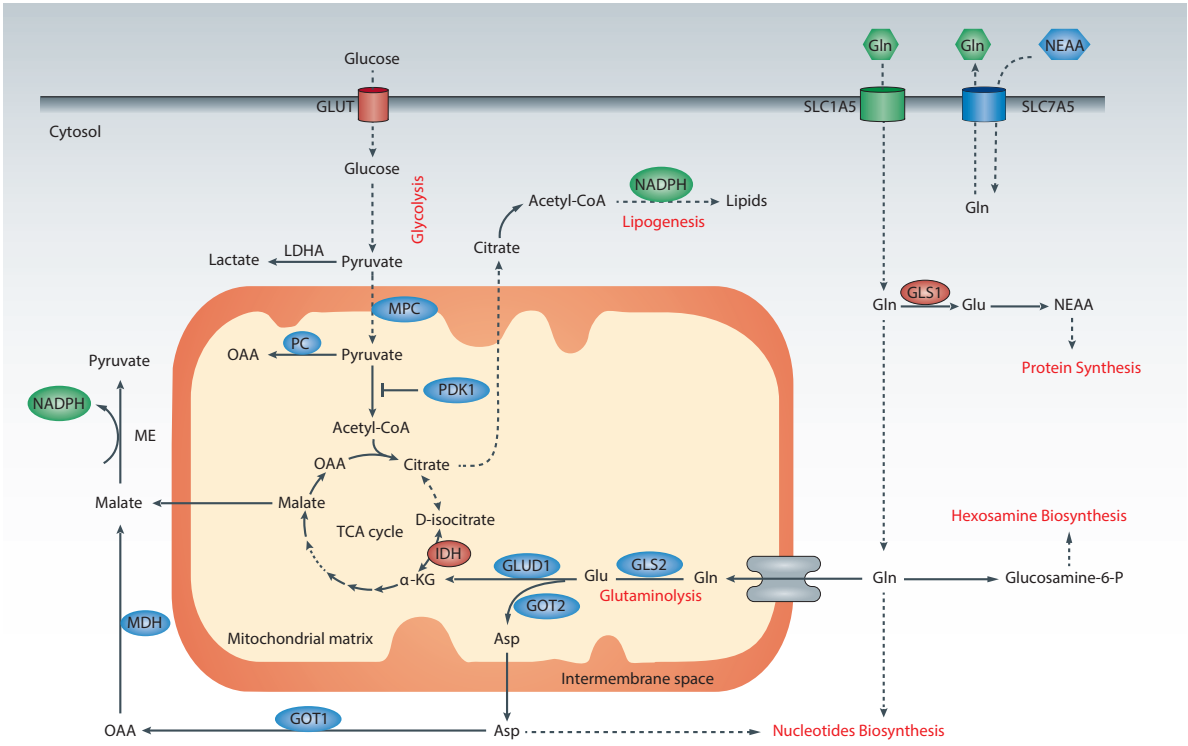

Figure 1. 6 Glutamine Metabolism in Cancer Cells

Glutamine serves as a nitrogen source for the biosynthesis of nucleotides and various nonessential amino acids. In addition, glutamine is an important carbon source for the replenishment of TCA cycle intermediates, which are diverted into various anabolic pathways during proliferation. Abbreviations: MPC, mitochondrial pyruvate carrier; PDK1, pyruvate dehydrogenase kinase; LDHA, lactate dehydrogenase; PC, pyruvate carboxylase; GLUD1, glutamate dehydrogenase 1; GLS1, glutaminase 1; GLS2, glutaminase 2; GOT1/2, glutamate oxaloacetate transaminase 1/2; MDH, malate dehydrogenase; IDH, isocitrate dehydrogenase; Gln, glutamine; Glu, glutamate; α-KG, α-ketoglutarate; OAA, oxaloacetate; Asp, aspartate. Adapted from[30, 38]

Glutamine, the most abundant amino acid found in the human blood, is a major nutrient source for most tumor cells to proliferate and survive. In fact, it donates not only carbon but also nitrogen for the *de novo* biosynthesis of a number of diverse nitrogen containing compounds, including nucleotides, hexosamine, and nonessential amino acids (NEAAs)[41, 87] (Figure 1.6). For instance, glutamine or glutamine-derived glycine and aspartate are required for the *de novo* synthesis of both purine and pyrimidine, therefore some transformed cells showed abortive S phase entrance in glutamine-deprived conditions due to a reduced supply of DNA[88]. Glutamine is also the obligate substrate that condenses with fructose-6-

phosphate to form glucosamine-6-phosphate, which is a precursor for glycosylation reactions[41-43]. It has also been demonstrated that intracellular glutamine exerts control over the uptake of various essential amino acids through the amino acid transporter SLC1A5 and SLC7A5[89].

Anaplerosis via glutamine metabolism in cancer cells replenishes the intermediates of TCA cycle[37, 90-94] (Figure 1.6). In some cells, glutamine fuels the majority of the cellular oxaloacetate (OAA) pool[95]. OAA is the essential substrate to maintain citrate production, which can donate acetyl-CoA groups for the synthesis of lipids[96]. Suppression of pyruvate import into the mitochondria through inhibiting the mitochondrial pyruvate carrier (MPC) activates GDH and reroutes glutamine metabolism to generate both OAA and acetyl-CoA, enabling persistent TCA cycle function[97]. Moreover, glutamine starvation from fibroblasts was shown to deplete intracellular pools of TCA cycle intermediates[98]. Real-time ^{13}C NMR spectroscopy in human glioblastoma cell line showed conclusively that glutamine replenishes the bulk of anaplerotic carbon to the TCA cycle[99]. The co-existence of robust glucose and glutamine metabolism in these cells resulted in production of citrate molecules containing two glucose-derived carbons (from acetyl-CoA) and four glutamine-derived carbons (from OAA).

Besides the contribution of glutamine to sustain metabolic intermediates, mitochondrial glutamine metabolism is in addition to the pentose phosphate pathway (PPP) a major producer of NADPH [37] (Figure 1.6). Export of glutamine-derived malate to the cytoplasm short-circuits the TCA cycle but delivers substrate to malic enzyme for NADPH production. Reduction of the NADPH/$NADP^+$ ratio diminishes cell proliferation and tumor formation by slowing down macromolecular biosynthesis and renders the transformed cells vulnerable to free radical-mediated damage[100]. Thus, NADPH is under most circumstances a limiting factor for cancer cell growth and survival[101]. Evidence suggests that glutamine metabolism can be the major source of NADPH in some tumor cells. For instance, in human glioblastoma cells, glutaminolysis was predicted to produce more than enough NADPH for fatty acid synthesis; the surplus could presumably be used for nucleotide biosynthesis and maintenance of the glutathione pool**.** Enzymes related to glutamine-derived NADPH generation, such as isocitrate dehydrogenases (IDH) and malic enzymes (ME) have also been shown to be in tight correlation with metabolic cancer profiles [102-104]. Moreover, a recent study identified a novel non-canonical pathway of glutamine use that is required for tumor growth in human pancreatic ductal adenocarcinoma (PDAC) cells[85]. In this pathway, glutamine-derived aspartate is transported into the cytoplasm where it can be converted into OAA by the enzyme glutamic-oxaloacetic transaminase 1 (GOT1). Subsequently, this OAA is converted into malate and then pyruvate, increasing the NADPH/$NADP^+$ ratio that can potentially maintain the cellular redox state during rapid cellular proliferation. GOT1 knockdown increased glutamine-derived aspartate, decreased OAA, and profoundly impaired PDAC growth in multiple PDAC cell lines and primary PDAC cells[85].

Because of these multifaceted functions of glutamine, cancer cells thus critically depend on glutamine to satisfy the anabolic demands of macromolecular biosynthesis and to maintain cellular redox[86], impairment of the glutamine pathway can significantly block tumorigenesis. In fact, glutamine-based PET imaging has recently shown promise in preclinical and early clinical studies[105, 106]. The use of 18F-labeled glutamine as a tracer appears to provide potentially useful information to detect tumors in regions where the use of 18F-fluorodeoxyglucose is not feasible, for instance, in imaging of tumors that are localized to sites of heavy glucose utilization, such as the brain.

Regulation of Glutamine Metabolism

Glutamine metabolism of proliferating cells serves to meet both anaplerotic and NADPH demands to maintain growth and proliferation. Both signaling pathways and transcriptional machinery can regulate cellular metabolism through coordinating glutamine utilization.

Oncogenic MYC has been shown to stimulate genes involved in glutamine metabolism at the transcriptional and posttranscriptional levels. MYC directly promotes mRNA expression of *glutaminase 1* (*Gls1*)[83, 107], which converts glutamine to glutamate for its oxidation in the TCA cycle and also for protein synthesis or glutathione synthesis. It appears that MYC could also indirectly regulate the protein expression of GLS1 through its repression of the microRNAs, miR23a and miR23b, which in turn suppress GLS1 expression[107]. This explains the observation that in the P493-6 B-cell model of human Burkitt's lymphoma GLS1 protein levels were much elevated by MYC induction while *Gls1* mRNA levels only modestly induced[107]. Pharmacological inhibition of GLS1 abrogated the growth of tumor xenografts from MYC-expressing B cells, indicating that glutamine metabolism is essential for MYC-dependent tumorigenesis[99]. Intriguingly, MYC induced glutamine metabolism appears to be important for cell survival under glucose- or oxygen-deprived conditions[99]. Using isotopic labeled glutamine as the tracer, Le et al. (2012) found that glutamine import and metabolism through the TCA cycle persisted under hypoxia, and glutamine contributed significantly to citrate carbons, while under glucose deprivation, glutamine-derived fumarate, malate, and citrate were all significantly increased[99]. In fact, human tumor cells whose growth is driven by the oncogene MYC are particularly sensitive to glutamine withdrawal; deficiency in glutamine but not glucose induces MYC-dependent apoptosis[98]. Glutamine depletion from MYC-transformed cells resulted in a rapid loss of TCA cycle intermediates and cell death[98]. Furthermore, this dependence on glutamine for survival is not related to the generation of ATP by glutamine metabolism. Metabolic flux tracking using 13C-labeled glucose or glutamine in a MYC-inducible P493-6 B-cell revealed that MYC drives a glucose-independent TCA cycle using glutamine as the substrate. The study also showed a significant contribution of glutamine to glutathione synthesis, particularly under hypoxic conditions[108]. In aerobic conditions, a marked amount of glutamine is also converted to proline through MYC-dependent regulation of proline oxidase/dehydrogenase (POX/PRODH) that are involved in proline biosynthesis[109]. A study on MYC-inducible liver cancer model indicated

that imported glutamine contributes to the production of alanine from pyruvate through transaminases in the premalignant livers[65]. In frank liver tumor cells, glutaminase levels and glutamine metabolism were increased by MYC. Glycolysis is also heightened with an increased rate of pyruvate to lactate conversion in these hepatic tumors[65]. Similarly, the MYC-inducible lung cancer model displayed increased glycolysis and glutaminolysis; however, in contrast to the liver tumors, MYC-induced lung cancer is also associated with increased glutamine synthetase[98, 110]. In this regard, these lung cancer cells can produce glutamine from glutamate in addition to their ability to import glutamine. Moreover, MYC also activates the transcription of *Slc1a5*, which encodes the Na^+-dependent amino acid transporter ASCT2 required for glutamine uptake[83, 111]. Taken together, these data provide further evidence that reprogrammed glutamine metabolism is critical to the growth and survival of MYC-driven malignancies.

The function of p53 as a tumor suppressor has been attributed to its ability of regulating glutamine metabolism. For instance, p53 activates of the expression of *Gls2*, which encodes a mitochondrial glutaminase, catalyzing the hydrolysis of glutamine to glutamate. Induction of GLS2 by P53 leads to increased levels of glutamate and α-KG, as well as mitochondrial respiration rates and glutathione (GSH) levels that protect the cell from oxidative stress-induced apoptosis. p53 also regulates cell metabolism and proliferation by controlling expression of ME1 and ME2, which are important for NADPH production and glutamine metabolism. Both malic enzyme isoforms are repressed at the transcriptional level by p53. As a result, p53-deficient cells exert enhanced levels of glutamine consumption and NADPH production. Silencing of ME1 or especially ME2 in $p53^{-/-}$ HCT116 cells markedly reduced the tumor sizes in the xenograft model[104]. In addition, p53 is also required for cellular survival and adaptation to low glutamine conditions[112]. Glutamine deprivation stimulates p53 by regulating protein phosphatase 2A (PP2A). B55α, one of the regulatory subunit of PP2A, was specifically induced during glutamine starvation in a ROS-dependent manner. B55α then activates p53 through direct binding and dephosphorylation of EDD, an inhibitor of p53. However, another study showed that in DMBA-induced mammary tumors, oral supplementation of glutamine increases phosphorylation of p53 and apoptosis[113]. Hence, there is still a controversy surrounding p53 activation and glutamine status including glutamine supplementation or deprivation, carefully designed studies should be performed to explore these complex relationships in different cell states.

HIF-1 plays very important roles in regulating glutamine metabolism to meet the demands of cancer cells and to prevent cancer cells from damage of hypoxic stress. Recent studies showed that glutamine is essential for the survival of many cancer cells under hypoxic stress. It was demonstrated that glutamine transport is enhanced in neuroblastoma cells under oxygen-limited conditions[114]. Furthermore, in rat pheochromocytoma cells, key enzymes relevant to glutamine metabolism and transport including glutamine synthetase (GS) and glutamate decarboxylase (GAD), GLS1, SLC1A2 and SLC1A3 were coordinated by hypoxia[115]. Exposure to hypoxia also led to an elevated rate of *de novo* glutamine synthesis[115]. As mentioned

above, HIF-1 limits fluxes of glucose-derived pyruvate into mitochondria through inhibition of PDH activity, thus inducing low intracellular levels of citrate that is critical for *de novo* lipogenesis. Alternatively, several independent groups have described a new pathway of citrate formation during hypoxia[99, 116-118]. Metabolic tracing demonstrated that glutamine import and metabolism through the glucose-independent TCA cycle persisted under hypoxia, and consumed glutamine contributed significantly to citrate production. This process is facilitated by cytosol isocitrate dehydrogenase 1 (IDH1) or mitochondrial isoform IDH2, which catalyze a reversible conversion from α-KG to isocitrate (Figure 1.7). Under hypoxia, HIF-1 regulates both IDH1 and IDH2 to facilitate glutamine-dependent reductive metabolism in order to sustain citrate formation and lipogenesis. Moreover, whole-genome sequencing has led to the identification of recurrent mutations of IDH1 and IDH2 in gliomas, acute myeloid leukemias (AML), and chondrosarcomas[119-121] (Figure 1.7). These mutations acquire a novel reductive activity to convert α-KG to 2-hydroxyglutarate (2-HG), a rare metabolite found at only trace amounts in mammalian cells under normal conditions[122]. Elevated levels of 2-HG competitively inhibit various α-KG-dependent dioxygenases including ten-eleven translocation 2 (TET2) DNA hydroxylases and JmjC histone demethylases that are involved in epigenetic regulations[123-126] (Figure 1.7). 2-HG has also been shown to suppress activity of prolyl hydroxylase domain 2 (PHD2) and subsequently maintain HIF-1 stability (Figure 1.7). However, several independent groups further claimed that they have failed to observe a direct link between 2-HG and PHD2 inhibition, and it is currently proposed that the regulation of HIF-1 stability through decreased PHD2 activity is not the primary effect of IDH mutations[120, 122, 127-130]. Collectively, these results illustrated how cancer cells reprogram glutamine metabolism under hypoxia conditions.

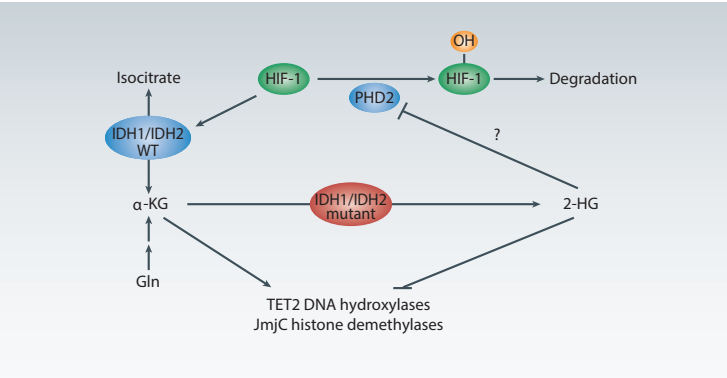

Figure 1. 7 HIF-1-dependent Glutamine Metabolism

IDH, isocitrate dehydrogenase; Gln, glutamine; Glu, glutamate; α-KG, α-ketoglutarate; 2-HG, 2-hydroxyglutarate; PHD2, prolyl hydroxylase domain protein 2. Adapted from[30]

The mechanistic target of rapamycin (TOR) is a conserved serine-threonine kinase that regulates cell growth and metabolism in response to nutritional status[131]. The importance of amino acids for TORC1 activation was initially documented in yeast, in which amino acid starvation recapitulated the effects of treat-

ment with the TORC1 inhibitor, rapamycin, in suppressing TORC1-induced protein translation and inducing autophagy. Moreover, in yeast, TORC1 was shown to be responsive to both glutamine and essential amino acids (EAAs)[132]. Substantial evidence indicates that mTORC1-signaling appears to respond most acutely to leucine, however glutamine is also necessary for maximal mTOR activation[133, 134]. Glutamine can regulate the mTORC1 pathway by facilitating the uptake of leucine [89] and by promoting mTORC1 assembly and lysosomal localization[135, 136], suggesting that glutamine serves both as an intermediary source or a signaling metabolite to promote mTOR pathway. To better understand the mechanism through which glutamine synergizes with EAAs to regulate mTORC1 activation, Nicklin et al. studied a cell line in which mTORC1 activation was dependent on the presence of both glutamine and the EAAs. The authors found that a portion of the glutamine taken up through the glutamine importer SLC1A5 was rapidly exported through the bidirectional amino acid transporter SLC7A5 in exchange for the uptake of extracellular EAAs. Knockdown of SLC1A5 in these cells impaired glutamine uptake and export, EAAs uptake, and mTORC1 activation, suggesting that glutamine uptake and export is required for EAAs activation of mTORC1[89]. Another study showed that glutamine in combination with leucine activates mTORC1 by enhancing glutaminolysis and α-ketoglutarate production. Elevated glutaminolysis or a cell-permeable α-ketoglutarate analog stimulated lysosomal translocation and activation of mTORC1[135]. Finally, cell growth and autophagy, two processes controlled by mTORC1, were regulated by glutaminolysis. A more recent study demonstrated that mTORC1 promotes glutamine anaplerosis by activating glutamate dehydrogenase (GDH), and this regulation requires transcriptional repression of mitochondrial-localized sirtuin 4 (SIRT4) that inhibits GDH[84].

1.2.3 Asparagine Metabolism in Cancer

Unlike glutamine, which is a well-established nutrient for cancer cells, the role of asparagine in cancer has been less documented. However, several studies have reported that certain types of tumors are susceptible to L-Asparaginase (L-ASNase) treatment, which lowers cellular asparagine levels by converting asparagine into aspartate and ammonia[137-139]. Furthermore, primary acute lymphoblastic leukemia (ALL) cells and many ALL cell lines are unusually sensitive to asparagine depletion. Therefore systemic reduction of asparagine levels by treatment of patients with the enzyme L-ASNase has become a approach to treat ALL. *De novo* synthesis of the non-essential amino acid asparagine is regulated by the enzyme asparagine synthetase (ASNS). ASNS catalyzes the conversion of aspartate and glutamine to asparagine and glutamate in an ATP-dependent reaction, thereby regulating the level of both glutamine and asparagine (Figure 1.8). Expression of ASNS is strongly increased in amino acid and glucose deficient environments such as tumors pointing to an important adaptive role of this enzyme in response to metabolic stress[140-142]. L-ASNase-resistant ALLs tend to overexpress ASNS to compensate for the lack of asparagine[137]. ASNS overexpression has furthermore been linked to other solid tumors, such as those of the pancreas[143], ovary[144], and appears

to be important for liver regeneration[145]. The expression of ASNS also correlates with the poor prognosis of glioma and neuroblastoma patients. Intriguingly, recent studies showed that ASNS overexpression or asparagine supplementation promotes cell survival and helps tumor cells to overcome the proliferation arrest induced by amino acid depletion[146]. In glioblastoma cells, asparagine is necessary and sufficient to suppress glutamine depletion induced apoptosis without restoring the levels of other nonessential amino acids or TCA cycle intermediates[147]. In these cells, knockdown of ASNS leads to cell death even in the presence of glutamine, which can be reversed by addition of exogenous asparagine[147]. ASNS silencing in melanoma cells was recently reported to result in cell cycle arrest[148]. Similarly, in sarcoma cells a striking inhibitory effect on proliferation was observed after the suppression of ASNS due to reduced proportion of cells in S phase and impeded synthesis of nascent polypeptide chains[149]. Collectively, these studies suggest a critical role of asparagine metabolism in maintaining metabolic homeostasis, and promoting cellular adaptation to metabolic stresses in tumor cells, making it a novel and attractive target for anti-tumor approaches.

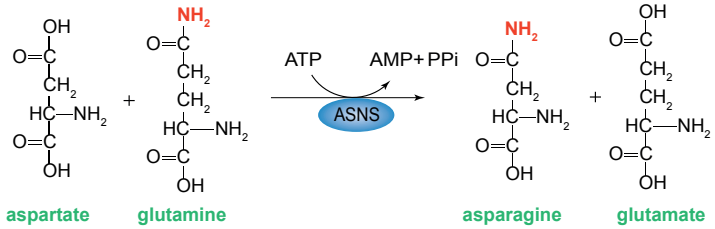

Figure 1. 8 Chemical Reaction Catalyzed by Asparagine Synthesis (ASNS)

The level of ASNS expression among tissues in adult animals varies considerably, with much higher expression in pancreas[138]. ASNS in tumor tissue has been linked to the trans-activating effects of oncogenic effectors such as TP53 mutant[150]. ASNS expression is also linked to various metabolic stresses[138]. For instance, in pancreatic cancer glucose deprivation up-regulates ASNS expression[143]. Similarly, ASNS is also elevated in response to amino acid restriction[142]. ASNS is a transcriptional target of ATF4 in response to amino acid starvation through the GCN2/eIF2a axis. The activation of the GCN2/eIF2a/ATF4 pathway has been reported in primary solid tumors, and GCN2- or ATF4-deficient cells failed to give rise to tumors in vivo[146, 151], suggesting that to maintain asparagine production is critical for solid tumor progression in their nutrient-limited environment. Moreover, several transcriptional regulators, including C/EBPβ, CHOP and members of the ATF family, have been reported to control ASNS expression[152-154]. The link between ATF4 and ASNS and its role in conferring adaptive cell responsiveness to nutrient deprivation has been particularly well studied. Amino acid deficiency is sensed by the protein kinase GCN2, which phosphorylates the translation factor eIF2α. This phosphorylation blocks translation of most mRNAs, but enhances translation of a limited set of mRNAs, such as that encoding ATF4. Increased translation of ATF4 protein in turn promotes the transcription of its target genes, among which ASNS. This signaling cascade thus ultimately en-

hances amino acid synthesis in an attempt to overcome nutrient shortage and to trigger a survival response. A recent study presented a previously unrecognized role for asparagine as an amino acid exchange factor. It is suggested that under normal growth and non-starvation conditions, intracellular asparagine exchanges with extracellular amino acids, especially serine, arginine and histidine, to promote mTORC1 activation, protein and nucleotide synthesis and cell proliferation[155]. Collectively, these results indicate that asparagine is an important regulator of cancer cell amino acid homeostasis, anabolic metabolism and proliferation.

1.3 Functions of LRH-1 in Health and Disease

1.3.1 Introduction of LRH-1

The liver receptor homolog-1 (LRH-1; NR5A2) is a member of the NR5A subfamily of nuclear receptors (NRs). It is also know as fushi tarazu factor 1 (Ftz-F1) [156-161], pancreas homolog receptor 1[162], α-fetoprotein transcription factor [163], human B1-binding factor [164] and CYP7A1 promoter binding factor[165]. Like other NRs, LRH-1 has a conserved modular structure that includes the A/B domain; the highly conserved DNA-binding domain (DBD or C domain); the ligand-binding domain (LBD or E domain), which contains an equally conserved ligand-dependent activation function 2 (AF2) motif that mediates coactivator interaction; and the D domain, which serves as a flexible hinge between DBD and LBD. Moreover, LRH-1 also contains a Ftz-F1 box between the C and DE domains, through which LRH-1 binds DNA with high affinity as monomers (Figure 1.9A).

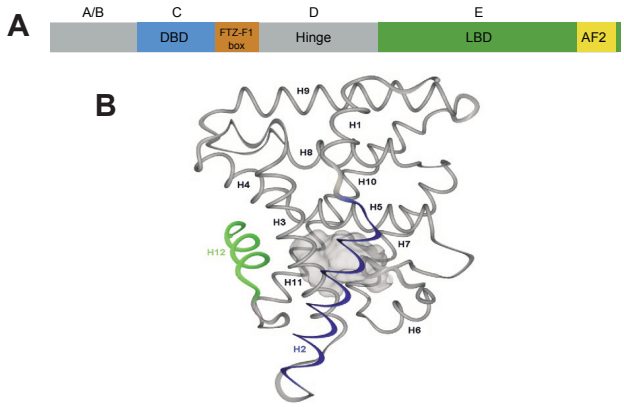

Figure 1. 9 Structure of the Mouse LRH-1

DBD, DNA-binding domain; LBD: ligand-binding domain; AF2: ligand-dependent activation function 2. Helix (H) 12, the position of which determines the active state of a nuclear receptor, is highlighted in green. The extended NR5A-specific H2 (blue) provides an additional layer to the canonical LBD fold and stabilizes the active position of H12 in the LRH-1 crystal structure. The empty ligand-binding pocket is shown in gray. Adapted from [166]

LRH-1 was initially considered as an orphan NR based on its constitutive activity and the absence of

established physiological ligands. Recent studies however revealed that phospholipid species, including phosphatidyl glycerol, phosphatidyl ethanolamine and phosphatidyl choline, as well as the second messengers phosphatidyl inositols, can bind to the large ligand binding pocket of LRH-1 (Figure 1.9B)[167-169]. Notably, two other studies further identified the phospholipid dilauroyl phosphatidylcholine (DLPC) as a potent ligand of LRH-1[170, 171]. Several synthetic agonists and antagonists of LRH-1 have been reported[172-176], indicating the receptor is a bona fide druggable target. Of equal importance, interactions with cofactors or other NRs, and posttranslational modifications (PTM) such as phosphorylation, acetylation and SUMOylation have emerged as mechanisms to fine-tune the activity of LRH-1[177-180].

LRH-1 is mainly expressed in enterohepatic tissues, exocrine pancreas and ovary, where it controls divergent biological processes in development, differentiation and metabolism[181] (Figure 1.10). In the pancreas, LRH-1 is critically required for adequate production and secretion of the pancreatic digestive juice[182, 183]. In the ovary, LRH-1 has been implicated as a key regulator in the regulation of steroidogenesis [184-187], ovulation[188] and maintenance of pregnancy[189]. The function of LRH-1 In the liver has been extensively investigated, and LRH-1 is shown to govern various metabolic pathways. LRH-1 is also implicated in different cancers including colorectal, pancreatic and breast cancer, where it promotes cell proliferation, tumor initiation and progression. The amplification of the chromosomal region harboring LRH-1 (1q32.1) has been found in liver and ovarian tumors, widening the spectrum of tumors in which LRH-1 might be involved[190-192]. The recent identification of LRH-1 in the control of stemness may furthermore provide new insights that could be directly relevant to understand the pro-tumorigenic actions of LRH-1.

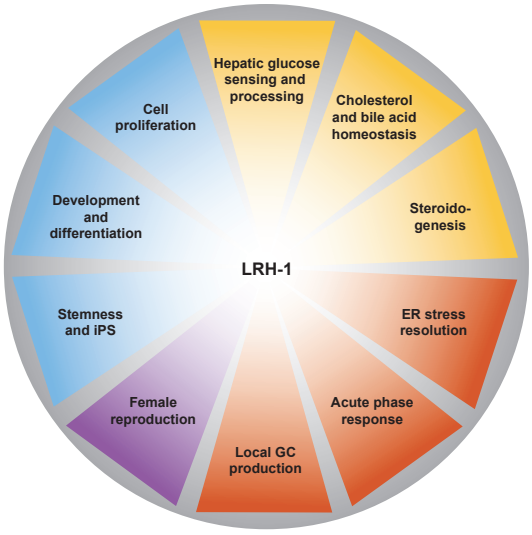

Figure 1. 10 Overview of the Diverse Functions of LRH-1

Yellow shading, metabolic processes; red shading, adaptive stress responses; violet shading, female reproduction; blue shading, stemness, development and proliferation. Adapted from[181].

1.3.2 Emerging Roles of LRH-1 in Liver Metabolism

Bile Acid Homeostasis

LRH-1 has been identified as a master regulator of bile acid (BA) homeostasis. LRH-1 positively regulates the expression of *Cyp7a1* and *Cyp8b1*, which are two key genes involved in BA synthesis[165, 193] (Figure 1.11). Moreover, SHP, an atypical member of the nuclear receptor family that lacks a DNA-binding domain, represses expression of CYP7A1 by inhibiting the activity of LRH-1[194, 195], while the peroxisome proliferator-activated receptor γ-coactivator-1α (PGC-1α) acts as a co-activator for LRH-1 and stimulates CYP7A1 expression[196]. Liver-specific deletion of LRH-1 and subsequent deficiency of *Cyp8b1* eliminate the production of cholic acid and its amino acid conjugate taurocholic acid, and thus increase the ratio towards more muricholic acid species. Interestingly, this effect is attributed to the dramatic reduction of *Cyp8b1*, but not *Cyp7a1*, which in fact was not reduced upon hepatocyte-specific LRH-1 deletion in mice[197-199]. Importantly, this altered BAs composition leads to a compromised intestinal lipid absorption and enhances the fecal excretion of lipids[198, 199]. In addition to its control of key enzymes involved in BA biosynthesis, LRH-1 also maintains hepatic BA levels through coordinating BA elimination and recycling. LRH-1 transcriptionally activates the *bile salt export pump* (*Bsep*) that encodes a transporter responsible for the canalicular secretion of BAs[200]. Multidrug-resistance protein 3 (MRP3) exports bile acids from enterocytes and hepatocytes into the blood, thereby preventing BAs intracellular accumulation. It is demonstrated that LRH-1 controls *Mrp3* expression in hepatocytes[201]. Therefore in the livers following bile duct ligation in rodents, as well as some cholestatic liver diseases in human, LRH-1 drives the induction of MRP3 to prevent hepatocellular injury induced by BAs during cholestasis.

Cholesterol Homeostasis

LRH-1 plays indispensable roles in sustaining cholesterol homeostasis by regulating a number of hepatic and intestinal genes critical for cholesterol metabolism. In the liver, LRH-1 critically modulates reverse cholesterol transport (RCT) (Figure 1.11), a process in which excessive cholesterol from peripheral tissues is transported to the liver and eventually excreted through the bile. LRH-1 positively regulates the expression of several genes involved in RCT, including scavenger receptor class B type I (SR-BI)[202], ATP binding cassette (ABC) half-transporters ABCG5 and ABCG8[203], apolipoprotein AI (APOAI)[204], and apolipoprotein M (APOM)[205]. By activating the expression of those genes, LRH-1 impacts diverse functions in the process of RCT. Transcriptional regulation of SR-BI receptors increases the transfer of mature HDL particles from plasma into hepatocytes. Induction of ABCG5/8 limits intestinal absorption and facilitates biliary secretion cholesterol. Increase in ApoA1 and APOM are associated with high-density lipoprotein (HDL) and facilitate cholesterol clearance[204, 205]. Of note, a recent study reported that SUMOylation of LRH-1 promotes its interaction with prospero homeobox protein 1 (PROX1) and leads to the trans-repression of hepatic RCT genes such as *Scarb1*, *Abcg5*, and *Abcg8*[206]. The increased biliary sterol excretion and RCT observed in an athero-

sclerosis-prone non-SUMOylatable *Lrh-1 K289R* mouse model, decreases the development of atherosclerosis[206]. Moreover, major LRH-1 gene targets that are involved in BA homeostasis including CYP7A1 and MRP3 have also been tightly implicated in cholesterol metabolism[201, 207], further highlighting the importance of LRH-1 in cholesterol homeostasis.

Glucose Homeostasis

LRH-1 has also emerged as a key factor in hepatic glucose metabolism (Figure 1.11). LRH-1 is identified as a direct upstream regulator of glucokinase (*Gck*). Under postprandial conditions, liver-specific *Lrh-1* deficient mice display reduced glucokinase (GCK) and glycogen synthase fluxes as a consequence of reduced availability of glucose-6-phosphate, the end product of GCK. Impaired glucokinase-mediated glucose phosphorylation in LRH-1-deficient livers was also associated with reduced glycogen synthesis, glycolysis, and de novo lipogenesis (DNL) in response to acute and prolonged glucose exposure. Accordingly, hepatic carbohydrate response element-binding protein (ChREBP) activity was reduced upon hepatic loss of LRH-1. These findings identify LRH-1 as a critical regulatory component of the hepatic glucose-sensing system required for proper integration of postprandial glucose and lipid metabolism[208]. Furthermore, the role of LRH-1 in glucose homeostasis has also been investigated in the condition of metabolic disorders. Treatment of dilauroylphosphatidylcholine (DLPC), an unusual phospholipid that binds to and stimulates LRH-1 activity, improves glucose homeostasis and decreases hepatic steatosis in two mouse models of insulin resistance. Both the antidiabetic and lipotropic effects are lost in liver-specific *Lrh-1* knockout mice[170]. Another study showed that the heterozygous *Lrh-1*+/-mice have a mild but significant body weight gain when exposed to a high-fat diet, but conversely do not exhibit changes in glucose or insulin tolerance[209]. These studies suggest that receptor activation has more pronounced metabolic effects on glucose homeostasis than genetic haploinsufficiency of *Lrh-1*.

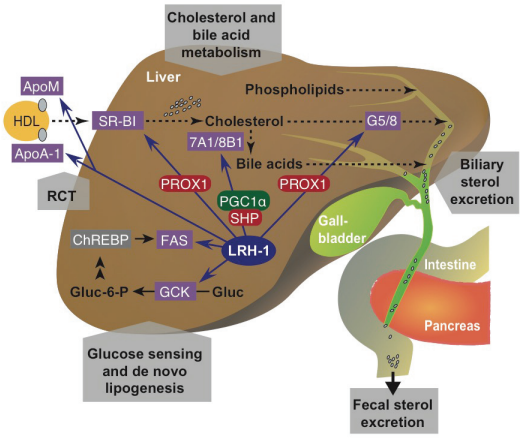

Figure 1. 11 Scheme Demonstrating the Main Hepatic Functions of LRH-1

RCT, reverse cholesterol transport; HDL, high-density lipoprotein; SR-BI, Scavenger receptor class B1; G5/G8, ABCG5/ABCG8; 7A1/8B1, CYP7A1/CYP8B1. Corepressors are illustrated in red, coactivators in green. Adapted from[181].

Hepatic Acute Response

Upon inflammatory stimuli due to injury, infection or chronic metabolic stress, immune cells secrete various cytokines into the bloodstream, which may activate the acute phase response in the liver. As described above, SUMOylation of hepatic LRH-1 leads to the recruitment of different co-repressors. Binding of SUMOylated LRH-1 to the NCOR1/HDAC3 complex via GPS2 mediates the transrepression of acute phase response genes[180, 210] and modulates this hepatic response. Besides transrepressing APPs, LRH- 1 induces the expression of interleukin-1 receptor antagonist (IL-1RA), a robust inhibitor of IL-1 signaling, thereby exerting additional anti-inflammatory roles in the liver[211].

ER Stress

Chronic endoplasmic reticulum (ER) stress results in toxicity that contributes to multiple human disorders. Mamrosh et al. recently reported that LRH-1 initiates a novel ER stress resolution that is independent of canonical unfolded protein response (UPR) pathways. LRH-1 induces expression of the kinase polo-like kinase 3 (PLK3), which phosphorylates and activates the transcription factor ATF2. In response to ER stress, despite a functional UPR, liver-specific *Lrh-1* knockout mice cannot resolve ER stress attributed to reduced PLK3 expression and ATF2 activity. Importantly, LRH-1 agonist treatment increases ER stress resistance and decreases cell death, this suggests targeting LRH-1 may be beneficial in human disorders associated with chronic ER stress[170].

Methyl-pool Homeostasis

A tight balance of labile methyl groups, typically found in choline, betaine, methionine, and folate, and a constant supply of methyl donors such as s-adenosylmethionine (SAM) are important for proper liver functions[212, 213]. A significant quantitative use of labile methyl groups occurs during the production of phosphatidylcholines (PCs), which are ligands for LRH-1. A recent study identified LRH-1 as a critical determinant of methyl-pool homeostasis in the liver[214] (Figure 1.12). Mechanistically, the authors showed that LRH-1 transcriptionally regulates glycine-n-methyltransferase (*Gnmt*), an abundant methyltransferase that transfers methyl group from SAM to glycine thereby generating sarcosine. LRH-1 also directly regulates multidrug-resistance protein 2 (*Mdr2*), which is a biliary phospholipid floppase that shuttles phospholipids from hepatocytes into bile. Upon hepatic loss of LRH-1, mice display increased SAM/SAH ratios and ablated biliary PC loss as a result of blunted GNMT and MDR2. Consequently, when exposed to a methionine and choline deficient (MCD) diet that harshly depletes methyl groups and results in a deleterious decrease in the PC-to-phosphatidylethanolamine (PE) ratio (Figure 1.12), liver-specific LRH-1 knockout mice do not show the expected decrease in methyl-pool and PC/PE ratio and are resistant to hepatitis and fibrosis normally induced by the diet[214].

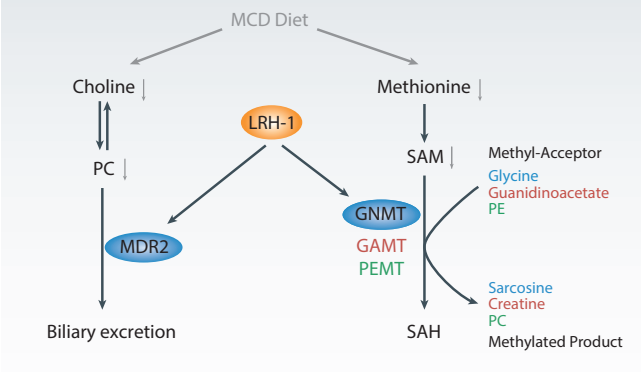

Figure 1. 12 Scheme of Methyl-group Cycling

MCD, methionine and choline deficient; PC, phosphatidylcholine; PE, phosphatidylethanolamine; MDR2, multidrug-resistance protein 2; GNMT, glycine N-methyltransferase; GAMT, guanidinoacetate N-methyltransferase; PEMT, phosphatidylethanolamine N-methyltransferase; Adapted from[214].

LRH-1 and Intestinal Cancer

Activation of the Wnt/β-catenin signaling pathway represents a critical event in the development of colorectal cancers (CRC)[215]. Noteworthy, It is shown that LRH-1 is highly expressed in the intestinal crypts, where it controls intestinal cell proliferation and renewal through crosstalk with the Wnt/β-catenin pathway[216]. More specifically, LRH-1 acts as a coactivator for β-catenin/Tcf4 to drive the expression of *cyclin D1* and other β-catenin/Tcf target genes, such as *c-Myc*. LRH-1 also interacts with β-catenin to directly promote the transcription of *cyclin E1*[216]. Through the synergy with β-catenin signaling, LRH-1 is proposed to contribute to gastrointestinal tumorigenesis. Consistently, haploinsufficiency of LRH-1 markedly reduced intestinal cancer development in both genetic (ApcMin/+) and chemical (azoxymethane) induced CRC mouse models[217]. Expression and subcellular localization of LRH-1 are also significantly altered in neoplastic colon compared with normal human colon[217]. Similarly, two isoforms of LRH-1, hLRH-1 and hLRH-1v1, are found to be co-expressed and significantly up regulated in human gastric cancer[218].

LRH-1 and Pancreatic Cancer

Several lines of evidence indicate that LRH-1 is also critically involved in development and progression of pancreatic cancer. Recent genome wide association studies (GWAS) have identified single nucleotide polymorphisms in the LRH-1 gene as being strongly linked with pancreatic cancer risk[219, 220]. Of note, *Lrh-1* transcripts are markedly elevated in human pancreatic cancer (PC) cells compared to normal pancreatic ductal epithelium[221, 222], which correlates with profound increase of LRH-1 protein expression in human pancreatic ductal adenocarcinomas compared to normal adult pancreas [222]. LRH-1 has also been found to promote PC cell proliferation and tumorigenicity in nude mice through the mediation of its downstream targets *cyclin D1/E1* and *c-Myc* [221, 222]. Conversely, suppression of LRH-1 significantly inhibits PC cell proliferation[222]. Of equal importance, LRH-1 also plays indispensible roles in promoting pancreatic cancer metastasis[222, 223]. PC

cells originating from metastatic tumors have significantly higher expression of LRH-1 than in primary tumor cells[222]. Overexpression of LRH-1 causes enhanced transcriptional activation *c-Myc*, *Matrix metalloproteinase* 2 (*Mmp2*), and *Mmp9* in PC cell lines, as well as prominent increases in PC cell migration, invasion, wound healing, and sphere formation in vivo[223]. This suggests that LRH-1 not only promotes tumor formation, but also confers a more aggressive malignant phenotype.

LRH-1 and Breast Cancer

Notably, LRH-1 is highly expressed and localized in the epithelial compartment of both invasive breast carcinoma and ductal carcinoma in situ[224, 225]. In addition, LRH-1 transcriptional program is also highly associated with a signature of poor clinical prognosis and high-grade of breast cancer[226]. Depletion of endogenous LRH-1 in breast cancer cells decreases cell proliferation, mobility, invasion and colony formation[224, 226-228]. A well-characterized mechanism for the roles of LRH-1 in breast cancer cells is its crosstalk with estrogen/oestrogen receptor α (ERα) signaling. It is reported that LRH-1 directly binds the promoter of ERα, and vice versa, expression of LRH-1 can also be directly regulated by ERα[224, 229]. LRH-1 cooperates with ERα to regulate estrogen-dependent genes such as growth regulation by estrogen in breast cancer 1 (GREB1) and trefoil factor 1 (TFF1) [230, 231]. Despite this positive feedback loop between LRH-1 and ERα, it was also observed that LRH-1 is expressed in ERα-negative breast cancer cells in which it controls cell migration and invasion[228, 232], suggesting that LRH-1 may also have an important role in hormone-independent cancers. A recent study demonstrated that inhibition of LRH-1 affects two- (2D) and three-dimensional (3D) cell proliferation of several breast cancer cells, including ERα-positive and ERα-negative cells. This phenotype is accompanied by the up-regulation of the cyclin-dependent kinase inhibitor CDKN1A in a p53-independent manner. Through cooperating with FOXA1, LRH-1 attenuates the expression of CDKN1A by the recruitment of histone deacetylase 2 (HDAC2) and controls cell proliferation independent of ERα and p53 status[227]. Finally LRH-1 may also promote breast cancer through an indirect mechanism. For instance, LRH-1 is observed highly expressed in breast adipose tissue and cancer-associated fibroblasts surrounding the tumor microenvironment where it stimulates the expression of CYP19A1, the essential enzyme required for production of estrogens, thereby favoring the proliferation of adjacent cancer cells in a paracrine manner[233, 234]. In summary, LRH-1 acts as a determinant in breast cancer development and progression through regulating a specific transcriptional program involved in cell proliferation in both antiestrogen-sensitive and antiestrogen-resistant breast cancer cells.

1.3.3 Emerging Roles of LRH-1 in Stemness

Increasing evidence shows that LRH-1 is a critical transcriptional modulator in several aspects of stem cell biology. LRH-1-deficient mice die at embryonic day 6.5–7.5 with features typical of visceral endoderm dysfunction, demonstrating its indispensible roles in early embryonic development[235]. Pluripotency of embry-

onic stem cells (ESCs) and early mouse embryo is controlled by several key transcription factors such as octamer-binding transcription factor 4 (Oct4), SRY-Box 2 (Sox2) and Nanog[236]. The regulation of these key factors is thus crucial for the maintenance of pluripotency and embryonic development. LRH-1 is known to be co-localized with Oct3/4 in the inner cell mass and the epiblast of embryos at early developmental stages[237]. A nuclear receptor screening also identified LRH-1 as one of the components of a transcription factor regulatory network that maintains pluripotency of mouse ESCs [236]. In early embryo and ESCs, embryonic *Lrh-1* expression is shown to be regulated by both Sox2 and GA-binding proteins (GABP) [238]. Another report revealed that LRH-1 expression can also be regulated by Wnt signaling pathway, through the binding of β-catenin to an embryonic-specific LRH-1 promoter. Moreover, one of the crucial pluripotency factors in maintaining ESCs pluripotency, Oct4, is directly regulated by LRH-1[237]. Strikingly, LRH-1 can even replace Oct4 in the reprogramming from mouse embryonic fibroblasts (MEFs, murine somatic cells) to induced pluripotent stem cells[237, 239], further demonstrating the vital role of LRH-1-Oct4 axis in the maintenance of pluripotency. In addition to Oct4, LRH-1 also mediates other key pluripotency factors of ESCs. For example, upon activation by β-catenin, LRH-1 subsequentially promotes the expression of Nanog and Tbx3[240]. LRH-1 also synergizes with Nanog to directly bind and stimulate expression of Dax1, which is a nuclear receptor found to be highly involved in ESCs biology[241]. Moreover, LRH-1 is involved in the differentiation of mESCs to ectodermal lineage and endodermal lineage. One study revealed that microRNA-134 enhances mESCs differentiation to ectodermal lineage, partially through its direct translational attenuation of Nanog and LRH1[242]. Moreover, it is reported that transcription factor c-Jun promotes mESCs differenciation towards endodermal lineage and blocks the generation of iPSCs from MEFs[242]. In particular, Jun dimerization protein 2 (Jdp2), which represses c-Jun mediated mESC differentiation, anchors LRH-1 to reprogram MEFs into iPSCs. This suggests a role for LRH-1 in mediating the conversion of somatic cells to iPSCs[243]. Furthermore, a recent study identified LRH-1 as a central node in controlling neural stem cell fate decisions during development. The authors revealed that LRH-1 blocks proliferation of neural stem/ progenitor cells (NSCs) and additionally induces neuronal differentiation via direct regulatory effects on Ink4/Arf locus, Prox1 gene, Notch1 and JAK/STAT pathways. Interestingly, LRH-1 is also upstream regulated by the major neuronal and astrocyte pathways, as well as Notch1 and JAK/STAT signaling. These observations suggest that could be a critical regulator of neural development and a potential therapeutic target for CNS-related diseases[182].

Chapter 2 Aim

Despite the rise in the prevalence of HCC, effective therapies are still lacking and novel therapeutic approaches are urgently needed. A better understanding of the molecular mechanisms underlying the metabolic processes that promote to HCC is therefore essential.

This doctoral work aimed to investigate the role of LRH-1 in the development of HCC and to gain more insights into the molecular mechanisms by which LRH-1 controls liver carcinogenesis. To achieve this, I took advantage of two mouse models, one carrying a hepatocyte-specific loss-of-function (LOF) mutation of LRH-1 (*Lrh1*$^{hep-/-}$*),* and one with a knock-in *Lrh1* K289R, which represents a selective gain-of-function (GOF) model for LRH-1.

I initially started by characterizing the role of LRH-1 in the process of liver carcinogenesis using LRH-1 LOF (Chapter 4) and GOF (Chapter 5) mouse models upon DEN exposure that favors the development of HCC. Next, I studied the molecular networks through which LRH-1 regulates glutamine metabolism (Chapter 4) and asparagine metabolism (Chapter 5) that contribute to liver cancer development.

The results from this thesis should lead to new insights into how LRH-1 converges with biochemical, molecular and signaling pathways in intermediary metabolism that are intimately linked with liver cancer development. The outcome should also spark future enthusiasm in the design and development of novel LRH-1 antagonists as a therapeutic strategy to fight HCC.

Chapter 3 Experimental Procedures

Animal studies

For the generation of LRH-1 floxed (LRH-1L2/L2) mice, genomic DNA covering the LRH-1 locus was amplified from the 129Sv strain by using high-fidelity PCR. The resulting DNA fragments were assembled into the targeting vector that, after linearization by NotI, was electroporated into 129Sv embryonic stem (ES) cells. G418-resistant colonies were selected and analyzed for homologous recombination by PCR and Southern blot hybridization. For the PCR screening strategy, primers ACE225 (5'GTCATAGGGAGTCAGGATACCATGG3'), ACE228 (5'GTTCTGACCACTTTCATCTCCTCACG3'), ACE229 (5'CTCAACTGCCGAAGAATGCTGCGG3'), and ACE231 (5'GTTAGCAATTTGGCAGATTTACGC3') were used. Positive clones were verified by Southern blot hybridization. Therefore, genomic DNA was prepared from ES cells (or mouse tails), digested with XbaI or SacI, subjected to electrophoresis on a 0.8% agarose gel, and transferred to a positively charged nylon transfer membrane (Amersham Biosciences, Saclay, France). A 0.5-kb DNA fragment (NotI-NheI) located between exons 6 and 7 (3' probe) and a 0.5-kb DNA fragment (NotI-SacII) placed between exons 2 and 3 (5' probe) were used as probes. The karyotype was verified, and several correctly targeted ES cell clones were injected into blastocysts from C57BL/6J mice. These blastocysts were transferred into pseudopregnant females, resulting in chimeric offspring that were mated to female C57BL/6J mice that express the Flp recombinase under the control of the ubiquitous cytomegalovirus promoter. Offspring that transmitted the mutated allele, in which the selection marker was excised, and that lost the Flp transgene (LRH-1+/L2 mice) were selected, mated with with serum albumin-Cre mice (The Jackson Laboratory), and then further intercrossed to generate hepatocyte-specific LRH-1 knockout (Alb-Cre; Lrh-$1^{hep-/-}$) and wild-type (Lrh-$1^{hep+/+}$) mice.

To generate Lrh-1 K289R mice, gDNA covering the Lrh-1 gene (NCBI Gene ID: 26424) was amplified from the C57BL/6J strain by using high-fidelity PCR. The point mutation of interest (AAG -> AGG) was introduced by PCR. The amplified DNA fragments were ligated into the targeting vector with a floxed Neo cassette (Institut Clinique de la Souris, Strasbourg). The construct was then electroporated into C57BL/6N ES cells. Colonies resistant to G418 were selected and evaluated by PCR for homologous recombination and PCR-positive clones were further validated by Southern blotting. Karyotype-verified ES cell clones were injected into blastocysts from BALB/c mice. These blastocysts were transferred to pseudo pregnant females. Chimeric offspring were mated to female C57BL/6J mice expressing the Cre-recombinase under the control of the ubiquitous cytomegalovirus promoter (CMV) to

delete the Neo cassette. Offspring transmitting the mutated allele, in which the selection marker was excised, and that lost the Cre transgene (Lrh1 L-/+ mice) were selected and inbred with to obtain Lrh1 L-/L- (Lrh-1 K289R) mice. Lrh-1 K289R and Lrh-1 WT mice were backcrossed for 6-7 generations onto commercial C57BL/6J purchased from the Jackson Laboratory.

For DEN-treated liver cancer cohorts, congenic neonatal mice at 14-day-old were intraperitoneally injected with DEN at a dose of 25 mg / kg body weight to initiate tumor formation. 6 months (mid-term DEN) or 10 months (long-term DEN) post-injection, mice were sacrificed and liver tissue was collected. The experiments with the AAV8-viruses have been described previously [208]. Five-week male BALB/c nu/nu mice were purchased from Charles River (France) and maintained in the animal facilities. All animal procedures were approved by the Swiss authorities (Canton of Vaud, animal protocols ID 2375 and 2768) and performed in accordance with our institutional guidelines.

Immunohistochemistry

Liver tissue was fixed overnight in phosphate-buffered 10% formalin and embedded in paraffin, sectioned in 4 µm, and stained with eosin/hematoxylin. Immunohistochemistry was performed using anti-BrdU antibody (AbD Serotec, OBT0030) and anti-Ki67 (Abcam, Ab16667) antibodies. For 5-bromo-2'-deoxyuridine (BrdU, Sigma) incorporation, mice were intraperitoneally injected with BrdU at the dose of 100 mg/kg body weight for 4 hours before sacrifice.

Cell culture, transfection, antibodies and reagents

Hepa 1.6 mouse hepatoma cells and HepG2 cells were cultured in DMEM 4.5 g/l glucose (Gibco) with 10% FBS (Gibco), 1% NEAA (Gibco), and 1% pen-strep (Gibco) at 37°C under a 5% CO_2 atmosphere. Dimethyl-ketoglutarate (DM-KG), N- acetyl-cysteine (NAC), and Asparagine were obtained from Sigma. For LRH-1 overexpression, Hepa 1.6 cells were transfected with pCMV-empty or pCMV-LRH-1 plasmids using jetPEI reagent (Polyplus, France) according to the manufacturer's instructions. For GLS2 overexpression, cells were transduced with either AdGFP or AdGLS2 viruses. siRNAs for LRH-1 and GLS2 were purchased from Microsynth, sequences of siRNA against LRH-1 were: 5'-GUGAACCAGAUGA GCCUCUCA-3', and 5'-CACCUCACAGCAGCC UGCA-3'; sequences of siRNA against GLS2 were: 5'-AGAGCCCACUGGAGGCAAA-3', and 5'-GAAAUCAUCAUGCCAACAA-3'. siRNAs were transfected into cells using Lipofectamine RNAiMAX transfection reagent (Invitrogen, 13778150). 48 hours after transfection or infection, cells were rinsed with cold PBS for 3 times and either lysed in TRIZOL Reagent (Invitrogen) for RNA isolation or RIPA buffer for protein extraction. shRNA for mouse LRH-1 was purchased from Sigma, TRCN0000025985, sequences are: CCGGCCCACAACAGACTGAGAAATTCTCGAGAATTTCTCAGTCTGTTGTGGGTTTTT. shRNA for human LRH-1 was purchased from Sigma, TRCN0000019656, sequences are: CCGGGCGTTGTCCTTACTGTCGTTTCTCGAGAAAC-GACAGTAAGGACAACGCTTTTT. shRNA for mouse GLS2 was purchased from Sigma, TRCN0000177991, sequences are: CCGGGAACCTGCTATTTGCTGCATACTCGAGTATGCAGCAAATAGCAGGTTCTTTTTTG. shRNA for

mouse ASNS was purchased from Sigma, TRCN0000031703, sequences are: CCGGCGCTATCAAGAAACGCTT-GATCTCGAGATCAAGCGTTTCTTGATAGCGTTTTTG. The antibodies used for this study are the following: p-S6K (Thr389, Cell signaling, 9205S), S6K (Cell signaling, 2708), Tubulin (Santa Cruz, sc-5286), p-4EBP1 (Thr37/46, Cell signaling, 2855S), 4EBP1 (Cell signaling, 9644), GLS2 (Abcam, ab113509), ACTIN (Santa Cruz, sc-47778), P62 (Progen, GP62-C), LC3 (Cell signaling, 4108S), HSP90 (BD Transduction Laboratories, 610418), CYP2E1 (Abcam, ab28146), ATF2 (Abcam, ab47476) and p-ATF2 (Thr 69/71, Cell signaling, 9225S), Total Caspase 3 (Cell signaling, 9662S), Cleaved Caspase-3 (Asp175, Cell signaling, 9661), ATF4 (Santa Cruz, sc-200), ASNS (Santa Cruz, sc-365809), VDAC (Abcam, ab14734).

DEN bioactivation and cancerogenicity analysis

Lrh-1$^{hep+/+}$ and *Lrh-1*$^{hep-/-}$ mice were injected with DEN (25 mg/kg body weight) on postnatal day 14. Livers were extracted 6, 24 and 48 hours after DEN administration (n=5-6 per group and time point) and gene and protein expression of relevant enzymes in DEN bioactivation were determined. Cancerogenicity of DEN was determined by evaluating the levels of 8-hydroxy-2'-deoxyguanosine (Nakae et al. 1997) and O^6-ethylguanine DNA adducts (Becker and Shank 1985). Concentration of 8-hydroxy-2'-deoxyguanosine (8-OHdG) was analyzed by enzyme immunoassay (Caymen Chemical, Cat. #589320). For detection of O^6-ethylguanine DNA adducts, DNA was isolated from liver biopsies using commercial kits (Macherey-nagel, Ref.740952.50), and denatured by heating for 10 min at 99 °C followed by the addition of 2 M ammonium acetate. 500ng of DNA was slot-blotted onto nylon membranes (GE Healthcare, Germany). The membrane was then fixed for 90 min at 90 °C and blocked with 5% (w/v) non-fat dry milk in TBS-T. O^6-ethyluanine was visualized with a monoclonal antibody (Axxora, EM2-1) followed by a secondary peroxidase-coupled antibody and enhanced chemoluminescence detection.

Luciferase assay

HEK-293A cells in 96-wells plates were co-transfected with pGL4-TK reporter constructs driven by a heterologous promoter consisting of multiple consensus LRH-1 response elements, in the presence of either pCMV-empty control or pCMV-LRH-1 constructs using jetPEI reagent (Polyplus, France) according to the manufacturer's instructions. Luciferase activities were measured 24 hours post transfection and normalized to β-galactosidase activities.

Gene expression and analysis

RNA was extracted from the livers or cells using TRIZOL (Invitrogen) and purified with the RNeasy cleanup kit for microarray analysis (Qiagen). For Q-RT-PCR, RNA was treated with DNase. cDNA was generated using the QuantiTect® reverse transcription kit (Qiagen), and analyzed by Q-PCR using a LightCycler® 480 Real-Time PCR System (Roche). Primers are listed in Table 1. Expression data were normalized to *cyclophilin*. Microarray analysis was performed using the Affymetrix MouseGene 2.0 ST array and normalized using the Robust Multi-array Average (RMA) method. Heatmaps were generated with GENE-E:

(http://www.broadinstitute.org/cancer/software/GENE-E/index.html).

Hyperpolarization via dissolution dynamic nuclear polarization

To measure *in vivo* glutamine metabolism, an injectable solution of hyperpolarized [5-^{13}C]glutamine was obtained using a custom-built 7-T DNP polarizer (Comment et al. 2007). The ^{13}C polarization was 20 ± 2 % at the time of injection, providing a ^{13}C signal 24,000 times larger than at thermal equilibrium. A frozen solution of cesium hydroxide monohydrate (40.8 mg, 0.24 mmol) and [5- ^{13}C]glutamine (36.3 mg, 0.24 mmol) (Sigma-Aldrich, Switzerland) was dissolved in 38 µL polarization medium containing 35 mM Ox063 radical (Albeda Research, Denmark) was placed inside the polarizer together with 12 µL of frozen HCl (%25) to neutralize the base during dissolution (Cabella et al. 2013). The solution was polarized at 1.00 ± 0.05 K and 196.8 GHz using a nominal output power of 55 mW measured at the output of the microwave source (ELVA- 1, Estonia). After 4 hours, the polarized frozen solution was rapidly dissolved in 5 ml preheated deuterated phosphate buffer (pH 7.5). The hyperpolarized [5-^{13}C]glutamine solution was automatically transferred into a separator/infusion pump located inside the bore of a 9.4-T/31-cm horizontal MR magnet (Varian/Magnex, USA) prior to be injected into a phantom or a mouse, 3 s after dissolution (Cheng et al. 2013).

^{35}S-labelled methionine incorporation for protein translation

Hepa 1.6 cells were pre-treated with methionine-free medium for 30 min, and then 100 µCi of ^{35}S-labelled methionine per mL was added to the cultures for 2 hr. Cells were lysed in RIPA buffer, and lysate were separated by SDS-10% polyacrylamide gels. Gels were then fixed and dried. Radiolabeled species were visualized by autoradiography. The radioactivity of each lane was also scanned by phosphorImager and analysed by ImageQuant analysis.

Cell proliferation assay

Cells were plated in 24-well plates at 2,000 cells per well in 0.5 ml of media. Media was not changed throughout the course of the experiment. At the indicated time points, cells were fixed in 10% formalin and stained with 0.1% crystal violet. Dye was extracted with 10% acetic acid and the relative viable cell number was determined by attenuance (D) at 595nm.

Caspase-glo 3/7 assay

Caspase-3 and -7 activities were determined using commercial kits (Promega, #TB323) according to the manufacturer's instructions.

Chromatin immunoprecipitation (ChIP)

ChIP analysis was performed as described previously with minor modifications [206]. DNA was purified using the PCR clean-up extraction kit (Macherey-Nagel), after which Q-RT-PCR was performed as described previously [198]. Data were normalized to the input (Fold differences=$2^{-(\text{Ct-sample} - \text{Ct-input})}$). ChIP primer sequences are listed in the Supplemental table 1.

Measurements of metabolites

For NADPH/$NADP^+$, GSH/GSSG and Asn/Asp ratios, liver biopsies were extracted with 70% ethanol. Biomass was separated by centrifugation for 10 min at 4000 rpm. Liquid extracts were then dried by vacuum-centrifugation, re-suspended in 10 µl water per mg wet weight, and analyzed by targeted-LC-MS/MS on a Thermo Quantum Ultra instrument equipped with a Waters Acquity UPLC. Intracellular α-KG levels were determined using commercial kits (Abcam, ab83431) according to the manufacturer's instructions.

***In vivo* hyperpolarized ^{13}C MR measurements**

DEN-treated *Lrh-1*$^{hep+/+}$ and *Lrh-1*$^{hep-/-}$ mice were anesthetized with isoflurane (~1.8%), 0.5% O_2 and 0.5% air. A 750 µl bolus containing a dose of 0.57 ± 0.02 mmol/kg hyperpolarized [5-^{13}C]glutamine was administered in 9 s. A series of 30^o BIR4 adiabatic RF excitation pulses were applied using a custom-built dual ^{1}H/^{13}C probe (two ^{1}H surface coils placed in quadrature on top of a ^{13}C single-loop surface coil) placed underneath the animal, onto the shaved skin located on top of the mouse liver. *In vivo* ^{13}C MRS measurements were respiratory-gated and triggered with simulated cardiac signal with a repetition time of 1 s. Acquisitions were performed with an INOVA spectrometer (Varian/ Magnex, USA). The peak integrals were obtained from summed spectra analysed using VNMRJ (Varian/Magnex, USA).

Allograft tumor study

Hepa 1.6 cells suspended in phosphate-buffered saline were injected subcutaneously into the left flanks of nude mice (4×10^6 cells per flank). The diameters of the tumors were measured every 3 days and tumor volumes (V) were calculated using the formula *V=L*W^2/2.* L, length; W, width.

Statistical analysis

Data represent mean ± S.E.M. Comparison of differences between two groups was assessed using two-tailed Student's *t*-tests. Multiple group comparisons were assessed by one-way analysis of variance (ANOVA) and Tukey's *post hoc* test. Differences under $P < 0.05$ were considered statistically significant (*$P < 0.05$, **$P < 0.01$, ***$P < 0.001$).

Acknowledgements

I thank S. Stein, V. Lemos, H. Demagny and MH. Oosterveer for assistance with in vivo and in vitro experiments. Many thanks to E. Can and H.A.I. Yoshihara for hyperpolarized 13C data analysis. Studies in this thesis were supported by École Polytechnique Fédérale de Lausanne funding, the Swiss Cancer League (KFS-2809-08-2011, KFS-3082-02-2013, and KFS-3444-08-2014), and the Swiss National Science Foundation (CRSII3_160798/1).

Gene	Forward primers	Reverse primers
Gls2	GACCGTGGTGAACCTGCTAT	TGCGGGAATCATAGTCCTTC
Got1	GACCATGAGATCCGAACTCA	TGACCAAATACTCGACCTGC
Gpt2	GGACAACGTGTACTCTCCAG	GGTGCAAATTGATCACCTCC
Me1	GATGATAAGGTCTTCCTCACC	TTACTGGTTGACTTTGGTCTGT
c-Myc	TGAGCCCCTAGTGCTGCAT	AGCCCGACTCCGACCTCTT
CyclinD1	CATCCATGCGGAAAATCGT	TCTACGCACTTCTGCTCCTCA
CyclinE1	CTGGCTGAATGTCTATGTCC	TCTTTGCTTGGGCTTTGTCC
Gls1	AGTGACTTGTGAATCAGCCAG	GTTGCCCATCTTATCCAGAGG
Got2	GAAGCAATGGTTGCAAGAGG	GTCATGTAGACCGAGAACTC
Pcx	AGGAAGGGGATGTTGGTCTT	TCGTCAAGGTCATTGCACAC
Cs	ATTCGTGGAAGAAGCACTGG	GCCATGGCTCTACTCACTGC
Aco2	GGTGACCAGGAGGCTGTAAG	CCCAACATACACAGACACAACA
Ogdh	AAGTGGTGGTGGGTAAGTGG	TGATGATGCTCCGGTAACTG
Suclg1	TAAGACCCGTGTCGTATCCC	CAACCATGGTCTCCAGCAG
Suclg2	AGTTGACGATCCCACCAAAG	TGGTGTAAAGGAAGCCCAAG
Pcca	TCCTTGGGCACTTTTTCAAG	AGGTGGAAACATGAGCATCC
Sdha	GGAACACTCCAAAAACAGACCT	CCACCACTGGGTATTGAGTAGAA
Sdhb	GGACCTATGGTGTTGGATGC	GTGTGCACGCCAGAGTATTG
Mdh1	TTCTGGACGGTGTCCTGATG	TTTCACATTGGCTTTCAGTAGGT
Mdh2	TTGGGCAACCCCTTTCACTC	GCCTTTCACATTTGCTCTGGTC
Gck	ACATTGTGCGCCGTGCCTGTGAA	AGCCTGCGCACACTGGCGTGAAA
Chrebp-a	CGACACTCACCCACCTCTTC	TTGTTCAGCCGGATCTTGTC
Chrebp-b	TCTGCAGATCGCGTGGAG	CTTGTCCCGGCATAGCAAC
Gdh1	CTATGGAGCTGGCCAAGAAG	CCTATGGTGCTGGCATAGGT
Plk3	ACCTACAGCACCGCCATATC	CGCAGGTAGTAGCGAACCTC
Cyp2e1	CTTAGGGAA AACCTCCGCAC	GGGACATTCCTGTGTTCCAG
Mgmt	CCTCTGTGGGGTCAGTGTTT	CCTCTGTGGGGTCAGTGTTT
Asns	GAGAAACTCTTCCCAGGCTTTG	CAAGCGTTTCTTGATAGCGTTGT
Atf5	AGAGCCCCTGGCAGGTGA	CAGAGGAAGGAGAGCTGTGAAGT

Promoter	Forward primers	Reverse primers
Gls2-1 and 2	AGAGGCAGGCGGATTTCT	AAGCCAGTGAACTCAAAATCTTC
Gls2-3	TGCCTGTAAGTGTGCACTGG	GTGCTCTGGTGCAGATGAAA
Gls2-4 and 5	TTTCATCTGCACCAGAGCAC	CTGGGACAGTCGGGACAC
Asns-1	AGATGGGTTCACCCTCCAAC	CCACAAGGGATGTACTGCAC
Asns-2	GTGCATGCATGTGTGTGTGT	AGCACTGTGGAGATGGAAGC
Asns-3	TCAACTTGATGGAGACTTTGTGA	TCCCTGCAGAGATTAAAAGCA

Table 1 Primers for qRT-PCR and ChIP-qPCR

Chapter 4 LRH-1 Coordinates Glutamine Metabolism to Promote Liver Cancer

4.1 Hepatic Loss of LRH-1 Prevents DEN-induced Liver Carcinogenesis

To investigate the specific contribution of hepatic LRH-1 on HCC formation, we used the well-established diethylnitrosamine (DEN) method to induce liver cancer[244]. Liver-specific *Lrh-1*-deficient (*Lrh-1*$^{hep-/-}$) and wild-type control (*Lrh-1*$^{hep+/+}$) mice were injected with DEN on postnatal day 14. Tumor burden was assessed 6 (mid-term) or 10 (long-term) months post-injection (Figure 4.1A). While long-term DEN-challenged *Lrh-1*$^{hep+/+}$ littermates developed multiple hepatic tumors, *Lrh-1*$^{hep-/-}$ mice were strikingly protected (Figure 4.1B-C).

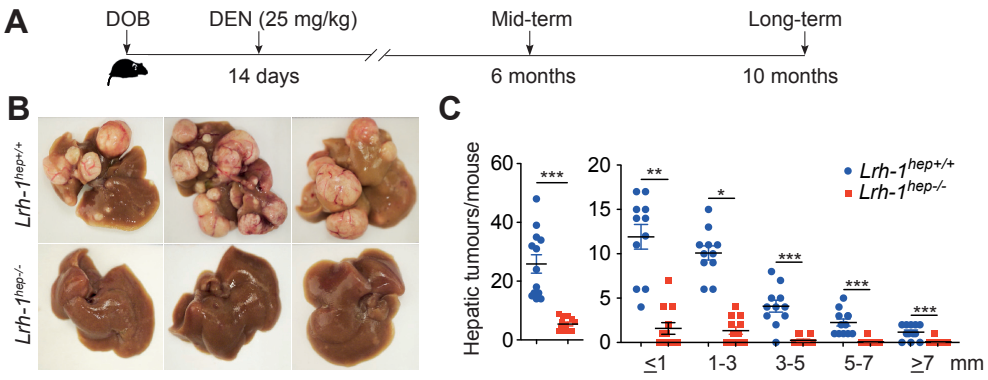

Figure 4. 1 Hepatic Loss of LRH-1 Prevents DEN-induced Liver Carcinogenesis

(A) Experimental strategies of DEN administration. DOB, date of birth. (B) Representative livers of 10 months DEN-treated *Lrh-1*$^{hep+/+}$ and *Lrh-1*$^{hep-/-}$ mice. (C) Hepatic tumor number (left) and tumor size (right) in the corresponding genotypes.

We first checked whether the robust reduction of total tumor number and size was caused by differences in DEN cancerogenicity. Bioactivation of DEN is a complex process that relies on many enzymes (Figure 4.2A). For instance, CYP2E1 catalyzes the initial step in a series of enzymatic reactions generating reactive alkylating agents, triggering DNA alkylation, and ultimately initiating oncogenesis[245]. However, these alkylation adducts are also removed by DNA repair enzymes, such as O^6-methylguanine-DNA methyltransferase (MGMT), which are known to counteract DEN-induced hepatocarcinogenesis[246].

To obtain an unbiased picture on how DEN is metabolized in our liver cancer model, *Lrh-1*$^{hep-/-}$ and control *Lrh-1*$^{hep+/+}$ mice were injected with DEN (25 mg/kg body weight) on postnatal day 14. Livers were col-

lected 6, 24 and 48 h after DEN administration[247], and *Cyp2e1* and *Mgmt* transcripts were both decreased after DEN injection in *Lrh-1*$^{hep-/-}$ livers (Figure 4.2B-C). These results suggest that loss of LRH-1 in hepatocytes may not only dampen the bioactivation of DEN but also blunt DNA repair capacity after DEN-induced DNA damage.

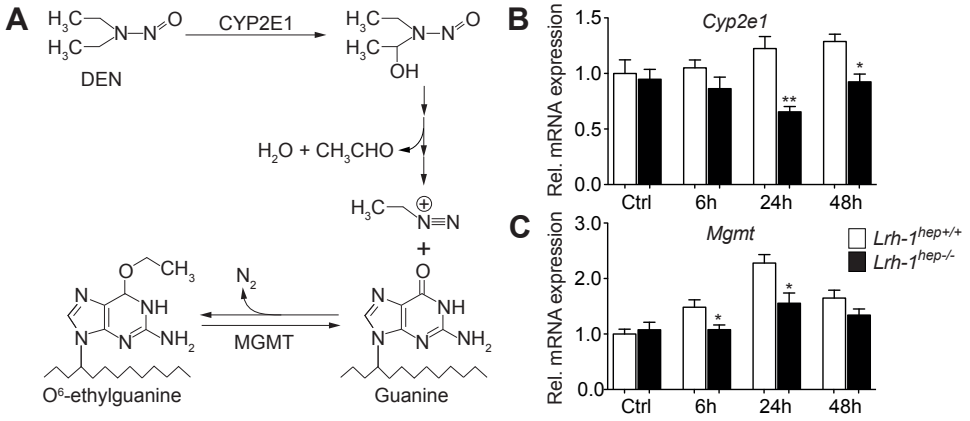

Figure 4. 2 DEN Bioactivation and DNA Repair Capacity in Livers of *Lrh-1*$^{hep+/+}$ and *Lrh-1*$^{hep-/-}$ Mice

(A) Graphical representation illustrating hepatic DEN bioactivation through DNA alkylation to initiate carcinogenesis. (B, C) Hepatic mRNA levels of *Cyp2e1* (B*)*, *Mgmt* (C) in *Lrh-1*$^{hep+/+}$ and *Lrh-1*$^{hep-/-}$ mice 6, 24 and 48 hours after DEN injection on postnatal day 14 (n=5-6 per group and time point).

Importantly, CYP2E1 is tightly regulated by post-translational mechanisms impacting on protein stability[248-250]. To take this additional layer of regulation into account we compared CYP2E1 protein expression in *Lrh-1*$^{hep+/+}$ and *Lrh-1*$^{hep-/-}$ livers and found no significant differences (Figure 4.3A), indicating that CYP2E1 dependent metabolism of DEN is most likely not affected by hepatic loss of LRH-1.

Based on the complexity of DEN bioactivation, we also directly evaluated the levels of DNA alkylation as it represents the most reliable readout for DEN-induced cancerogenicity. To do so, we assessed O^6-ethylguanine DNA adducts[251] in *Lrh-1*$^{hep+/+}$ and *Lrh-1*$^{hep-/-}$ livers. Formation of the DNA adduct O^6-ethylguanine is recognized as the initial step of DEN-induced oncogenesis. DEN triggered a dramatic accumulation of O^6-ethylguanine and the induction of this alkylation product was maintained up to 48 h after DEN exposure (Figure 4.3B-C). However, no significant differences in O^6-ethylguanine contents were observed between *Lrh-1*$^{hep+/+}$ and *Lrh-1*$^{hep-/-}$ livers (Figure 4.3B-C), indicating equal levels of DEN activation between the two genotypes. We further measured the oxidative DNA damage marker 8-hydroxydeoxyguanosine (8-OHdG) in *Lrh-1*$^{hep+/+}$ and *Lrh-1*$^{hep-/-}$ livers. While 8-OHdG formation was found to be significantly increased after DEN exposure, the two genotypes were indistinguishable (Figure 4.3D). Taken together, our results strongly suggest that hepatic LRH-1 does not directly affect the level of DEN-induced DNA damage and that our DEN model is appropriate to study liver carcinogenesis.

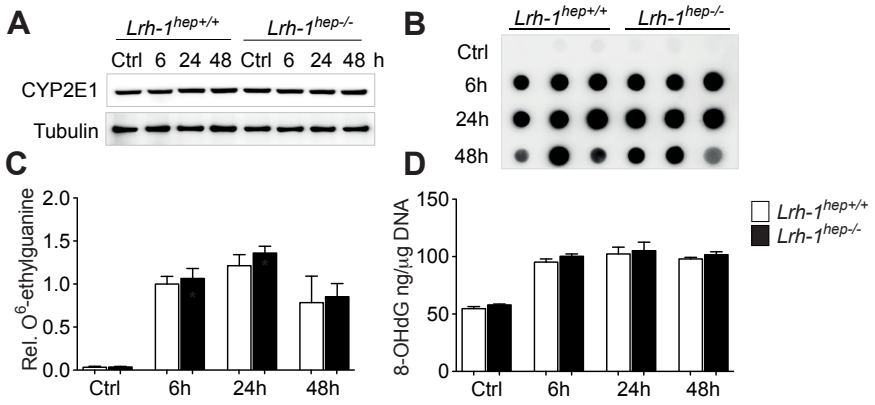

Figure 4. 3 Hepatic Loss of LRH-1 Does not Affect DEN-Induced DNA Damage

(A) Hepatic protein levels of CYP2E1, (B) Hepatic O^6-ethylguanine DNA adducts, (C) Quantification of relative O^6-ethylguanine DNA adduct contents, (D) Hepatic concentration of 8-OHdG 6, 24 and 48 hours after DEN injection to 14-day-old *Lrh-1*$^{hep+/+}$ and *Lrh-1*$^{hep-/-}$ mice (n=5-6 per genotype and time point).

We next asked whether the abundance of LRH-1 or its translocation is induced upon the administration of DEN. To this end, we performed immunoblotting assay to evaluate LRH-1 abundance and translocation in livers from unchallenged, mid-term or long-term DEN-challenged *Lrh-1*$^{hep+/+}$ and *Lrh-1*$^{hep-/-}$ mice. As shown in Figure 4.4, DEN moderately increased LRH-1 protein abundance, but did not affect its nuclear compartmentalization.

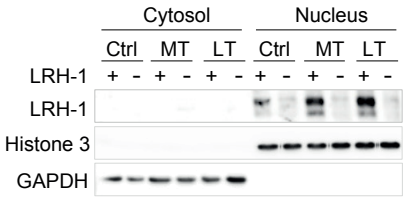

Figure 4. 4 Compartmentalization of LRH-1 protein in response to DEN treatment

Protein levels of LRH-1 in cytosol and nucleus fractions of livers from *Lrh-1*$^{hep+/+}$ and *Lrh-1*$^{hep-/-}$ mice with untreat-ed control (Ctrl), 6 months DEN-treated (MT) and 10 months DEN-treated (LT).

Furthermore, We then performed histological and immunohistochemical analysis on the long-term DEN-treated liver sections. H&E staining of *Lrh-1*$^{hep-/-}$ liver sections demonstrated less microscopic tumor foci while BrdU and Ki67 staining confirmed reduced cell proliferation in *Lrh-1*-deficient livers (Figure 4.5A). Moreover, long-term DEN-treated *Lrh-1*$^{hep-/-}$ livers were significantly lighter compared to *Lrh-1*$^{hep+/+}$ livers, while the body weight did not differ between the two genotypes (Figure 4.5B-D). Together, these results indicate that LRH-1 is required for efficient HCC induction and progression in response to DEN treatment.

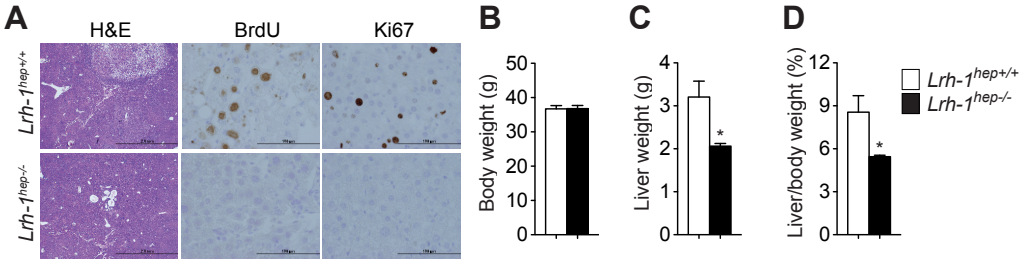

Figure 4. 5 Histology, Body and Liver Weight of DEN-treated *Lrh-1*$^{hep+/+}$ and *Lrh-1*$^{hep-/-}$ Mice

(A) Representative images of H&E, BrdU and Ki67 staining of liver sections of 10 months DEN-treated *Lrh-1*$^{hep+/+}$ and *Lrh-1*$^{hep-/-}$ mice. (B-D) Body weight (B), liver weight (C) and normalized liver weight to body weight (D) of mice described in (A).

4.2 Hepatic Loss of LRH-1 Inhibits Non-canonical Glutamine Processing

LRH-1 coordinates intestinal cell renewal and tumor formation through crosstalk with the β-catenin pathway[216, 217]. It is also required for hepatic endoplasmic reticulum (ER) stress resolution through transcriptional control of *polo-like kinase 3* (*Plk3*) and subsequent phosphorylation of activating transcription factor 2 (ATF2) [252]. To understand the robust tumor suppressive phenotype, we first assessed the β-catenin pathway in mid-term DEN-treated livers, in which tumors were not yet developed (Figure 4.6A). In contrast to the findings in intestinal crypts of germline *Lrh-1*$^{+/-}$ mice[216], β-catenin targets, *c-Myc, Ccnd1 and Ccne1*, were not reduced in the unchallenged (Figure 4.6B) or DEN-challenged (Figure 4.6C) *Lrh-1*$^{hep-/-}$ livers.

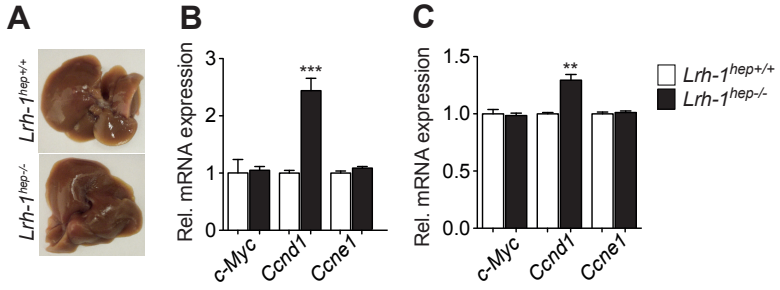

Figure 4. 6 β-catenin Pathway in Mid-term DEN-treated *Lrh-1*$^{hep+/+}$ and *Lrh-1*$^{hep-/-}$ Livers

(A) Representative images of livers from 6 months DEN-treated *Lrh-1*$^{hep+/+}$ and *Lrh-1*$^{hep-/-}$ mice. (B, C) Hepatic mRNA levels of *c-Myc*, *Ccnd1* and *Ccne1* in *Lrh-1*$^{hep+/+}$ and *Lrh-1*$^{hep-/-}$ mice under unchallenged (B) and DEN-challenged (C) conditions.

We also evaluated the Plk3-ATF2 cascade in response to acute DEN exposure. *Plk3* mRNA levels and ATF2 phosphorylation levels were not induced by DEN (Figure 4.7), indicating that in our model LRH-1 impacts on hepatocarcinogenesis via other mechanisms.

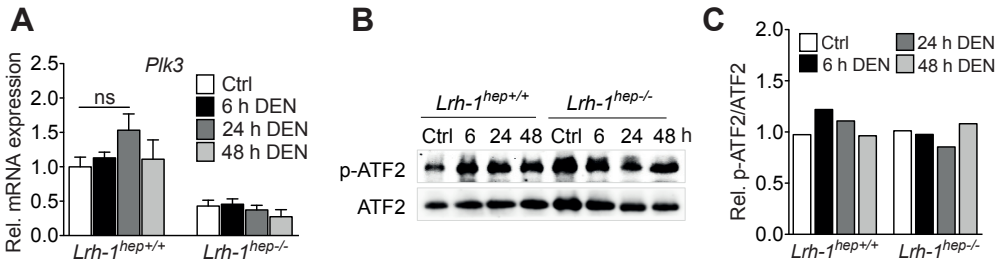

Figure 4. 7 PLK3-ATF2 Cascade upon DEN Administration

(A-C) Relative hepatic mRNA expression of *Plk3* (A), protein levels of p-ATF2 and ATF2 (B), and quantification of relative p-ATF2 to ATF2 ratios (C) in control *Lrh-1*$^{hep+/+}$ and *Lrh-1*$^{hep-/-}$ mice treated with DEN.

We then performed microarray analysis to compare the transcriptomes of mid-term DEN-exposed *Lrh-1*$^{hep+/+}$ and *Lrh-1*$^{hep-/-}$ livers. As expected, gene set enrichment analysis (GSEA) confirmed previously established functions and target pathways of LRH-1, such as synthesis of bile acids (Figure 4.8). Of interest, metabolism of amino acid and derivatives scored amongst the most significantly enriched pathways (Figure 4.8A).

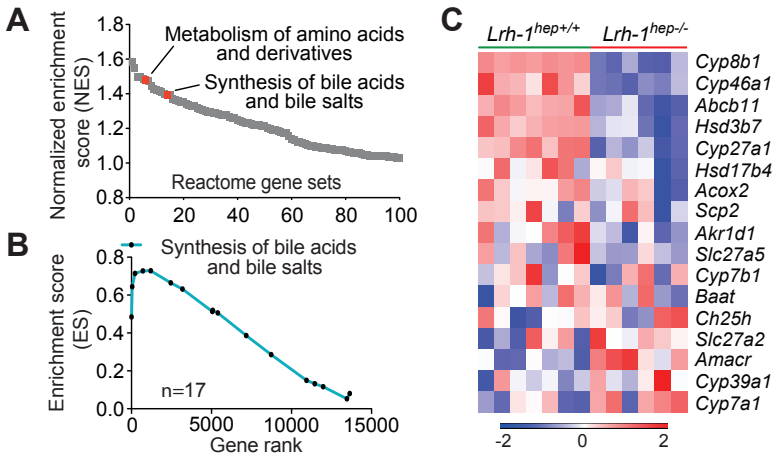

Figure 4. 8 Gene Set Enrichment Analysis (GSEA) Confirmed Established Target Pathways of LRH-1

(A) GSEA demonstrates down-regulated pathways that were ranked by normalized enrichment scores (NES) in livers of 6 months DEN-treated *Lrh-1*$^{hep-/-}$ (n=6) mice compared to *Lrh-1*$^{hep+/+}$ (n=7) mice. Specific pathways are indicated. (B-C) GSEA enrichment profile (B) and heatmap displaying core enriched genes (C) of bile acid and bile salt synthesis in livers of mice described in (A).

We next analyzed this gene set in more detail. While transcripts of several proteasomal subunits were down-regulated in *Lrh-1*$^{hep-/-}$ livers, a more striking reduction of several enzymes involved in glutamine catabolism was observed (Figure 4.9A).

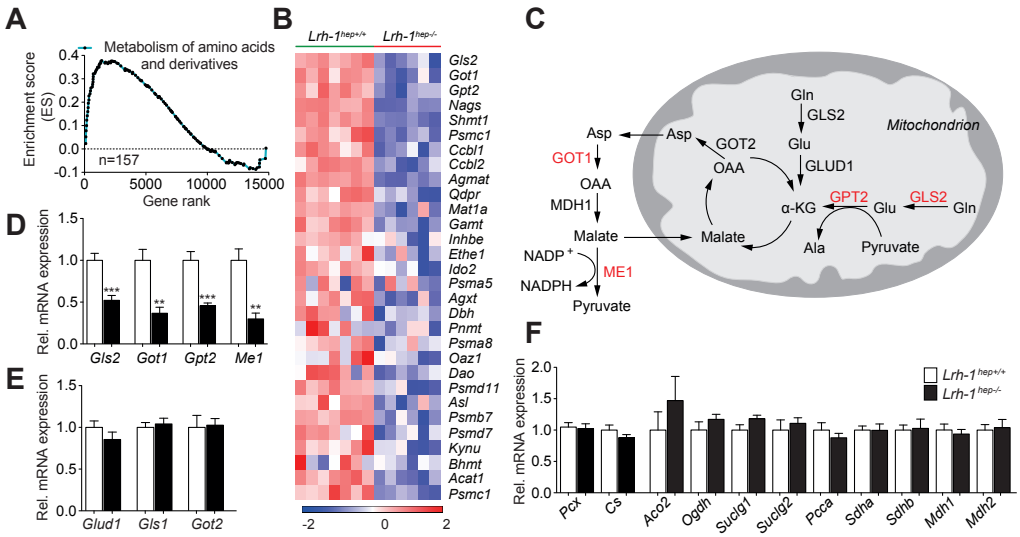

Figure 4. 9 Glutamine Processing Pathway Between DEN-treated *Lrh-1*$^{hep+/+}$ and *Lrh-1*$^{hep-/-}$ Livers

(A) Gene Set Enrichment Analysis (GSEA) demonstrates down-regulated pathways that were ranked by normalized enrichment scores (NES) in livers of 6 months DEN-treated *Lrh-1*$^{hep-/-}$ (n=6) mice compared to *Lrh-1*$^{hep+/+}$ (n=7) mice. Specific pathways are indicated. (B) Heatmap displaying core enriched genes of amino acids and derivatives metabolism pathway that positively correlate with LRH-1 in livers of mice described in A. (C) Graphical representation of enzymes involved in glutamine breakdown and metabolism. Enzymes highlighted in red are reduced in *Lrh-1*$^{hep-/-}$ livers as shown in panel (D). (D) Hepatic mRNA levels of *Gls2*, *Got1, Gpt2* and *Me1* in livers of mice as described in (A). (E-F) Hepatic mRNA levels of *Glud1*, *Gls1* and *Got2* (E), TCA cycle related genes (F) in 6 months DEN-treated *Lrh-1*$^{hep-/-}$ (n=6) and *Lrh-1*$^{hep+/+}$ (n=7) mice. *Glud1, glutamate dehydrogenase 1; Gls1, glutaminase 1; Got2, glutamate oxaloacetate transaminase 2; Pcx, pyruvate carboxylase; Cs, citrate synthase; Aco2, aconitase 2, mitochondrial; Ogdh, alpha-ketoglutarate dehydrogenase; Suclg1, succinate-CoA ligase, alpha subunit; Suclg2, succinate-Coenzyme A ligase, beta subunit; Pcca, propionyl-Coenzyme A carboxylase, alpha polypeptide; Sdha, succinate dehydrogenase complex, subunit A; Sdhb, succinate dehydrogenase complex, subunit B; Mdh1, malate dehydrogenase 2, cytosol; Mdh2, malate dehydrogenase 2, mitochondrial.* Data are represented as mean ± S.E.M. **P* < 0.05; ***P* < 0.01; ****P* < 0.001 by two-tailed Student's *t*-test.

Glutamine plays an essential role in tumor growth to support anaplerosis and reductive biosynthesis [37]. Several genes involved in the processing of glutamine were reduced in mid-term DEN-exposed *Lrh-1*$^{hep-/-}$ livers, including mitochondrial *glutaminase 2* (*Gls2)*), cytosolic *glutamate oxaloacetate transaminase 1* (*Got1*) and mitochondrial *glutamate pyruvate transaminase 2* (*Gpt2*) (Figure 4.9B-C). This pathway is reminiscent to a non-canonical pathway of glutamine breakdown that was earlier reported in human glioma[83], and in pancreatic ductal adenocarcinoma (PDAC) cells as an alternative mechanism to support NADPH production via malic enzyme[85]. Not only these genes, but also *malic enzyme 1* (*Me1*), were significantly blunted, as confirmed by Q-RT-PCR (Figure 4.9D).

Many cancer cells typically rely on GLUD1 to fuel the TCA cycle through repleting α-KG[37]. Transcript levels of *Glud1*, however, remain unchanged upon hepatic loss-of-function (LOF) of LRH-1 (Figure 4.9E). Moreover, mRNA expression of *glutaminase 1 (Gls1)*, *glutamate oxaloacetate transaminase 2 (Got2)* and TCA cycle related genes were not altered between the two genotypes (Figure 4.9E-F). Collectively, these

data indicate that an alternative pathway involved in hepatic glutamine processing is most likely compromised in *Lrh-1*$^{hep-/-}$ mice.

4.3 LRH-1 Regulates Reductive Biosynthesis Fueled By Glutamine Processing

We previously showed that LRH-1 coordinates glucose intermediary metabolism via glucokinase (GCK) activation and subsequent ChREBP nuclear translocation[208]. Consistent with this study, the ChREBP pathway was significantly enriched between both genotypes (Figure 4.10A).

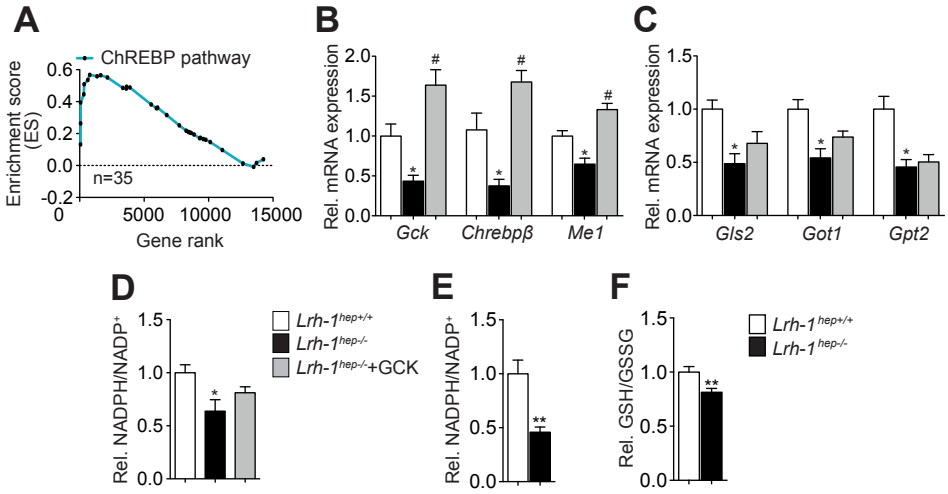

Figure 4. 10 NADPH Production in *Lrh-1*$^{hep+/+}$ and *Lrh-1*$^{hep-/-}$ Livers

(A) GSEA enrichment profile of the ChREBP pathway in 6 months DEN-treated *Lrh-1*$^{hep+/+}$ (n=7) and *Lrh-1*$^{hep-/-}$ (n=6) livers. (B-D) Hepatic mRNA levels of *Gck*, *Chrebpβ* and *Me1* (B), *Gls2*, *Got1* and *Gpt2* (C), Relative NADPH/NADP$^+$ levels (D) in control virus infected *Lrh-1*$^{hep+/+}$ and *Lrh-1*$^{hep-/-}$ mice, and AAV8-GCK virus infected *Lrh-1*$^{hep-/-}$ mice (n=4-5 per group). Data are represented as mean ± S.E.M. **P < 0.05* versus *Lrh-1*$^{hep+/+}$; #*P < 0.05* versus *Lrh-1*$^{hep-/-}$ by one-way ANOVA and Tukey's *post hoc* test. (E) Relative NADPH/NADP$^+$, (F) GSH/GSSG levels in livers of mice described in (A). Data represent mean ± S.E.M. ***P* < 0.01; ****P* < 0.001 by two-tailed Student's *t*-test.

Because *Me1* is a known ChREBP target gene[253, 254], we first analyzed if the reduction of our candidate genes (Figure 4.9D) results from impaired GCK-ChREBP signaling. GCK reconstitution in *Lrh-1*$^{hep-/-}$ livers restored *Chrebpβ* and *Me1* (Figure 4.10B), but not *Gls2*, *Got1 or Gpt2* expression (Figure 4.10C), indicating that LRH-1 regulates only *Me1* via the GCK-ChREBP axis.

In parallel to the reduced *Me1* expression, NADPH/NADP$^+$ levels were significantly reduced in unchallenged (Figure 4.10D) or DEN-challenged (Figure 4.10E) *Lrh-1*$^{hep-/-}$ livers, and was accompanied by a corresponding reduction of the GSH/GSSG ratio in DEN-treated livers (Figure 4.10F). Although *Me1* was readily rescued upon GCK reconstitution (Figure 4.10B), normalization of NADPH/NADP$^+$ levels was still incomplete (Figure 4.10D), supporting the notion that the generation of NADPH from glutamine is also attenuated in *Lrh-1*$^{hep-/-}$ livers.

We next investigated the molecular mechanism through which LRH-1 regulates glutamine metabolism. Overexpression of LRH-1 in mouse hepatoma Hepa 1.6 cells resulted in an increase of GLS2 transcripts and protein, while *Got1* and *Gpt2* transcripts were unchanged (Figure 4.11A-B). Conversely, siRNA-mediated silencing of LRH-1 exclusively reduced the expression of GLS2 mRNA and protein (Figure 4.11C-D). Also in *Lrh-1*$^{hep-/-}$ mice, reduced hepatic *Gls2* mRNA expression (Figure 4.9D) translated into lower GLS2 protein levels (Figure 4.11E).

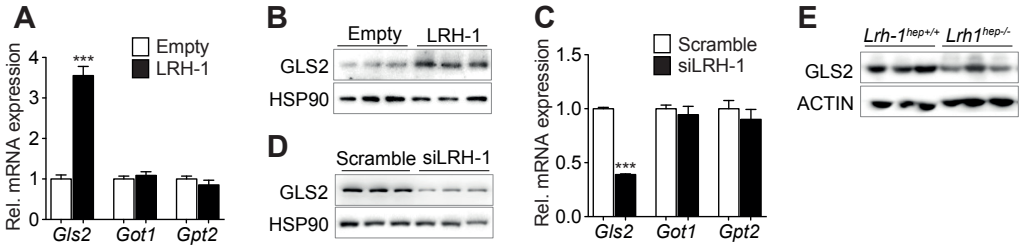

Figure 4. 11 LRH-1 Directly Activates GLS2 Expression

(A-B) mRNA levels of *Gls2*, *Got1* and *Gpt2* (A), and protein levels of GLS2 (B) in Hepa 1.6 cells transfected with control or *Lrh-1* expression plasmids (n=3 per group). (C-D) mRNA levels of *Gls2*, *Got1* and *Gpt2* (C), and protein levels of GLS2 (D) in Hepa 1.6 cells transfected with with scrambled or *Lrh-1*-targeted siRNAs (n=3 per group). Data represent mean ± S.E.M. ***P* < 0.01; ****P* < 0.001 by two-tailed Student's *t*-test. (E) Hepatic protein levels of GLS2 in livers of 6 months DEN-treated *Lrh-1*$^{hep+/+}$ (n=7) and *Lrh-1*$^{hep-/-}$ (n=6) mice.

Of interest, *Gls2* is highly expressed in liver compared to *Gls1* (Figure 4.12A). GLS2 deaminates mitochondrial glutamine, thus controlling a major anaplerotic step for hepatic glutamine utilization [86]. We then asked whether *Gls2* is subjected to direct transcriptional regulation by LRH-1. Analysis of a genome-wide hepatic LRH-1 chromatin immunoprecipitation (ChIP)-seq dataset[255] revealed LRH-1 recruitment at the *Gls2* promoter (Figure 4.12B), and computational analysis identified five putative LRH-1 response elements within the *Gls2* promoter under the LRH-1 ChIP-seq peak (Figure 4.12C). Site-specific ChIP assays using DNA from mid-term DEN-treated *Lrh-1*$^{hep+/+}$ and *Lrh-1*$^{hep-/-}$ livers revealed LRH-1 recruitment to putative binding sites 1, 2 and 3 (Figure 4.12D). Mutation of these binding sites in mouse *Gls2*-luciferase reporter constructs further mapped site 3, which is conserved in the human *Gls2* promoter (Figure 4.12F), as the major site that confers LRH-1 responsiveness (Figure 4.12E). Accordingly, silencing of LRH-1 in human hepatoma HepG2 cells also led to a significant reduction of *Gls2* transcripts (Figure 4.12G).

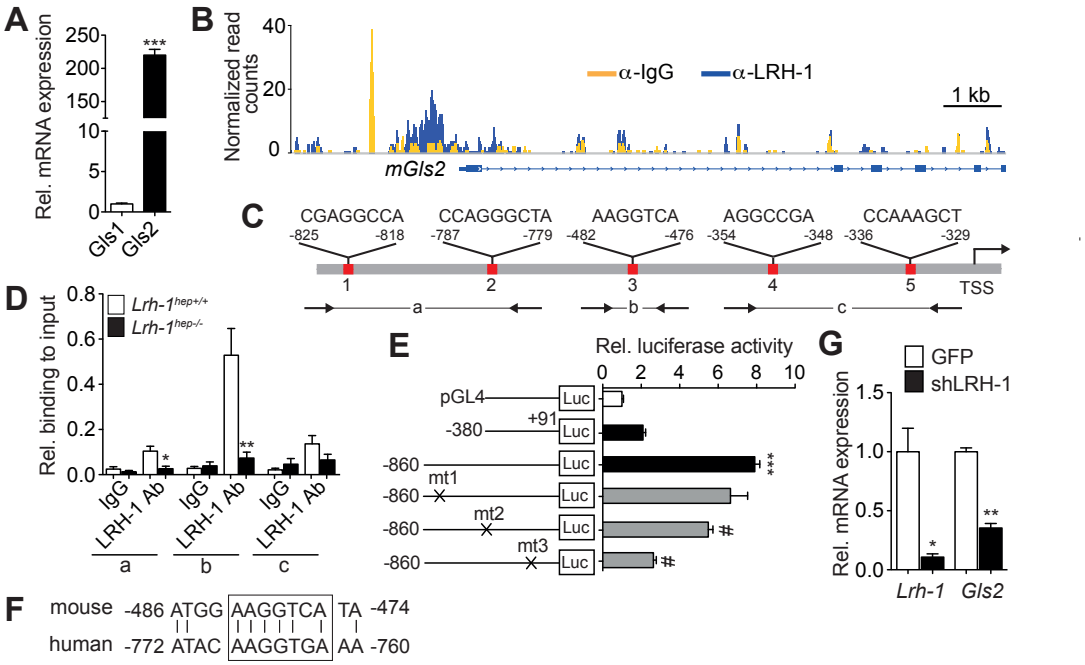

Figure 4. 12 *Gls2* Is A Direct Transcriptional Target of LRH-1

(A) Hepatic mRNA levels of *Gls1* and *Gls2* in basal *Lrh-1*$^{hep+/+}$ mice. (B) UCSC genome browser (mm9) view displaying the occupancy of mouse *Gls2* by IgG and LRH-1^{255}. (C) Schematic representation of the 5 putative LRH-1 response elements in the proximal mouse *Gls2* promoter. (D) ChIP-qPCR assay evaluating the relative LRH-1 binding to the mouse *Gls2* promoter. Amplified regions (a, b and c) are depicted in (C). (E) Luciferase activities in HEK-293A cells after co-transfection of a *Lrh-1* expression vector or with empty luciferase reporter (pGL4), long or short *Gls2* promoter constructs with or without the indicated mutations. Data represent mean ± S.E.M. ***$P < 0.001$ versus empty reporter (pGL4); #$P < 0.05$ versus long *Gls2* promoter construct by one-way ANOVA and Tukey's *post hoc* test. (F) *Gls2* promoter alignment between mouse and human species. (G) mRNA levels of *Lrh-1* and *Gls2* in HepG2 cells infected with either GFP or LRH-1 targeting lentiviruses (n=3 per group). Data are represented as mean ± S.E.M. *$P < 0.05$; **$P < 0.01$ by two-tailed Student's *t*-test.

4.4 LRH-1 Regulates GLS2 to Promote Glutamine-induced Anaplerosis

Given the marked reduction of GLS2 in *Lrh-1*$^{hep-/-}$ mice, we hypothesized that hepatic loss of LRH-1 blunts the conversion of glutamine to glutamate. To test the flux through GLS2 *in vivo*, we performed ^{13}C magnetic resonance spectroscopy measurements following hyperpolarized [5-^{13}C]glutamine injection[256, 257]. [5-^{13}C]glutamine was hyperpolarized using dissolution dynamic nuclear polarization (DNP) and rapidly injected into DEN-treated *Lrh-1*$^{hep-/-}$ and *Lrh-1*$^{hep+/+}$ mice, followed by real time recording of its conversion to [5-^{13}C]glutamate (Figure 4.13A-B). As expected, *Lrh-1*$^{hep-/-}$ showed a strong decrease in hepatic [5-^{13}C]glutamate content compared to *Lrh-1*$^{hep+/+}$ mice (Figure 4.13C). Unlike the expression levels of glutamine transporters *Slc1a5* and *Slc7a5*, which were unchanged (Figure 4.13D), hepatic α-KG levels were diminished in *Lrh-1*$^{hep-/-}$ mice (Figure 4.13E), indicating that LRH-1 LOF may attenuate glutamine-fueled anaplerosis.

To further explore the direct roles of LRH-1 and GLS2 in maintaining glutaminolysis and intracellular α-KG pools, we examined the effect of glutamine metabolism on α-KG levels. Hepa 1.6 cells were starved of glutamine for 6 hours, and removal of glutamine significantly reduced the intracellular levels of α-KG (Figure 4.13F), demonstrating that glutamine sustains glutaminolysis. We then acutely modulated LRH-1 or GLS2 expression in Hepa 1.6 cells. In line with the reduced α-KG abundance in *Lrh-1*$^{hep-/-}$ livers, overexpression of LRH-1 or GLS2 increased, while siRNA-mediated silencing of LRH-1 or GLS2 decreased α-KG levels in Hepa 1.6 cells (Figure 4.13G-J). Together, these results demonstrate that LRH-1 promotes glutamine-induced anaplerosis via the induction of GLS2.

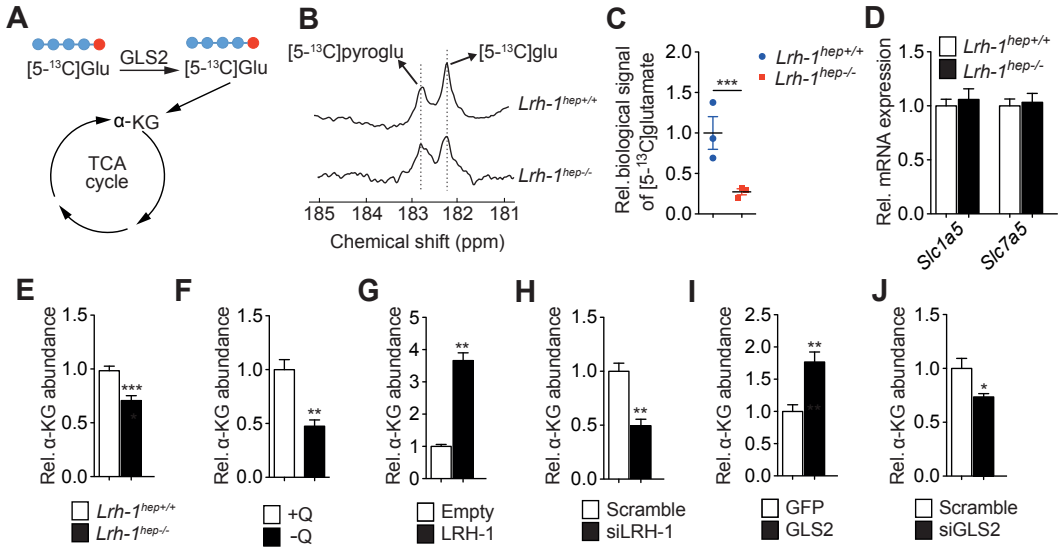

Figure 4. 13 LRH-1 Controls Glutamine-induced Anaplerosis and Sustains α-KG Availability

(A) GLS2 mediated biochemical reaction with hyperpolarized [5-^{13}C]glutamine. Red dots indicate the labeling of C5. (B-C) Representative *in vivo* ^{13}C-NMR spectra showing hyperpolarized [5-^{13}C]glutamate production with the by-product signal of hyperpolarized [5-^{13}C]pyroglutamate (B), The mean signal intensity of the hyperpolarized [5-^{13}C]glutamate formed via glutaminase (C) in the livers of DEN-treated *Lrh-1*$^{hep+/+}$ and *Lrh-1*$^{hep-/-}$ mice. (D) Hepatic mRNA levels of *Slc1a5* and *Slc7a5* in the livers of DEN-treated *Lrh-1*$^{hep+/+}$ and *Lrh-1*$^{hep-/-}$ mice. (E-J) Intracellular α-KG levels in the livers of 6 months DEN-treated *Lrh-1*$^{hep+/+}$ and *Lrh-1*$^{hep-/-}$ mice (E), Hepa 1.6 cells cultured with or without glutamine for 6 hr (F), Hepa 1.6 cells transfected with either control or *Lrh-1* expression plasmids (n=3 per group) (G), transfected with either scrambled or *Lrh-1*-targeted siRNAs (n=3 per group) (H), transduced with either AdGFP or AdGLS2 viruses (n=3 per group) (I), or transfected with scrambled or *Gls2*-targeted siRNAs (n=3 per group) (J). Data represent mean ± S.E.M. **P* < 0.05, ***P* < 0.01, ****P* < 0.001 by two-tailed Student's *t*-test. Data in Figure A-C were obtained through collaborations with Prof. Arnaud Comment's lab.

4.5 LRH-1 Modulates mTORC1 Pathway in a α-KG-dependent Manner

Glutamine is metabolized through glutaminolysis to produce α-KG. Previous studies showed that increased glutamine[135, 258] or α-KG availability[135] stimulates the mTORC1 signaling pathway. Of note, a robust reduction of mTORC1 activation was observed in *Lrh-1*$^{hep-/-}$ livers, as evidenced by the decreased phosphorylation of 4EBP1 and S6K (Figure 4.14A).

We then investigated the importance of glutamine in the activation of mTORC1 in Hepa1.6 cells. Depletion of glutamine for 6 hours reduced α-KG levels (Figure 4.13F) and inhibited mTORC1 activity (Figure 4.14B). Moreover, supplementation of a cell-permeable α-KG analogue dimethyl-KG (DM-KG) restored the activation of mTORC1 signaling upon glutamine deprivation (Figure 4.14C), indicating that intracellular glutamine and its derived α-KG are essential to stimulate mTORC1.

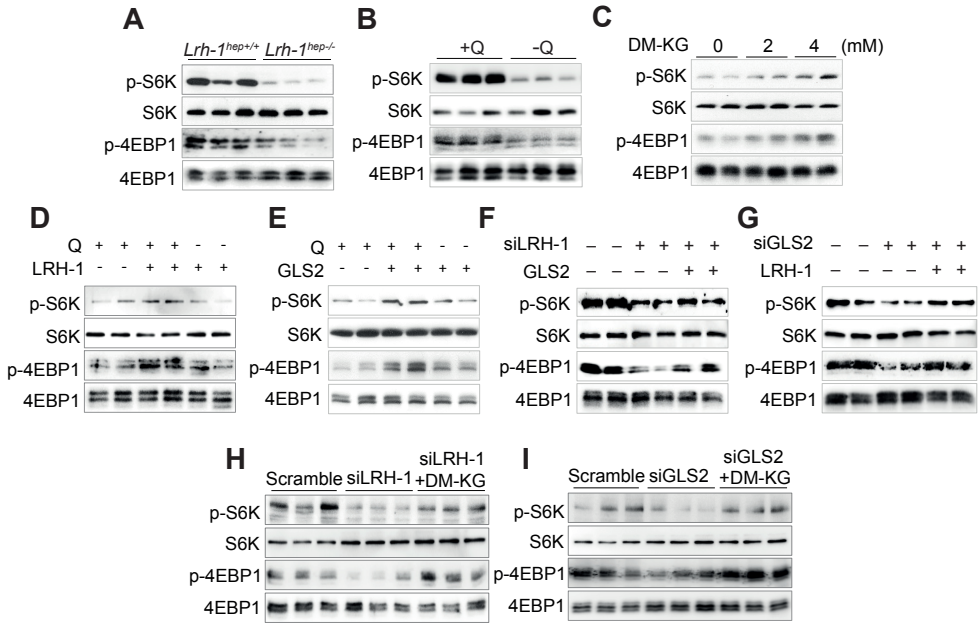

Figure 4. 14 LRH-1-GLS2 Axis Modulates mTORC1 Pathway in a α-KG-dependent Manner

(A) Phosphorylation levels of S6K and 4EBP1 in livers of 6 months DEN-treated *Lrh-1*$^{hep+/+}$ and *Lrh-1*$^{hep-/-}$ mice. (B-K) Phosphorylation levels of S6K and 4EBP1 in Hepa 1.6 cells cultured with or without glutamine for 6 hr (B), with DM-KG supplementation at different concentrations (C), transfected with either control or *Lrh-1* expression plasmids (n=3 per group) cultured with or without glutamine for 6 hr (D), transduced with either AdGFP or AdGLS2 viruses (n=3 per group) cultured with or without glutamine for 6 hr (E), transfected with either scrambled or *Lrh-1*-targeted siRNAs (n=3 per group) with or without GLS2 overexpression (F), transfected with scrambled or *Gls2*-targeted siRNAs (n=3 per group) with or without LRH-1 overexpression (G), transfected with either scrambled or *Lrh-1*-targeted siRNAs (n=3 per group) with or without DM-KG supplementation (H), transfected with scrambled or *Gls2*-targeted siRNAs (n=3 per group) with or without DM-KG supplementation (I).

Based on these results, we overexpressed LRH-1 or GLS2 in Hepa 1.6 cells. In both settings, mTORC1 activity was induced in the presence of glutamine (Figure 4.14D-E). These effects were reversed upon glutamine starvation (Figure 4.14D-E). Furthermore, RNAi-mediated suppression of LRH-1 or GLS2 interfered with phosphorylation of 4EBP-1 and S6K in the presence of glutamine, while overexpression of GLS2 or LRH-1 (Figure 4.14F-G), addition of DM-KG (Figure 4.14H-I), respectively, rescued mTORC1 activities. These data hence suggest that the LRH-1-GLS2 axis increases α-KG levels and consequently activates mTORC1.

4.6 The LRH-1-GLS2 Axis Promotes Cell Proliferation

Activation of mTORC1 inhibits autophagy[259], activates protein translation[260] and promotes cell growth[261]. To investigate the importance of the LRH-1-GLS2-mTORC1 pathway, we first assessed autophagy in mid-term DEN-treated livers. As expected, disruption of LRH-1 induced autophagy, as evidenced by reduced phosphorylation of ULK-1 at ser[757], blunted P62 and increased LC3-II levels (Figure 4.15A). Silencing of LRH-1 or GLS2 decreased global protein translation as measured by incorporation of ^{35}S-labeled methionine in Hepa 1.6 cells (Figure 4.15B-C), while their overexpression enhanced translation (Figure 4.15D-E).

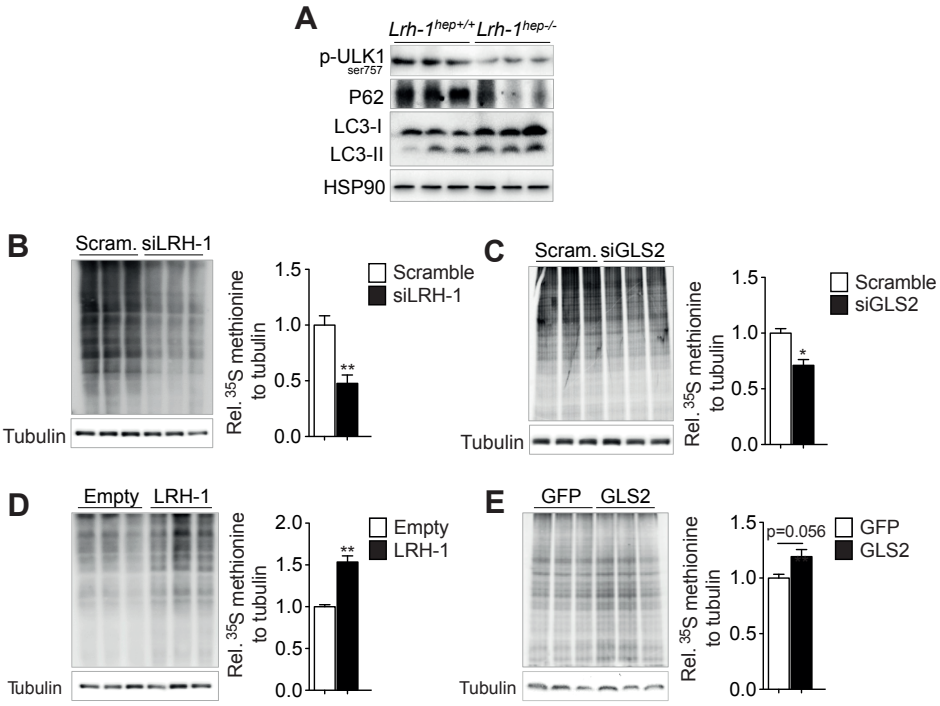

Figure 4. 15 The LRH-1-GLS2 Axis Inhibits Autophagy and Promotes Protein Translation

(A) Immunoblots of phosphorylated ULK-1 at Ser[757], P62, LC3-I, LC3-II and HSP90 in whole lysate from 6 months DEN-treated *Lrh-1*$^{hep+/+}$ and *Lrh-1*$^{hep-/-}$ livers. (B-E) Global protein synthesis measured by ^{35}S-labelled methionine incorporation in Hepa1.6 cells transfected with either scrambled or *Lrh-1*-targeted siRNAs (n=3 per group) (B), scrambled or *Gls2*-targeted siRNAs (n=3 per group) (C), transfected with either control or wildtype *Lrh-1* plasmids (n=3 per group) (D), infected with either AdGFP or AdGLS2 viruses (n=3 per group) (E). Relative ^{35}S-labelled methionine signals were normalized to Tubulin. Data are represented as mean ± S.E.M. ***P* < 0.01 by two-tailed Student's *t*-test.

We then evaluated the link between LRH-1-GLS2 axis, α-KG and cell proliferation. As expected, LRH-1 or GLS2 overexpression promoted cell proliferation, while additional glutamine deprivation prevented the increase in cell proliferation (Figure 4.16A-B). Conversely, inhibition of glutaminolysis by LRH-1 or GLS2 silencing inhibited cell proliferation, while addition of DM-KG rescued this effect (Figure 4.16C-D).

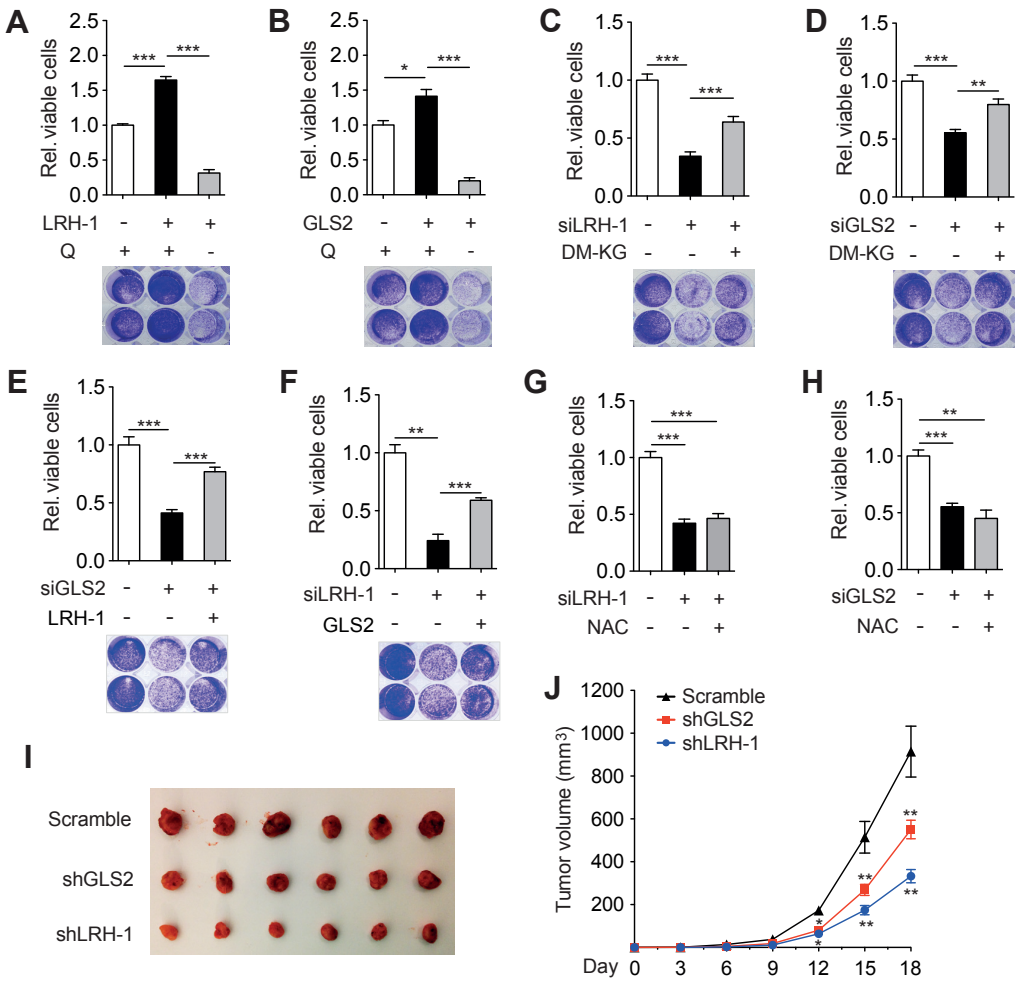

Figure 4. 16 The LRH-1-GLS2 Axis Promotes Cell Proliferation and Tumor Growth

(A-F) Relative viable cells and representative crystal violet staining images of Hepa 1.6 cells transfected with either control or *Lrh-1* expression plasmids (n=3 per group) (A), transduced either with AdGFP or AdGLS2 viruses (n=3 per group) (B) with or without glutamine deprivation, scrambled or *Lrh-1*-targeted siRNAs (n=3 per group) (C), scrambled or *Gls2*-targeted siRNAs (n=3 per group) (D) with or without DM-KG supplementation, scrambled or *Gls2*-targeted siRNAs (n=3 per group) (E), scrambled or *Lrh-1*-targeted siRNAs (n=3 per group) (F) with or without overexpression of LRH-1 or GLS2. (G-H) Relative viable cells of Hepa1.6 cells transfected with scrambled or *Lrh-1*-targeted siRNAs (n=3 per group) (G), scrambled or *Gls2*-targeted siRNAs (n=3 per group) (H) with or without NAC supplementation. NAC, N-acetyl-cysteine. Data represent mean ± S.E.M. **P* < 0.05; ****P* < 0.001 by one-way ANOVA and Tukey's *post hoc* test. (I-J) Comparison of tumor volume (I) and growth (J) of mice subcutaneously injected with Hepa 1.6 cells that were transduced with scrambled, LRH-1-, or GLS2-targeted shRNA (n = 6 per group). Data are represented as mean ± S.E.M. ***P* < 0.01 by two-tailed Student's *t*-test.

In addition, diminished cell proliferation upon LRH-1 or GLS2 suppression could also be rescued by over-expressing of LRH-1 or GLS2 (Figure 4.16E-F). Collectively, these results indicate that the LRH-1-GLS2 axis activates cell proliferation in a α-KG-dependent manner. It has been shown that GLS2-catalyzed deamination of glutamine is also essential for the control of intracellular ROS levels[262]. Supplementation with the antioxidant N-acetyl-cysteine (NAC), however, could not rescue the inhibited cell proliferation upon LRH-1 or GLS2 silencing in Hepa 1.6 cells (Figure 4.16G-H), suggesting that reduced mTORC1 signaling, rather than

induced oxidative stress, accounts for the reduction in cell proliferation. Furthermore, Hepa 1.6 cells silenced for LRH-1 or GLS2 induced significantly less tumor growth after propagation in athymic nude mice (Figure 4.16I-J). Taken together, these findings highlight that LRH-1 promotes cell proliferation through glutaminolysis and mTORC1 signaling.

4.7 Discussion and Future Studies

Glutamine is an abundant and versatile nutrient required for the survival and growth of a large subset of tumors [37, 38]. Glutamine metabolism not only replenishes TCA cycle intermediates via conversion to α-KG, but also contributes to the production of the biological reductant NADPH that is required for macromolecular biosynthesis and defense against oxidative stress[37, 83, 85, 262]. Glutaminases favor the conversion of glutamine to glutamate, representing gatekeepers of glutamine processing to maintain TCA cycle and anabolic outcomes[86]. Two distinct glutaminase genes have been identified in mammals, GLS1 and GLS2[263]. While GLS1 is considered as a cancer therapeutic target, the biological role of GLS2 in cancer remains largely unexplored, especially in hepatocytes, where GLS2 is considered as the predominant glutaminase[263]. In the study of this chapter, we observed a profound and consistent reduction of hepatic GLS2 upon chronic and acute deletion of LRH-1. Consistent with the low abundance of GLS1 in hepatocytes and the absence of any significant difference in *Gls1* transcripts, non-invasive *in vivo* hyperpolarized MR spectroscopy confirmed that the glutamine flux through GLS2 is significantly blunted in DEN-challenged *Lrh-1*-deficient livers. By means of ChIP analysis and site-directed mutagenesis, we have firmly established that LRH-1 directly controls *Gls2* transcription. Furthermore, our findings revealed that LRH-1 more largely coordinates an alternative route of glutamine processing, which fuels glutamine-dependent anaplerosis and NADPH production. This pathway is reminiscent to a non-canonical pathway of glutamine breakdown that was earlier reported in human glioma[83] and pancreatic ductal adenocarcinoma (PDAC) cells[85]. Consistent with these studies emphasizing the role of transaminases rather than GLUD1 in glutamine processing, our findings revealed that LRH-1 LOF significantly reduced the expression of mitochondrial *Gpt2* and cytosolic *Got1*, while no changes could be observed in mitochondrial *Glud1*, which in hepatocytes encodes for the predominant enzyme that converts glutamate into α-KG. Of interest, recent studies identified the cytosolic transaminase GOT1 as a crucial factor to sustain proliferation in cells with mitochondrial electron transport chain (ETC) defects[264]. In this particular context of electron acceptor deficiency, exogenous aspartate or GOT1-mediated aspartate biosynthesis could restore proliferation of ETC defective cells[264, 265]. Although transcript levels of *Got1* were markedly reduced in *Lrh-1*-deficient livers, our data based on genome-wide promoter recruitment analysis in *Lrh-1*$^{hep-/-}$ and *Lrh-1*$^{hep+/+}$ livers and LRH-1 LOF and GOF studies in hepatoma cell lines indicate that *Got1* is rather an indirect target of LRH-1.

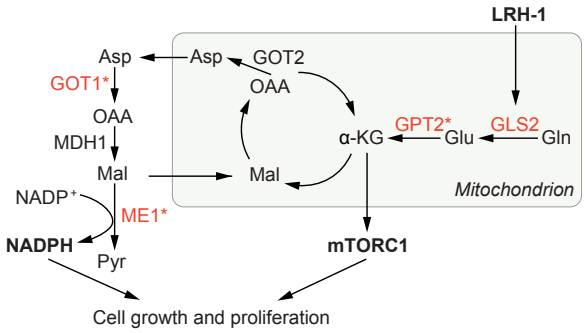

Figure 4. 17 Glutamine Processing Pathway Regulated by LRH-1

Graphical summary illustrating how LRH-1 promotes glutamine-induced anaplerosis and reductive biosynthesis in hepatic cancer cells. Enzymes highlighted in red are reduced in *Lrh-1*$^{hep-/-}$ livers, * indicates indirect regulation by LRH-1.

One of the most striking findings in this study is the observation that mice lacking LRH-1 in hepatocytes are robustly protected against hepatocarcinogenesis upon DEN induction. Unlike the role of LRH-1 in the intestine and pancreas, the oncogenic potential of hepatic LRH-1 is independent from the β-catenin/Wnt-signaling pathway. Instead, our data are in support of a role of LRH-1 in glutamine-dependent anaplerosis and NADPH production, two biochemical processes that are required for uncontrolled proliferation of cancer cells (Figure 4.17). Moreover, the enhanced mTORC1 signaling upon LRH-1-induced glutaminolysis indicates that the effect of LRH-1 on glutamine processing also impinges on established kinases in cell growth and cancer, thereby further amplifying the overall growth stimulating effect (Figure 4.17). These observations together with our previous findings linking LRH-1 to glucose-dependent fatty acid biosynthesis via ChREBP activation[208] support the notion that LRH-1 confers a pro-tumorigenic status to hepatocytes by promoting the metabolism of the two principal fuel substrates of cancer cells, glucose and glutamine. The stimulatory effect of LRH-1 on both glucose and glutamine metabolism is significantly attenuated in the livers of *Lrh-1*$^{hep-/-}$ mice, and may hence provide an explanation for the pronounced protection against tumorigenesis in DEN challenged *Lrh-1*$^{hep-/-}$ liver.

Chapter 5 LRH-1 Coordinates Asparagine Metabolism to Promote Liver Cancer

5.1 *Lrh-1 K289R* Promotes DEN-induced Liver Carcinogenesis

Those abovementioned data from Chapter 4 of the LRH-1 LOF mouse model support a pro-tumorigenic role for LRH-1 in promoting liver cancer development. Furthermore, it is known that LRH-1 can be targeted for SUMOylation by E3-SUMO ligases at several lysine residues, and this conserved reversible posttranslational modification affects its transcriptional activity[177, 179, 180, 266, 267]. Previously, our lab has generated a *Lrh-1 K289R* mouse model, in which substitution of lysine 289 by arginine (K289R) prevents SUMO modification of LRH-1 and leads to increased LRH-1 transcriptional activity. We then hypothesized that gain-of-function (GOF) of LRH-1 in whole body *Lrh-1 K289R* knock-in mice would enhance HCC formation in contrast to LRH-1 LOF.

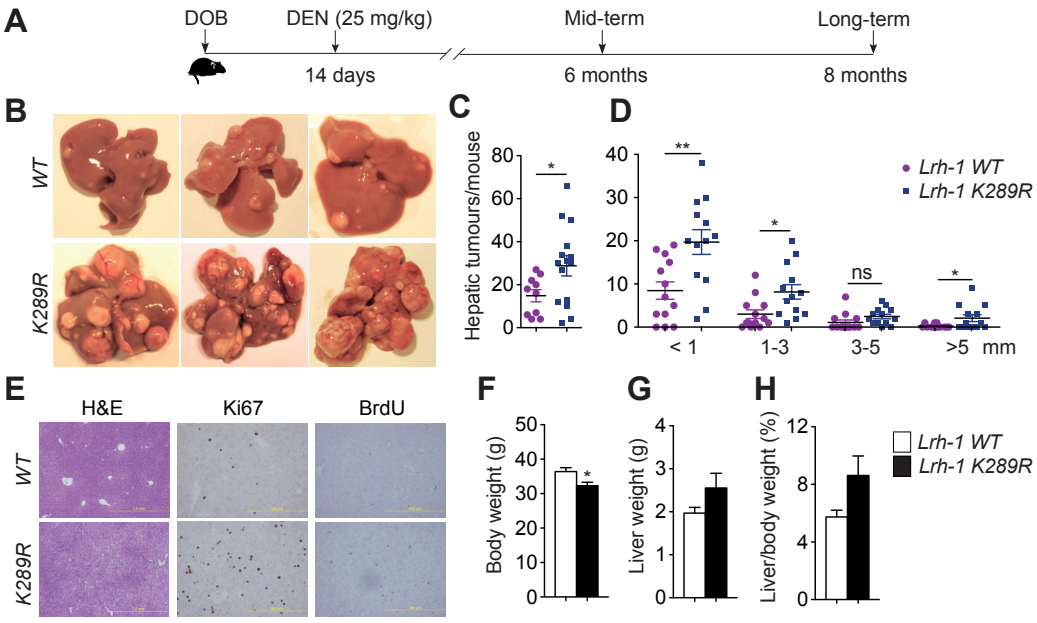

Figure 5. 1 *Lrh-1 K289R* Promotes DEN-induced Liver Cancer

(A) Experimental strategies of DEN administration. DOB, date of birth. (B) Representative livers of 8 months DEN-treated *Lrh-1 WT* and *Lrh-1 K289R* mice. (C, D) Hepatic tumor number (C), tumor size (D) in the corresponding genotypes. (E) Representative images of H&E, BrdU and Ki67 staining of liver sections of 8 months DEN-treated *Lrh-1 WT* and *Lrh-1 K289R* mice. (F-H) Body weight (F), liver weight (G) and normalized liver weight to body weight (H) of mice described in (A).

Following the same method[244], *Lrh-1 WT* and *Lrh-1 K289R* mice were injected with DEN at 25 mg/ kg body weight on postnatal day 14 (Figure 5.1A). Six (mid-term) or eight (long-term) months after injection, tumor load of the mice were evaluated. In line with our previous data, *Lrh-1 K289R* mice developed more hepatic tumors than the control *Lrh-1 WT* littermates after a long-term DEN treatment (Figure 5.1B), which was reflected in increased tumor number and size (Figure 5.1C-D). Consistently, H&E staining of long-term DEN treated liver sections demonstrated more microscopic tumor foci, immunohistochemical staining of BrdU and Ki67 confirmed increased cell proliferation in *Lrh-1 K289R* livers (Figure 5.1E). Although no significant changes in body weight were observed, a small increase of liver weight of *Lrh-1 K289R* mice was noticed (Figure 5.1F-H). Collectively, these results corroborate our previous finding that LRH-1 promotes DEN-induced hepatocarcinogenesis.

5.2 *Lrh-1 K289R* Induces Asparagine Metabolism

We previously demonstrated that LRH-1 coordinates glutamine metabolism through controlling the expression of GLS2 to promote cell proliferation and tumor formation. We then assessed whether the increased tumor formation in the *Lrh-1 K289R* livers is attributed to an enhanced activity of the LRH-1-GLS2 axis. To this end, we performed microarray analysis and assessed the transcriptome between *Lrh-1 WT* and *Lrh-1 K289R* livers. Although dramatically reduced in LRH-1-deficient livers (Figure 4.9D), the mRNA levels of *Gls2, Got1 Gpt2 and Me1* were not significantly enhanced in mid-term DEN-challenged *Lrh-1 K289R* livers (Figure 5.2A-B). Noteworthy, *Lrh-1 K289R* exhibits increased transcriptional activity only on a selected subset of the known LRH-1 target genes and thus cannot be described as a global constitutively active LRH-1 form[206]. This suggested that the LRH-1-GLS2 cascade does not contribute to the tumor promoting phenotype in *Lrh-1 K289R* livers upon DEN administration (Figure 5.2C). Strikingly, one of the most significantly enhanced transcripts observed in the DEN-treated livers of *Lrh-1 K289R* mice compared to control *Lrh-1 WT* mice was *asparagine synthetase (Asns)* (Figure 5.2A-B). ASNS sits at the crossroads of glutamine and asparagine metabolism where it catalyzes the biosynthesis of asparagine from glutamine and aspartate through an ATP-dependent transamination reaction (Figure 5.2C). In parallel, altered mRNA levels of *Asns* were also translated into significant changes in ASNS protein levels (Figure 5.2D), which were found to be solely expressed in the cytosol (Figure 5.2E), suggesting a solid regulatory relationship between LRH-1 and ASNS.

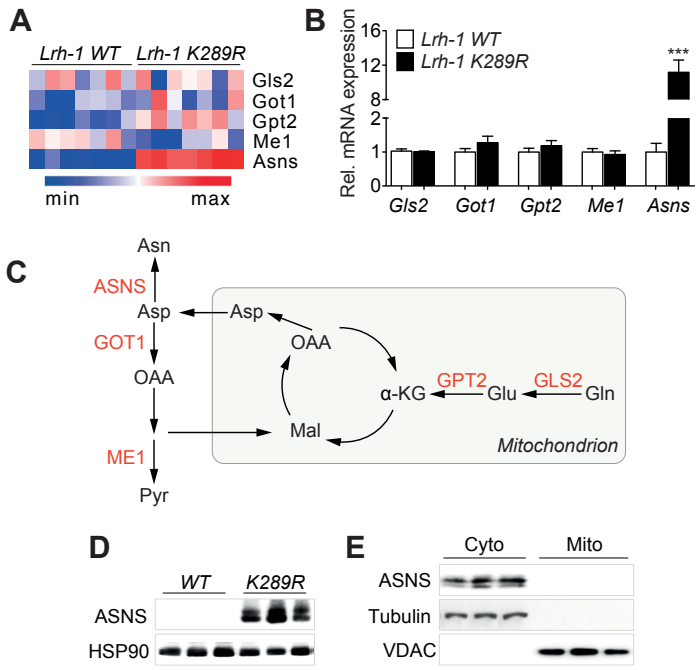

Figure 5. 2 LRH-1 Controls ASNS Expression *In Vivo*

(A) Heatmap displaying mRNA levels of *Gls2*, *Got1*, *Gpt2*, *Me1 and Asns* in livers of DEN-treated *Lrh-1 WT* (n=7) and *Lrh-1 K289R* (n=7) mice. (B) Relative hepatic mRNA expression of *Gls2*, *Got1*, *Gpt2*, *Me1* and *Asns* in livers of DEN-treated *Lrh-1 WT* (n=10) and *Lrh-1 K289R* (n=12) mice. (C) Graphical representation of enzymes involved in glutamine and asparagine metabolism. (D) Protein levels of ASNS in livers of DEN-treated *Lrh-1 WT* and *Lrh-1 K289R* mice. (E) Cytosolic and mitochondrial protein levels of ASNS in livers of DEN-treated *Lrh-1 WT* and *Lrh-1 K289R* mice. Data are represented as mean ± S.E.M.****P* < 0.001 by two-tailed Student's *t*-test.

Given the robust changes in ASNS expression, we hypothesized that hepatic GOF of LRH-1 affects the conversion of aspartate to asparagine (Figure 5.3A). In this regard, we performed targeted liquid chromatography mass spectrometry (LC-MS) analysis of intracellular glutamine (Gln), glutamate (Glu), asparagine (Asn) and aspartate (Asp). While the Gln/Glu ratio showed no difference (Figure 5.3B), a significant increase of Asn/Asp levels in the livers of *Lrh-1 K289R* mice was observed (Figure 5.3C), indicating LRH-1 participates in the regulation of asparagine metabolism.

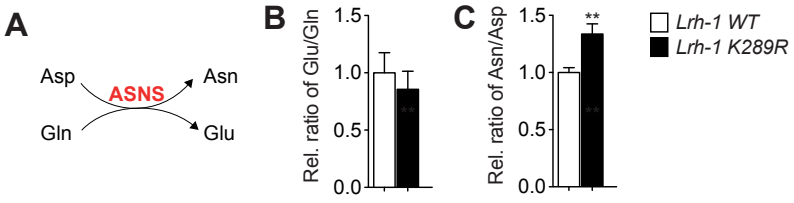

Figure 5. 3 LRH-1 Regulates Asn/Asp Levels

(A) Chemical reaction catalyzed by ASNS. (B-C) Relative Gln/Glu (B), Asn/Asp (C) levels in livers of *Lrh-1 WT* (n=10) and *Lrh-1 K289R* (n=12) mice. Data are represented as mean ± S.E.M.***P* < 0.01 by two-tailed Student's *t*-test.

Recent work has implied essential roles of asparagine metabolism in maintaining metabolic homeostasis and promoting cellular adaptation to metabolic stress in tumor cells. In one study, it was demonstrated that asparagine is sufficient to suppress apoptosis induced by glutamine depletion[147]. Silencing of ASNS leads to cell death even in the presence of glutamine, which can be reversed by addition of exogenous asparagine[147]. This observation, however, has only been reported in glioblastoma cells. We thus asked whether asparagine exhibits similar impact in hepatoma cells. To address this question, Hepa1.6 cells were deprived with glutamine, and then supplemented with asparagine. Removal of glutamine significantly induced apoptosis, as evidenced by enhanced cleavage of Caspase 3 and Caspase 7 (Figure 5.4A-B), and cell death (Figure 5.4C). Moreover, supplementation of asparagine attenuated glutamine withdrawal-induced apoptosis and cell death (Figure 5.4), indicating that asparagine is essential for hepatoma Hepa1.6 cells to evade glutamine-deprivation triggered apoptosis and cell death.

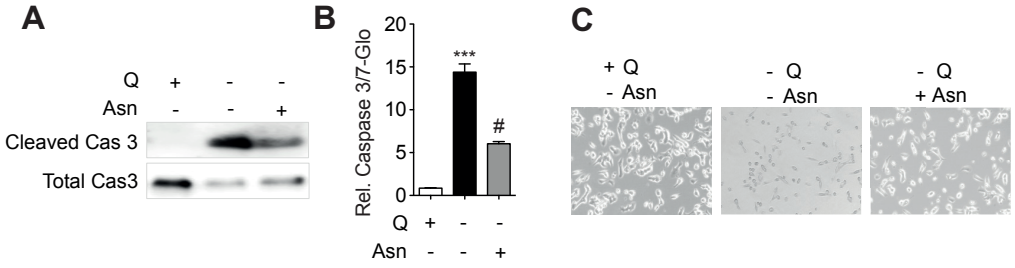

Figure 5. 4 Asparagine Suppresses Glutamine-depletion Induced Apoptosis

(A-C) Cleavage of Caspase-3 (A), Caspase 3 and 7 activation (B), Representative images captured with a Leica DM microscope at x40 bright field (C) of Hepa 1.6 cells cultured with or without glutamine (Q), and with or without asparagine (Asn) supplementation (n = 3 per group) for 24 hr. Data are represented as mean ± S.E.M. **P < 0.05* versus with Q; #*P < 0.05* versus without Q and without Asn by one-way ANOVA and Tukey's *post hoc* test.

5.3 *Lrh-1 K289R* Maintains Asparagine to Suppress Apoptosis

The evidence above implicated a critical role for asparagine in suppressing apoptosis. We then asked whether the anti-apoptotic function of asparagine depends on the ability of ASNS, which is the only enzyme maintains intracellular levels of asparagine. To address this question, we used shRNA to silence ASNS in Hepa1.6 cells. Suppression of ASNS led to apoptosis (Figure 5.5A) and impeded cell survival (Figure 5.5B) in the absence of asparagine. These effects were reversed by exogenous addition of asparagine (Figure 5.5A-B), supporting the notion that expression of ASNS is required for glutamine-dependent survival. Furthermore, suppression of ASNS inhibited cell proliferation in the absence of asparagine (Figure 5.5C), demonstrating that ASNS is also required for cell proliferation.

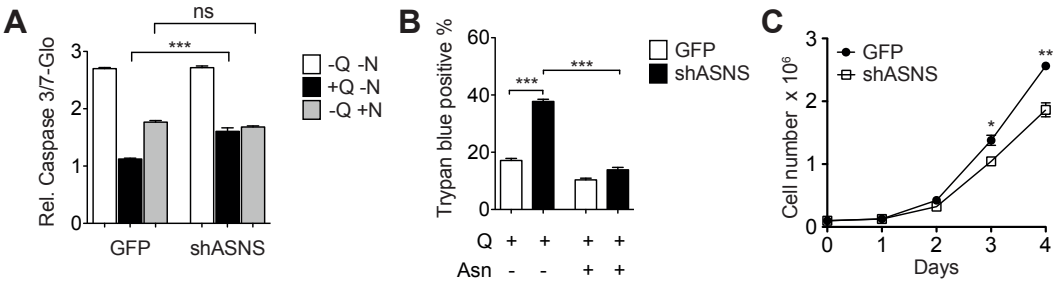

Figure 5. 5 Loss of ASNS Induces Apoptosis

(A-B) Caspase 3 and 7 activation (A), Trypan blue staining (B) of Hepa 1.6 cells infected with either GFP or ASNS silencing lentiviruses (n=3 per group) cultured with or without glutamine (Q), and with or without asparagine (N or Asn) supplementation (n = 3 per group) for 24 hr. (C) Cell proliferation of Hepa 1.6 cells infected with either GFP or ASNS silencing lentiviruses (n=3 per group) cultured with glutamine, and without asparagine supplementation (n = 3 per group). Data are represented as mean ± S.E.M. ***P < 0.01* and *** *P < 0.001* by one-way ANOVA and Tukey's *post hoc* test.

Overcoming cell death is a marked feature of cancer cells[31], and metabolic reprogramming supports cancer cell survival to eventually favor tumor formation in vivo. Given the strong association between apoptosis and cell survival in HCC development[268, 269], and the marked increase of Asn/Asp ratio in livers of *Lrh-1 K289R* mice, we then asked whether apoptosis is reduced in DEN-treated *Lrh-1 K289R* livers. To do so, we evaluated Caspase 3 activation in DEN-treated *Lrh-1 WT* and *Lrh-1 K289R* livers, and observed a striking reduction of cleaved Caspase 3 in the *Lrh-1 K289R* livers (Figure 5.6A), indicating that *Lrh-1 K289R* promotes hepatic cell survival upon DEN challenge. Of interest, we also observed an increased phosphorylation of 4EBP1, suggesting that the mTORC1 pathway is activated in DEN-treated *Lrh-1 K289R* livers. In line with the unaltered expression of *Gls2*, no significant differences in α-KG levels were observed between livers of *Lrh-1 WT* and *Lrh-1 K289R* mice (Figure 5.6B). Moreover, depletion of glutamine in Hepa1.6 cells inhibited mTORC1 activity, while supplementation of asparagine restored the activation of mTORC1 signaling (Figure 5.6C). Taken together, these results demonstrate that LRH-1 *K289R* suppresses apoptosis in DEN-treated livers, and *LRH-1 K289R* may stimulate mTORC1 signaling pathway in an Asn-dependent manner.

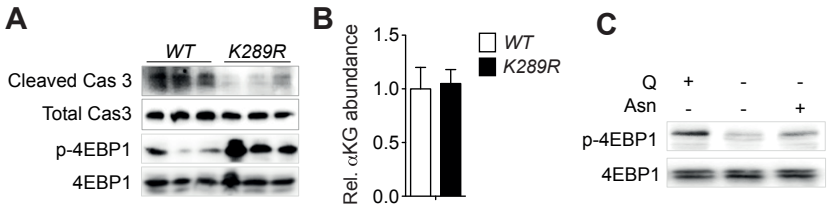

Figure 5. 6 *Lrh-1 K289R* Suppresses Apoptosis and Activates mTORC1 Signaling in DEN-treated Livers

(A-B) Cleavage of Caspase-3 and phosphorylation of 4EBP1 (A), intracellular α-KG levels (B) in livers of 8 months DEN-treated *Lrh-1 WT* and *Lrh-1 K289R* mice. (C) Phosphorylation levels of 4EBP1 in Hepa 1.6 cells cultured with or without glutamine or Asn supplementation.

5.4 Define the Role of Asparagine Synthetase in Liver Tumorigenesis

ASNS overexpression has been linked to solid tumor formation, such as those of the pancreas [143] and ovary [144], and is shown to be important for liver regeneration[145]. Despite the numerous existing correlations between L-asparaginase treatment and ALL pathology, *in vivo* studies demonstrating a causal link between ASNS activity and tumorigenesis are currently lacking. Moreover, conflicting studies propose ASNS as a tumor suppressor rather than as a tumor promoter, which would argue against a role for ASNS in HCC[270]. There is hence a crucial need to unequivocally establish whether ASNS is a relevant cancer target *in vivo*. Therefore, our lab has generated liver-specific ASNS mutant mice from C57BL/6N ES cells with floxed *Asns* alleles (www.mousephenotype.org). These ASNS L2/L2 mice were then bred with liver-specific albumin-CRE transgenic mice (http://jaxmice.jax.org/strain /003574.html) to generate liver-specific *Asns*$^{hep-/-}$ mice, which have been validated (Figure 5.7A-C). We are now using these mice to investigate the role of ASNS in the development of HCC by applying the DEN induced liver cancer model. These ASNS L2/L2 mice were also under breeding with CMV-CRE transgenic mice (https://www.jax.org/strain/006054) to generate whole body *Asns*$^{-/-}$ mice.

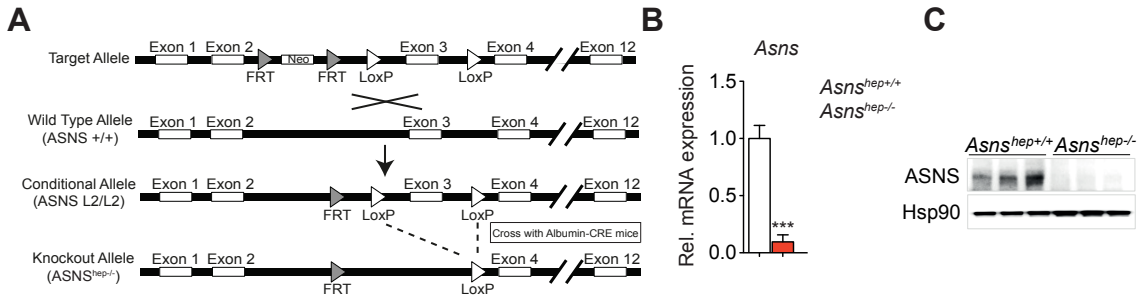

Figure 5. 7 Generation and Validation of Mice with a Targeted Mutation of ASNS in Hepatocytes

(A) Schematic map of the ASNS genomic locus, the floxed allele with a neomycin cassette (neo). White boxes represent the respective exons. Mice carrying the floxed ASNS alleles were crossed with liver-specific albumin-CRE transgenic mice to induce Cre-mediated recombination of the floxed ASNS alleles in hepatocytes. (B-C) ASNS mRNA (B) and protein (C) levels in primary hepatocytes isolated from *ASNS*$^{hep+/+}$ mice and *ASNS*$^{hep-/-}$ mice.

5.5 Dissect the Regulatory Network of LRH-1-ASNS Cascade

Given the solid correlation between LRH-1 and ASNS, we intended to dissect the molecular network through which LRH-1 governs ASNS expression. We first tested whether *Asns* is a direct transcriptional target of LRH-1. Analysis of the same genome-wide hepatic LRH-1 ChIP-seq dataset as described previously[255] revealed a weak LRH-1 recruitment at the mouse *Asns* promoter (Figure 5.8A), and extensive computational analyses identified three putative binding sites in this region of the promoter (Figure 5.8B). Site-specific ChIP analysis using DNA from mid-term DEN-treated *Lrh-1*$^{hep+/+}$ and *Lrh-1*$^{hep-/-}$ livers, however, revealed no LRH-1 recruitment to those three putative binding sites (Figure 5.8C). Especially when compared to LRH-1

binding strength to the promoter of *Shp*, which is a well-established LRH-1 target, the recruitment of LRH-1 to *Asns* promoter appears to be very weak (Figure 5.8A and C). Taken together, these results suggest that *Asns* transcription is most likely not directly regulated by LRH-1.

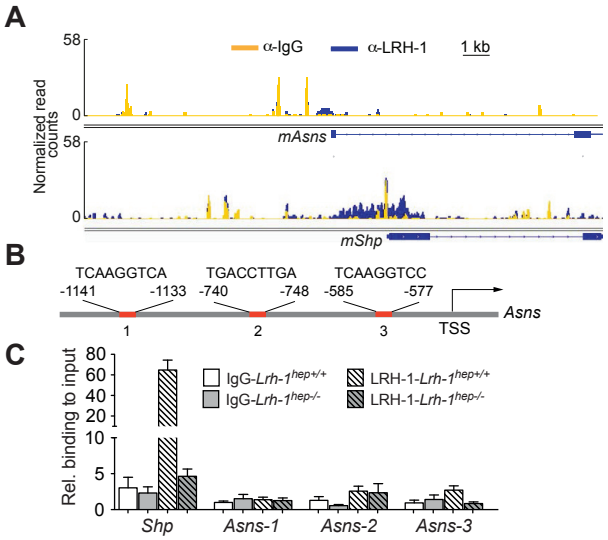

Figure 5. 8 *Asns* Is an Indirect Transcriptional Target of LRH-1

(A) UCSC genome browser (mm9) view displaying the occupancy of mouse *Asns* and *Shp* by IgG and LRH-1[255]. (B) Schematic representation of the 3 putative LRH-1 response elements in the proximal mouse *Asns* promoter. (D) ChIP-qPCR assay to evaluate the relative LRH-1 binding to the mouse *Asns* promoter. Data represent mean ± S.E.M.

Earlier report revealed a role for the GCN2-eIF2α-ATF4-ASNS pathway in the survival and proliferation of cells derived from colon carcinoma or fibrosarcoma[146]. Given the known role of ATF4 in the regulation of ASNS gene expression, we initially examined ATF4 protein levels in livers of mid-term DEN-treated *Lrh-1 WT* and *Lrh-1 K289R mice*, yet no significant differences were observed between the two genotypes (Figure 5.9A). Moreover, previous reports demonstrated that activating transcription factor 5 (ATF5) directly drives *Asns* transcription by binding to its promoter[271, 272]. We thus analyzed if the increase of ASNS in livers of *Lrh-1 K289R* mice results from ATF5 stimulation. We first assessed the mRNA expression of *Atf5* in mid-term DEN-treated mice, and detected a strong induction of *Atf5* in *Lrh-1 K289R* livers (Figure 5.9B). In parallel, ATF5 reconstitution in *Lrh-1*$^{hep-/-}$ livers restored *Asns* expression (Figure 5.9C). Analysis of the previously described genome-wide hepatic LRH-1 ChIP-seq dataset[255] revealed a LRH-1 recruitment at the mouse *Atf5* promoter (Figure 5.8D). Notably, early study has described an important role of ATF5 in promoting cell survival[272, 273]. We hence hypothesized that LRH-1 may regulate ASNS expression through ATF5 to support cell survival[273, 274273, 274272, 273]. More experiments are currently ongoing to define the molecular mechanism in the LRH-1/ATF5/ASNS axis.

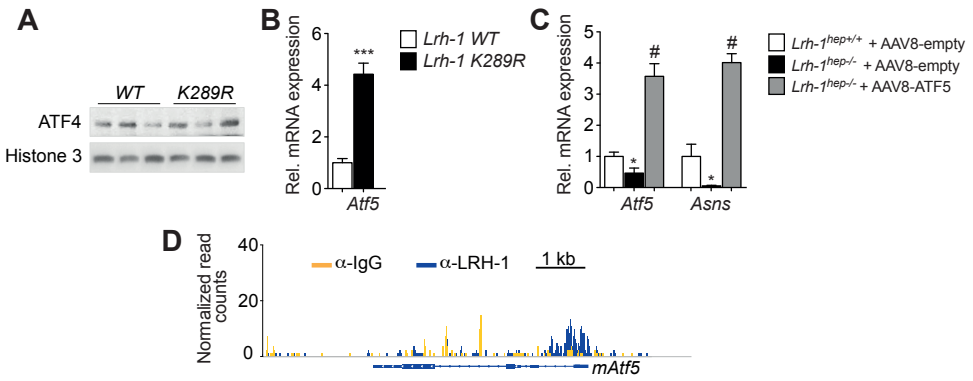

Figure 5. 9 ATF5 Regulates *Asns* Expression

(A-B) Hepatic protein levels of ATF4 (A), Relative hepatic mRNA expression of *Atf5* (B) in livers of DEN-treated *Lrh-1 WT* (n=10) and *Lrh-1 K289R* (n=12) mice. Data are represented as mean ± S.E.M. ***$P < 0.001$ versus *Lrh-1 WT* by two-tailed Student's *t*-test. (C) Relative hepatic mRNA expression of *Atf5* and *Asns* in livers of control virus infected *Lrh-1*$^{hep+/+}$ and *Lrh-1*$^{hep-/-}$ mice, and AAV8-ATF5 virus infected *Lrh-1*$^{hep-/-}$ mice (n=4-5 per group). Data are represented as mean ± S.E.M. *$P < 0.05$ versus *Lrh-1*$^{hep+/+}$; #$P < 0.05$ versus *Lrh-1*$^{hep-/-}$ by one-way ANOVA and Tukey's *post hoc* test. (D) UCSC genome browser (mm9) view displaying the occupancy of mouse *Atf5* by IgG and LRH-1[255].

5.6 Discussion and Future Studies

The biological contributions of glutamine to transformed cells are versatile and complex. Glutamine provides carbon and nitrogen for macromolecule biosynthesis, it is also involved in many cellular processes, including anti-oxidative stress, mTOR signaling and autophagy[37, 83, 89, 135]. In addition, glutamine also contributes to biosynthesis of several amino acids including asparagine that requires glutamine for *de novo* synthesis via the enzyme ASNS. The importance of asparagine for tumor growth has been demonstrated by the effectiveness of asparaginase in treating low-ASNS-expressing leukemia. Earlier studies on metabolic profiling have identified a number of metabolites that are heavily consumed by cancer cells, including asparagine[275]. Recently, genetic silencing of ASNS in sarcoma cells combined with depletion of plasma asparagine levels via asparaginase was shown to blunt tumor growth *in vivo*[149]. ASNS expression in solid tumors correlates with high tumor grade and poor prognosis[147]. Thus, cancer cells appear to have high demand for asparagine. However, the mechanisms behind this asparagine-dependency are largely unexplored.

In the study of this chapter, we explored the role of ASNS and its end-product asparagine in the context of liver cancer using a selective gain-of-function (GOF) LRH-1 mouse model, in which one mutation of lysine residue 289 to arginine (K289R) abolishes SUMO modification of LRH-1 and interferes with co-repressor interactions, subsequently leading to selectively increased transcriptional activity of LRH-1. We observed that *Lrh-1 K289R* mice developed more hepatic tumors compared to control littermates upon DEN exposure. This supports our previous finding that LRH-1 confers a pro-tumorigenic role in liver cancer development.

Our results in chapter 4 demonstrated that LRH-1 coordinates glutamine metabolism in promoting liver cancer progression. We thus assessed whether the previously identified mechanistic basis reliant on GLS2/GPT2/GOT1/ME1 accounts for the tumor promoting phenotype in DEN-treated *Lrh-1 K289R* livers. Notably, none of those genes were significantly changed in the livers upon GOF of LRH-1. Accordingly, intracellular levels of α-KG showed no significant differences between livers of the two genotypes. Noteworthy, a striking increase of ASNS expression was observed in *Lrh-1 K289R* livers, along with a significant induction of Asn/Asp ratios, indicating a strong association between LRH-1 and asparagine metabolism.

Particularly, our results revealed that asparagine plays an important role in the regulation of the cellular adaptation to glutamine depletion. We showed that glutamine deprivation induced apoptosis in hepatoma cells, while asparagine was necessary and sufficient to suppress glutamine-withdrawal-induced apoptosis. Moreover, we found that deletion of ASNS led to cell death even when glutamine was present and asparagine was not available. Addition of extracellular asparagine restored apoptosis and cell survival under these conditions, indicating ASNS is required for glutamine-dependent cell survival. These results are consistent with the findings of another study in N-Myc amplified neuroblastoma cell lines[147], suggesting that adequate availability of intrinsic or extrinsic asparagine may act as a critical apoptosis suppressor in different cancer cell types.

Moreover, a recent study identified a novel role for asparagine as an amino acid exchange factor. It was shown that intracellular asparagine exchanges with extracellular amino acids, especially serine, arginine and histidine, to promote mTORC1 activation, protein and nucleotide synthesis and cell proliferation. In chapter 4, we have demonstrated that LRH-1 stimulates mTORC1 activation in a α-KG dependent manner to further promote cell proliferation. We then evaluated LRH-1/α-KG/mTORC1 cascade in the selective GOF LRH-1 mouse model. Although mRNA levels of *Gls2* and intracellular availability of α-KG were not changed between DEN-treated *Lrh-1 WT* and *Lrh-1 K289R* livers, enhanced mTORC1 activation was observed in *Lrh-1 K289R* livers. Moreover, extracellular supplementation of asparagine rescued the inhibited mTORC1 activity upon glutamine deprivation in Hepa1.6 cells, suggesting that LRH-1 may also stimulate mTORC1 signaling pathway through regulating ASNS expression and its product asparagine.

Collectively, the results in this chapter assigned a potential role for ASNS and asparagine in hepatoma cell survival and cell proliferation (Figure 5.10), and raised a crucial need of establishing the *in vivo* relevance of ASNS/asparagine in cancer. We are now assessing the effects of DEN treatment on $ASNS^{hep+/+}$ and $ASNS^{hep-/-}$ mice, and this ongoing study will provide more evidence on the importance of ASNS in liver cancer. Moreover, we are currently injecting DEN-treated *Lrh-1 WT* and *Lrh-1 K289R* mice with asparaginase, which is an enzyme able to deplete circulating asparagine. Tumor burden, apoptosis and mTORC1 signaling will be assessed in those mice to determine the contribution of ASNS/asparagine to the tumor promoting phenotype in DEN-treated *Lrh-1 K289R* livers.

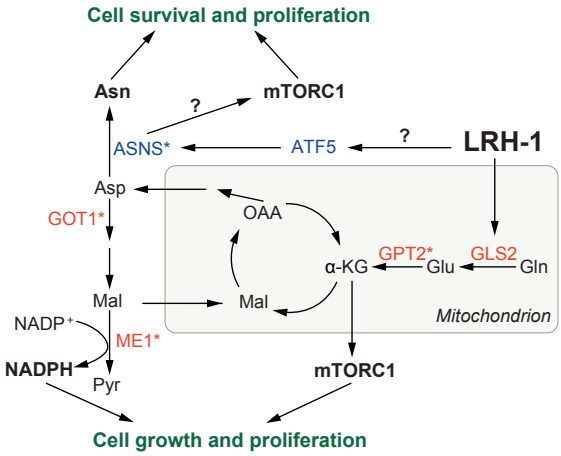

Figure 5. 10 Glutamine and Asparagine Metabolism Regulated by LRH-1

Graphical summary illustrating how LRH-1 promotes glutamine and asparagine metabolism in hepatic cancer cells. Enzymes highlighted in red are reduced in *Lrh-1*$^{hep-/-}$ livers, in blue are induced in *Lrh-1 K289R* livers, * indicates indirect regulation by LRH-1.

Mechanistically, we performed ChIP analysis and demonstrated that *Asns* is not a direct transcriptional target of LRH-1. ATF4 and ATF5 have previously been shown to regulate *Asns* transcription. No differences in ATF4 protein levels were observed between livers of *Lrh-1 WT* and *Lrh-1 K289R* mice. However, we found that ATF5 follows the same regulation patterns as ASNS in both LOF and GOF of LRH-1 mice models. More importantly, ATF5 reconstitution in *Lrh-1*$^{hep-/-}$ restored ASNS expression, suggesting that ATF5 may act as the intermediary mediator links LRH-1 and ASNS.

ATF5 is a member of the ATF/cAMP response element-binding protein family. Increased levels of ATF5 have been observed in many types of tumors including glioblastoma[273], epithelial ovarian neoplasms[276], breast cancers[274, 277] and rectal cancer[278]. Previous studies demonstrated that ATF5 acts as an important anti-apoptotic factor and is required for cancer cell survival. A genome-wide RNAi screen revealed an essential ATF5-mediated survival pathway in malignant glioma, whereby activation of a RAS-mitogen-activated protein kinase (RAS-MAPK) or phosphoinositide-3-kinase (PI3K) signaling cascade leads to induction of the transcription factor cAMP response element-binding protein-3-like-2 (CREB3L2), which directly activates ATF5 expression. ATF5, in turn, promotes survival by stimulating transcription of myeloid cell leukemia sequence-1 (MCL-1)[273]. In addition, another anti-apoptotic factor B-cell leukemia lymphoma-2 (BCL-2) was also identified as a downstream target of ATF5, and was shown to mediate the prosurvival function of ATF5 in glioma cells[274], breast cancer cells[274], and ovarian cancer cells[276]. Given the important role of ATF5 in promoting cancer cell survival, and the strong association between LRH-1, ATF5 and ASNS, we speculate that LRH-1 promotes cell survival through ATF5-mediated regulation of ASNS and its product asparagine. Further investigations are required to dissect the molecuar network and the anti-apoptotic function of the LRH-1/ATF5/ASNS axis.

Chapter 6 Conclusion and Perspectives

6.1 Achieved Results

In this thesis, I focused on deciphering the role of nuclear receptor LRH-1 in liver intermediary metabolism and cancer. LRH-1 has previously been linked with the development of several cancers, such as colorectal, breast, and pancreatic cancer. However, until now our knowledge on the roles of LRH-1 in the development of another major cancer type, hepatocellular carcinoma is much lacking. Furthermore, previous studies have focused on the elucidation of how LRH-1 intersects with a number of pro-tumorigenic signaling pathways, where the crosstalk with β-catenin pathway represents a prevalent mechanism for LRH-1 function in several cancer events, evidence on how LRH-1 affects tumor cell metabolism is largely unexplored. Our findings indicated a key role of LRH-1 in the regulation of hepatic intermediary metabolism with major implication in the pathogenesis of liver cancer.

More specifically, in this thesis, I identified mitochondrial glutamine processing and glutamine-dependent asparagine biosynthesis as key mechanisms to sustain cell proliferation and cell survival in models of hepatocellular carcinoma (HCC) and pinpoint the nuclear receptor LRH-1 as a critical regulator of these biochemical processes. The significance of the role of LRH-1 in HCC development is supported by the observation that mice with a liver-specific disruption of LRH-1 function no longer developed tumors after exposure to carcinogen diethylnitrosamine (DEN) known to trigger HCC, while mice carrying a knock-in *Lrh1 K289R*, which represents a selective gain-of-function (GOF) model for LRH-1, developed more tumors after the exposure to DEN. Using non-invasive *in vivo* hyperpolarized MR technology, I demonstrated that diminished glutamine fluxes account for the robust tumor suppressive phenotype in LRH-1 deficient livers, ultimately compromising glutamine-fueled anaplerosis and mTORC1 signaling. More specifically, I demonstrated that LRH-1 governs the hepatic expression of the mitochondrial gatekeeper of glutamine catabolism, GLS2, to stimulate glutaminolysis, α-ketoglutarate (α-KG) replenishment, and subsequent mTORC1 activation. Unlike the more ubiquitously expressed isozyme GLS1, GLS2 expression is highly enriched in hepatocytes, underscoring its therapeutic relevance to target liver cancer without undue adverse effects in other tissues. I conclude that the LRH-1-GLS2 axis is crucial in coordinating the availability of α-KG to drive glutamine-induced anabolic cancer metabolism in the liver. Furthermore, I found that LRH-1 also maintains NADPH production through coordinating the alternative route of glutamine processing reliant on GPT2, GOT1 and ME1. I showed that NADPH/$NADP^+$ ratio was significantly diminished in LRH-1-deficient livers,

which can also further contribute the striking tumor suppressive phenotype in the livers of *Lrh-1*$^{hep-/-}$ mice.

In addition, LRH-1 also plays a crucial role in regulating glutamine-dependent asparagine homeostasis. Hepatic expression of ASNS, the only identified enzyme for *de novo* synthesis of asparagine is down-regulated upon LOF of LRH-1 and increased upon GOF of LRH-1, with sequential modulations on intracellular Asn/Asp levels. Moreover, I also showed that ASNS or asparagine is required to suppress apoptosis and cell death induced by glutamine removal, suggesting that LRH-1 may promote cell survival through its regulation of ASNS-mediated asparagine biosynthesis.

In conclusion, studies in this thesis assigned a critical role to LRH-1 in hepatic fuel metabolism with a striking impact on hepatic tumorigenesis. These findings demonstrated for the first time the existence of a nuclear receptor-mediated mechanism that links intermediary metabolism to cancer growth.

6.2 Perspectives

In this thesis, I found that LRH-1 loss dramatically reduces the tumor burden in mice treated with the carcinogen DEN. Integrative molecular, cellular and metabolic profiling demonstrated that LRH-1 up-regulates glutamine-dependent anaplerosis which coincides with activated mTORC1 signaling and increased cell proliferation. However, GSEA enrichment analysis demonstrated several other pathways that are significant altered between *Lrh-1*$^{hep+/+}$ and *Lrh-1*$^{hep-/-}$ livers, although less enriched than glutamine processing pathway. For instance, I noticed that some proteasomal subunits are downregulated in LRH-1 knockout livers. Considering the sensitivity of many cancers to proteasome inhibition, it is conceivable that decreased proteasome activity may have anti-tumorigenic effects. Therefore, it would be interesting in future to test whether impaired proteasomal function upon LRH-1 loss contributes the tumor suppressive phenotype.

Moreover, recent studies identified cytosolic transaminase GOT1 as a crucial factor for sustaining proliferation in cells with mitochondrial electron transport chain (ETC) defects[264, 265]. In the study of chapter 4, transcript levels of *Got1* were markedly reduced in *Lrh-1*-deficient livers. However, our overall data based on genome-wide promoter recruitment analysis in *Lrh-1*$^{hep-/-}$ and *Lrh-1*$^{hep+/+}$ livers and LRH-1 LOF and GOF studies in hepatoma cell lines indicated that *Got1* is rather an indirect target of LRH-1. Given the essential role of ETC and GOT1 in cell proliferation, it will be of interest to investigate to what extent the GOT1-ETC axis may account for the anti-tumorigenic effects in DEN-treated *Lrh-1*-deficient livers. In this context, further studies are warranted to dissect the exact mechanistic basis by which LRH-1 governs *Got1* expression.

The existing evidence suggests that maintenance of the TCA cycle is critical for glutamine-dependent survival. Particularly, a cell permeable form of α-KG, DM-KG, has been shown to rescue MYC-transformed cells from cell death upon glutamine withdrawal[83, 147]. Interestingly, compared to *Lrh-1*$^{hep+/+}$, I observed a strong induction of apoptosis in DEN-treated *Lrh-1*$^{hep-/-}$ livers. Moreover, Asn and α-KG levels were both reduced upon hepatic loss of LRH-1, I thus speculate that the increased apoptosis levels in *Lrh-1*$^{hep-/-}$ may

attribute from reduced availability of asparagine and α-KG. Therefore, the effect of LRH-1/GLS2/α-KG axis on glutamine-deprivation induced apoptosis may also be interesting to study in more detail.

Furthermore, intracellular α-KG has also been tightly linked with epigenetics that have important implication in many cancers[279, 280]. α-KG is one of the cofactors for several dioxygenases, including histone demethylases, prolyl hydroxylases, and the TET2 DNA hydroxylases. Altered α-KG availability affects α-KG-dependent dioxygenases with consequent regulation of genome-wide DNA methylation and histone modification[281, 282]. In chapter 4, I observed a significant reduction of α-KG levels in LRH-1 knockout livers, it hence would be very interesting in future to assess whether LRH-1 regulates cancer cell growth and proliferation through mediating α-KG-dependent chromatin modification.

Although many facets of ASNS regulation and function have been characterized, there are still several major gaps remaining in our knowledge. The exact roles and physiological importance of ASNS are largely unexplored. For example, studies on ASNS have so far only implied its function on asparagine synthesis, while its activity could also have a significant impact on the substrate aspartate. Especially, aspartate carries reducing equivalents in the malate-aspartate shuttle[85, 264, 265], it has also been shown to restore apoptosis[283] and to promote cell proliferation[264, 265]. Increased aspartate levels after ASNS knockdown may thus confer a beneficial response. It is hence necessary to evaluate the levels and effects of both Asn and Asp when modulating ASNS expression *in vivo* or in *vitro*.

Finally, the identification of small molecule agonists and antagonists as well as the discovery that specific phospholipid species act as endogenous agonists of LRH-1[170, 172, 175, 176] suggest that the receptor could be a druggable target. In this doctoral work, I demonstrated that LRH-1 acts as a tumor-promoting factor during liver cancer development. I also evaluated the effects of several commercially available LRH-1 antagonists[173, 284] on established LRH-1 target genes, cell proliferation and cell survival, the results, however, demonstrated that these LRH-1 antagonists are neither not highly potent nor specific. Therefore, the identification and evaluation of novel potent and specific LRH-1 antagonists is needed and may offer interesting therapeutic perspectives to treat liver cancer. Moreover, some cancers evade asparaginase sensitivity by up-regulating ASNS expression[285], presumably to recover intracellular asparagine pools via ASNS-catalyzed synthesis from glutamine, thus I speculate coupling asparaginase treatment with a glutamine-low diet may improve efficacy of asparaginase treatment.

References

1. CANCER, I.A.F.R.O.
2. El-Serag, H.B. Epidemiology of viral hepatitis and hepatocellular carcinoma. *Gastroenterology* **142**, 1264-1273 e1 (2012).
3. Pascual, S., Herrera, I. & Irurzun, J. New advances in hepatocellular carcinoma. *World J Hepatol* **8**, 421-38 (2016).
4. Parkin, D.M., Bray, F., Ferlay, J. & Pisani, P. Global cancer statistics, 2002. *CA Cancer J Clin* **55**, 74-108 (2005).
5. Bralet, M.P., Regimbeau, J.M., Pineau, P., Dubois, S., Loas, G., Degos, F., Valla, D., Belghiti, J., Degott, C. & Terris, B. Hepatocellular carcinoma occurring in nonfibrotic liver: epidemiologic and histopathologic analysis of 80 French cases. *Hepatology* **32**, 200-4 (2000).
6. El-Serag, H.B., Richardson, P.A. & Everhart, J.E. The role of diabetes in hepatocellular carcinoma: a case-control study among United States Veterans. *Am J Gastroenterol* **96**, 2462-7 (2001).
7. Marrero, J.A., Fontana, R.J., Fu, S., Conjeevaram, H.S., Su, G.L. & Lok, A.S. Alcohol, tobacco and obesity are synergistic risk factors for hepatocellular carcinoma. *J Hepatol* **42**, 218-24 (2005).
8. Marcellin, P., Pequignot, F., Delarocque-Astagneau, E., Zarski, J.P., Ganne, N., Hillon, P., Antona, D., Bovet, M., Mechain, M., Asselah, T., Desenclos, J.C. & Jougla, E. Mortality related to chronic hepatitis B and chronic hepatitis C in France: evidence for the role of HIV coinfection and alcohol consumption. *J Hepatol* **48**, 200-7 (2008).
9. Franceschi, S. & Raza, S.A. Epidemiology and prevention of hepatocellular carcinoma. *Cancer Lett* **286**, 5-8 (2009).
10. Chang, M.H., You, S.L., Chen, C.J., Liu, C.J., Lee, C.M., Lin, S.M., Chu, H.C., Wu, T.C., Yang, S.S., Kuo, H.S., Chen, D.S. & Taiwan Hepatoma Study, G. Decreased incidence of hepatocellular carcinoma in hepatitis B vaccinees: a 20-year follow-up study. *J Natl Cancer Inst* **101**, 1348-55 (2009).
11. Organization., W.H. 405-420 (2009).
12. Bolondi, L. Screening for hepatocellular carcinoma in cirrhosis. *J Hepatol* **39**, 1076-84 (2003).
13. Kim, C.K., Lim, J.H. & Lee, W.J. Detection of hepatocellular carcinomas and dysplastic nodules in cirrhotic liver: accuracy of ultrasonography in transplant patients. *J Ultrasound Med* **20**, 99-104 (2001).
14. Kobayashi, K., Sugimoto, T., Makino, H., Kumagai, M., Unoura, M., Tanaka, N., Kato, Y. & Hattori, N. Screening methods for early detection of hepatocellular carcinoma. *Hepatology* **5**, 1100-5 (1985).
15. Yamashita, T., Forgues, M., Wang, W., Kim, J.W., Ye, Q., Jia, H., Budhu, A., Zanetti, K.A., Chen, Y., Qin, L.X., Tang, Z.Y. & Wang, X.W. EpCAM and alpha-fetoprotein expression defines novel prognostic subtypes of hepatocellular carcinoma. *Cancer Res* **68**, 1451-61 (2008).
16. European Association For The Study Of The, L., European Organisation For, R. & Treatment Of, C. EASL-EORTC clinical practice guidelines: management of hepatocellular carcinoma. *J Hepatol* **56**, 908-43 (2012).
17. Llovet, J.M., Schwartz, M. & Mazzaferro, V. Resection and liver transplantation for hepatocellular carcinoma. *Semin Liver Dis* **25**, 181-200 (2005).
18. Mazzaferro, V., Bhoori, S., Sposito, C., Bongini, M., Langer, M., Miceli, R. & Mariani, L. Milan criteria in liver transplantation for hepatocellular carcinoma: an evidence-based analysis of 15 years of experience. *Liver Transpl* **17 Suppl 2**, S44-57 (2011).
19. Lencioni, R. Loco-regional treatment of hepatocellular carcinoma. *Hepatology* **52**, 762-73 (2010).

20. Lo, C.M., Ngan, H., Tso, W.K., Liu, C.L., Lam, C.M., Poon, R.T., Fan, S.T. & Wong, J. Randomized controlled trial of transarterial lipiodol chemoembolization for unresectable hepatocellular carcinoma. *Hepatology* **35**, 1164-71 (2002).
21. Pelletier, G., Ducreux, M., Gay, F., Luboinski, M., Hagege, H., Dao, T., Van Steenbergen, W., Buffet, C., Rougier, P., Adler, M., Pignon, J.P. & Roche, A. Treatment of unresectable hepatocellular carcinoma with lipiodol chemoembolization: a multicenter randomized trial. Groupe CHC. *J Hepatol* **29**, 129-34 (1998).
22. Boucher, E., Corbinais, S., Rolland, Y., Bourguet, P., Guyader, D., Boudjema, K., Meunier, B. & Raoul, J.L. Adjuvant intra-arterial injection of iodine-131-labeled lipiodol after resection of hepatocellular carcinoma. *Hepatology* **38**, 1237-41 (2003).
23. Lau, W.Y., Leung, T.W., Ho, S.K., Chan, M., Machin, D., Lau, J., Chan, A.T., Yeo, W., Mok, T.S., Yu, S.C., Leung, N.W. & Johnson, P.J. Adjuvant intra-arterial iodine-131-labelled lipiodol for resectable hepatocellular carcinoma: a prospective randomised trial. *Lancet* **353**, 797-801 (1999).
24. Salem, R., Lewandowski, R.J., Mulcahy, M.F., Riaz, A., Ryu, R.K., Ibrahim, S., Atassi, B., Baker, T., Gates, V., Miller, F.H., Sato, K.T., Wang, E., Gupta, R., Benson, A.B., Newman, S.B., Omary, R.A., Abecassis, M. & Kulik, L. Radioembolization for hepatocellular carcinoma using Yttrium-90 microspheres: a comprehensive report of long-term outcomes. *Gastroenterology* **138**, 52-64 (2010).
25. Abou-Alfa, G.K., Schwartz, L., Ricci, S., Amadori, D., Santoro, A., Figer, A., De Greve, J., Douillard, J.Y., Lathia, C., Schwartz, B., Taylor, I., Moscovici, M. & Saltz, L.B. Phase II study of sorafenib in patients with advanced hepatocellular carcinoma. *J Clin Oncol* **24**, 4293-300 (2006).
26. Cheng, A.L., Kang, Y.K., Chen, Z., Tsao, C.J., Qin, S., Kim, J.S., Luo, R., Feng, J., Ye, S., Yang, T.S., Xu, J., Sun, Y., Liang, H., Liu, J., Wang, J., Tak, W.Y., Pan, H., Burock, K., Zou, J., Voliotis, D. & Guan, Z. Efficacy and safety of sorafenib in patients in the Asia-Pacific region with advanced hepatocellular carcinoma: a phase III randomised, double-blind, placebo-controlled trial. *Lancet Oncol* **10**, 25-34 (2009).
27. Iavarone, M., Cabibbo, G., Piscaglia, F., Zavaglia, C., Grieco, A., Villa, E., Camma, C., Colombo, M. & group, S.s. Field-practice study of sorafenib therapy for hepatocellular carcinoma: a prospective multicenter study in Italy. *Hepatology* **54**, 2055-63 (2011).
28. Hanahan, D. & Weinberg, R.A. Hallmarks of cancer: the next generation. *Cell* **144**, 646-74 (2011).
29. Warburg, O., Wind, F. & Negelein, E. The Metabolism of Tumors in the Body. *J Gen Physiol* **8**, 519-30 (1927).
30. Ward, P.S. & Thompson, C.B. Metabolic reprogramming: a cancer hallmark even warburg did not anticipate. *Cancer Cell* **21**, 297-308 (2012).
31. Hanahan, D. & Weinberg, R.A. The hallmarks of cancer. *Cell* **100**, 57-70 (2000).
32. Warburg, O.W., F. Negelein, E. . The metabolism of tumors in the body. *The Journal of General Physiology* **8**, 519-530 (1927).
33. Som, P., Atkins, H.L., Bandoypadhyay, D., Fowler, J.S., MacGregor, R.R., Matsui, K., Oster, Z.H., Sacker, D.F., Shiue, C.Y., Turner, H., Wan, C.N., Wolf, A.P. & Zabinski, S.V. A fluorinated glucose analog, 2-fluoro-2-deoxy-D-glucose (F-18): nontoxic tracer for rapid tumor detection. *J Nucl Med* **21**, 670-5 (1980).
34. Almuhaideb, A., Papathanasiou, N. & Bomanji, J. 18F-FDG PET/CT imaging in oncology. *Ann Saudi Med* **31**, 3-13 (2011).
35. Czernin, J. & Phelps, M.E. Positron emission tomography scanning: current and future applications. *Annu Rev Med* **53**, 89-112 (2002).

36. Gatenby, R.A. & Gillies, R.J. Why do cancers have high aerobic glycolysis? *Nat Rev Cancer* **4**, 891-9 (2004).
37. DeBerardinis, R.J., Lum, J.J., Hatzivassiliou, G. & Thompson, C.B. The biology of cancer: metabolic reprogramming fuels cell growth and proliferation. *Cell Metab* **7**, 11-20 (2008).
38. Vander Heiden, M.G., Cantley, L.C. & Thompson, C.B. Understanding the Warburg effect: the metabolic requirements of cell proliferation. *Science* **324**, 1029-33 (2009).
39. Locasale, J.W. & Cantley, L.C. Metabolic flux and the regulation of mammalian cell growth. *Cell Metab* **14**, 443-51 (2011).
40. Patra, K.C. & Hay, N. The pentose phosphate pathway and cancer. *Trends Biochem Sci* **39**, 347-54 (2014).
41. Wellen, K.E., Lu, C., Mancuso, A., Lemons, J.M., Ryczko, M., Dennis, J.W., Rabinowitz, J.D., Coller, H.A. & Thompson, C.B. The hexosamine biosynthetic pathway couples growth factor-induced glutamine uptake to glucose metabolism. *Genes Dev* **24**, 2784-99 (2010).
42. Spiro, R.G. Protein glycosylation: nature, distribution, enzymatic formation, and disease implications of glycopeptide bonds. *Glycobiology* **12**, 43R-56R (2002).
43. Pinho, S.S. & Reis, C.A. Glycosylation in cancer: mechanisms and clinical implications. *Nat Rev Cancer* **15**, 540-55 (2015).
44. Possemato, R., Marks, K.M., Shaul, Y.D., Pacold, M.E., Kim, D., Birsoy, K., Sethumadhavan, S., Woo, H.K., Jang, H.G., Jha, A.K., Chen, W.W., Barrett, F.G., Stransky, N., Tsun, Z.Y., Cowley, G.S., Barretina, J., Kalaany, N.Y., Hsu, P.P., Ottina, K., Chan, A.M., Yuan, B., Garraway, L.A., Root, D.E., Mino-Kenudson, M., Brachtel, E.F., Driggers, E.M. & Sabatini, D.M. Functional genomics reveal that the serine synthesis pathway is essential in breast cancer. *Nature* **476**, 346-50 (2011).
45. Lunt, S.Y. & Vander Heiden, M.G. Aerobic glycolysis: meeting the metabolic requirements of cell proliferation. *Annu Rev Cell Dev Biol* **27**, 441-64 (2011).
46. Hsu, P.P. & Sabatini, D.M. Cancer cell metabolism: Warburg and beyond. *Cell* **134**, 703-7 (2008).
47. Bensaad, K., Tsuruta, A., Selak, M.A., Vidal, M.N., Nakano, K., Bartrons, R., Gottlieb, E. & Vousden, K.H. TIGAR, a p53-inducible regulator of glycolysis and apoptosis. *Cell* **126**, 107-20 (2006).
48. Matoba, S., Kang, J.G., Patino, W.D., Wragg, A., Boehm, M., Gavrilova, O., Hurley, P.J., Bunz, F. & Hwang, P.M. p53 regulates mitochondrial respiration. *Science* **312**, 1650-3 (2006).
49. Schwartzenberg-Bar-Yoseph, F., Armoni, M. & Karnieli, E. The tumor suppressor p53 down-regulates glucose transporters GLUT1 and GLUT4 gene expression. *Cancer Res* **64**, 2627-33 (2004).
50. Kondoh, H., Lleonart, M.E., Gil, J., Wang, J., Degan, P., Peters, G., Martinez, D., Carnero, A. & Beach, D. Glycolytic enzymes can modulate cellular life span. *Cancer Res* **65**, 177-85 (2005).
51. Contractor, T. & Harris, C.R. p53 negatively regulates transcription of the pyruvate dehydrogenase kinase Pdk2. *Cancer Res* **72**, 560-7 (2012).
52. Jiang, P., Du, W., Wang, X., Mancuso, A., Gao, X., Wu, M. & Yang, X. p53 regulates biosynthesis through direct inactivation of glucose-6-phosphate dehydrogenase. *Nat Cell Biol* **13**, 310-6 (2011).
53. Semenza, G.L. Regulation of metabolism by hypoxia-inducible factor 1. *Cold Spring Harb Symp Quant Biol* **76**, 347-53 (2011).
54. Yeung, S.J., Pan, J. & Lee, M.H. Roles of p53, MYC and HIF-1 in regulating glycolysis - the seventh hallmark of cancer. *Cell Mol Life Sci* **65**, 3981-99 (2008).
55. Brahimi-Horn, M.C., Chiche, J. & Pouyssegur, J. Hypoxia signalling controls metabolic demand. *Curr Opin Cell Biol* **19**, 223-9 (2007).

56. Papandreou, I., Cairns, R.A., Fontana, L., Lim, A.L. & Denko, N.C. HIF-1 mediates adaptation to hypoxia by actively downregulating mitochondrial oxygen consumption. *Cell Metab* **3**, 187-97 (2006).
57. Kim, J.W., Tchernyshyov, I., Semenza, G.L. & Dang, C.V. HIF-1-mediated expression of pyruvate dehydrogenase kinase: a metabolic switch required for cellular adaptation to hypoxia. *Cell Metab* **3**, 177-85 (2006).
58. Lum, J.J., Bui, T., Gruber, M., Gordan, J.D., DeBerardinis, R.J., Covello, K.L., Simon, M.C. & Thompson, C.B. The transcription factor HIF-1alpha plays a critical role in the growth factor-dependent regulation of both aerobic and anaerobic glycolysis. *Genes Dev* **21**, 1037-49 (2007).
59. Shen, G.M., Zhang, F.L., Liu, X.L. & Zhang, J.W. Hypoxia-inducible factor 1-mediated regulation of PPP1R3C promotes glycogen accumulation in human MCF-7 cells under hypoxia. *FEBS Lett* **584**, 4366-72 (2010).
60. Osthus, R.C., Shim, H., Kim, S., Li, Q., Reddy, R., Mukherjee, M., Xu, Y., Wonsey, D., Lee, L.A. & Dang, C.V. Deregulation of glucose transporter 1 and glycolytic gene expression by c-Myc. *J Biol Chem* **275**, 21797-800 (2000).
61. Kim, J.W., Gao, P., Liu, Y.C., Semenza, G.L. & Dang, C.V. Hypoxia-inducible factor 1 and dysregulated c-Myc cooperatively induce vascular endothelial growth factor and metabolic switches hexokinase 2 and pyruvate dehydrogenase kinase 1. *Mol Cell Biol* **27**, 7381-93 (2007).
62. Valera, A., Pujol, A., Gregori, X., Riu, E., Visa, J. & Bosch, F. Evidence from transgenic mice that myc regulates hepatic glycolysis. *FASEB J* **9**, 1067-78 (1995).
63. Subramanian, A. & Miller, D.M. Structural analysis of alpha-enolase. Mapping the functional domains involved in down-regulation of the c-myc protooncogene. *J Biol Chem* **275**, 5958-65 (2000).
64. Shim, H., Dolde, C., Lewis, B.C., Wu, C.S., Dang, G., Jungmann, R.A., Dalla-Favera, R. & Dang, C.V. c-Myc transactivation of LDH-A: implications for tumor metabolism and growth. *Proc Natl Acad Sci U S A* **94**, 6658-63 (1997).
65. Hu, S., Balakrishnan, A., Bok, R.A., Anderton, B., Larson, P.E., Nelson, S.J., Kurhanewicz, J., Vigneron, D.B. & Goga, A. 13C-pyruvate imaging reveals alterations in glycolysis that precede c-Myc-induced tumor formation and regression. *Cell Metab* **14**, 131-42 (2011).
66. David, C.J., Chen, M., Assanah, M., Canoll, P. & Manley, J.L. HnRNP proteins controlled by c-Myc deregulate pyruvate kinase mRNA splicing in cancer. *Nature* **463**, 364-8 (2010).
67. Plas, D.R. & Thompson, C.B. Akt-dependent transformation: there is more to growth than just surviving. *Oncogene* **24**, 7435-42 (2005).
68. Luo, J., Manning, B.D. & Cantley, L.C. Targeting the PI3K-Akt pathway in human cancer: rationale and promise. *Cancer Cell* **4**, 257-62 (2003).
69. Franke, T.F., Hornik, C.P., Segev, L., Shostak, G.A. & Sugimoto, C. PI3K/Akt and apoptosis: size matters. *Oncogene* **22**, 8983-98 (2003).
70. Rathmell, J.C., Fox, C.J., Plas, D.R., Hammerman, P.S., Cinalli, R.M. & Thompson, C.B. Akt-directed glucose metabolism can prevent Bax conformation change and promote growth factor-independent survival. *Mol Cell Biol* **23**, 7315-28 (2003).
71. Gottlob, K., Majewski, N., Kennedy, S., Kandel, E., Robey, R.B. & Hay, N. Inhibition of early apoptotic events by Akt/PKB is dependent on the first committed step of glycolysis and mitochondrial hexokinase. *Genes Dev* **15**, 1406-18 (2001).

72. Deprez, J., Vertommen, D., Alessi, D.R., Hue, L. & Rider, M.H. Phosphorylation and activation of heart 6-phosphofructo-2-kinase by protein kinase B and other protein kinases of the insulin signaling cascades. *J Biol Chem* **272**, 17269-75 (1997).
73. Laplante, M. & Sabatini, D.M. mTOR signaling in growth control and disease. *Cell* **149**, 274-93 (2012).
74. Wieman, H.L., Wofford, J.A. & Rathmell, J.C. Cytokine stimulation promotes glucose uptake via phosphatidylinositol-3 kinase/Akt regulation of Glut1 activity and trafficking. *Mol Biol Cell* **18**, 1437-46 (2007).
75. Edinger, A.L. & Thompson, C.B. Akt maintains cell size and survival by increasing mTOR-dependent nutrient uptake. *Mol Biol Cell* **13**, 2276-88 (2002).
76. Duvel, K., Yecies, J.L., Menon, S., Raman, P., Lipovsky, A.I., Souza, A.L., Triantafellow, E., Ma, Q., Gorski, R., Cleaver, S., Vander Heiden, M.G., MacKeigan, J.P., Finan, P.M., Clish, C.B., Murphy, L.O. & Manning, B.D. Activation of a metabolic gene regulatory network downstream of mTOR complex 1. *Mol Cell* **39**, 171-83 (2010).
77. Schieke, S.M., Phillips, D., McCoy, J.P., Jr., Aponte, A.M., Shen, R.F., Balaban, R.S. & Finkel, T. The mammalian target of rapamycin (mTOR) pathway regulates mitochondrial oxygen consumption and oxidative capacity. *J Biol Chem* **281**, 27643-52 (2006).
78. Ramanathan, A. & Schreiber, S.L. Direct control of mitochondrial function by mTOR. *Proc Natl Acad Sci U S A* **106**, 22229-32 (2009).
79. Cunningham, J.T., Rodgers, J.T., Arlow, D.H., Vazquez, F., Mootha, V.K. & Puigserver, P. mTOR controls mitochondrial oxidative function through a YY1-PGC-1alpha transcriptional complex. *Nature* **450**, 736-40 (2007).
80. Bentzinger, C.F., Romanino, K., Cloetta, D., Lin, S., Mascarenhas, J.B., Oliveri, F., Xia, J., Casanova, E., Costa, C.F., Brink, M., Zorzato, F., Hall, M.N. & Ruegg, M.A. Skeletal muscle-specific ablation of raptor, but not of rictor, causes metabolic changes and results in muscle dystrophy. *Cell Metab* **8**, 411-24 (2008).
81. Dang, C.V. Links between metabolism and cancer. *Genes Dev* **26**, 877-90 (2012).
82. DeBerardinis, R.J., Mancuso, A., Daikhin, E., Nissim, I., Yudkoff, M., Wehrli, S. & Thompson, C.B. Beyond aerobic glycolysis: transformed cells can engage in glutamine metabolism that exceeds the requirement for protein and nucleotide synthesis. *Proc Natl Acad Sci U S A* **104**, 19345-50 (2007).
83. Wise, D.R., DeBerardinis, R.J., Mancuso, A., Sayed, N., Zhang, X.Y., Pfeiffer, H.K., Nissim, I., Daikhin, E., Yudkoff, M., McMahon, S.B. & Thompson, C.B. Myc regulates a transcriptional program that stimulates mitochondrial glutaminolysis and leads to glutamine addiction. *Proc Natl Acad Sci U S A* **105**, 18782-7 (2008).
84. Csibi, A., Fendt, S.M., Li, C., Poulogiannis, G., Choo, A.Y., Chapski, D.J., Jeong, S.M., Dempsey, J.M., Parkhitko, A., Morrison, T., Henske, E.P., Haigis, M.C., Cantley, L.C., Stephanopoulos, G., Yu, J. & Blenis, J. The mTORC1 pathway stimulates glutamine metabolism and cell proliferation by repressing SIRT4. *Cell* **153**, 840-54 (2013).
85. Son, J., Lyssiotis, C.A., Ying, H., Wang, X., Hua, S., Ligorio, M., Perera, R.M., Ferrone, C.R., Mullarky, E., Shyh-Chang, N., Kang, Y., Fleming, J.B., Bardeesy, N., Asara, J.M., Haigis, M.C., DePinho, R.A., Cantley, L.C. & Kimmelman, A.C. Glutamine supports pancreatic cancer growth through a KRAS-regulated metabolic pathway. *Nature* **496**, 101-5 (2013).
86. Hensley, C.T., Wasti, A.T. & DeBerardinis, R.J. Glutamine and cancer: cell biology, physiology, and clinical opportunities. *J Clin Invest* **123**, 3678-84 (2013).

87. DeBerardinis, R.J. & Cheng, T. Q's next: the diverse functions of glutamine in metabolism, cell biology and cancer. *Oncogene* **29**, 313-24 (2010).
88. Gaglio, D., Soldati, C., Vanoni, M., Alberghina, L. & Chiaradonna, F. Glutamine deprivation induces abortive s-phase rescued by deoxyribonucleotides in k-ras transformed fibroblasts. *PLoS One* **4**, e4715 (2009).
89. Nicklin, P., Bergman, P., Zhang, B., Triantafellow, E., Wang, H., Nyfeler, B., Yang, H., Hild, M., Kung, C., Wilson, C., Myer, V.E., MacKeigan, J.P., Porter, J.A., Wang, Y.K., Cantley, L.C., Finan, P.M. & Murphy, L.O. Bidirectional transport of amino acids regulates mTOR and autophagy. *Cell* **136**, 521-34 (2009).
90. Portais, J.C., Voisin, P., Merle, M. & Canioni, P. Glucose and glutamine metabolism in C6 glioma cells studied by carbon 13 NMR. *Biochimie* **78**, 155-64 (1996).
91. Walther, J.L., Metallo, C.M., Zhang, J. & Stephanopoulos, G. Optimization of 13C isotopic tracers for metabolic flux analysis in mammalian cells. *Metab Eng* **14**, 162-71 (2012).
92. Goltsov, A., Faratian, D., Langdon, S.P., Mullen, P., Harrison, D.J. & Bown, J. Features of the reversible sensitivity-resistance transition in PI3K/PTEN/AKT signalling network after HER2 inhibition. *Cell Signal* **24**, 493-504 (2012).
93. Qing, G., Li, B., Vu, A., Skuli, N., Walton, Z.E., Liu, X., Mayes, P.A., Wise, D.R., Thompson, C.B., Maris, J.M., Hogarty, M.D. & Simon, M.C. ATF4 regulates MYC-mediated neuroblastoma cell death upon glutamine deprivation. *Cancer Cell* **22**, 631-44 (2012).
94. Qu, W., Oya, S., Lieberman, B.P., Ploessl, K., Wang, L., Wise, D.R., Divgi, C.R., Chodosh, L.A., Thompson, C.B. & Kung, H.F. Preparation and characterization of L-[5-11C]-glutamine for metabolic imaging of tumors. *J Nucl Med* **53**, 98-105 (2012).
95. Boroughs, L.K. & DeBerardinis, R.J. Metabolic pathways promoting cancer cell survival and growth. *Nat Cell Biol* **17**, 351-9 (2015).
96. Holleran, A.L., Briscoe, D.A., Fiskum, G. & Kelleher, J.K. Glutamine metabolism in AS-30D hepatoma cells. Evidence for its conversion into lipids via reductive carboxylation. *Mol Cell Biochem* **152**, 95-101 (1995).
97. Yang, C., Ko, B., Hensley, C.T., Jiang, L., Wasti, A.T., Kim, J., Sudderth, J., Calvaruso, M.A., Lumata, L., Mitsche, M., Rutter, J., Merritt, M.E. & DeBerardinis, R.J. Glutamine oxidation maintains the TCA cycle and cell survival during impaired mitochondrial pyruvate transport. *Mol Cell* **56**, 414-24 (2014).
98. Yuneva, M., Zamboni, N., Oefner, P., Sachidanandam, R. & Lazebnik, Y. Deficiency in glutamine but not glucose induces MYC-dependent apoptosis in human cells. *J Cell Biol* **178**, 93-105 (2007).
99. Le, A., Lane, A.N., Hamaker, M., Bose, S., Gouw, A., Barbi, J., Tsukamoto, T., Rojas, C.J., Slusher, B.S., Zhang, H., Zimmerman, L.J., Liebler, D.C., Slebos, R.J., Lorkiewicz, P.K., Higashi, R.M., Fan, T.W. & Dang, C.V. Glucose-independent glutamine metabolism via TCA cycling for proliferation and survival in B cells. *Cell Metab* **15**, 110-21 (2012).
100. Cairns, R.A., Harris, I.S. & Mak, T.W. Regulation of cancer cell metabolism. *Nat Rev Cancer* **11**, 85-95 (2011).
101. Carracedo, A., Cantley, L.C. & Pandolfi, P.P. Cancer metabolism: fatty acid oxidation in the limelight. *Nat Rev Cancer* **13**, 227-32 (2013).
102. Smolkova, K. & Jezek, P. The Role of Mitochondrial NADPH-Dependent Isocitrate Dehydrogenase in Cancer Cells. *Int J Cell Biol* **2012**, 273947 (2012).
103. Yan, H., Parsons, D.W., Jin, G., McLendon, R., Rasheed, B.A., Yuan, W., Kos, I., Batinic-Haberle, I., Jones, S., Riggins, G.J., Friedman, H., Friedman, A., Reardon, D., Herndon, J., Kinzler, K.W.,

Velculescu, V.E., Vogelstein, B. & Bigner, D.D. IDH1 and IDH2 mutations in gliomas. *N Engl J Med* **360**, 765-73 (2009).

104. Jiang, P., Du, W., Mancuso, A., Wellen, K.E. & Yang, X. Reciprocal regulation of p53 and malic enzymes modulates metabolism and senescence. *Nature* **493**, 689-93 (2013).
105. Lieberman, B.P., Ploessl, K., Wang, L., Qu, W., Zha, Z., Wise, D.R., Chodosh, L.A., Belka, G., Thompson, C.B. & Kung, H.F. PET imaging of glutaminolysis in tumors by 18F-(2S,4R)4-fluoroglutamine. *J Nucl Med* **52**, 1947-55 (2011).
106. Venneti, S., Dunphy, M.P., Zhang, H., Pitter, K.L., Zanzonico, P., Campos, C., Carlin, S.D., La Rocca, G., Lyashchenko, S., Ploessl, K., Rohle, D., Omuro, A.M., Cross, J.R., Brennan, C.W., Weber, W.A., Holland, E.C., Mellinghoff, I.K., Kung, H.F., Lewis, J.S. & Thompson, C.B. Glutamine-based PET imaging facilitates enhanced metabolic evaluation of gliomas in vivo. *Sci Transl Med* **7**, 274ra17 (2015).
107. Gao, P., Tchernyshyov, I., Chang, T.C., Lee, Y.S., Kita, K., Ochi, T., Zeller, K.I., De Marzo, A.M., Van Eyk, J.E., Mendell, J.T. & Dang, C.V. c-Myc suppression of miR-23a/b enhances mitochondrial glutaminase expression and glutamine metabolism. *Nature* **458**, 762-5 (2009).
108. Murphy, T.A., Dang, C.V. & Young, J.D. Isotopically nonstationary 13C flux analysis of Myc-induced metabolic reprogramming in B-cells. *Metab Eng* **15**, 206-17 (2013).
109. Liu, W., Le, A., Hancock, C., Lane, A.N., Dang, C.V., Fan, T.W. & Phang, J.M. Reprogramming of proline and glutamine metabolism contributes to the proliferative and metabolic responses regulated by oncogenic transcription factor c-MYC. *Proc Natl Acad Sci U S A* **109**, 8983-8 (2012).
110. Yuneva, M.O., Fan, T.W., Allen, T.D., Higashi, R.M., Ferraris, D.V., Tsukamoto, T., Mates, J.M., Alonso, F.J., Wang, C., Seo, Y., Chen, X. & Bishop, J.M. The metabolic profile of tumors depends on both the responsible genetic lesion and tissue type. *Cell Metab* **15**, 157-70 (2012).
111. Ren, P., Yue, M., Xiao, D., Xiu, R., Gan, L., Liu, H. & Qing, G. ATF4 and N-Myc coordinate glutamine metabolism in MYCN-amplified neuroblastoma cells through ASCT2 activation. *J Pathol* **235**, 90-100 (2015).
112. Reid, M.A., Wang, W.I., Rosales, K.R., Welliver, M.X., Pan, M. & Kong, M. The B55alpha subunit of PP2A drives a p53-dependent metabolic adaptation to glutamine deprivation. *Mol Cell* **50**, 200-11 (2013).
113. Todorova, V.K., Kaufmann, Y., Luo, S. & Klimberg, V.S. Modulation of p53 and c-myc in DMBA-induced mammary tumors by oral glutamine. *Nutr Cancer* **54**, 263-73 (2006).
114. Soh, H., Wasa, M. & Fukuzawa, M. Hypoxia upregulates amino acid transport in a human neuroblastoma cell line. *J Pediatr Surg* **42**, 608-12 (2007).
115. Kobayashi, S. & Millhorn, D.E. Hypoxia regulates glutamate metabolism and membrane transport in rat PC12 cells. *J Neurochem* **76**, 1935-48 (2001).
116. Metallo, C.M., Gameiro, P.A., Bell, E.L., Mattaini, K.R., Yang, J., Hiller, K., Jewell, C.M., Johnson, Z.R., Irvine, D.J., Guarente, L., Kelleher, J.K., Vander Heiden, M.G., Iliopoulos, O. & Stephanopoulos, G. Reductive glutamine metabolism by IDH1 mediates lipogenesis under hypoxia. *Nature* **481**, 380-4 (2012).
117. Mullen, A.R., Wheaton, W.W., Jin, E.S., Chen, P.H., Sullivan, L.B., Cheng, T., Yang, Y., Linehan, W.M., Chandel, N.S. & DeBerardinis, R.J. Reductive carboxylation supports growth in tumour cells with defective mitochondria. *Nature* **481**, 385-8 (2012).
118. Wise, D.R., Ward, P.S., Shay, J.E., Cross, J.R., Gruber, J.J., Sachdeva, U.M., Platt, J.M., DeMatteo, R.G., Simon, M.C. & Thompson, C.B. Hypoxia promotes isocitrate dehydrogenase-dependent

carboxylation of alpha-ketoglutarate to citrate to support cell growth and viability. *Proc Natl Acad Sci U S A* **108**, 19611-6 (2011).

119. Parsons, D.W., Jones, S., Zhang, X., Lin, J.C., Leary, R.J., Angenendt, P., Mankoo, P., Carter, H., Siu, I.M., Gallia, G.L., Olivi, A., McLendon, R., Rasheed, B.A., Keir, S., Nikolskaya, T., Nikolsky, Y., Busam, D.A., Tekleab, H., Diaz, L.A., Jr., Hartigan, J., Smith, D.R., Strausberg, R.L., Marie, S.K., Shinjo, S.M., Yan, H., Riggins, G.J., Bigner, D.D., Karchin, R., Papadopoulos, N., Parmigiani, G., Vogelstein, B., Velculescu, V.E. & Kinzler, K.W. An integrated genomic analysis of human glioblastoma multiforme. *Science* **321**, 1807-12 (2008).
120. Mardis, E.R., Ding, L., Dooling, D.J., Larson, D.E., McLellan, M.D., Chen, K., Koboldt, D.C., Fulton, R.S., Delehaunty, K.D., McGrath, S.D., Fulton, L.A., Locke, D.P., Magrini, V.J., Abbott, R.M., Vickery, T.L., Reed, J.S., Robinson, J.S., Wylie, T., Smith, S.M., Carmichael, L., Eldred, J.M., Harris, C.C., Walker, J., Peck, J.B., Du, F., Dukes, A.F., Sanderson, G.E., Brummett, A.M., Clark, E., McMichael, J.F., Meyer, R.J., Schindler, J.K., Pohl, C.S., Wallis, J.W., Shi, X., Lin, L., Schmidt, H., Tang, Y., Haipek, C., Wiechert, M.E., Ivy, J.V., Kalicki, J., Elliott, G., Ries, R.E., Payton, J.E., Westervelt, P., Tomasson, M.H., Watson, M.A., Baty, J., Heath, S., Shannon, W.D., Nagarajan, R., Link, D.C., Walter, M.J., Graubert, T.A., DiPersio, J.F., Wilson, R.K. & Ley, T.J. Recurring mutations found by sequencing an acute myeloid leukemia genome. *N Engl J Med* **361**, 1058-66 (2009).
121. Amary, M.F., Bacsi, K., Maggiani, F., Damato, S., Halai, D., Berisha, F., Pollock, R., O'Donnell, P., Grigoriadis, A., Diss, T., Eskandarpour, M., Presneau, N., Hogendoorn, P.C., Futreal, A., Tirabosco, R. & Flanagan, A.M. IDH1 and IDH2 mutations are frequent events in central chondrosarcoma and central and periosteal chondromas but not in other mesenchymal tumours. *J Pathol* **224**, 334-43 (2011).
122. Dang, L., White, D.W., Gross, S., Bennett, B.D., Bittinger, M.A., Driggers, E.M., Fantin, V.R., Jang, H.G., Jin, S., Keenan, M.C., Marks, K.M., Prins, R.M., Ward, P.S., Yen, K.E., Liau, L.M., Rabinowitz, J.D., Cantley, L.C., Thompson, C.B., Vander Heiden, M.G. & Su, S.M. Cancer-associated IDH1 mutations produce 2-hydroxyglutarate. *Nature* **462**, 739-44 (2009).
123. Xu, W., Yang, H., Liu, Y., Yang, Y., Wang, P., Kim, S.H., Ito, S., Yang, C., Wang, P., Xiao, M.T., Liu, L.X., Jiang, W.Q., Liu, J., Zhang, J.Y., Wang, B., Frye, S., Zhang, Y., Xu, Y.H., Lei, Q.Y., Guan, K.L., Zhao, S.M. & Xiong, Y. Oncometabolite 2-hydroxyglutarate is a competitive inhibitor of alpha-ketoglutarate-dependent dioxygenases. *Cancer Cell* **19**, 17-30 (2011).
124. Lu, C., Ward, P.S., Kapoor, G.S., Rohle, D., Turcan, S., Abdel-Wahab, O., Edwards, C.R., Khanin, R., Figueroa, M.E., Melnick, A., Wellen, K.E., O'Rourke, D.M., Berger, S.L., Chan, T.A., Levine, R.L., Mellinghoff, I.K. & Thompson, C.B. IDH mutation impairs histone demethylation and results in a block to cell differentiation. *Nature* **483**, 474-8 (2012).
125. Guo, J.U., Su, Y., Zhong, C., Ming, G.L. & Song, H. Hydroxylation of 5-methylcytosine by TET1 promotes active DNA demethylation in the adult brain. *Cell* **145**, 423-34 (2011).
126. Figueroa, M.E., Abdel-Wahab, O., Lu, C., Ward, P.S., Patel, J., Shih, A., Li, Y., Bhagwat, N., Vasanthakumar, A., Fernandez, H.F., Tallman, M.S., Sun, Z., Wolniak, K., Peeters, J.K., Liu, W., Choe, S.E., Fantin, V.R., Paietta, E., Lowenberg, B., Licht, J.D., Godley, L.A., Delwel, R., Valk, P.J., Thompson, C.B., Levine, R.L. & Melnick, A. Leukemic IDH1 and IDH2 mutations result in a hypermethylation phenotype, disrupt TET2 function, and impair hematopoietic differentiation. *Cancer Cell* **18**, 553-67 (2010).
127. Williams, S.C., Karajannis, M.A., Chiriboga, L., Golfinos, J.G., von Deimling, A. & Zagzag, D. R132H-mutation of isocitrate dehydrogenase-1 is not sufficient for HIF-1alpha upregulation in adult glioma. *Acta Neuropathol* **121**, 279-81 (2011).

128. Metellus, P., Colin, C., Taieb, D., Guedj, E., Nanni-Metellus, I., de Paula, A.M., Colavolpe, C., Fuentes, S., Dufour, H., Barrie, M., Chinot, O., Ouafik, L. & Figarella-Branger, D. IDH mutation status impact on in vivo hypoxia biomarkers expression: new insights from a clinical, nuclear imaging and immunohistochemical study in 33 glioma patients. *J Neurooncol* **105**, 591-600 (2011).
129. Jin, G., Reitman, Z.J., Spasojevic, I., Batinic-Haberle, I., Yang, J., Schmidt-Kittler, O., Bigner, D.D. & Yan, H. 2-hydroxyglutarate production, but not dominant negative function, is conferred by glioma-derived NADP-dependent isocitrate dehydrogenase mutations. *PLoS One* **6**, e16812 (2011).
130. Chowdhury, R., Yeoh, K.K., Tian, Y.M., Hillringhaus, L., Bagg, E.A., Rose, N.R., Leung, I.K., Li, X.S., Woon, E.C., Yang, M., McDonough, M.A., King, O.N., Clifton, I.J., Klose, R.J., Claridge, T.D., Ratcliffe, P.J., Schofield, C.J. & Kawamura, A. The oncometabolite 2-hydroxyglutarate inhibits histone lysine demethylases. *EMBO Rep* **12**, 463-9 (2011).
131. Wullschleger, S., Loewith, R. & Hall, M.N. TOR signaling in growth and metabolism. *Cell* **124**, 471-84 (2006).
132. Crespo, J.L., Powers, T., Fowler, B. & Hall, M.N. The TOR-controlled transcription activators GLN3, RTG1, and RTG3 are regulated in response to intracellular levels of glutamine. *Proc Natl Acad Sci U S A* **99**, 6784-9 (2002).
133. Hara, K., Yonezawa, K., Weng, Q.P., Kozlowski, M.T., Belham, C. & Avruch, J. Amino acid sufficiency and mTOR regulate p70 S6 kinase and eIF-4E BP1 through a common effector mechanism. *J Biol Chem* **273**, 14484-94 (1998).
134. Krause, U., Bertrand, L., Maisin, L., Rosa, M. & Hue, L. Signalling pathways and combinatory effects of insulin and amino acids in isolated rat hepatocytes. *Eur J Biochem* **269**, 3742-50 (2002).
135. Duran, R.V., Oppliger, W., Robitaille, A.M., Heiserich, L., Skendaj, R., Gottlieb, E. & Hall, M.N. Glutaminolysis activates Rag-mTORC1 signaling. *Mol Cell* **47**, 349-58 (2012).
136. Kim, S.G., Hoffman, G.R., Poulogiannis, G., Buel, G.R., Jang, Y.J., Lee, K.W., Kim, B.Y., Erikson, R.L., Cantley, L.C., Choo, A.Y. & Blenis, J. Metabolic stress controls mTORC1 lysosomal localization and dimerization by regulating the TTT-RUVBL1/2 complex. *Mol Cell* **49**, 172-85 (2013).
137. Richards, N.G. & Kilberg, M.S. Asparagine synthetase chemotherapy. *Annu Rev Biochem* **75**, 629-54 (2006).
138. Balasubramanian, M.N., Butterworth, E.A. & Kilberg, M.S. Asparagine synthetase: regulation by cell stress and involvement in tumor biology. *Am J Physiol Endocrinol Metab* **304**, E789-99 (2013).
139. Balasubramanian, M.N., Shan, J. & Kilberg, M.S. Dynamic changes in genomic histone association and modification during activation of the ASNS and ATF3 genes by amino acid limitation. *Biochem J* **449**, 219-29 (2013).
140. Andrulis, I.L., Hatfield, G.W. & Arfin, S.M. Asparaginyl-tRNA aminoacylation levels and asparagine synthetase expression in cultured Chinese hamster ovary cells. *J Biol Chem* **254**, 10629-33 (1979).
141. Arfin, S.M., Simpson, D.R., Chiang, C.S., Andrulis, I.L. & Hatfield, G.W. A role for asparaginyl-tRNA in the regulation of asparagine synthetase in a mammalian cell line. *Proc Natl Acad Sci U S A* **74**, 2367-9 (1977).
142. Gong, S.S., Guerrini, L. & Basilico, C. Regulation of asparagine synthetase gene expression by amino acid starvation. *Mol Cell Biol* **11**, 6059-66 (1991).
143. Cui, H., Darmanin, S., Natsuisaka, M., Kondo, T., Asaka, M., Shindoh, M., Higashino, F., Hamuro, J., Okada, F., Kobayashi, M., Nakagawa, K., Koide, H. & Kobayashi, M. Enhanced expression of asparagine synthetase under glucose-deprived conditions protects pancreatic cancer cells from apoptosis induced by glucose deprivation and cisplatin. *Cancer Res* **67**, 3345-55 (2007).

144. Lorenzi, P.L., Llamas, J., Gunsior, M., Ozbun, L., Reinhold, W.C., Varma, S., Ji, H., Kim, H., Hutchinson, A.A., Kohn, E.C., Goldsmith, P.K., Birrer, M.J. & Weinstein, J.N. Asparagine synthetase is a predictive biomarker of L-asparaginase activity in ovarian cancer cell lines. *Mol Cancer Ther* **7**, 3123-8 (2008).
145. Patterson, M.K., Jr. & Orr, G.R. Regeneration, tumor, dietary, and L-asparaginase effects on asparagine biosynthesis in rat liver. *Cancer Res* **29**, 1179-83 (1969).
146. Ye, J., Kumanova, M., Hart, L.S., Sloane, K., Zhang, H., De Panis, D.N., Bobrovnikova-Marjon, E., Diehl, J.A., Ron, D. & Koumenis, C. The GCN2-ATF4 pathway is critical for tumour cell survival and proliferation in response to nutrient deprivation. *EMBO J* **29**, 2082-96 (2010).
147. Zhang, J., Fan, J., Venneti, S., Cross, J.R., Takagi, T., Bhinder, B., Djaballah, H., Kanai, M., Cheng, E.H., Judkins, A.R., Pawel, B., Baggs, J., Cherry, S., Rabinowitz, J.D. & Thompson, C.B. Asparagine plays a critical role in regulating cellular adaptation to glutamine depletion. *Mol Cell* **56**, 205-18 (2014).
148. Li, H., Zhou, F., Du, W., Dou, J., Xu, Y., Gao, W., Chen, G., Zuo, X., Sun, L., Zhang, X. & Yang, S. Knockdown of asparagine synthetase by RNAi suppresses cell growth in human melanoma cells and epidermoid carcinoma cells. *Biotechnol Appl Biochem* **63**, 328-33 (2016).
149. Hettmer, S., Schinzel, A.C., Tchessalova, D., Schneider, M., Parker, C.L., Bronson, R.T., Richards, N.G., Hahn, W.C. & Wagers, A.J. Functional genomic screening reveals asparagine dependence as a metabolic vulnerability in sarcoma. *Elife* **4** (2015).
150. Scian, M.J., Stagliano, K.E., Deb, D., Ellis, M.A., Carchman, E.H., Das, A., Valerie, K., Deb, S.P. & Deb, S. Tumor-derived p53 mutants induce oncogenesis by transactivating growth-promoting genes. *Oncogene* **23**, 4430-43 (2004).
151. Horiguchi, M., Koyanagi, S., Okamoto, A., Suzuki, S.O., Matsunaga, N. & Ohdo, S. Stress-regulated transcription factor ATF4 promotes neoplastic transformation by suppressing expression of the INK4a/ARF cell senescence factors. *Cancer Res* **72**, 395-401 (2012).
152. Siu, F., Bain, P.J., LeBlanc-Chaffin, R., Chen, H. & Kilberg, M.S. ATF4 is a mediator of the nutrient-sensing response pathway that activates the human asparagine synthetase gene. *J Biol Chem* **277**, 24120-7 (2002).
153. Siu, F., Chen, C., Zhong, C. & Kilberg, M.S. CCAAT/enhancer-binding protein-beta is a mediator of the nutrient-sensing response pathway that activates the human asparagine synthetase gene. *J Biol Chem* **276**, 48100-7 (2001).
154. Su, N. & Kilberg, M.S. C/EBP homology protein (CHOP) interacts with activating transcription factor 4 (ATF4) and negatively regulates the stress-dependent induction of the asparagine synthetase gene. *J Biol Chem* **283**, 35106-17 (2008).
155. Krall, A.S., Xu, S., Graeber, T.G., Braas, D. & Christofk, H.R. Asparagine promotes cancer cell proliferation through use as an amino acid exchange factor. *Nat Commun* **7**, 11457 (2016).
156. Ellinger-Ziegelbauer, H., Hihi, A.K., Laudet, V., Keller, H., Wahli, W. & Dreyer, C. FTZ-F1-related orphan receptors in Xenopus laevis: transcriptional regulators differentially expressed during early embryogenesis. *Mol Cell Biol* **14**, 2786-97 (1994).
157. Galarneau, L., Pare, J.F., Allard, D., Hamel, D., Levesque, L., Tugwood, J.D., Green, S. & Belanger, L. The alpha1-fetoprotein locus is activated by a nuclear receptor of the Drosophila FTZ-F1 family. *Mol Cell Biol* **16**, 3853-65 (1996).
158. Kudo, T. & Sutou, S. Molecular cloning of chicken FTZ-F1-related orphan receptors. *Gene* **197**, 261-8 (1997).

159. Liu, D., Le Drean, Y., Ekker, M., Xiong, F. & Hew, C.L. Teleost FTZ-F1 homolog and its splicing variant determine the expression of the salmon gonadotropin IIbeta subunit gene. *Mol Endocrinol* **11**, 877-90 (1997).
160. Boerboom, D., Pilon, N., Behdjani, R., Silversides, D.W. & Sirois, J. Expression and regulation of transcripts encoding two members of the NR5A nuclear receptor subfamily of orphan nuclear receptors, steroidogenic factor-1 and NR5A2, in equine ovarian cells during the ovulatory process. *Endocrinology* **141**, 4647-56 (2000).
161. Nakajima, T., Takase, M., Miura, I. & Nakamura, M. Two isoforms of FTZ-F1 messenger RNA: molecular cloning and their expression in the frog testis. *Gene* **248**, 203-12 (2000).
162. Becker-Andre, M., Andre, E. & DeLamarter, J.F. Identification of nuclear receptor mRNAs by RT-PCR amplification of conserved zinc-finger motif sequences. *Biochem Biophys Res Commun* **194**, 1371-9 (1993).
163. Galarneau, L., Drouin, R. & Belanger, L. Assignment of the fetoprotein transcription factor gene (FTF) to human chromosome band 1q32.11 by in situ hybridization. *Cytogenet Cell Genet* **82**, 269-70 (1998).
164. Li, M., Xie, Y.H., Kong, Y.Y., Wu, X., Zhu, L. & Wang, Y. Cloning and characterization of a novel human hepatocyte transcription factor, hB1F, which binds and activates enhancer II of hepatitis B virus. *J Biol Chem* **273**, 29022-31 (1998).
165. Nitta, M., Ku, S., Brown, C., Okamoto, A.Y. & Shan, B. CPF: an orphan nuclear receptor that regulates liver-specific expression of the human cholesterol 7alpha-hydroxylase gene. *Proc Natl Acad Sci U S A* **96**, 6660-5 (1999).
166. Sablin, E.P., Krylova, I.N., Fletterick, R.J. & Ingraham, H.A. Structural basis for ligand-independent activation of the orphan nuclear receptor LRH-1. *Mol Cell* **11**, 1575-85 (2003).
167. Krylova, I.N., Sablin, E.P., Moore, J., Xu, R.X., Waitt, G.M., MacKay, J.A., Juzumiene, D., Bynum, J.M., Madauss, K., Montana, V., Lebedeva, L., Suzawa, M., Williams, J.D., Williams, S.P., Guy, R.K., Thornton, J.W., Fletterick, R.J., Willson, T.M. & Ingraham, H.A. Structural analyses reveal phosphatidyl inositols as ligands for the NR5 orphan receptors SF-1 and LRH-1. *Cell* **120**, 343-55 (2005).
168. Wang, W., Zhang, C., Marimuthu, A., Krupka, H.I., Tabrizizad, M., Shelloe, R., Mehra, U., Eng, K., Nguyen, H., Settachatgul, C., Powell, B., Milburn, M.V. & West, B.L. The crystal structures of human steroidogenic factor-1 and liver receptor homologue-1. *Proc Natl Acad Sci U S A* **102**, 7505-10 (2005).
169. Sablin, E.P., Blind, R.D., Uthayaruban, R., Chiu, H.J., Deacon, A.M., Das, D., Ingraham, H.A. & Fletterick, R.J. Structure of Liver Receptor Homolog-1 (NR5A2) with PIP3 hormone bound in the ligand binding pocket. *J Struct Biol* **192**, 342-8 (2015).
170. Lee, J.M., Lee, Y.K., Mamrosh, J.L., Busby, S.A., Griffin, P.R., Pathak, M.C., Ortlund, E.A. & Moore, D.D. A nuclear-receptor-dependent phosphatidylcholine pathway with antidiabetic effects. *Nature* **474**, 506-10 (2011).
171. Musille, P.M., Pathak, M.C., Lauer, J.L., Hudson, W.H., Griffin, P.R. & Ortlund, E.A. Antidiabetic phospholipid-nuclear receptor complex reveals the mechanism for phospholipid-driven gene regulation. *Nat Struct Mol Biol* **19**, 532-7, S1-2 (2012).
172. Benod, C., Carlsson, J., Uthayaruban, R., Hwang, P., Irwin, J.J., Doak, A.K., Shoichet, B.K., Sablin, E.P. & Fletterick, R.J. Structure-based discovery of antagonists of nuclear receptor LRH-1. *J Biol Chem* **288**, 19830-44 (2013).

173. Corzo, C.A., Mari, Y., Chang, M.R., Khan, T., Kuruvilla, D., Nuhant, P., Kumar, N., West, G.M., Duckett, D.R., Roush, W.R. & Griffin, P.R. Antiproliferation activity of a small molecule repressor of liver receptor homolog 1. *Mol Pharmacol* **87**, 296-304 (2015).
174. Rey, J., Hu, H., Kyle, F., Lai, C.F., Buluwela, L., Coombes, R.C., Ortlund, E.A., Ali, S., Snyder, J.P. & Barrett, A.G. Discovery of a new class of liver receptor homolog-1 (LRH-1) antagonists: virtual screening, synthesis and biological evaluation. *ChemMedChem* **7**, 1909-14 (2012).
175. Whitby, R.J., Dixon, S., Maloney, P.R., Delerive, P., Goodwin, B.J., Parks, D.J. & Willson, T.M. Identification of small molecule agonists of the orphan nuclear receptors liver receptor homolog-1 and steroidogenic factor-1. *J Med Chem* **49**, 6652-5 (2006).
176. Whitby, R.J., Stec, J., Blind, R.D., Dixon, S., Leesnitzer, L.M., Orband-Miller, L.A., Williams, S.P., Willson, T.M., Xu, R., Zuercher, W.J., Cai, F. & Ingraham, H.A. Small molecule agonists of the orphan nuclear receptors steroidogenic factor-1 (SF-1, NR5A1) and liver receptor homologue-1 (LRH-1, NR5A2). *J Med Chem* **54**, 2266-81 (2011).
177. Lee, M.B., Lebedeva, L.A., Suzawa, M., Wadekar, S.A., Desclozeaux, M. & Ingraham, H.A. The DEAD-box protein DP103 (Ddx20 or Gemin-3) represses orphan nuclear receptor activity via SUMO modification. *Mol Cell Biol* **25**, 1879-90 (2005).
178. Lee, Y.K., Choi, Y.H., Chua, S., Park, Y.J. & Moore, D.D. Phosphorylation of the hinge domain of the nuclear hormone receptor LRH-1 stimulates transactivation. *J Biol Chem* **281**, 7850-5 (2006).
179. Chalkiadaki, A. & Talianidis, I. SUMO-dependent compartmentalization in promyelocytic leukemia protein nuclear bodies prevents the access of LRH-1 to chromatin. *Mol Cell Biol* **25**, 5095-105 (2005).
180. Venteclef, N., Jakobsson, T., Ehrlund, A., Damdimopoulos, A., Mikkonen, L., Ellis, E., Nilsson, L.M., Parini, P., Janne, O.A., Gustafsson, J.A., Steffensen, K.R. & Treuter, E. GPS2-dependent corepressor/SUMO pathways govern anti-inflammatory actions of LRH-1 and LXRbeta in the hepatic acute phase response. *Genes Dev* **24**, 381-95 (2010).
181. Stein, S. & Schoonjans, K. Molecular basis for the regulation of the nuclear receptor LRH-1. *Curr Opin Cell Biol* **33**, 26-34 (2015).
182. Stergiopoulos, A. & Politis, P.K. Nuclear receptor NR5A2 controls neural stem cell fate decisions during development. *Nat Commun* **7**, 12230 (2016).
183. Holmstrom, S.R., Deering, T., Swift, G.H., Poelwijk, F.J., Mangelsdorf, D.J., Kliewer, S.A. & MacDonald, R.J. LRH-1 and PTF1-L coregulate an exocrine pancreas-specific transcriptional network for digestive function. *Genes Dev* **25**, 1674-9 (2011).
184. Kim, J.W., Havelock, J.C., Carr, B.R. & Attia, G.R. The orphan nuclear receptor, liver receptor homolog-1, regulates cholesterol side-chain cleavage cytochrome p450 enzyme in human granulosa cells. *J Clin Endocrinol Metab* **90**, 1678-85 (2005).
185. Liu, D.L., Liu, W.Z., Li, Q.L., Wang, H.M., Qian, D., Treuter, E. & Zhu, C. Expression and functional analysis of liver receptor homologue 1 as a potential steroidogenic factor in rat ovary. *Biol Reprod* **69**, 508-17 (2003).
186. Peng, N., Kim, J.W., Rainey, W.E., Carr, B.R. & Attia, G.R. The role of the orphan nuclear receptor, liver receptor homologue-1, in the regulation of human corpus luteum 3beta-hydroxysteroid dehydrogenase type II. *J Clin Endocrinol Metab* **88**, 6020-8 (2003).
187. Saxena, D., Escamilla-Hernandez, R., Little-Ihrig, L. & Zeleznik, A.J. Liver receptor homolog-1 and steroidogenic factor-1 have similar actions on rat granulosa cell steroidogenesis. *Endocrinology* **148**, 726-34 (2007).

188. Duggavathi, R., Volle, D.H., Mataki, C., Antal, M.C., Messaddeq, N., Auwerx, J., Murphy, B.D. & Schoonjans, K. Liver receptor homolog 1 is essential for ovulation. *Genes Dev* **22**, 1871-6 (2008).
189. Zhang, C., Large, M.J., Duggavathi, R., DeMayo, F.J., Lydon, J.P., Schoonjans, K., Kovanci, E. & Murphy, B.D. Liver receptor homolog-1 is essential for pregnancy. *Nat Med* **19**, 1061-6 (2013).
190. Leung, T.H., Wong, N., Lai, P.B., Chan, A., To, K.F., Liew, C.T., Lau, W.Y. & Johnson, P.J. Identification of four distinct regions of allelic imbalances on chromosome 1 by the combined comparative genomic hybridization and microsatellite analysis on hepatocellular carcinoma. *Mod Pathol* **15**, 1213-20 (2002).
191. Sun, H.C. & Tang, Z.Y. Angiogenesis in hepatocellular carcinoma: the retrospectives and perspectives. *J Cancer Res Clin Oncol* **130**, 307-19 (2004).
192. Wang, G., Zhao, Y., Liu, X., Wang, L., Wu, C., Zhang, W., Liu, W., Zhang, P., Cong, W., Zhu, Y., Zhang, L., Chen, S., Wan, D., Zhao, X., Huang, W. & Gu, J. Allelic loss and gain, but not genomic instability, as the major somatic mutation in primary hepatocellular carcinoma. *Genes Chromosomes Cancer* **31**, 221-7 (2001).
193. del Castillo-Olivares, A. & Gil, G. Alpha 1-fetoprotein transcription factor is required for the expression of sterol 12alpha -hydroxylase, the specific enzyme for cholic acid synthesis. Potential role in the bile acid-mediated regulation of gene transcription. *J Biol Chem* **275**, 17793-9 (2000).
194. Goodwin, B., Jones, S.A., Price, R.R., Watson, M.A., McKee, D.D., Moore, L.B., Galardi, C., Wilson, J.G., Lewis, M.C., Roth, M.E., Maloney, P.R., Willson, T.M. & Kliewer, S.A. A regulatory cascade of the nuclear receptors FXR, SHP-1, and LRH-1 represses bile acid biosynthesis. *Mol Cell* **6**, 517-26 (2000).
195. Lu, T.T., Makishima, M., Repa, J.J., Schoonjans, K., Kerr, T.A., Auwerx, J. & Mangelsdorf, D.J. Molecular basis for feedback regulation of bile acid synthesis by nuclear receptors. *Mol Cell* **6**, 507-15 (2000).
196. Shin, D.J. & Osborne, T.F. Peroxisome proliferator-activated receptor-gamma coactivator-1alpha activation of CYP7A1 during food restriction and diabetes is still inhibited by small heterodimer partner. *J Biol Chem* **283**, 15089-96 (2008).
197. Lee, Y.K., Schmidt, D.R., Cummins, C.L., Choi, M., Peng, L., Zhang, Y., Goodwin, B., Hammer, R.E., Mangelsdorf, D.J. & Kliewer, S.A. Liver receptor homolog-1 regulates bile acid homeostasis but is not essential for feedback regulation of bile acid synthesis. *Mol Endocrinol* **22**, 1345-56 (2008).
198. Mataki, C., Magnier, B.C., Houten, S.M., Annicotte, J.S., Argmann, C., Thomas, C., Overmars, H., Kulik, W., Metzger, D., Auwerx, J. & Schoonjans, K. Compromised intestinal lipid absorption in mice with a liver-specific deficiency of liver receptor homolog 1. *Mol Cell Biol* **27**, 8330-9 (2007).
199. Out, C., Hageman, J., Bloks, V.W., Gerrits, H., Sollewijn Gelpke, M.D., Bos, T., Havinga, R., Smit, M.J., Kuipers, F. & Groen, A.K. Liver receptor homolog-1 is critical for adequate up-regulation of Cyp7a1 gene transcription and bile salt synthesis during bile salt sequestration. *Hepatology* **53**, 2075-85 (2011).
200. Song, X., Kaimal, R., Yan, B. & Deng, R. Liver receptor homolog 1 transcriptionally regulates human bile salt export pump expression. *J Lipid Res* **49**, 973-84 (2008).
201. Bohan, A., Chen, W.S., Denson, L.A., Held, M.A. & Boyer, J.L. Tumor necrosis factor alpha-dependent up-regulation of Lrh-1 and Mrp3(Abcc3) reduces liver injury in obstructive cholestasis. *J Biol Chem* **278**, 36688-98 (2003).
202. Schoonjans, K., Annicotte, J.S., Huby, T., Botrugno, O.A., Fayard, E., Ueda, Y., Chapman, J. & Auwerx, J. Liver receptor homolog 1 controls the expression of the scavenger receptor class B type I. *EMBO Rep* **3**, 1181-7 (2002).

203. Freeman, L.A., Kennedy, A., Wu, J., Bark, S., Remaley, A.T., Santamarina-Fojo, S. & Brewer, H.B., Jr. The orphan nuclear receptor LRH-1 activates the ABCG5/ABCG8 intergenic promoter. *J Lipid Res* **45**, 1197-206 (2004).
204. Delerive, P., Galardi, C.M., Bisi, J.E., Nicodeme, E. & Goodwin, B. Identification of liver receptor homolog-1 as a novel regulator of apolipoprotein AI gene transcription. *Mol Endocrinol* **18**, 2378-87 (2004).
205. Venteclef, N., Haroniti, A., Tousaint, J.J., Talianidis, I. & Delerive, P. Regulation of anti-atherogenic apolipoprotein M gene expression by the orphan nuclear receptor LRH-1. *J Biol Chem* **283**, 3694-701 (2008).
206. Stein, S., Oosterveer, M.H., Mataki, C., Xu, P., Lemos, V., Havinga, R., Dittner, C., Ryu, D., Menzies, K.J., Wang, X., Perino, A., Houten, S.M., Melchior, F. & Schoonjans, K. SUMOylation-dependent LRH-1/PROX1 interaction promotes atherosclerosis by decreasing hepatic reverse cholesterol transport. *Cell Metab* **20**, 603-13 (2014).
207. Pullinger, C.R., Eng, C., Salen, G., Shefer, S., Batta, A.K., Erickson, S.K., Verhagen, A., Rivera, C.R., Mulvihill, S.J., Malloy, M.J. & Kane, J.P. Human cholesterol 7alpha-hydroxylase (CYP7A1) deficiency has a hypercholesterolemic phenotype. *J Clin Invest* **110**, 109-17 (2002).
208. Oosterveer, M.H., Mataki, C., Yamamoto, H., Harach, T., Moullan, N., van Dijk, T.H., Ayuso, E., Bosch, F., Postic, C., Groen, A.K., Auwerx, J. & Schoonjans, K. LRH-1-dependent glucose sensing determines intermediary metabolism in liver. *J Clin Invest* **122**, 2817-26 (2012).
209. Hattori, T., Iizuka, K., Horikawa, Y. & Takeda, J. LRH-1 heterozygous knockout mice are prone to mild obesity. *Endocr J* **61**, 471-80 (2014).
210. Venteclef, N., Smith, J.C., Goodwin, B. & Delerive, P. Liver receptor homolog 1 is a negative regulator of the hepatic acute-phase response. *Mol Cell Biol* **26**, 6799-807 (2006).
211. Venteclef, N. & Delerive, P. Interleukin-1 receptor antagonist induction as an additional mechanism for liver receptor homolog-1 to negatively regulate the hepatic acute phase response. *J Biol Chem* **282**, 4393-9 (2007).
212. Lu, S.C. & Mato, J.M. S-adenosylmethionine in liver health, injury, and cancer. *Physiol Rev* **92**, 1515-42 (2012).
213. Mato, J.M., Martinez-Chantar, M.L. & Lu, S.C. Methionine metabolism and liver disease. *Annu Rev Nutr* **28**, 273-93 (2008).
214. Wagner, M., Choi, S., Panzitt, K., Mamrosh, J.L., Lee, J.M., Zaufel, A., Xiao, R., Wooton-Kee, R., Stahlman, M., Newgard, C.B., Boren, J. & Moore, D.D. Liver receptor homolog-1 is a critical determinant of methyl-pool metabolism. *Hepatology* **63**, 95-106 (2016).
215. MacDonald, B.T., Tamai, K. & He, X. Wnt/beta-catenin signaling: components, mechanisms, and diseases. *Dev Cell* **17**, 9-26 (2009).
216. Botrugno, O.A., Fayard, E., Annicotte, J.S., Haby, C., Brennan, T., Wendling, O., Tanaka, T., Kodama, T., Thomas, W., Auwerx, J. & Schoonjans, K. Synergy between LRH-1 and beta-catenin induces G1 cyclin-mediated cell proliferation. *Mol Cell* **15**, 499-509 (2004).
217. Schoonjans, K., Dubuquoy, L., Mebis, J., Fayard, E., Wendling, O., Haby, C., Geboes, K. & Auwerx, J. Liver receptor homolog 1 contributes to intestinal tumor formation through effects on cell cycle and inflammation. *Proc Natl Acad Sci U S A* **102**, 2058-62 (2005).
218. Wang, S.L., Zheng, D.Z., Lan, F.H., Deng, X.J., Zeng, J., Li, C.J., Wang, R. & Zhu, Z.Y. Increased expression of hLRH-1 in human gastric cancer and its implication in tumorigenesis. *Mol Cell Biochem* **308**, 93-100 (2008).

219. Petersen, G.M., Amundadottir, L., Fuchs, C.S., Kraft, P., Stolzenberg-Solomon, R.Z., Jacobs, K.B., Arslan, A.A., Bueno-de-Mesquita, H.B., Gallinger, S., Gross, M., Helzlsouer, K., Holly, E.A., Jacobs, E.J., Klein, A.P., LaCroix, A., Li, D., Mandelson, M.T., Olson, S.H., Risch, H.A., Zheng, W., Albanes, D., Bamlet, W.R., Berg, C.D., Boutron-Ruault, M.C., Buring, J.E., Bracci, P.M., Canzian, F., Clipp, S., Cotterchio, M., de Andrade, M., Duell, E.J., Gaziano, J.M., Giovannucci, E.L., Goggins, M., Hallmans, G., Hankinson, S.E., Hassan, M., Howard, B., Hunter, D.J., Hutchinson, A., Jenab, M., Kaaks, R., Kooperberg, C., Krogh, V., Kurtz, R.C., Lynch, S.M., McWilliams, R.R., Mendelsohn, J.B., Michaud, D.S., Parikh, H., Patel, A.V., Peeters, P.H., Rajkovic, A., Riboli, E., Rodriguez, L., Seminara, D., Shu, X.O., Thomas, G., Tjonneland, A., Tobias, G.S., Trichopoulos, D., Van Den Eeden, S.K., Virtamo, J., Wactawski-Wende, J., Wang, Z., Wolpin, B.M., Yu, H., Yu, K., Zeleniuch-Jacquotte, A., Fraumeni, J.F., Jr., Hoover, R.N., Hartge, P. & Chanock, S.J. A genome-wide association study identifies pancreatic cancer susceptibility loci on chromosomes 13q22.1, 1q32.1 and 5p15.33. *Nat Genet* **42**, 224-8 (2010).

220. Ueno, M., Ohkawa, S., Morimoto, M., Ishii, H., Matsuyama, M., Kuruma, S., Egawa, N., Nakao, H., Mori, M., Matsuo, K., Hosono, S., Nojima, M., Wakai, K., Nakamura, K., Tamakoshi, A., Takahashi, M., Shimada, K., Nishiyama, T., Kikuchi, S. & Lin, Y. Genome-wide association study-identified SNPs (rs3790844, rs3790843) in the NR5A2 gene and risk of pancreatic cancer in Japanese. *Sci Rep* **5**, 17018 (2015).

221. Lin, Q., Aihara, A., Chung, W., Li, Y., Huang, Z., Chen, X., Weng, S., Carlson, R.I., Wands, J.R. & Dong, X. LRH1 as a driving factor in pancreatic cancer growth. *Cancer Lett* **345**, 85-90 (2014).

222. Benod, C., Vinogradova, M.V., Jouravel, N., Kim, G.E., Fletterick, R.J. & Sablin, E.P. Nuclear receptor liver receptor homologue 1 (LRH-1) regulates pancreatic cancer cell growth and proliferation. *Proc Natl Acad Sci U S A* **108**, 16927-31 (2011).

223. Lin, Q., Aihara, A., Chung, W., Li, Y., Chen, X., Huang, Z., Weng, S., Carlson, R.I., Nadolny, C., Wands, J.R. & Dong, X. LRH1 promotes pancreatic cancer metastasis. *Cancer Lett* **350**, 15-24 (2014).

224. Annicotte, J.S., Chavey, C., Servant, N., Teyssier, J., Bardin, A., Licznar, A., Badia, E., Pujol, P., Vignon, F., Maudelonde, T., Lazennec, G., Cavailles, V. & Fajas, L. The nuclear receptor liver receptor homolog-1 is an estrogen receptor target gene. *Oncogene* **24**, 8167-75 (2005).

225. Miki, Y., Clyne, C.D., Suzuki, T., Moriya, T., Shibuya, R., Nakamura, Y., Ishida, T., Yabuki, N., Kitada, K., Hayashi, S. & Sasano, H. Immunolocalization of liver receptor homologue-1 (LRH-1) in human breast carcinoma: possible regulator of insitu steroidogenesis. *Cancer Lett* **244**, 24-33 (2006).

226. Bianco, S., Brunelle, M., Jangal, M., Magnani, L. & Gevry, N. LRH-1 governs vital transcriptional programs in endocrine-sensitive and -resistant breast cancer cells. *Cancer Res* **74**, 2015-25 (2014).

227. Bianco, S., Jangal, M., Garneau, D. & Gevry, N. LRH-1 controls proliferation in breast tumor cells by regulating CDKN1A gene expression. *Oncogene* **34**, 4509-18 (2015).

228. Chand, A.L., Herridge, K.A., Thompson, E.W. & Clyne, C.D. The orphan nuclear receptor LRH-1 promotes breast cancer motility and invasion. *Endocr Relat Cancer* **17**, 965-75 (2010).

229. Thiruchelvam, P.T., Lai, C.F., Hua, H., Thomas, R.S., Hurtado, A., Hudson, W., Bayly, A.R., Kyle, F.J., Periyasamy, M., Photiou, A., Spivey, A.C., Ortlund, E.A., Whitby, R.J., Carroll, J.S., Coombes, R.C., Buluwela, L. & Ali, S. The liver receptor homolog-1 regulates estrogen receptor expression in breast cancer cells. *Breast Cancer Res Treat* **127**, 385-96 (2011).

230. Chand, A.L., Wijayakumara, D.D., Knower, K.C., Herridge, K.A., Howard, T.L., Lazarus, K.A. & Clyne, C.D. The orphan nuclear receptor LRH-1 and ERalpha activate GREB1 expression to induce breast cancer cell proliferation. *PLoS One* **7**, e31593 (2012).

231. Lai, C.F., Flach, K.D., Alexi, X., Fox, S.P., Ottaviani, S., Thiruchelvam, P.T., Kyle, F.J., Thomas, R.S., Launchbury, R., Hua, H., Callaghan, H.B., Carroll, J.S., Charles Coombes, R., Zwart, W., Buluwela, L. & Ali, S. Co-regulated gene expression by oestrogen receptor alpha and liver receptor homolog-1 is a feature of the oestrogen response in breast cancer cells. *Nucleic Acids Res* **41**, 10228-40 (2013).
232. Lazarus, K.A., Zhao, Z., Knower, K.C., To, S.Q., Chand, A.L. & Clyne, C.D. Oestradiol reduces liver receptor homolog-1 mRNA transcript stability in breast cancer cell lines. *Biochem Biophys Res Commun* **438**, 533-9 (2013).
233. Chand, A.L., Herridge, K.A., Howard, T.L., Simpson, E.R. & Clyne, C.D. Tissue-specific regulation of aromatase promoter II by the orphan nuclear receptor LRH-1 in breast adipose stromal fibroblasts. *Steroids* **76**, 741-4 (2011).
234. Knower, K.C., Chand, A.L., Eriksson, N., Takagi, K., Miki, Y., Sasano, H., Visvader, J.E., Lindeman, G.J., Funder, J.W., Fuller, P.J., Simpson, E.R., Tilley, W.D., Leedman, P.J., Graham, J., Muscat, G.E., Clarke, C.L. & Clyne, C.D. Distinct nuclear receptor expression in stroma adjacent to breast tumors. *Breast Cancer Res Treat* **142**, 211-23 (2013).
235. Pare, J.F., Malenfant, D., Courtemanche, C., Jacob-Wagner, M., Roy, S., Allard, D. & Belanger, L. The fetoprotein transcription factor (FTF) gene is essential to embryogenesis and cholesterol homeostasis and is regulated by a DR4 element. *J Biol Chem* **279**, 21206-16 (2004).
236. Zhou, Q., Chipperfield, H., Melton, D.A. & Wong, W.H. A gene regulatory network in mouse embryonic stem cells. *Proc Natl Acad Sci U S A* **104**, 16438-43 (2007).
237. Gu, P., Goodwin, B., Chung, A.C., Xu, X., Wheeler, D.A., Price, R.R., Galardi, C., Peng, L., Latour, A.M., Koller, B.H., Gossen, J., Kliewer, S.A. & Cooney, A.J. Orphan nuclear receptor LRH-1 is required to maintain Oct4 expression at the epiblast stage of embryonic development. *Mol Cell Biol* **25**, 3492-505 (2005).
238. Kanno, M., Yazawa, T., Kawabe, S., Imamichi, Y., Usami, Y., Ju, Y., Matsumura, T., Mizutani, T., Fujieda, S. & Miyamoto, K. Sex-determining region Y-box 2 and GA-binding proteins regulate the transcription of liver receptor homolog-1 in early embryonic cells. *Biochim Biophys Acta* **1839**, 406-14 (2014).
239. Heng, J.C., Feng, B., Han, J., Jiang, J., Kraus, P., Ng, J.H., Orlov, Y.L., Huss, M., Yang, L., Lufkin, T., Lim, B. & Ng, H.H. The nuclear receptor Nr5a2 can replace Oct4 in the reprogramming of murine somatic cells to pluripotent cells. *Cell Stem Cell* **6**, 167-74 (2010).
240. Wagner, R.T., Xu, X., Yi, F., Merrill, B.J. & Cooney, A.J. Canonical Wnt/beta-catenin regulation of liver receptor homolog-1 mediates pluripotency gene expression. *Stem Cells* **28**, 1794-804 (2010).
241. Kelly, V.R. & Hammer, G.D. LRH-1 and Nanog regulate Dax1 transcription in mouse embryonic stem cells. *Mol Cell Endocrinol* **332**, 116-24 (2011).
242. Tay, Y.M., Tam, W.L., Ang, Y.S., Gaughwin, P.M., Yang, H., Wang, W., Liu, R., George, J., Ng, H.H., Perera, R.J., Lufkin, T., Rigoutsos, I., Thomson, A.M. & Lim, B. MicroRNA-134 modulates the differentiation of mouse embryonic stem cells, where it causes post-transcriptional attenuation of Nanog and LRH1. *Stem Cells* **26**, 17-29 (2008).
243. Liu, J., Han, Q., Peng, T., Peng, M., Wei, B., Li, D., Wang, X., Yu, S., Yang, J., Cao, S., Huang, K., Hutchins, A.P., Liu, H., Kuang, J., Zhou, Z., Chen, J., Wu, H., Guo, L., Chen, Y., Chen, Y., Li, X., Wu, H., Liao, B., He, W., Song, H., Yao, H., Pan, G., Chen, J. & Pei, D. The oncogene c-Jun impedes somatic cell reprogramming. *Nat Cell Biol* **17**, 856-67 (2015).
244. Bakiri, L. & Wagner, E.F. Mouse models for liver cancer. *Mol Oncol* **7**, 206-23 (2013).
245. Kang, J.S., Wanibuchi, H., Morimura, K., Gonzalez, F.J. & Fukushima, S. Role of CYP2E1 in diethylnitrosamine-induced hepatocarcinogenesis in vivo. *Cancer Res* **67**, 11141-6 (2007).

246. Nakatsuru, Y., Matsukuma, S., Nemoto, N., Sugano, H., Sekiguchi, M. & Ishikawa, T. O6-methylguanine-DNA methyltransferase protects against nitrosamine-induced hepatocarcinogenesis. *Proc Natl Acad Sci U S A* **90**, 6468-72 (1993).
247. Shirakami, Y., Gottesman, M.E. & Blaner, W.S. Diethylnitrosamine-induced hepatocarcinogenesis is suppressed in lecithin:retinol acyltransferase-deficient mice primarily through retinoid actions immediately after carcinogen administration. *Carcinogenesis* **33**, 268-74 (2012).
248. Perez, M.J. & Cederbaum, A.I. Proteasome inhibition potentiates CYP2E1-mediated toxicity in HepG2 cells. *Hepatology* **37**, 1395-404 (2003).
249. Roberts, B.J., Song, B.J., Soh, Y., Park, S.S. & Shoaf, S.E. Ethanol induces CYP2E1 by protein stabilization. Role of ubiquitin conjugation in the rapid degradation of CYP2E1. *J Biol Chem* **270**, 29632-5 (1995).
250. Wang, Y., Guan, S., Acharya, P., Koop, D.R., Liu, Y., Liao, M., Burlingame, A.L. & Correia, M.A. Ubiquitin-dependent proteasomal degradation of human liver cytochrome P450 2E1: identification of sites targeted for phosphorylation and ubiquitination. *J Biol Chem* **286**, 9443-56 (2011).
251. Becker, R.A. & Shank, R.C. Kinetics of formation and persistence of ethylguanines in DNA of rats and hamsters treated with diethylnitrosamine. *Cancer Res* **45**, 2076-84 (1985).
252. Mamrosh, J.L., Lee, J.M., Wagner, M., Stambrook, P.J., Whitby, R.J., Sifers, R.N., Wu, S.P., Tsai, M.J., Demayo, F.J. & Moore, D.D. Nuclear receptor LRH-1/NR5A2 is required and targetable for liver endoplasmic reticulum stress resolution. *Elife* **3**, e01694 (2014).
253. Chambers, K.T., Chen, Z., Lai, L., Leone, T.C., Towle, H.C., Kralli, A., Crawford, P.A. & Finck, B.N. PGC-1beta and ChREBP partner to cooperatively regulate hepatic lipogenesis in a glucose concentration-dependent manner. *Mol Metab* **2**, 194-204 (2013).
254. Iizuka, K., Bruick, R.K., Liang, G., Horton, J.D. & Uyeda, K. Deficiency of carbohydrate response element-binding protein (ChREBP) reduces lipogenesis as well as glycolysis. *Proc Natl Acad Sci U S A* **101**, 7281-6 (2004).
255. Chong, H.K., Biesinger, J., Seo, Y.K., Xie, X. & Osborne, T.F. Genome-wide analysis of hepatic LRH-1 reveals a promoter binding preference and suggests a role in regulating genes of lipid metabolism in concert with FXR. *BMC Genomics* **13**, 51 (2012).
256. Cabella, C., Karlsson, M., Canape, C., Catanzaro, G., Colombo Serra, S., Miragoli, L., Poggi, L., Uggeri, F., Venturi, L., Jensen, P.R., Lerche, M.H. & Tedoldi, F. In vivo and in vitro liver cancer metabolism observed with hyperpolarized [5-(13)C]glutamine. *J Magn Reson* **232**, 45-52 (2013).
257. Cheng, T., Mishkovsky, M., Bastiaansen, J.A., Ouari, O., Hautle, P., Tordo, P., van den Brandt, B. & Comment, A. Automated transfer and injection of hyperpolarized molecules with polarization measurement prior to in vivo NMR. *NMR Biomed* **26**, 1582-8 (2013).
258. Bar-Peled, L. & Sabatini, D.M. Regulation of mTORC1 by amino acids. *Trends Cell Biol* **24**, 400-6 (2014).
259. Kim, J., Kundu, M., Viollet, B. & Guan, K.L. AMPK and mTOR regulate autophagy through direct phosphorylation of Ulk1. *Nat Cell Biol* **13**, 132-41 (2011).
260. Ma, X.M. & Blenis, J. Molecular mechanisms of mTOR-mediated translational control. *Nat Rev Mol Cell Biol* **10**, 307-18 (2009).
261. Schmelzle, T. & Hall, M.N. TOR, a central controller of cell growth. *Cell* **103**, 253-62 (2000).
262. Hu, W., Zhang, C., Wu, R., Sun, Y., Levine, A. & Feng, Z. Glutaminase 2, a novel p53 target gene regulating energy metabolism and antioxidant function. *Proc Natl Acad Sci U S A* **107**, 7455-60 (2010).

263. Martin-Rufian, M., Tosina, M., Campos-Sandoval, J.A., Manzanares, E., Lobo, C., Segura, J.A., Alonso, F.J., Mates, J.M. & Marquez, J. Mammalian glutaminase Gls2 gene encodes two functional alternative transcripts by a surrogate promoter usage mechanism. *PLoS One* **7**, e38380 (2012).
264. Birsoy, K., Wang, T., Chen, W.W., Freinkman, E., Abu-Remaileh, M. & Sabatini, D.M. An Essential Role of the Mitochondrial Electron Transport Chain in Cell Proliferation Is to Enable Aspartate Synthesis. *Cell* **162**, 540-51 (2015).
265. Sullivan, L.B., Gui, D.Y., Hosios, A.M., Bush, L.N., Freinkman, E. & Vander Heiden, M.G. Supporting Aspartate Biosynthesis Is an Essential Function of Respiration in Proliferating Cells. *Cell* **162**, 552-63 (2015).
266. Talamillo, A., Herboso, L., Pirone, L., Perez, C., Gonzalez, M., Sanchez, J., Mayor, U., Lopitz-Otsoa, F., Rodriguez, M.S., Sutherland, J.D. & Barrio, R. Scavenger receptors mediate the role of SUMO and Ftz-f1 in Drosophila steroidogenesis. *PLoS Genet* **9**, e1003473 (2013).
267. Ward, J.D., Bojanala, N., Bernal, T., Ashrafi, K., Asahina, M. & Yamamoto, K.R. Sumoylated NHR-25/NR5A regulates cell fate during C. elegans vulval development. *PLoS Genet* **9**, e1003992 (2013).
268. Columbano, A., Endoh, T., Denda, A., Noguchi, O., Nakae, D., Hasegawa, K., Ledda-Columbano, G.M., Zedda, A.I. & Konishi, Y. Effects of cell proliferation and cell death (apoptosis and necrosis) on the early stages of rat hepatocarcinogenesis. *Carcinogenesis* **17**, 395-400 (1996).
269. Hara, A., Yoshimi, N., Yamada, Y., Matsunaga, K., Kawabata, K., Sugie, S. & Mori, H. Effects of Fas-mediated liver cell apoptosis on diethylnitrosamine-induced hepatocarcinogenesis in mice. *Br J Cancer* **82**, 467-71 (2000).
270. Zhang, B., Dong, L.W., Tan, Y.X., Zhang, J., Pan, Y.F., Yang, C., Li, M.H., Ding, Z.W., Liu, L.J., Jiang, T.Y., Yang, J.H. & Wang, H.Y. Asparagine synthetase is an independent predictor of surgical survival and a potential therapeutic target in hepatocellular carcinoma. *Br J Cancer* **109**, 14-23 (2013).
271. Zhang, Y.P., Lambert, M.A., Cairney, A.E., Wills, D., Ray, P.N. & Andrulis, I.L. Molecular structure of the human asparagine synthetase gene. *Genomics* **4**, 259-65 (1989).
272. Al Sarraj, J., Vinson, C. & Thiel, G. Regulation of asparagine synthetase gene transcription by the basic region leucine zipper transcription factors ATF5 and CHOP. *Biol Chem* **386**, 873-9 (2005).
273. Sheng, Z., Li, L., Zhu, L.J., Smith, T.W., Demers, A., Ross, A.H., Moser, R.P. & Green, M.R. A genome-wide RNA interference screen reveals an essential CREB3L2-ATF5-MCL1 survival pathway in malignant glioma with therapeutic implications. *Nat Med* **16**, 671-7 (2010).
274. Dluzen, D., Li, G., Tacelosky, D., Moreau, M. & Liu, D.X. BCL-2 is a downstream target of ATF5 that mediates the prosurvival function of ATF5 in a cell type-dependent manner. *J Biol Chem* **286**, 7705-13 (2011).
275. Jain, M., Nilsson, R., Sharma, S., Madhusudhan, N., Kitami, T., Souza, A.L., Kafri, R., Kirschner, M.W., Clish, C.B. & Mootha, V.K. Metabolite profiling identifies a key role for glycine in rapid cancer cell proliferation. *Science* **336**, 1040-4 (2012).
276. Chen, A., Qian, D., Wang, B., Hu, M., Lu, J., Qi, Y. & Liu, D.X. ATF5 is overexpressed in epithelial ovarian carcinomas and interference with its function increases apoptosis through the downregulation of Bcl-2 in SKOV-3 cells. *Int J Gynecol Pathol* **31**, 532-7 (2012).
277. Monaco, S.E., Angelastro, J.M., Szabolcs, M. & Greene, L.A. The transcription factor ATF5 is widely expressed in carcinomas, and interference with its function selectively kills neoplastic, but not nontransformed, breast cell lines. *Int J Cancer* **120**, 1883-90 (2007).
278. Kong, X., Meng, W., Zhou, Z., Li, Y., Zhou, B., Wang, R. & Zhan, L. Overexpression of activating transcription factor 5 in human rectal cancer. *Exp Ther Med* **2**, 827-831 (2011).
279. Morgan, M.A. & Shilatifard, A. Chromatin signatures of cancer. *Genes Dev* **29**, 238-49 (2015).

280. Yun, J., Johnson, J.L., Hanigan, C.L. & Locasale, J.W. Interactions between epigenetics and metabolism in cancers. *Front Oncol* **2**, 163 (2012).
281. Esteller, M. Epigenetics in cancer. *N Engl J Med* **358**, 1148-59 (2008).
282. Gut, P. & Verdin, E. The nexus of chromatin regulation and intermediary metabolism. *Nature* **502**, 489-98 (2013).
283. Wong, C.C., Qian, Y., Li, X., Xu, J., Kang, W., Tong, J.H., To, K.F., Jin, Y., Li, W., Chen, H., Go, M.Y., Wu, J.L., Cheng, K.W., Ng, S.S., Sung, J.J., Cai, Z. & Yu, J. SLC25A22 Promotes Proliferation and Survival of Colorectal Cancer Cells With KRAS Mutations, and Xenograft Tumor Progression in Mice, via Intracellular Synthesis of Aspartate. *Gastroenterology* (2016).
284. Busby, S., Nuhant, P., Cameron, M., Mercer, B.A., Hodder, P., Roush, W.R. & Griffin, P.R. in Probe Reports from the NIH Molecular Libraries Program (Bethesda (MD), 2010).
285. Holleman, A., Cheok, M.H., den Boer, M.L., Yang, W., Veerman, A.J., Kazemier, K.M., Pei, D., Cheng, C., Pui, C.H., Relling, M.V., Janka-Schaub, G.E., Pieters, R. & Evans, W.E. Gene-expression patterns in drug-resistant acute lymphoblastic leukemia cells and response to treatment. *N Engl J Med* **351**, 533-42 (2004).

List of Abbreviations

Hepatocellular carcinoma	HCC
4E-binding protein 1	4EBP1
Asparagine synthetase	ASNS
Activating transcription factor 5	ATF5
Chromatin immunoprecipitation	ChIP
Dimethyl-ketoglutarate	DM-KG
Dynamic nuclear polarization	DNP
Glucokinase	GCK
Glutaminase 2	GLS2
Gain-of-function	GOF
Glutamic-oxaloacetic transaminase 1	GOT1
Glutamate pyruvate transaminase 2	GPT2
L-Asparaginase	L-ASNase
Loss-of-function	LOF
Liver receptor homolog-1	LRH-1
Malic enzyme 1	ME1
Magnetic resonance	MR
Mechanistic target of rapamycin complex 1	mTORC1
N-acetyl-cysteine	NAC
Nonessential amino acids	NEAAs
Nuclear receptor	NR
Oxaloacetate	OAA
Reactive oxygen species	ROS
S6 kinase 1	S6K1
Tricarboxylic acid	TCA
α-ketoglutarate	α-KG

Curriculum Vitae

Personal Details

Name: Pan Xu
Nationality: China
Gender: Female
Date of birth: 19.09.1986

Education

8.2012-present PhD student in Biochemistry and Molecular Biology
Supervisor: Professor Kristina Schoonjans
École Polytechnique Fédérale de Lausanne (EPFL), Lausanne, Switzerland

9.2009-6.2012 Master of Science in Analytical Chemistry
Supervisor: Professor Zhining Xia
Chongqing University, Chongqing, China

9.2005-6.2009 Bachelor of Technology in Pharmaceutical Engineering
Chongqing University, Chongqing, China

Honors & Awards

10.2005 and 11.2006	National Scholarship Award of China by the Chinese Ministry of Education (The highest achievable scholarship in China, awarded to students that are among top 0.2% nationwide)
9.2006 and 9.2007	Excellent Student Cadre Honor of Chongqing University
11.2007 and 12.2008	Model Student of Academic Records Award of Chongqing University
11.2007	Wong Kin Hang Scholarship Award
6.2008	Excellent Leader of the Student Union Award
6.2009	Excellent Graduate Award of Chongqing University
10.2010	Excellent Postgraduate Award of Chongqing University
9.2011	First-Class Postgraduate Scholarship of Chongqing University

Research Experiences

(8.2012-present)
Elucidating the role of LRH-1 in liver intermediary metabolism and hepatocellular carcinoma

(9.2009-6.2012)
Drug discovery: Identifying novel peroxisome proliferator-activated receptor (PPAR) agonists from traditional Chinese medicine

(11.2007-5.2009)
Pharmaco-engineering: Microwave assisted organic synthesis of non-classical beta-lactam antibiotics

(9.2006-10.2007)
Pharmacokinetics: Testing drug-protein interactions by capillary electrophoresis

Publications

1. Stein S*, Lemos V*, Xu P, Wang X, Ryu D, Oosterveer MH, Schoonjans K. A SUMO- dependent LRH-1/OSBP pathway promoting nonalcoholic fatty liver disease. ***The Journal of Clinical Investigation***. Under revision. (* Equal contribution)
2. Xu P, Oosterveer MH, Stein S, Demagny H, Ryu D, Moullan N, Wang X, Can E, Zamboni N, Comment A, Auwerx J, Schoonjans K. LRH-1-dependent programming of mitochondrial glutamine processing drives liver cancer. ***Genes & Development***. 2016. 30: 1255-60.
3. Gao D, Zhang YL, Xu P, Lin YX, Yang FQ, Liu JH, Zhu HW, Xia ZN. In vitro evaluation of dual agonists for PPARγ/β from the flower of Edgeworthia gardneri (wall.) Meisn. ***Journal of Ethnopharmacology***. 2015,162: 14-9.
4. Stein S, Oosterveer MH, Mataki C, Xu P, Lemos V, Havinga R, Dittner C, Ryu D, Menzies KJ, Wang X, Perino A, Houten SM, Melchior F, Schoonjans K. SUMOylation-dependent LRH-1/PROX1 interaction promotes atherosclerosis by decreasing hepatic reverse cholesterol transport. ***Cell Metabolism***. 2014,20(4): 603-13.
5. Xia ZN, Lin YX, Guo LX, Yang FQ, Xu P, Zhang YL, Liu JH. Development of a cell-based high-throughput peroxisome proliferator-activated receptors (PPARs) screening model and its application for evaluation of the extracts from Rhizoma Coptis. ***Journal of Asian Natural Products Research***. 2013,15(3): 225-34.
6. Xu P, Xia ZN, Lin YX. Chemical constituents from Edgeworthia gardneri (Thymelaeaceae). ***Biochemical Systematics and Ecology***. 2012,45:148-150.
7. Yang FQ, Yang J, Zhang XM, Xu P, Xia ZN. Analysis of volatile components in Curcuma rhizome by microemulsion electrokinetic chromatography. ***Journal of Chromatographic Science***. 2013,51(2): 155-60.
8. Xiong CQ, Xia ZN, Huang R, Chen H, Xu P. Establishment and application of a new method for the determination of kinetic parameters by plug-plug kinetic capillary electrophoresis (ppKCE). ***Science in China, Series B: Chemistry***. 2008, 51: 1087-92.

Oral and Poster Presentations

1. Xu P, Oosterveer MH, Schoonjans K. Role of nuclear receptors in nutrient sensing and cancer metabolism. Nestlé Conference on Cancer and Nutrition. Lausanne, Switzerland. July 2015. Oral Presentation.
2. Xu P, Stein S, Oosterveer MH, Ryu D, Wang X, Can E, Comment A, Auwerx J, Schoonjans K. LRH-1 promotes liver carcinogenesis by coordinating glutamine-induced anaplerosis. EMBO Meeting, Nuclear receptors: From molecules to humans. Ajaccio, France. September 2015. Poster Presentation.

Techniques and Skills

Animal handling and experiences:

Completed the animal experimentation course provided by Lemanic Animal Facility Network (RESAL) in Switzerland. Animal experiences include: Mouse strain breeding / Adeno-associated virus (AAV)-mediated gene delivery / Anesthesia / Genotyping / Metabolic phenotyping / CT scanning / Dietary manipulation

Molecular and cellular biology:

Cell culture / Primary hepatocytes isolation and culture / Western immunoblotting / Tissue nuclear and cytosolic fractionation / Immunohistochemistry / ROS measurements / qRT-PCR / Luciferase assay / Microscopy / Flow cytometry / Metabolic flux analysis / Chromatin immunoprecipitation (ChIP) / Lentivirus- or adenovirus-mediated gene delivery / Microarray analysis / Bioinformatic analysis of (HCC) databases

Analytical and pharmaceutical chemistry:
Capillary electrophoresis / GC- or LC-MS / Infrared spectroscopy / Spectrometer / Organic biochemical synthesis / Pharmaceutical analysis / Traditional Chinese Medicine (TCM) / Natural product chemistry

Teaching Experiences

(8.2012-present)
Teaching assistant of advanced undergraduate course Biological Chemistry II (BIO212) at École Polytechnique

RESEARCH COMMUNICATION

LRH-1-dependent programming of mitochondrial glutamine processing drives liver cancer

Pan Xu,[1] Maaike H. Oosterveer,[2,6] Sokrates Stein,[1,6] Hadrien Demagny,[1] Dongryeol Ryu,[3] Norman Moullan,[1,3] Xu Wang,[3] Emine Can,[4] Nicola Zamboni,[5] Arnaud Comment,[4] Johan Auwerx,[3] and Kristina Schoonjans[1]

[1]Metabolic Signaling, Institute of Bioengineering, Ecole Polytechnique Fédérale de Lausanne, CH-1015 Lausanne, Switzerland; [2]Department of Pediatrics, Center for Liver Digestive and Metabolic Diseases, University of Groningen, NL-9700 RB Groningen, The Netherlands; [3]Laboratory of Integrative and Systems Physiology, Institute of Bioengineering, Ecole Polytechnique Fédérale de Lausanne, CH-1015 Lausanne, Switzerland; [4]Institute of the Physics of Biological Systems, School of Basic Sciences, Ecole Polytechnique Fédérale de Lausanne, CH-1015 Lausanne, Switzerland; [5]Department of Biology, Institute for Molecular Systems Biology, Eidgenössische Technische Hochschule Zürich, CH-8093 Zurich, Switzerland

Various tumors develop addiction to glutamine to support uncontrolled cell proliferation. Here we identify the nuclear receptor liver receptor homolog 1 (LRH-1) as a key regulator in the process of hepatic tumorigenesis through the coordination of a noncanonical glutamine pathway that is reliant on the mitochondrial and cytosolic transaminases glutamate pyruvate transaminase 2 (GPT2) and glutamate oxaloacetate transaminase 1 (GOT1), which fuel anabolic metabolism. In particular, we show that gain and loss of function of hepatic LRH-1 modulate the expression and activity of mitochondrial glutaminase 2 (GLS2), the first and rate-limiting step of this pathway. Acute and chronic deletion of hepatic LRH-1 blunts the deamination of glutamine and reduces glutamine-dependent anaplerosis. The robust reduction in glutaminolysis and the limiting availability of α-ketoglutarate in turn inhibit mTORC1 signaling to eventually block cell growth and proliferation. Collectively, these studies highlight the importance of LRH-1 in coordinating glutamine-induced metabolism and signaling to promote hepatocellular carcinogenesis.

Supplemental material is available for this article.

Received January 7, 2016; revised version accepted May 12, 2016.

During tumorigenesis, cancer cells usually switch from oxidative metabolism to a highly glycolytic metabolic status (Vander Heiden et al. 2009). While glucose is predominantly metabolized into lactate rather than entering the tricarboxylic acid (TCA) cycle, cancer cells particularly rely on glutamine to replenish TCA cycle intermediates. This process, termed anaplerosis, is accomplished through the conversion of glutamine to α-ketoglutarate (α-KG) via a two-step deamination reaction catalyzed by glutaminases and then by glutamate dehydrogenase 1 (GLUD1) or transaminases (DeBerardinis et al. 2008; Wise et al. 2008; Csibi et al. 2013; Son et al. 2013). Cancer cells therefore critically depend on glutamine as a fuel for proliferation, and abrogation of glutamine metabolism blocks tumorigenesis, indicating an accessible therapeutic window for cancer treatment (Hensley et al. 2013).

Liver receptor homolog 1 (LRH-1; also called NR5A2) is a nuclear receptor that is enriched in enterohepatic tissues, where it has diverse molecular and physiological functions (Stein and Schoonjans 2015). LRH-1 has been linked to cell proliferation and cancer development in the intestine (Botrugno et al. 2004; Schoonjans et al. 2005) and pancreas (Petersen et al. 2010; Benod et al. 2011). In the liver, LRH-1 regulates various metabolic processes, including bile acid synthesis (Mataki et al. 2007; Lee et al. 2008; Out et al. 2011), glucose sensing and processing (Oosterveer et al. 2012), and reverse cholesterol transport (Stein et al. 2014). Although the function of LRH-1 in the liver has been extensively studied, its commanding role in intermediary metabolism has never been connected to tumorigenesis.

In this study, we report that LRH-1 promotes diethylnitrosamine (DEN)-induced hepatocellular carcinoma (HCC) by coordinating glutamine-induced anabolic metabolism. We demonstrate that LRH-1 facilitates the production of NADPH from glutamine by favoring a noncanonical glutamine pathway that optimizes reductive biosynthesis. Importantly, chronic and acute disruption of LRH-1 also impairs glutamine-induced anaplerosis and α-KG availability, ultimately leading to reduced mTORC1 signaling. These results unveil an unexpected role of LRH-1 in cancer intermediary metabolism with broad-ranging implications on mTORC1 signaling.

Results and Discussion

Hepatic loss of LRH-1 prevents DEN-induced liver carcinogenesis

To investigate the specific contribution of hepatic LRH-1 on HCC formation, we used the well-established DEN method to induce liver cancer (Bakiri and Wagner 2013). Liver-specific *Lrh-1*-deficient ($Lrh\text{-}1^{hep-/-}$) and wild-type control ($Lrh\text{-}1^{hep+/+}$) mice were injected with DEN on postnatal day 14. Tumor burden was assessed 6 mo (mid-term) or 10 mo (long-term) after injection (Fig. 1A). While long-term DEN-challenged $Lrh\text{-}1^{hep+/+}$ littermates developed multiple hepatic tumors, $Lrh\text{-}1^{hep-/-}$ mice were strikingly protected (Fig. 1B,C). The robust reduction of total tumor number and size was not caused by differences in DEN carcinogenicity as evidenced by the equal accumulation of DNA adducts induced by DEN

[*Keywords*: Hepatocellular carcinoma; cancer metabolism; nuclear receptor NR5A2; mitochondria; anaplerosis; mTOR; NADPH]
[6]These authors contributed equally to this work.
Corresponding author: kristina.schoonjans@epfl.ch
Article is online at http://www.genesdev.org/cgi/doi/10.1101/gad.277483.116. Freely available online through the *Genes & Development* Open Access option.

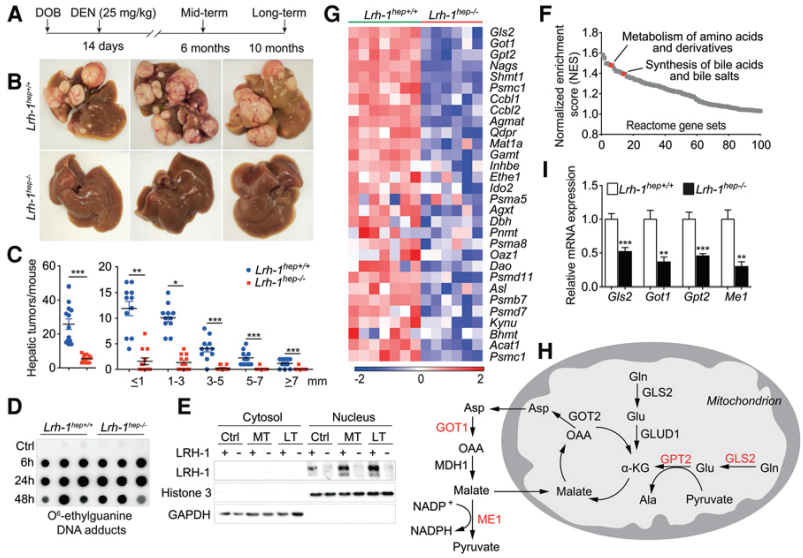

Figure 1. Hepatic *Lrh-1*-deficient mice are protected against DEN-induced HCC formation and display reduced glutamine-dependent anaplerosis. (*A*) Experimental strategies of DEN administration. (DOB) Date of birth. (*B*) Representative livers of 10-mo DEN-treated *Lrh-1*$^{hep+/+}$ and *Lrh-1*$^{hep-/-}$ mice. (*C*) Hepatic tumor number (*left*) and tumor size (*right*) in the corresponding genotypes. (*D*) Hepatic O^6-ethylguanine DNA adducts 6, 24, and 48 h after DEN injection to 14-d-old *Lrh-1*$^{hep+/+}$ and *Lrh-1*$^{hep-/-}$ mice. $n = 5$–6 per genotype and time point. (*E*) LRH-1 protein levels in cytosol and nucleus fractions of livers from untreated control (Ctrl), 6-mo DEN-treated (MT), and 10-mo DEN-treated (LT) *Lrh-1*$^{hep+/+}$ and *Lrh-1*$^{hep-/-}$ mice. (*F*) Gene set enrichment analysis (GSEA) demonstrates down-regulated pathways that were ranked by normalized enrichment scores (NES) in livers of 6-mo DEN-treated *Lrh-1*$^{hep-/-}$ ($n = 6$) mice compared with *Lrh-1*$^{hep+/+}$ ($n = 7$) mice. Specific pathways are indicated. (*G*) Heat map displaying the core-enriched gene set "metabolism of amino acids and derivatives," expressed in the livers of the mice described in *F*. (*H*) Graphical representation of enzymes involved in glutamine breakdown and metabolism. Enzymes highlighted in red are reduced in *Lrh-1*$^{hep-/-}$ livers, as shown in *I*. (*I*) Hepatic mRNA levels of *glutaminase 2* (*Gls2*), *glutamate oxaloacetate transaminase 1* (*Got1*), *glutamate pyruvate transaminase 2* (*Gpt2*), and *malic enzyme 1* (*Me1*) in livers of mice described in *F*. Data represent mean ± SEM. (*) $P < 0.05$; (**) $P < 0.01$; (***) $P < 0.001$ by two-tailed Student's *t*-test.

exposure in 14-d-old *Lrh-1*$^{hep+/+}$ and *Lrh-1*$^{hep-/-}$ livers (Fig. 1D; see the Supplemental Material for more details). Furthermore, DEN moderately increased LRH-1 protein abundance but did not affect its nuclear compartmentalization (Fig. 1E). We then performed histological and immunohistochemical analysis on the long-term DEN-treated liver sections. H&E staining of *Lrh-1*$^{hep-/-}$ liver sections demonstrated fewer microscopic tumor foci, while BrdU and Ki67 staining confirmed reduced cell proliferation in *Lrh-1*-deficient livers (Supplemental Fig. S1A). Moreover, long-term DEN-treated *Lrh-1*$^{hep-/-}$ livers were significantly lighter compared with *Lrh-1*$^{hep+/+}$ livers, while the body weight did not differ between the two genotypes (Supplemental Fig. S1B–D). Together, these results indicate that LRH-1 is required for efficient HCC induction and progression in response to DEN treatment.

Hepatic loss of LRH-1 inhibits noncanonical glutamine processing

LRH-1 coordinates intestinal cell renewal and tumor formation through cross-talk with the β-catenin pathway (Botrugno et al. 2004; Schoonjans et al. 2005). It is also required for hepatic endoplasmic reticulum (ER) stress resolution through transcriptional control of *polo-like kinase 3* (*Plk3*) and subsequent phosphorylation of activating transcription factor 2 (ATF2) (Mamrosh et al. 2014). To understand the robust tumor-suppressive phenotype, we first assessed the β-catenin pathway in mid-term DEN-treated livers in which tumors were not yet developed (Supplemental Fig. S1E). In contrast to the findings in intestinal crypts of germline *Lrh-1*$^{+/-}$ mice (Botrugno et al. 2004), β-catenin targets *c-Myc*, *Ccnd1*, and *Ccne1* were not reduced in the unchallenged (Supplemental Fig. S1F) or DEN-challenged (Supplemental Fig. S1G) *Lrh-1*$^{hep-/-}$ livers. We also evaluated the Plk3–ATF2 cascade in response to acute DEN exposure. *Plk3* mRNA levels and ATF2 phosphorylation were not induced by DEN (Supplemental Fig. S1H; data not shown), indicating that, in our model, LRH-1 impacts hepatocarcinogenesis via other mechanisms. We then performed microarray analysis to compare the transcriptomes of mid-term DEN-exposed *Lrh-1*$^{hep+/+}$ and *Lrh-1*$^{hep-/-}$ livers. As expected, gene set enrichment analysis (GSEA) confirmed previously established functions and target pathways of LRH-1, such as synthesis of bile acids (Fig. 1F; Supplemental Fig. S1I,J). Of interest, metabolism of amino acid and derivatives scored among the most significantly enriched pathways (Fig. 1F; Supplemental Fig. S1K). We next analyzed this gene set in more detail. While transcripts of several proteasomal subunits were down-regulated in *Lrh-1*$^{hep-/-}$ livers, a more striking reduction of several enzymes involved in glutamine catabolism was observed (Fig. 1G). Glutamine plays an essential role in tumor growth to support anaplerosis and reductive biosynthesis (DeBerardinis et al. 2008). Several genes involved in the processing of glutamine were reduced in mid-term DEN-exposed *Lrh-1*$^{hep-/-}$ livers, including mitochondrial *glutaminase 2* (*Gls2*), cytosolic *glutamate oxaloacetate transaminase 1* (*Got1*), and mitochondrial *glutamate pyruvate transaminase 2* (*Gpt2*) (Fig. 1G,H). This pathway is reminiscent of a noncanonical pathway of glutamine breakdown that was earlier reported in human glioma (Wise et al. 2008) and pancreatic ductal adenocarcinoma (PDAC) cells as an alternative mechanism to support NADPH production via malic enzyme (Son et al. 2013). Not only these genes but also *malic enzyme 1* (*Me1*) were significantly blunted, as confirmed by quantitative RT–PCR (qRT–PCR) (Fig. 1I). Many cancer cells typically rely on GLUD1 to fuel the TCA cycle through repleting α-KG (DeBerardinis et al. 2008). Transcript levels of *Glud1*, however, remained unchanged upon hepatic loss of function (LOF) of LRH-1 (Supplemental Fig. S1L). Moreover, mRNA expression of *Gls1*, *Got2*, and TCA cycle-related genes was not altered between the two

genotypes (Supplemental Fig. S1L,M). Collectively, these data indicate that an alternative pathway involved in hepatic glutamine processing is most likely compromised in *Lrh-1*$^{hep-/-}$ mice.

LRH-1 regulates reductive biosynthesis fueled by glutamine processing

We previously showed that LRH-1 coordinates glucose intermediary metabolism via glucokinase (GCK) activation and subsequent carbohydrate response element-binding protein (ChREBP) nuclear translocation (Oosterveer et al. 2012). Consistent with this study, the ChREBP pathway was significantly enriched between both genotypes (Supplemental Fig. S2A,B). Because *Me1* is a known ChREBP target gene (Iizuka et al. 2004; Chambers et al. 2013), we first analyzed whether the reduction of our candidate genes (Fig. 1I) results from impaired GCK–ChREBP signaling. GCK reconstitution in *Lrh-1*$^{hep-/-}$ livers restored *Chrebp*β and *Me1* (Fig. 2A), but not *Gls2*, *Got1*, or *Gpt2* expression (Supplemental Fig. S2C), indicating that LRH-1 regulates only *Me1* via the GCK–ChREBP axis. In parallel to the reduced *Me1* expression, NADPH/NADP$^+$ levels were significantly reduced in unchallenged (Fig. 2B) or DEN-challenged (Fig. 2C) *Lrh-1*$^{hep-/-}$ livers and was accompanied by a corresponding reduction of the GSH/GSSG ratio in DEN-treated livers (Fig. 2D). Although *Me1* was readily rescued upon GCK reconstitution (Fig. 2A), normalization of NADPH/NADP$^+$ levels was still incomplete (Fig. 2B), supporting the notion that the generation of NADPH from glutamine is also attenuated in *Lrh-1*$^{hep-/-}$ livers.

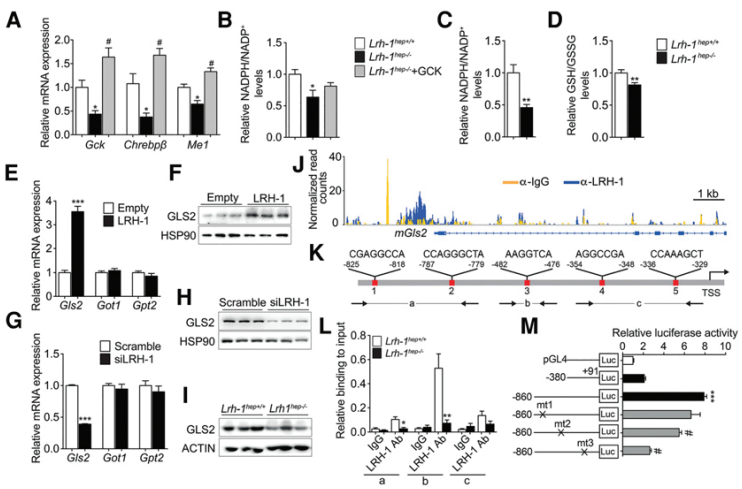

Figure 2. *Gls2* is a direct transcriptional target of LRH-1. (*A*,*B*) Hepatic mRNA levels of *Gck*, *Chrebp*β, and *Me1* (*A*) and NADPH/NADP$^+$ levels (*B*) in control virus-infected *Lrh-1*$^{hep+/+}$ and *Lrh-1*$^{hep-/-}$ mice and AAV8-GCK virus-infected *Lrh-1*$^{hep-/-}$ mice. $n = 4$–5 per group. Data represent mean ± SEM. (*) $P < 0.05$ versus *Lrh-1*$^{hep+/+}$; (#) $P < 0.05$ versus *Lrh-1*$^{hep-/-}$ by one-way ANOVA and Tukey's post-hoc test. (*C*,*D*) Relative NADPH/NADP$^+$ (*C*) and GSH/GSSG (*D*) levels in livers of 6-mo DEN-treated *Lrh-1*$^{hep+/+}$ ($n = 7$) and *Lrh-1*$^{hep-/-}$ ($n = 6$) mice. (*E*,*F*) mRNA levels of *Gls2*, *Got1*, and *Gpt2* (*E*) and protein levels of GLS2 (*F*) in Hepa 1.6 cells transfected with control or *Lrh-1* expression plasmids. $n = 3$ per group. (*G*,*H*) mRNA levels of *Gls2*, *Got1*, and *Gpt2* (*G*) and protein levels of GLS2 (*H*) in Hepa 1.6 cells transfected with scrambled or *Lrh-1* targeted siRNAs. $n = 3$ per group. Data represent mean ± SEM. (**) $P < 0.01$; (***) $P < 0.001$ by two-tailed Student's *t*-test. (*I*) Hepatic protein levels of GLS2 in mice described in *C*. (*J*) University of California at Santa Cruz (UCSC) genome browser (mm9) view displaying the occupancy of mouse *Gls2* by IgG and LRH-1 (Chong et al. 2012). (*K*) Schematic representation of the five putative LRH-1 response elements in the proximal mouse *Gls2* promoter. (*L*) ChIP-qPCR (chromatin immunoprecipitation [ChIP] combined with qPCR) assay to evaluate the relative LRH-1 binding to the mouse *Gls2* promoter. Amplified regions (a, b and c) are depicted in Figure 1K. (*M*) Luciferase activities in HEK293A cells after cotransfection of a *Lrh-1* expression vector and with empty luciferase reporter (pGL4) and long or short *Gls2* promoter constructs with or without the indicated mutations. Data represent mean ± SEM. (***) $P < 0.001$ versus empty reporter (pGL4); (#) $P < 0.05$ versus long *Gls2* promoter construct by one-way ANOVA and Tukey's post-hoc test.

We next investigated the molecular mechanism through which LRH-1 regulates glutamine metabolism. Overexpression of LRH-1 in mouse hepatoma Hepa 1.6 cells resulted in an increase of GLS2 transcripts and protein, while *Got1* and *Gpt2* transcripts were unchanged (Fig. 2E,F). Conversely, siRNA-mediated silencing of LRH-1 exclusively reduced the expression of GLS2 mRNA and protein (Fig. 2G,H). In *Lrh-1*$^{hep-/-}$ mice, reduced hepatic *Gls2* mRNA expression (Fig. 1H) translated into lower GLS2 protein levels (Fig. 2I). Of interest, *Gls2* is highly expressed in the liver compared with *Gls1* (Supplemental Fig. S2D). GLS2 deaminates mitochondrial glutamine, thus controlling a major anaplerotic step for hepatic glutamine utilization (Hensley et al. 2013). We then asked whether *Gls2* is subjected to direct transcriptional regulation by LRH-1. Analysis of a genome-wide hepatic LRH-1 ChIP-seq (chromatin immunoprecipitation [ChIP] combined with high-throughput sequencing) data set (Chong et al. 2012) revealed LRH-1 recruitment at the *Gls2* promoter (Fig. 2J), and computational analysis identified five putative LRH-1 response elements within the *Gls2* promoter under the LRH-1 ChIP-seq peak (Fig. 2K). Site-specific ChIP assays using DNA from mid-term DEN-treated *Lrh-1*$^{hep+/+}$ and *Lrh-1*$^{hep-/-}$ livers revealed LRH-1 recruitment to putative binding sites 1, 2, and 3 (Fig. 2L). Mutation of these binding sites in mouse *Gls2*-luciferase reporter constructs further mapped site 3, which is conserved in the human *Gls2* promoter (Supplemental Fig. S2E), as the major site that confers LRH-1 responsiveness (Fig. 2M). Accordingly, silencing of LRH-1 in human hepatoma HepG2 cells also led to a significant reduction of *Gls2* transcripts (Supplemental Fig. S2F).

LRH-1 regulates GLS2 to promote glutamine-induced anaplerosis

Given the marked reduction of GLS2 in *Lrh-1*$^{hep-/-}$ mice, we hypothesized that hepatic loss of LRH-1 blunts the conversion of glutamine to glutamate. To test the flux through GLS2 in vivo, we performed ^{13}C nuclear magnetic resonance (^{13}C MR) spectroscopy measurements following hyperpolarized [5-^{13}C]glutamine injection (Cabella et al. 2013; Cheng et al. 2013). [5-^{13}C]glutamine was hyperpolarized using dissolution dynamic nuclear polarization (DNP) and rapidly injected into DEN-treated *Lrh-1*$^{hep-/-}$ and *Lrh-1*$^{hep+/+}$ mice followed by real-time recording of its conversion to [5-^{13}C]glutamate (Fig. 3A,B). As expected, *Lrh-1*$^{hep-/-}$ showed a strong decrease in hepatic

[5-^{13}C]glutamate content compared with *Lrh-1*$^{hep+/+}$ mice (Fig. 3C). Unlike the expression levels of glutamine transporters *Slc1a5* and *Slc7a5*, which were unchanged (Supplemental Fig. S3A), hepatic α-KG levels were diminished in *Lrh-1*$^{hep-/-}$ mice (Fig. 3D), indicating that LRH-1 LOF may attenuate glutamine-fueled anaplerosis. To further explore the direct roles of LRH-1 and GLS2 in maintaining glutaminolysis and intracellular α-KG pools, we examined the effect of glutamine metabolism on α-KG levels. Hepa 1.6 cells were starved of glutamine for 6 h, and removal of glutamine significantly reduced the intracellular levels of α-KG (Supplemental Fig. S3B), demonstrating that glutamine sustains glutaminolysis. We then acutely modulated LRH-1 or GLS2 expression in Hepa 1.6 cells. In line with the reduced α-KG abundance in *Lrh-1*$^{hep-/-}$ livers, overexpression of LRH-1 or GLS2 increased, while siRNA-mediated silencing of LRH-1 or GLS2 decreased, α-KG levels in Hepa 1.6 cells (Fig. 3E–H). Together, these results demonstrate that LRH-1 promotes glutamine-induced anaplerosis via the induction of GLS2.

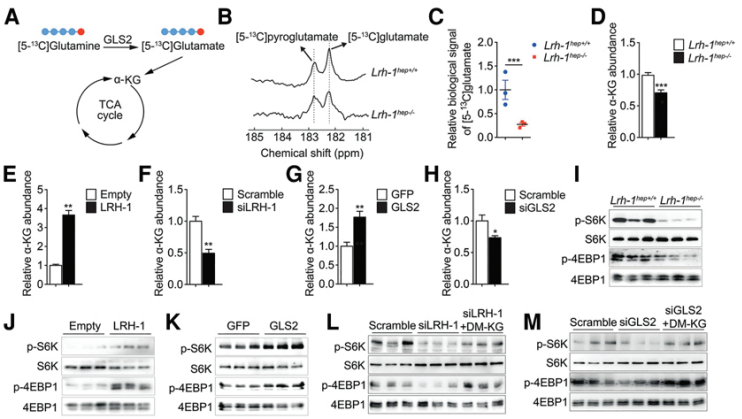

Figure 3. LRH-1 controls glutamine-induced anaplerosis and regulates mTORC1 activity. (*A*) GLS2-mediated biochemical reaction with hyperpolarized [5-^{13}C]glutamine. Red dots indicate the labelling of C5. (*B–D*) Representative in vivo ^{13}C MR spectra showing hyperpolarized [5-^{13}C]glutamate production with the by-product signal of hyperpolarized [5-^{13}C]pyroglutamate (*B*), the mean signal intensity of the hyperpolarized [5-^{13}C]glutamate formed via glutaminase (*C*), and intracellular α-KG levels (*D*) in the livers of DEN-treated *Lrh-1*$^{hep+/+}$ and *Lrh-1*$^{hep-/-}$ mice. (*E–H*) Intracellular α-KG levels in Hepa 1.6 cells transfected with either control or *Lrh-1* expression plasmids ($n = 3$ per group) (*E*) or scrambled or *Lrh-1* targeted siRNAs ($n = 3$ per group) (*F*), transduced with either AdGFP or AdGLS2 viruses ($n = 3$ per group) (*G*), or transfected with scrambled or *Gls2* targeted siRNAs ($n = 3$ per group) (*H*). (*I*) Phosphorylation states of S6K and 4EBP1 in the livers of mice described in *B*. (*J–M*) Phosphorylation states of S6K and 4EBP1 in Hepa 1.6 cells transfected as in *E* (*J*), transduced as in *G* (*K*), transfected as in *F* (*L*), or transfected as in *H* (*M*) with or without dimethyl-KG (DM-KG) supplementation (*L*,*M*). Data represent mean ± SEM. (*) $P < 0.05$; (**) $P < 0.01$; (***) $P < 0.001$ by two-tailed Student's *t*-test.

LRH-1 modulates the mTORC1 pathway in an α-KG-dependent manner

Glutamine is metabolized through glutaminolysis to produce α-KG. Previous studies showed that increased glutamine (Duran et al. 2012; Bar-Peled and Sabatini 2014) or α-KG (Duran et al. 2012) availability stimulates the mTORC1 signaling pathway. Of note, a robust reduction of mTORC1 activation was observed in *Lrh-1*$^{hep-/-}$ livers, as evidenced by the decreased phosphorylation of 4EBP1 and S6K (Fig. 3I). We then investigated the importance of glutamine in the activation of mTORC1 in Hepa 1.6 cells. Depletion of glutamine for 6 h reduced α-KG levels (Supplemental Fig. S3B) and inhibited mTORC1 activity (Supplemental Fig. S3C). Moreover, supplementation of a cell-permeable α-KG analog, dimethyl-KG (DM-KG), restored the activation of mTORC1 signaling upon glutamine deprivation (Supplemental Fig. S3D), indicating that intracellular glutamine and its derived α-KG are essential to stimulate mTORC1. Based on these results, we overexpressed LRH-1 or GLS2 in Hepa 1.6 cells. In both settings, mTORC1 activity was induced in the presence of glutamine (Fig. 3J,K). These effects were reversed upon glutamine starvation (Supplemental Fig. S3E,F). Furthermore, RNAi-mediated suppression of LRH-1 or GLS2 interfered with phosphorylation of 4EBP1 and S6K in the presence of glutamine, while addition of DM-KG or overexpression of GLS2 or LRH-1, respectively, rescued mTORC1 activities (Fig. 3L,M; Supplemental Fig. S3G,H). These data hence suggest that the LRH-1–GLS2 axis increases α-KG levels and consequently activates mTORC1.

The LRH-1–GLS2 axis promotes cell proliferation

Activation of mTORC1 inhibits autophagy (Kim et al. 2011), activates protein translation (Ma and Blenis 2009), and promotes cell growth (Schmelzle and Hall 2000). To investigate the importance of the LRH-1–GLS2–mTORC1 pathway, we first assessed autophagy in mid-term DEN-treated livers. As expected, disruption of LRH-1 induced autophagy, as evidenced by reduced phosphorylation of ULK-1 at Ser757, blunted P62, and increased LC3-II levels (Supplemental Fig. S4A). Silencing of LRH-1 or GLS2 decreased global protein translation as measured by incorporation of ^{35}S-labelled methionine in Hepa 1.6 cells (Fig. 4A, B), while their overexpression enhanced translation (Supplemental Fig. S4B,C). We then evaluated the link between LRH-1, α-KG, and cell proliferation. As expected, LRH-1 or GLS2 overexpression promoted cell proliferation, while additional glutamine deprivation prevented the increase in cell proliferation (Fig. 4C,D). Conversely, inhibition of glutaminolysis by LRH-1 or GLS2 silencing inhibited cell proliferation, while overexpression of LRH-1 or GLS2 rescued this effect (Supplemental Fig. S4D,E). Moreover, diminished cell proliferation upon LRH-1 or GLS2 suppression could also be rescued by addition of DM-KG (Fig. 4E,F), indicating that the LRH-1–GLS2 axis activates cell proliferation in an α-KG-dependent manner. It has been shown that GLS2-catalyzed deamination of glutamine is also essential for the control of intracellular reactive oxygen species (ROS) levels (Hu et al. 2010). Supplementation with the antioxidant N-acetyl-cysteine (NAC), however, could not rescue the inhibited cell proliferation upon LRH-1 or GLS2 silencing in Hepa 1.6 cells (Supplemental Fig. S4F,G), suggesting that reduced mTORC1 signaling rather than induced oxidative stress accounts for the reduction in cell proliferation. Furthermore, Hepa 1.6 cells silenced for LRH-1 or GLS2 induced significantly less tumor growth after propagation in athymic nude mice (Fig. 4G). Taken together, these findings

highlight that LRH-1 promotes cell proliferation through glutaminolysis and mTORC1 signaling.

In conclusion, our study assigns a critical role to LRH-1 in hepatic fuel metabolism with a striking impact on hepatic tumorigenesis. Unlike the role of LRH-1 in the intestine and pancreas, the oncogenic potential of hepatic LRH-1 is independent from the β-catenin/Wnt signaling pathway and is instead driven by the regulation of specific gene programs involved in mitochondrial glutamine catabolism (Fig. 4H). The enhanced mTORC1 signaling upon LRH-1-induced glutaminolysis indicates that the effect of LRH-1 on glutamine processing also impinges on established kinases in cell growth and cancer, thereby further amplifying the overall growth-stimulating effect. These observations, together with our previous findings linking LRH-1 to glucose-dependent fatty acid biosynthesis via ChREBP activation (Oosterveer et al. 2012), support the notion that LRH-1 confers a protumorigenic status to hepatocytes by promoting the metabolism of the principal fuel substrates of cancer cells. Further studies are warranted to fully understand its role in human HCC and explore its potential as a drug target.

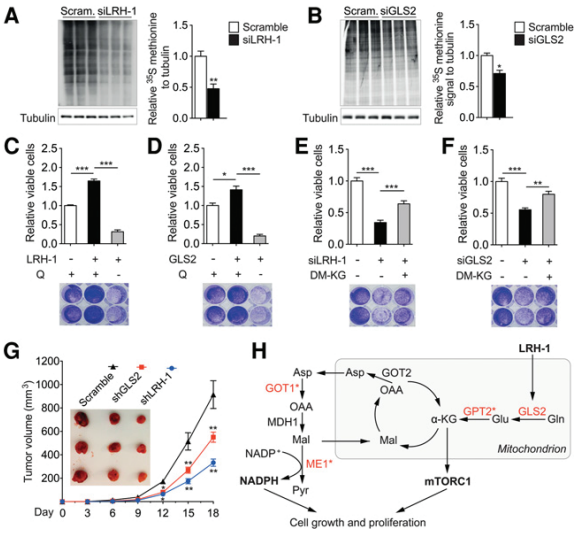

Figure 4. The LRH-1–GLS2 axis promotes protein translation and cell proliferation. (*A*,*B*) Global protein synthesis measured by ^{35}S-labelled methionine incorporation in Hepa 1.6 cells transfected with either scrambled or *Lrh-1* targeted siRNAs ($n = 3$ per group) (*A*) or scrambled or *Gls2* targeted siRNAs ($n = 3$ per group) (*B*). Relative ^{35}S methionine signals were normalized to Tubulin. Data represent mean ± SEM. (*) $P < 0.05$; (**) $P < 0.01$ by two-tailed Student's *t*-test. (*C*–*F*) Relative viable cells and representative Crystal Violet staining images of Hepa 1.6 cells transfected with either control or *Lrh-1* expression plasmids ($n = 3$ per group) (*C*) or transduced with either AdGFP or AdGLS2 viruses ($n = 3$ per group) (*D*) with or without glutamine deprivation or scrambled or *Lrh-1* targeted siRNAs ($n = 3$ per group) (*E*) or scrambled or *Gls2* targeted siRNAs ($n = 3$ per group) (*F*) with or without DM-KG supplementation. Data represent mean ± SEM. (*) $P < 0.05$; (***) $P < 0.001$ by one-way ANOVA and Tukey's post-hoc test. (*G*) Comparison of tumor growth and volume of mice subcutaneously injected with Hepa 1.6 cells that were transduced with scrambled, LRH-1 targeted, or GLS2 targeted shRNA. $n = 6$ per group. (*H*) Graphical summary illustrating how LRH-1 promotes glutamine-induced anaplerosis and reductive biosynthesis in hepatic cancer cells. Enzymes highlighted in red are reduced in *Lrh-1*$^{hep-/-}$ livers, and an asterisk indicates indirect regulation by LRH-1.

Materials and methods

Animal studies

Hepatocyte-specific LRH-1 knockout (*Lrh-1*$^{hep-/-}$) and wild-type (*Lrh-1*$^{hep+/+}$) mice were previously reported (Oosterveer et al. 2012). Congenic neonatal mice at 14 d old were intraperitoneally injected with DEN at a dose of 25 mg per kilogram of body weight to initiate tumor formation. Six months (mid-term DEN) or 10 mo (long-term DEN) after injection, mice were sacrificed, and liver tissue was collected. The experiments with the AAV8 viruses have been described previously (Oosterveer et al. 2012). Five-week-old male BALB/c nu/nu mice were purchased from Charles River and maintained in the animal facilities. All animal procedures were approved by the Swiss authorities (Canton of Vaud, animal protocol IDs 2375 and 2768) and performed in accordance with our institutional guidelines.

ChIP

ChIP analysis was performed as described previously with minor modifications (Stein et al. 2014). DNA was purified using the PCR clean-up extraction kit (Macherey-Nagel), after which qRT-PCR was performed as described previously (Mataki et al. 2007). Data were normalized to the input [fold differences = $2^{-[Ct\ sample - Ct\ input]}$]. ChIP primer sequences are listed in Supplemental Table 1.

Measurements of metabolites

For NADPH/NADP$^+$ and GSH/GSSG ratios, liver biopsies were extracted with 70% ethanol, and biomass was separated by centrifugation at 4000 rpm for 10 min. Liquid extracts were then dried by vacuum centrifugation, resuspended in 10 µL of water per milligram of wet weight, and analyzed by targeted liquid chromatography-tandem mass spectrometry on a Thermo Quantum Ultra instrument equipped with a Waters Acquity ultra high performance liquid chromatographer (UPLC). Intracellular α-KG levels were determined using commercial kits (Abcam, ab83431) according to the manufacturer's instructions.

In vivo hyperpolarized ^{13}C MR measurements

DEN-treated *Lrh-1*$^{hep+/+}$ and *Lrh-1*$^{hep-/-}$ mice were anesthetized with ~1.8% isoflurane, 0.5% O_2, and 0.5% air. A 750-µL bolus containing a dose of 0.57 mmol/kg ± 0.02 mmol/kg hyperpolarized [5-^{13}C]glutamine was administered in 9 sec. A series of 30°C BIR4 adiabatic RF excitation pulses were applied using a custom-built dual ^{1}H/^{13}C probe (two ^{1}H surface coils placed in quadrature on top of a ^{13}C single-loop surface coil) placed under the animal on the shaved skin located above the mouse's liver. In vivo ^{13}C MR measurements were respiratory-gated and triggered with simulated cardiac signal with a repetition time of 1 sec. Acquisitions were performed with an INOVA spectrometer (Varian/Magnex). The peak integrals were obtained from summed spectra analyzed using VNMRJ.

Allograft tumor study

Hepa 1.6 cells suspended in phosphate-buffered saline were injected subcutaneously into the left flanks of nude mice (4×10^6 cells per flank). The diameters of the tumors were measured every 3 d, and tumor volumes (V) were calculated using the formula $V = L \times W^2/2$, where L is length, and W is width.

Statistical analysis

Data represent mean ± SEM. Comparison of differences between two groups was assessed using two-tailed Student's *t*-tests. Multiple group comparisons were assessed by one-way ANOVA and Tukey's post-hoc test. Differences under $P < 0.05$ were considered statistically significant ($P < 0.05$ [*], $P < 0.01$ [**], and $P < 0.001$ [***]).

More experimental Materials and Methods are included in the Supplemental Material.

Acknowledgments

We thank V. Lemos for assistance with in vivo experiments, and H.A.I. Yoshihara for hyperpolarized ^{13}C data analysis. This study was supported by École Polytechnique Fédérale de Lausanne funding, the Swiss Cancer League (KFS-2809-08-2011, KFS-3082-02-2013, and KFS-3444-08-2014), and the Swiss National Science Foundation (CRSII3_160798/1). S.S. is supported by a post-doctoral fellowship from the Novartis Consumer Health Foundation, and J.A. is the Nestle Chair in Energy Metabolism.

References

Bakiri L, Wagner EF. 2013. Mouse models for liver cancer. *Mol Oncol* **7:** 206–223.

Bar-Peled L, Sabatini DM. 2014. Regulation of mTORC1 by amino acids. *Trends Cell Biol* **24:** 400–406.

Benod C, Vinogradova MV, Jouravel N, Kim GE, Fletterick RJ, Sablin EP. 2011. Nuclear receptor liver receptor homologue 1 (LRH-1) regulates pancreatic cancer cell growth and proliferation. *Proc Natl Acad Sci* **108:** 16927–16931.

Botrugno OA, Fayard E, Annicotte JS, Haby C, Brennan T, Wendling O, Tanaka T, Kodama T, Thomas W, Auwerx J, et al. 2004. Synergy between LRH-1 and β-catenin induces G1 cyclin-mediated cell proliferation. *Mol Cell* **15:** 499–509.

Cabella C, Karlsson M, Canape C, Catanzaro G, Colombo Serra S, Miragoli L, Poggi L, Uggeri F, Venturi L, Jensen PR, et al. 2013. In vivo and in vitro liver cancer metabolism observed with hyperpolarized [5-^{13}C]glutamine. *J Magn Reson* **232:** 45–52.

Chambers KT, Chen Z, Lai L, Leone TC, Towle HC, Kralli A, Crawford PA, Finck BN. 2013. PGC-1β and ChREBP partner to cooperatively regulate hepatic lipogenesis in a glucose concentration-dependent manner. *Mol Metab* **2:** 194–204.

Cheng T, Mishkovsky M, Bastiaansen JA, Ouari O, Hautle P, Tordo P, van den Brandt B, Comment A. 2013. Automated transfer and injection of hyperpolarized molecules with polarization measurement prior to in vivo NMR. *NMR Biomed* **26:** 1582–1588.

Chong HK, Biesinger J, Seo YK, Xie X, Osborne TF. 2012. Genome-wide analysis of hepatic LRH-1 reveals a promoter binding preference and suggests a role in regulating genes of lipid metabolism in concert with FXR. *BMC Genomics* **13:** 51.

Csibi A, Fendt SM, Li C, Poulogiannis G, Choo AY, Chapski DJ, Jeong SM, Dempsey JM, Parkhitko A, Morrison T, et al. 2013. The mTORC1 pathway stimulates glutamine metabolism and cell proliferation by repressing SIRT4. *Cell* **153:** 840–854.

DeBerardinis RJ, Lum JJ, Hatzivassiliou G, Thompson CB. 2008. The biology of cancer: metabolic reprogramming fuels cell growth and proliferation. *Cell Metab* **7:** 11–20.

Duran RV, Oppliger W, Robitaille AM, Heiserich L, Skendaj R, Gottlieb E, Hall MN. 2012. Glutaminolysis activates Rag-mTORC1 signaling. *Mol Cell* **47:** 349–358.

Hensley CT, Wasti AT, DeBerardinis RJ. 2013. Glutamine and cancer: cell biology, physiology, and clinical opportunities. *J Clin Invest* **123:** 3678–3684.

Hu W, Zhang C, Wu R, Sun Y, Levine A, Feng Z. 2010. Glutaminase 2, a novel p53 target gene regulating energy metabolism and antioxidant function. *Proc Natl Acad Sci* **107:** 7455–7460.

Iizuka K, Bruick RK, Liang G, Horton JD, Uyeda K. 2004. Deficiency of carbohydrate response element-binding protein (ChREBP) reduces lipogenesis as well as glycolysis. *Proc Natl Acad Sci* **101:** 7281–7286.

Kim J, Kundu M, Viollet B, Guan KL. 2011. AMPK and mTOR regulate autophagy through direct phosphorylation of Ulk1. *Nat Cell Biol* **13:** 132–141.

Lee YK, Schmidt DR, Cummins CL, Choi M, Peng L, Zhang Y, Goodwin B, Hammer RE, Mangelsdorf DJ, Kliewer SA. 2008. Liver receptor homolog-1 regulates bile acid homeostasis but is not essential for feedback regulation of bile acid synthesis. *Mol Endocrinol* **22:** 1345–1356.

Ma XM, Blenis J. 2009. Molecular mechanisms of mTOR-mediated translational control. *Nat Rev Mol Cell Biol* **10:** 307–318.

Mamrosh JL, Lee JM, Wagner M, Stambrook PJ, Whitby RJ, Sifers RN, Wu SPO, Tsai MJ, Demayo FJ, Moore DD. 2014. Nuclear receptor LRH-1/NR5A2 is required and targetable for liver endoplasmic reticulum stress resolution. *Elife* **3:** e01694.

Mataki C, Magnier BC, Houten SM, Annicotte JS, Argmann C, Thomas C, Overmars H, Kulik W, Metzger D, Auwerx J, et al. 2007. Compromised intestinal lipid absorption in mice with a liver-specific deficiency of liver receptor homolog 1. *Mol Cell Biol* **27:** 8330–8339.

Oosterveer MH, Mataki C, Yamamoto H, Harach T, Moullan N, van Dijk TH, Ayuso E, Bosch F, Postic C, Groen AK, et al. 2012. LRH-1-dependent glucose sensing determines intermediary metabolism in liver. *J Clin Invest* **122:** 2817–2826.

Out C, Hageman J, Bloks VW, Gerrits H, Sollewijn Gelpke MD, Bos T, Havinga R, Smit MJ, Kuipers F, Groen AK. 2011. Liver receptor homolog-1 is critical for adequate up-regulation of Cyp7a1 gene transcription and bile salt synthesis during bile salt sequestration. *Hepatology* **53:** 2075–2085.

Petersen GM, Amundadottir L, Fuchs CS, Kraft P, Stolzenberg-Solomon RZ, Jacobs KB, Arslan AA, Bueno-de-Mesquita HB, Gallinger S, Gross M, et al. 2010. A genome-wide association study identifies pancreatic cancer susceptibility loci on chromosomes 13q22.1, 1q32.1 and 5p15.33. *Nat Genet* **42:** 224–228.

Schmelzle T, Hall MN. 2000. TOR, a central controller of cell growth. *Cell* **103:** 253–262.

Schoonjans K, Dubuquoy L, Mebis J, Fayard E, Wendling O, Haby C, Geboes K, Auwerx J. 2005. Liver receptor homolog 1 contributes to intestinal tumor formation through effects on cell cycle and inflammation. *Proc Natl Acad Sci* **102:** 2058–2062.

Son J, Lyssiotis CA, Ying H, Wang X, Hua S, Ligorio M, Perera RM, Ferrone CR, Mullarky E, Shyh-Chang N, et al. 2013. Glutamine supports pancreatic cancer growth through a KRAS-regulated metabolic pathway. *Nature* **496:** 101–105.

Stein S, Schoonjans K. 2015. Molecular basis for the regulation of the nuclear receptor LRH-1. *Curr Opin Cell Biol* **33:** 26–34.

Stein S, Oosterveer MH, Mataki C, Xu P, Lemos V, Havinga R, Dittner C, Ryu D, Menzies KJ, Wang X, et al. 2014. SUMOylation-dependent LRH-1/PROX1 interaction promotes atherosclerosis by decreasing hepatic reverse cholesterol transport. *Cell Metab* **20:** 603–613.

Vander Heiden MG, Cantley LC, Thompson CB. 2009. Understanding the Warburg effect: the metabolic requirements of cell proliferation. *Science* **324:** 1029–1033.

Wise DR, DeBerardinis RJ, Mancuso A, Sayed N, Zhang XY, Pfeiffer HK, Nissim I, Daikhin E, Yudkoff M, McMahon SB, et al. 2008. Myc regulates a transcriptional program that stimulates mitochondrial glutaminolysis and leads to glutamine addiction. *Proc Natl Acad Sci* **105:** 18782–18787.

LRH-1-dependent programming of mitochondrial glutamine processing drives liver cancer

Pan Xu, Maaike H. Oosterveer, Sokrates Stein, et al.

Genes Dev. 2016 30: 1255-1260
Access the most recent version at doi:10.1101/gad.277483.116

Cell Metabolism
Article

SUMOylation-Dependent LRH-1/PROX1 Interaction Promotes Atherosclerosis by Decreasing Hepatic Reverse Cholesterol Transport

Sokrates Stein,[1] Maaike H. Oosterveer,[2] Chikage Mataki,[1] Pan Xu,[1] Vera Lemos,[1] Rick Havinga,[2] Claudia Dittner,[3,4] Dongryeol Ryu,[1] Keir J. Menzies,[1] Xu Wang,[1] Alessia Perino,[1] Sander M. Houten,[5] Frauke Melchior,[3] and Kristina Schoonjans[1,*]

[1]Metabolic Signaling, Institute of Bioengineering, School of Life Sciences, Ecole Polytechnique Fédérale de Lausanne, 1015 Lausanne, Switzerland
[2]Department of Pediatrics, Center for Liver Digestive and Metabolic Diseases, University of Groningen, University Medical Center Groningen, 9700 RB Groningen, the Netherlands
[3]Zentrum für Molekulare Biologie Heidelberg (ZMBH), DKFZ-ZMBH Alliance, 69120 Heidelberg, Germany
[4]Joint Division Molecular Metabolic Control, Zentrum für Molekulare Biologie Heidelberg, Deutsches Krebsforschungszentrum (DKFZ) and University Hospital Heidelberg, DKFZ-ZMBH Alliance, 69120 Heidelberg, Germany
[5]Department of Genetics and Genomic Sciences, Icahn School of Medicine at Mount Sinai, New York, NY 10029, USA
*Correspondence: kristina.schoonjans@epfl.ch
http://dx.doi.org/10.1016/j.cmet.2014.07.023

SUMMARY

Reverse cholesterol transport (RCT) is an antiatherogenic process in which excessive cholesterol from peripheral tissues is transported to the liver and finally excreted from the body via the bile. The nuclear receptor liver receptor homolog 1 (LRH-1) drives expression of genes regulating RCT, and its activity can be modified by different posttranslational modifications. Here, we show that atherosclerosis-prone mice carrying a mutation that abolishes SUMOylation of LRH-1 on K289R develop less aortic plaques than control littermates when exposed to a high-cholesterol diet. The mechanism underlying this atheroprotection involves an increase in RCT and its associated hepatic genes and is secondary to a compromised interaction of LRH-1 K289R with the corepressor prospero homeobox protein 1 (PROX1). Our study reveals that the SUMOylation status of a single nuclear receptor lysine residue can impact the development of a complex metabolic disease such as atherosclerosis.

INTRODUCTION

Atherosclerosis is a disease characterized by excessive cholesterol accumulation in vessel walls. It evolves from a complex interplay between hypercholesterolemia, dyslipidemia, and chronic inflammation and encompasses several tissues and organs (Weber and Noels, 2011). Rupture of an atherosclerotic plaque may lead to a myocardial infarction or stroke, two of the primary causes of morbidity and mortality in the world (Weber and Noels, 2011).

Liver receptor homolog 1 (LRH-1 or NR5A2) is a member of the NR5A subfamily of nuclear receptors (NRs) that binds as a monomer to its response elements (Fayard et al., 2004). The transcriptional activity of LRH-1 is governed by multiple factors, including the binding of ligands and posttranslational modifications, which together define its interaction with transcriptional coregulators (Fernandez-Marcos et al., 2011; Lee and Moore, 2008). LRH-1 is highly expressed in tissues of the enterohepatic axis, where it has diverse molecular and physiological functions (Fayard et al., 2004) ranging from local glucocorticoid production in the intestine (Coste et al., 2007) to glucose sensing in the liver (Oosterveer et al., 2012). Interestingly, one of the first described LRH-1 target genes is *scavenger receptor B type 1* (*Scarb1*) (Schoonjans et al., 2002), a gene that is expressed in many tissues and plays important functions in reverse cholesterol transport (RCT), an antiatherogenic process in which excessive cholesterol from peripheral tissues is transported to the liver and finally excreted via the bile (Rosenson et al., 2012). Although several other LRH-1 target genes involved in cholesterol metabolism have been identified, including *carboxl ester lipase* (*Cel*) (Fayard et al., 2003), *ATP binding cassette member subfamily G5* (*Abcg5*), *Abcg8* (Freeman et al., 2004), and *apolipoprotein M* (*Apom*) (Venteclef et al., 2008), so far no study has demonstrated that LRH-1 activity is critical for proper RCT or atherogenesis.

LRH-1 is targeted for SUMOylation by E3-SUMO ligases at several lysine residues, and this conserved reversible posttranslational modification affects its transcriptional activity (Chalkiadaki and Talianidis, 2005; Lee et al., 2005; Talamillo et al., 2013; Venteclef et al., 2010; Ward et al., 2013). SUMOylation of human LRH-1 is considered to attenuate its transcriptional activity, yet the mechanistic basis underlying this repression is poorly understood. Although one study reported that the SUMOylated form of LRH-1 is sequestered into promyelocytic leukemia (PML) protein bodies (Chalkiadaki and Talianidis, 2005), another study proposed that SUMO modification of LRH-1 stabilizes the recruitment of the transcriptional nuclear receptor corepressor 1 and histone deacetylase 3 (NCoR1/Hdac3) corepressor complex through its association with G protein pathway suppressor 2 (GPS2) (Venteclef et al., 2010).

In this study, we demonstrate that mice carrying a mutation on lysine 289 of LRH-1 (*Lrh1 K289R* mice) display reduced LRH-1

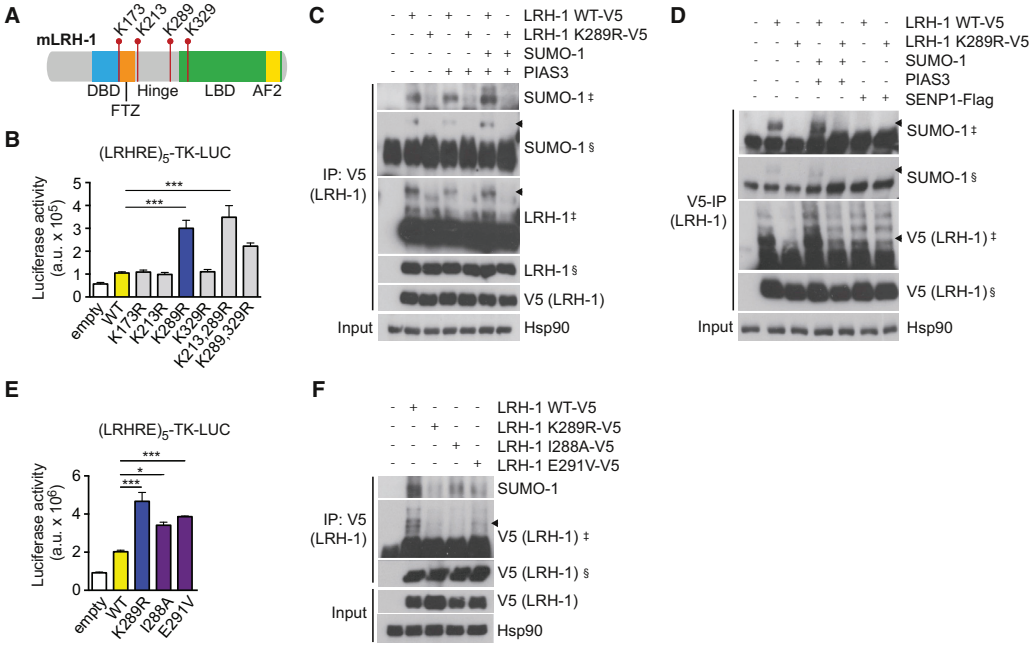

Figure 1. Non-SUMOylatable LRH-1 K289R Displays Increased Reporter Activity and Impaired SUMOylation In Vitro

(A) Schematic overview of LRH-1 highlighting the lysine residues that were mutated. DBD, DNA binding domain; FTZ, fushi tarazu homology domain; LBD, ligand binding domain; AF2, activation function 2 domain.

(B) Luciferase assay performed in HEK293T cells that were cotransfected with a pGL3::$(LRHRE)_5$-TK-LUC and a pCMV plasmid coding for LRH-1 WT or the outlined mutant constructs. n = 3. The experiment was replicated three times.

(C) Immunoprecipitation of V5-tagged LRH-1 to detect the SUMOylated band of LRH-1 (arrowheads). HEK293T cells were transfected with pCMV-V5::LRH-1 WT or pCMV-V5::LRH-1 K289R, pCMV::PIAS3, and/or pcDNA-HA::SUMO-1-HA. The experiment was replicated at least three times.

(D) Immunoprecipitation of V5-tagged LRH-1 to detect the SUMOylated band of LRH-1 in HEK293T cells that were transfected with pCMV-V5::LRH-1 (WT or K289R) and pCMV-FLAG::SENP1. The experiment was replicated at least three times.

(E) Residues adjacent to K289 are required for SUMOylation and function of LRH-1 activity. Luciferase assay was performed in HEK293T cells that were cotransfected with a pGL3::$(LRHRE)_5$-TK-LUC and pCMV plasmid coding for LRH-1 WT or the outlined mutant constructs. n = 3 from three separate experiments.

(F) Immunoprecipitation of V5-tagged LRH-1 to detect SUMOylation of the different mutant constructs used in (E).

Data are represented as means ± SEM. *$p < 0.05$, **$p < 0.01$, ***$p < 0.001$ relative to *Lrh-1 WT*, as determined by ANOVA and Bonferonni post hoc or Student's t test. Arrowheads, LRH-1*SUMO-1 band; §, short exposure; ‡,long exposure.

SUMOylation and increased expression of genes regulating cholesterol transport. When crossbred to atherosclerosis-prone *low-density lipoprotein receptor* (*Ldlr*) knockout mice, *Ldlr−/− Lrh-1 K289R* mice show improved RCT and diminished atherosclerosis development in comparison to control mice. Mechanistically, this effect is attributed to the specific loss of interaction of the mutated form of LRH-1 with the corepressor PROX1, thereby increasing the expression of LRH-1 target genes involved in RCT.

RESULTS

Non-SUMOylatable LRH-1 K289R Displays Increased Transcriptional Activity In Vitro

The murine LRH-1 protein has several lysine (K) residues that could be SUMOylated. They are located in the DNA binding domain, hinge region, or ligand binding domain (Figure 1A). On the basis of previous studies (Lee et al., 2005), we mutated the most relevant K residues to non-SUMOylatable arginines (R) and analyzed their potential to *trans*-activate a heterologous LRH-1 reporter by transient transfection assays (Figure 1B). Interestingly, the K289R mutation displayed the highest transcriptional activity, whereas the remaining K mutations (K173R, K213R, or K329R) had neither an effect as single mutations nor an additive effect when mutated together with K289R (Figure 1B). Next, we analyzed whether the enhanced activity of LRH-1 K289R was also associated with a reduction in the SUMOylation status. Human embryonic kidney 293T (HEK293T) cells transfected with either LRH-1 wild-type (WT) or LRH-1 K289R were cotransfected with either PIAS3 SUMO ligase alone or in combination with SUMO-1 substrate. Basal LRH-1 WT SUMOylation was clearly detectable, whereas it was nearly undetectable in LRH-1 K289R (Figure 1C). Cotransfection with PIAS3 and SUMO-1 slightly increased SUMOylation of LRH-1 WT (Figure 1C). Notably, LRH-1 K289R SUMOylation remained low after PIAS3 and SUMO-1 cotransfection, showing that mutating a single K residue can affect the total SUMOylation status of the transcription factor (Figure 1C). Moreover, cotransfection of LRH-1 WT or LRH-1 K289R with the isopeptidase sentrin/SUMO-specific protease 1 (SENP1) efficiently removed the SUMO modification from only LRH-1 WT (Figure 1D). The SUMO acceptor

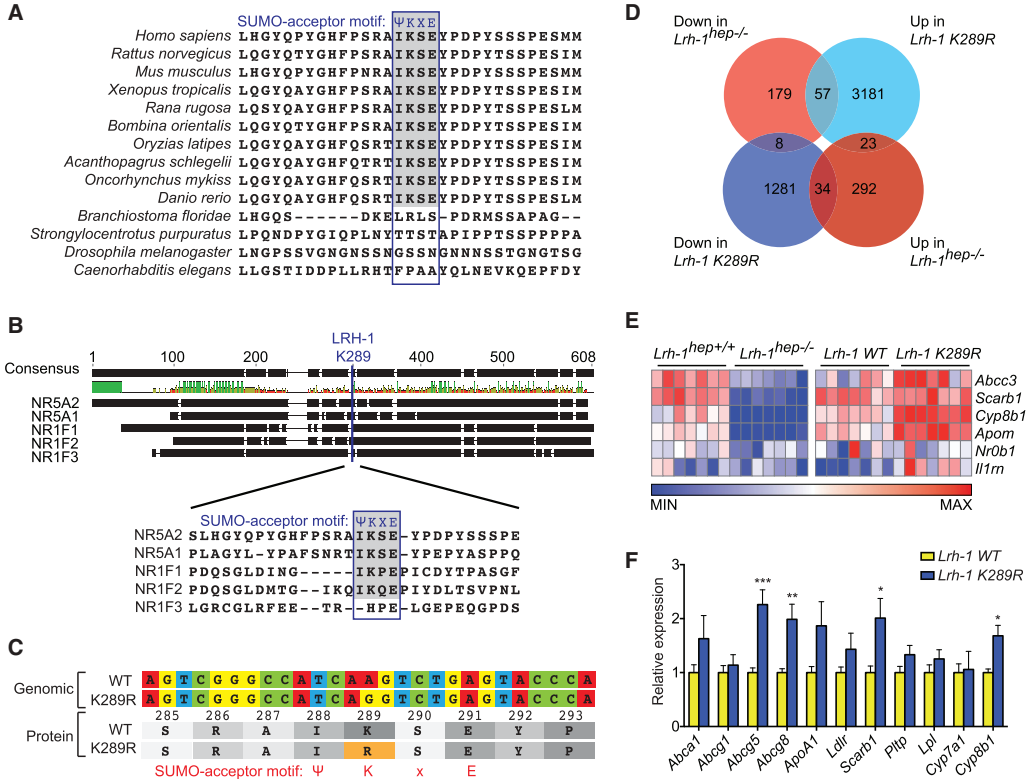

Figure 2. The LRH-1 SUMO Acceptor Motif Is Conserved in Vertebrates, and Mutation of Its Lysine Triggers Activation of Cholesterol Homeostasis Genes In Vivo

(A) Alignment of the amino acid sequence surrounding the murine LRH-1 K289 residue with other species. The blue-lined box highlights the aligned amino acids homologous to the SUMO acceptor motif, and the gray shading marks the sequences with an intact SUMO acceptor sequence.

(B) Protein alignment of LRH-1 (NR5A2) with other monomeric NR showing conserved sequences surrounding the LRH-1 K289 residue. Green, high homology; red, low homology.

(C) Overview of the genomic and protein sequence surrounding the K289R mutation. Mutation of a single nucleotide (AAG → AGG) at genomic level leads to K289R mutation of the translated protein.

(D) Venn diagram depicting the number of genes that are significantly up- or downregulated in *Lrh-1*$^{hep-/-}$ (n = 8) in comparison to *Lrh-1*$^{hep+/+}$ (Oosterveer et al., 2012) (n = 8) as well as *Lrh-1 K289R* (n = 7) in comparison to *Lrh-1 WT* (n = 7) mice.

(E) Heatmap displaying the expression of selected LRH-1 target genes in the corresponding genotypes (n = 4 per genotype).

(F) Hepatic expression of genes that regulate cholesterol homeostasis in *Lrh-1 WT* (n = 8) and *Lrh-1 K289R* (n = 9) mice.

Data are represented as means ± SEM. *p < 0.05, **p < 0.01, ***p < 0.001 relative to *Lrh-1 WT*, as determined by Student's t test. See also Figures S1 and S2.

motif Ψ-K-x-E is found in many SUMOylated proteins. Although the lysine residue can be targeted for SUMOylation, the adjacent hydrophobic (Ψ) and acidic glutamate (E) residues are also necessary to mediate the conjugation with the SUMO E2 enzyme Ubc9 (Bernier-Villamor et al., 2002). Mutation of these two sites (I288A and E291V) also increased LRHRE-driven reporter activity (Figure 1E) and reduced LRH-1 SUMOylation (Figure 1F), showing that not only the lysine but also an intact SUMO acceptor motif is crucial for the SUMO-dependent function of LRH-1.

LRH-1 K289R Activates Selected Target Genes In Vivo

To understand the relevance of this particular SUMO acceptor lysine residue, we carried out comparative alignment studies. Alignment of the amino acids surrounding the murine LRH-1 K289 with other species demonstrated that this particular SUMO acceptor motif is highly conserved in vertebrates but not in the chordate lancelet (*Branchiostoma floridae*), sea urchin (*Strongylocentrotus purpuratus*), fruit fly (*Drosophila melanogaster*), or roundworm (*Caenorhabditis elegans*; Figures 2A; Figure S1A available online). However, homologous proteins in *C. elegans* and *D. melanogaster* have other sites that can be targeted for SUMOylation (Talamillo et al., 2013; Ward et al., 2013). Next, we compared the murine LRH-1 protein sequence with other monomeric NRs with special focus on the highly variable and intrinsically disordered hinge region (Krasowski et al., 2008). Besides the close homolog NR5A1 (SF-1), only the retinoic-acid-receptor-related orphan receptors (RORs:NR1F1, NR1F2, and NR1F3) displayed somewhat homologous hinge regions (Figure S1B). Closer alignment of LRH-1 with NR5A1 and the three RORs showed that only NR1F1 and NR1F2 contain

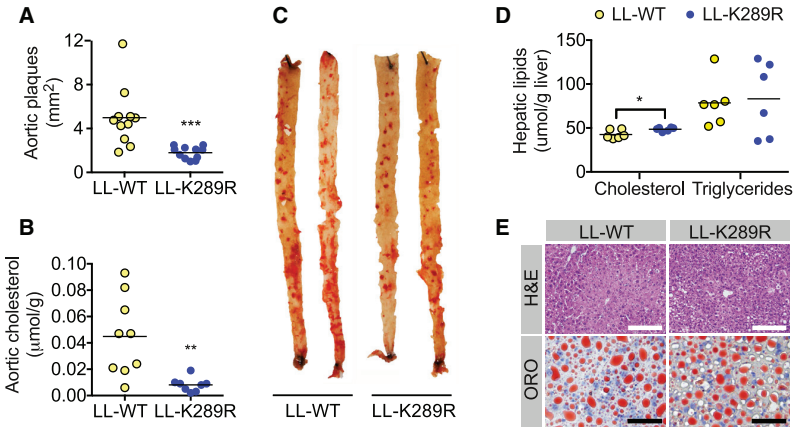

Figure 3. LRH-1 K289R Protects against Atherosclerosis Progression

(A) Quantification of aortic plaque area in *Ldlr*$^{-/-}$ *Lrh-1 WT* (LL-WT) or *Ldlr*$^{-/-}$ *Lrh-1 K289R* (LL-K289R) mice. n = 11 per genotype.

(B) Quantification of the cholesterol content in aortic lipid extracts of LL-WT (n = 9) and LL-K289R (n = 8) mice.

(C) Representative aortas of LL-WT and LL-K289R mice stained with Oil-Red O.

(D) Quantification of cholesterol and triglyceride contents in hepatic lipid extracts of LL-WT and LL-K289R mice. n = 6 per genotype.

(E) Representative images of hematoxylin and eosin and Oil-Red O (ORO) staining of hepatic sections of LL-WT and LL-K289R mice. The white scale bar represents 200 μm, and the black scale bar represents 50 μm.

Data are represented as means ± SEM. *p < 0.05, **p < 0.01, ***p < 0.001 relative to LL-WT, as determined by Mann-Whitney U or Student's t tests. See also Figure S3.

the conserved SUMO acceptor motif (Figure 2B). These bioinformatic data suggest that SUMOylation of this site is specific for a very small subset of NRs and highlights the functional importance of the hinge region in these selected NRs.

To analyze the physiological impact of the K289R mutation on LRH-1 function in vivo, we generated a knockin mouse line containing the K289R mutation *Lrh-1 K289R* (Figures 2C and S2A). The offspring of *Lrh-1 K289R* breeders were born under normal Mendelian and sex ratios, and no apparent dysmorphic phenotype could be observed in these mice (data not shown). The mutation did not affect the expression of LRH-1 in the liver in comparison to *Lrh-1 WT* and hepatocyte-specific *Lrh-1*$^{hep+/+}$ mice (Figure S2B). Then, we performed microarray analyses on livers in order to compare the transcriptome of hepatocyte-specific *Lrh-1*$^{hep-/-}$ (Oosterveer et al., 2012) and *Lrh-1 K289R* mice to their corresponding controls. Only 57 of the 244 genes (23.4%) whose expression was decreased in *Lrh-1*$^{hep-/-}$ mice were induced in *Lrh-1 K289R* mice (Figure 2D and Table S1). Several of the established LRH-1 target genes that are reduced in *Lrh-1*$^{hep-/-}$ mice were oppositely regulated in *Lrh-1 K289R* mice (Figure 2E). Intriguingly, most of the selected hepatic LRH-1 target genes involved in cholesterol metabolism were increased in *Lrh-1 K289R* in comparison to *Lrh-1 WT* mice, as determined by qPCR analyses (Figure 2F). Although hepatic expression of *Cyp8b1* was nearly absent in hepatocyte-specific *Lrh-1*$^{hep-/-}$ mice (Mataki et al., 2007), it was only mildly enhanced in *Lrh-1 K289R* mice (Figure 2F). This was reflected in the composition of bile acids in the gallbladder. Although the total bile acid content did not differ, *Lrh-1 K289R* mice had slightly increased tauro-conjugated cholic acid (tCA) and less tauro-conjugated muricholic acid (tMCA) (Figure S2C). Altogether, these data show that LRH-1 K289R exhibits increased transcriptional activity on a selected subset of LRH-1 target genes and cannot be described as a global constitutive active LRH-1 form.

LRH-1 K289R Protects against Atherosclerosis Development

Given that many of the genes affected in *Lrh-1 K289R* mice are involved in cholesterol homeostasis, we hypothesized that LRH-1 K289R may affect cholesterol metabolism, and hence hypercholesterolemia-driven diseases, such as atherosclerosis. To study the role of LRH-1 K289R in atherosclerosis, we crossbred *Lrh-1 WT* and *Lrh-1 K289R* mice to atherosclerotic-prone *Ldlr* knockout mice in order to generate *Ldlr*$^{-/-}$ *Lrh-1 WT* (LL-WT) or *Ldlr*$^{-/-}$ *Lrh-1 K289R* (LL-K289R) mice. Then, 8-week-old LL-WT or LL-K289R mice were subjected to a high-cholesterol diet (HCD) for 14 weeks. Body and liver weight (Figures S3A and S3B), and also gross morphology of other organs, were similar between the different genotypes (data not shown). Notably, en face plaque analyses of the thoraco-abdominal aorta demonstrated that LL-K289R mice developed significantly less atherosclerotic plaques than LL-WT mice and also accumulated less cholesterol in their aortas (Figures 3A–3C). Advanced plaque analyses of the aortic sinus stained for collagen imaging revealed no changes in necrotic core size, cap thickness, or collagen content in LL-K289R in comparison to LL-WT mice (Figures S3C–S3E). Total plasma cholesterol did not differ between the mice, and plasma triglyceride levels were only slightly reduced before administering the HCD and were not significantly changed upon HCD feeding (Figures S3F and S3G). Although no changes in triglyceride content were observed in the lipoprotein fractions, a small reduction in the cholesterol content of the low-density lipoprotein subfraction of LL-K289R mice could be noticed (Figures S3H and S3I). Furthermore, hepatic triglyceride content was not changed in overnight fasted LL-K289R mice, whereas cholesterol content was only slightly increased (Figure 3D). Stainings of liver cryosections showed no apparent difference in neutral lipid content and cellular morphology between the two genotypes (Figure 3E). These data demonstrate that LL-K289R mice develop less atherosclerosis, possibly as a consequence of improved RCT.

To assess a potential contribution of macrophages in the observed phenotype, we measured *Lrh-1* in isolated thioglycolate-elicited peritoneal macrophages. In comparison to its expression in the liver, *Lrh-1* was barely detectable in macrophages under the conditions analyzed (Figure S4A; bioGPS *Lrh-1* expression pattern, http://biogps.org/#goto=genereport&id=26424). Furthermore, treatment with acetylated LDL (acLDL) to trigger

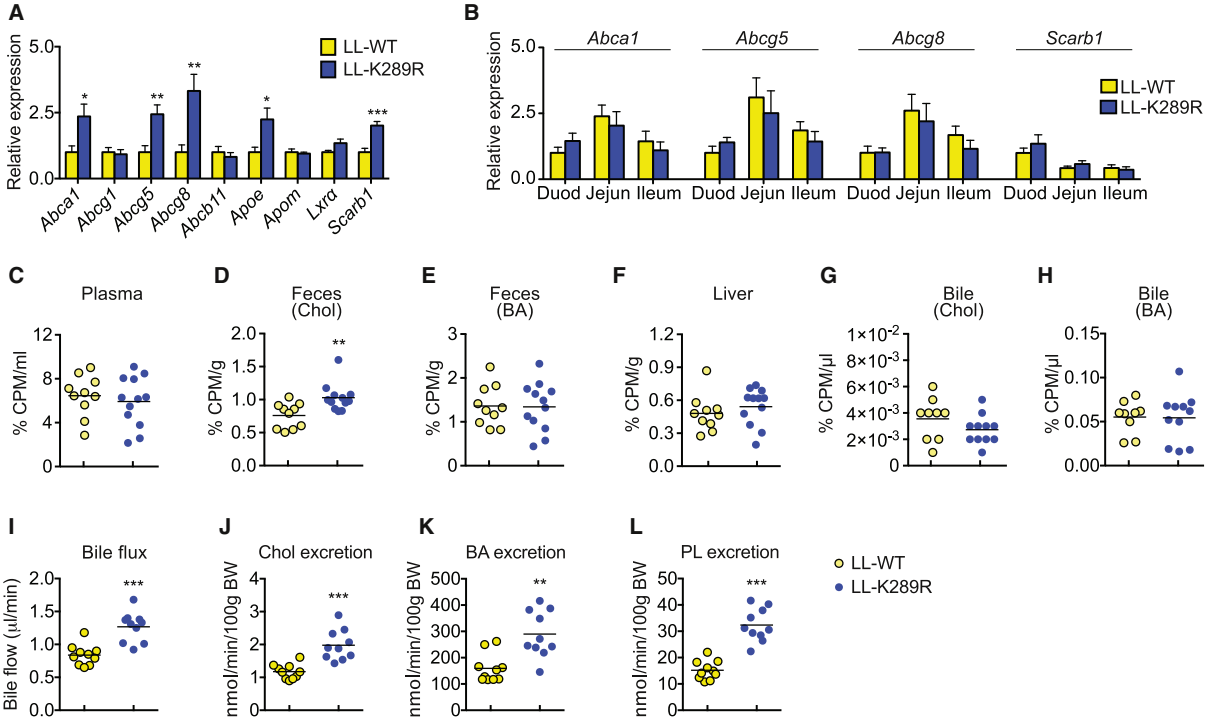

Figure 4. Improved Reverse Cholesterol Transport and Biliary Sterol Excretion in LL-K289R Mice

(A) Hepatic expression of genes affecting cholesterol metabolism in LL-WT and LL-K289R mice. n = 9 per genotype.

(B) Intestinal expression of genes affecting cholesterol metabolism in LL-WT and LL-K289R mice. Duod, duodenum; Jejun, jejunum. n = 9 per genotype.

(C–H) LL-WT and LL-K289R mice were injected with ^{3}H-cholesterol loaded LL-WT macrophages. Detection of ^{3}H-tracer in plasma (C), fecal cholesterol (Chol; D), fecal bile acids (BA; E), liver (F), bile cholesterol fraction (G), and bile BA fraction (H). n = 10 LL-WT; n = 12 LL-K289R.

(I–L) Bile excretion (I) and biliary secretion rates of Chol (J), BA (K), and phospholipids (PL; L). n = 10 per genotype.

Data are represented as means ± SEM. *p < 0.05, **p < 0.01, ***p < 0.001 relative to LL-WT, as determined by Mann-Whitney U or Student's t tests. See also Figure S4.

foam cell formation or lipopolysaccharide (LPS) in order to evaluate the inflammatory response did not trigger any significant difference in acetylated LDL accumulation, *Scarb1* expression, or inflammatory markers between *Lrh-1 WT* and *K289R* macrophages (Figures S4B–S4H), suggesting that the effects on aortic lipid accumulation are not likely related to differential macrophage function.

LRH-1 K289R Protects against Atherosclerosis by Promoting RCT

Intrigued by the marked decrease of atherosclerotic lesions in LL-K289R mice and the increased expression of genes involved in hepatic cholesterol homeostasis in *Lrh-1 K289R* mice (Figure 2F), we analyzed the expression of genes involved in RCT in the liver. Notably, hepatic expression of *Abca1*, *Abcg5*, *Abcg8*, *Apoe*, and *Scarb1* was significantly increased in LL-K289R in comparison to LL-WT mice (Figure 4A). Given that many of these genes are also expressed in the intestine and contribute to whole-body cholesterol homeostasis, we analyzed their expression pattern in the duodenum, jejunum, and ileum. Surprisingly, none of these transcripts was increased in any of the three intestinal sections (Figure 4B). Moreover, microarray analyses of jejunal sections from *Lrh-1 K289R* and *Lrh-1 WT* mice did not display differential expression of cholesterol and lipoprotein regulators that are expressed in livers and intestine (Figure S4I), indicating that LRH-1 K289R specifically induces the expression of cholesterol transport regulators in the liver.

To analyze whether the increased expression of RCT genes has physiological consequences, we performed in vivo macrophage-to-feces RCT and biliary flux studies. In vivo RCT analysis was performed by injecting peritoneal macrophages that were loaded with [^{3}H]-cholesterol (^{3}H tracer) ex vivo into recipient LL-K289R and LL-WT mice. ^{3}H-tracer counts were significantly increased in the fecal cholesterol fraction of LL-K289R in comparison to LL-WT mice, whereas no major differences were observed in the fecal bile acid pool or the plasma, hepatic, or biliary pools (Figures 4C–4H). Furthermore, gallbladder cannulation revealed that bile flow was increased in LL-K289R in comparison to LL-WT mice (Figure 4I). In line with the increased bile flow, biliary cholesterol, bile acids, and phospholipids excretion were also enhanced in LL-K289R in comparison to LL-WT mice (Figures 4J–4L). These data establish LRH-1 K289R as a potent mediator of bile secretion and RCT in vivo.

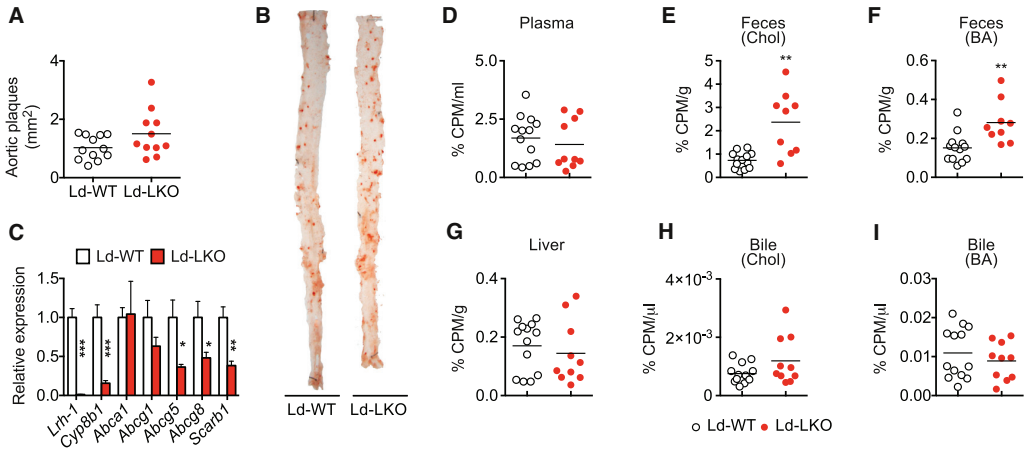

Figure 5. Liver-Specific *Lrh-1* Knockout Mice Do Not Develop More Atherosclerosis

(A) Quantification of aortic plaque area in *Ldlr*$^{-/-}$ *Lrh-1*$^{hep+/+}$ (Ld-WT, n = 12) or *Ldlr*$^{-/-}$ *Lrh-1*$^{hep-/-}$ (Ld-LKO, n = 11) mice.

(B) Representative aortas of Ld-WT and Ld-LKO mice stained with Oil-Red O.

(C) Hepatic expression of genes affecting cholesterol metabolism in Ld-WT and Ld-LKO mice. n = 9 per genotype.

(D–I) Ld-WT and Ld-LKO mice were injected with ^{3}H-cholesterol loaded Ld-WT macrophages. Detection of ^{3}H tracer in plasma (D), fecal cholesterol (E), fecal BA (F), liver (G), bile Chol fraction (H), and bile BA fraction (I). n = 13 Ld-WT; n = 10 Ld-LKO.

Data are represented as means ± SEM. *p < 0.05, **p < 0.01, ***p < 0.001 relative to LL-WT, as determined by Student's t test. See also Figure S5.

Liver-Specific *Lrh-1* Knockout Mice Do Not Develop Increased Atherosclerosis

Even though the transcriptome and targeted gene expression analyses argue against Lrh-1 K289R as a simple constitutively active form of LRH-1 (Figures 2D–2F), we nevertheless explored whether the hepatocyte-specific *Lrh-1*$^{hep-/-}$ mice would yield an opposite phenotype on RCT and atherosclerosis development. Therefore, we crossbred hepatocyte-specific *Lrh-1*$^{hep-/-}$ with *Ldlr*$^{-/-}$ mice in order to generate *Ldlr*$^{-/-}$ *Lrh-1*$^{hep+/+}$ (Ld-WT) or *Ldlr*$^{-/-}$ *Lrh-1*$^{hep-/-}$ (Ld-LKO) mice and fed them an HCD for 12 weeks. Body and liver weight did not differ between the genotypes (Figures S5A and S5B). Interestingly, Ld-LKO did not develop more atherosclerotic lesions than Ld-WT mice (Figures 5A and 5B), although the expression of the RCT regulators (Figure 5C) and binding of LRH-1 to the *Abcg5/Abcg8* intergenic promoter (Freeman et al., 2004) (Figure S5C) was significantly lower in the Ld-LKO liver. Moreover, in vivo RCT analysis demonstrated an increased fecal sterol content in Ld-LKO mice, which could explain why these mice do not develop more atherosclerotic lesions (Figures 5D–5I). The increase of fecal sterols in *Lrh-1*$^{hep-/-}$ mice most likely stems from the compromised intestinal sterol absorption, which was previously reported to be the consequence of reduced *Cyp8b1* in the liver shifting the bile acid pool toward more hydrophilic bile acids (Figure 5C) (Mataki et al., 2007; Out et al., 2011).

Compromised Binding of LRH-1 K289R with the Corepressor PROX1 Derepresses Hepatic RCT Genes

Several corepressors have been reported to fine-tune the activity of LRH-1 in a context specific manner. In the liver, corepressors such as small heterodimer partner (SHP or NR0B2) and prospero homeobox protein 1 (PROX1) as well as the NCOR1/HDAC3 corepressor complex can repress LRH-1 activity (Goodwin et al., 2000; Lee and Moore, 2002; Lu et al., 2000; Qin et al., 2004; Venteclef et al., 2010). To test the assumption that LRH-1 SUMOylation affects the interaction of LRH-1 with potential corepressors, we carried out coimmunoprecipitation experiments in HEK293T cells transfected with LRH-1 WT or LRH-1 K289R in the presence of the corepressor SHP, PROX1, or NCOR1. Surprisingly, we observed that the interaction between LRH-1 and PROX1 was lost or much weaker when LRH-1 K289R was ectopically expressed (Figure 6A), whereas no difference in interaction was observed with SHP or detected with NCOR1 (data not shown). This would suggest that optimal PROX1-LRH-1 interaction may at least require transient SUMOylation of K289 of LRH-1 WT. To assess this possibility, we coexpressed the isopeptidase SENP1 in order to enzymatically remove SUMO from its substrates. SENP1 robustly reduced the interaction between LRH-1 WT and PROX1, supporting the hypothesis that the SUMOylation status affects the interaction (Figure 6B), which might be direct or be mediated by a third partner. Interestingly, the weaker interaction observed between PROX1 and LRH-1 K289R was further reduced by addition of SENP1, suggesting that other SUMOylatable sites in the protein complex may enhance the interaction between the two proteins (Figure 6B). Given that loss of binding to the corepressor PROX1 would provide a mechanistic basis for explaining the enhanced activity of LRH-1 K289R, we next explored whether differential *Prox1* expression between liver and intestine could explain the absence of effects on intestinal RCT genes in *Lrh-1 K289R* mice (Figure 4B). Interestingly, *Prox1* mRNA was almost undetectable in the small intestine and only marginally expressed in the colon in comparison to liver (Figure 6C; bioGPS *Prox1* expression pattern, http://biogps.org/#goto=genereport&id=26424), thus most likely contributing to the differential expression of RCT genes between liver and intestine.

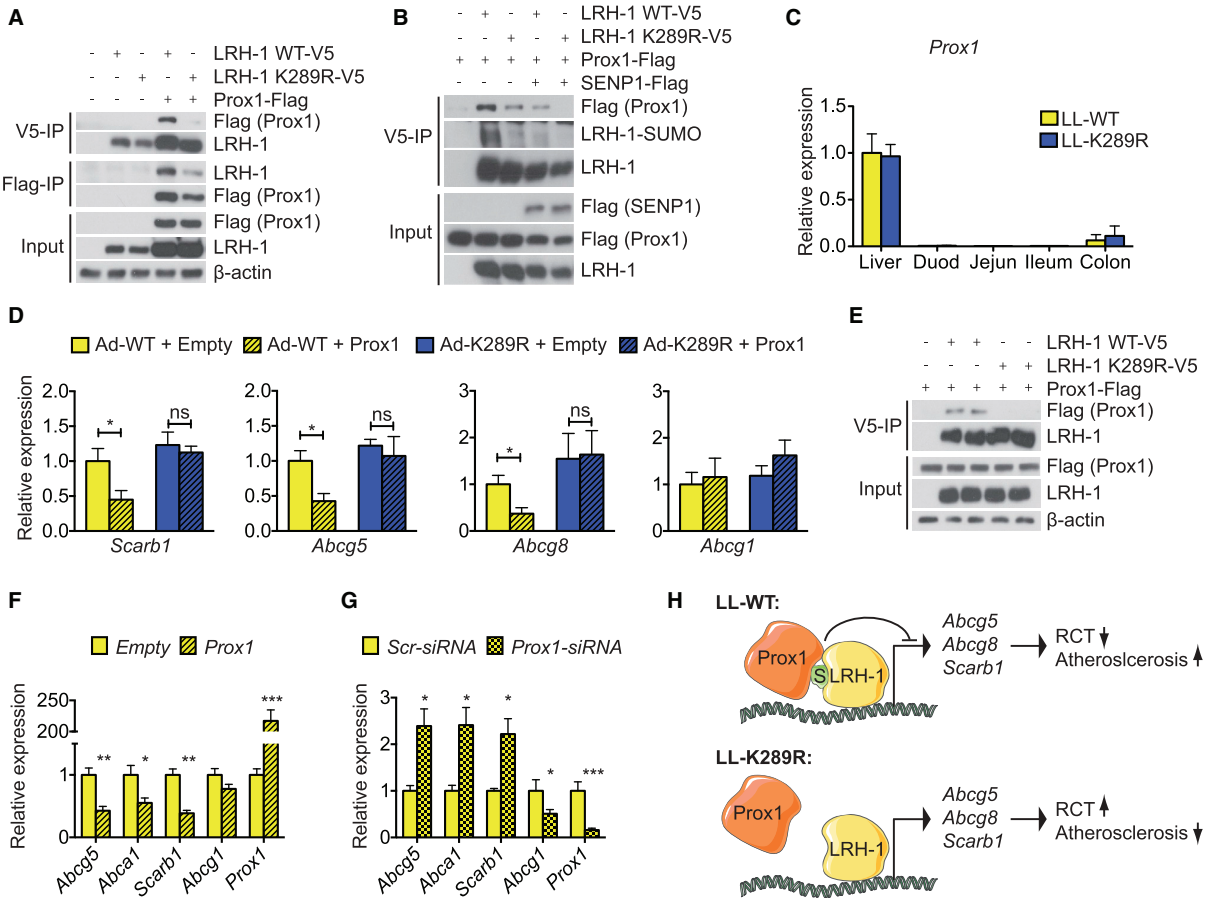

Figure 6. Compromised Binding of LRH-1 K289R with Prox1 Derepresses Hepatic RCT Genes

(A) LRH-1/Prox1 CoIP in HEK293T cells overexpressing V5-tagged LRH-1 (WT or K289R) and FLAG-tagged Prox1. The experiment was replicated at least three times.

(B) LRH-1/Prox1 CoIP in HEK293T cells overexpressing V5-tagged LRH-1 (WT or K289R), FLAG-tagged Prox1, and FLAG-tagged SENP1. The experiment was replicated three times.

(C) Comparative *Prox1* expression in liver, duodenum (Duod), jejunum (Jejun), ileum, and colon of LL-WT and LL-K289R mice. n = 9 per genotype.

(D) Expression of *Scarb1*, *Abcg5*, *Abcg8*, *Abca1*, and *Abcg1* in *Lrh-1*$^{hep-/-}$ primary hepatocytes that were infected or transfected with LRH-1 (WT or K289R) and Prox1. n = 3. The experiment was replicated with three batches of primary cells.

(E) LRH-1/Prox1 CoIP in primary hepatocytes that were infected or transfected with V5-tagged LRH-1 (WT or K289R) and FLAG-tagged Prox1. n = 2 from independent batches of primary hepatocytes.

(F and G) Effect of overexpression (F) and small-interfering-RNA-mediated silencing (G) of *Prox1* in WT primary hepatocytes n = 3. The experiment was replicated with two batches of primary cells.

(H) Model showing how LRH-1 WT and LRH-1 K289R regulate the expression of key genes controlling hepatic cholesterol transport and its consequence on RCT and atherosclerosis. S, SUMO-1.

Data are represented as means ± SEM. *p < 0.05 and **p < 0.01 relative to non-*Prox-1*-transfected controls, as determined by Student's t test. See also Figure S6.

To study the molecular effect of the PROX1-LRH-1 interaction in more detail, we decided to use primary hepatocytes. Notably, both *Lrh-1* and *Prox1* transcripts were reduced to ~25% of their expression in whole livers but were clearly detectable (Figure S6A). We isolated primary hepatocytes from *Lrh-1*$^{hep-/-}$ mice and infected them with an adenovirus containing the LRH-1 WT or K289R followed by ectopic expression of PROX1. Interestingly, while expression of *Abcg1* was not affected or rather increased in cells overexpressing PROX1, the expression of *Scarb1*, *Abcg5*, and *Abcg8* was diminished in cells in which LRH-1 WT, but not LRH-1 K289R, was reconstituted (Figures 6D and S6B), demonstrating that the repressive function of PROX1 on LRH-1 activity depends on an intact LRH-1 K289 SUMOylation site. Furthermore, LRH-1 K289R failed to bind PROX1 in transfected primary hepatocytes, whereas LRH-1 WT/PROX1 interaction was intact (Figure 6E), demonstrating that the LRH-1/PROX1 complex can assemble in vitro and ex vivo. To assess whether we could mimic the effect

of LRH-1/PROX1 interaction in a physiologically relevant cell model, we next overexpressed or silenced *Prox1* in WT primary hepatocytes. While overexpression of *Prox1* reduced the expression of the RCT regulators (Figure 6F), silencing of *Prox1* had the opposite effect (Figure 6G). Altogether, our data suggest that SUMOylated LRH-1 WT recruits the corepressor PROX1 and hence is unable to selectively activate the transcription of important cholesterol receptors and transporters (Figure 6H). If SUMOylation of LRH-1 is defective as in our LRH-1 K289R mutant, then the PROX1-mediated repression is weakened or lost, thereby facilitating the induction of RCT genes and diminishing the progression of atherosclerosis (Figure 6H).

DISCUSSION

Posttranslational modification by SUMO affects the function of a large number of nuclear proteins, including NRs (Geiss-Friedlander and Melchior, 2007; Treuter and Venteclef, 2011). Although various NRs have emerged as reversible SUMO targets modulating almost every aspect of NR function in cell models, very few studies have established in vivo functional roles of NR SUMOylation in health or disease. This is rather surprising given the prominent role of NRs in the pathogenesis of diseases and the repressive imprint of SUMOylation on NR activity. In this study, we have generated a mouse model harboring a K289R mutation that strongly affects LRH-1 SUMOylation and function. We demonstrate that loss of SUMOylation by mutating the critical lysine acceptor site in the LRH-1 protein is sufficient to protect mice against the development of a chronic metabolic disease such as atherosclerosis. More importantly, we provide evidence that the beneficial effect on atherosclerosis is caused by enhancing the transcription of hepatic RCT genes, such as *Abca1*, *Abcg5*, *Abcg8*, and *Scarb1*, without any involvement of gut- or macrophage-specific RCT genes. These findings are consistent with a recent study in *Drosophila* showing that SUMOylation of the LRH-1 homolog *Ftz-f1* affects the expression of the scavenger receptor *Snmp1*, which is required for cellular cholesterol uptake and subsequent steroid synthesis (Talamillo et al., 2013), suggesting that LRH-1 SUMOylation may impact on a similar physiologically conserved pathway.

Alignment of the protein sequence of LRH-1 with other NRs revealed that, aside from SF-1, only members of the ROR family have a hinge region that is comparable to that of LRH-1 (Figure 2B). Although in SF-1, mutation of two conserved SUMO acceptor lysine residues in the hinge region leads to a striking developmental phenotype in mice, characterized by inappropriate sonic hedgehog signaling and impaired endocrine tissue development (Lee et al., 2011a), our study shows that disruption of only one of these conserved SUMO sites in LRH-1 has a significant impact on adult homeostasis and protects against the development of a chronic disease. Surprisingly, SUMOylation of the homologous motif in RORα seems to activate instead of repressing its transcriptional activity (Hwang et al., 2009); however, its physiological properties have not been reported. These studies collectively indicate that SUMOylation of the hinge region has profound functional consequences among a very small subset of NRs.

The mechanistic features by which SUMO modulates the activity of NRs vary considerably and can range from interference with- to promotion of protein-protein interactions or alternatively competition with other PTMs (Geiss-Friedlander and Melchior, 2007; Jentsch and Psakhye, 2013). Our data suggest a role for LRH-1 SUMOylation in promoting protein-protein interactions. This finding is in line with previous studies showing that SUMOylation of LRH-1 K224, the human lysine residue corresponding to mouse LRH-1 K289, binds to a transcriptional corepressor complex consisting of NCOR1, HDAC3, and GPS2 and regulates the expression of acute phase response genes in human hepatoma cells (Venteclef et al., 2010). Interestingly, this study further demonstrated that mouse LRH-1 binding to the *haptoglobin* promoter was reduced in *Sumo1* knockout in comparison to WT livers. In our study, we reveal an unanticipated mechanism by demonstrating that LRH-1 K289R fails to bind another corepressor (i.e., PROX1), and we furthermore show that this impacts on the RCT genes, ultimately leading to enhanced bile flow and atheroprotection. The study by Venteclef et al. (2010), along with our work, propose that SUMOylation of a single K residue of LRH-1 promotes the recruitment of specific corepressor complexes. Importantly, our data demonstrate that the effect of LRH-1 SUMOylation depends on tissue-specific corepressor interaction.

The physiological stimuli and timing that affect LRH-1 SUMOylation in the liver are unknown. In primary granulosa cells, SUMO-driven sequestration of LRH-1 into nuclear bodies is abruptly reversed by cAMP and results in the induction of LRH-1 target genes (Yang et al., 2009). Intriguingly, this is accompanied by a robust reduction of the *Ubc9* and *Pias3* genes, which are part of the SUMO conjugation machinery. Conversely, expression of the SUMO-specific isopeptidase *Senp2* was increased. Although the crosstalk with the cAMP signaling has not been evaluated in the context of LRH-1 SUMOylation in liver cells, it is tempting to speculate that different physiological and/or pharmacological cues could trigger specific posttranslational modifications in LRH-1, which in turn could recruit specific corepressor complexes.

Several studies have identified natural or synthetic LRH-1 activators and inhibitors (Ingraham and Redinbo, 2005). A recent study has identified the unusual phospholipid dilauroyl phosphatidylcholine as an LRH-1 ligand (Lee et al., 2011b). Future studies should test whether ligand activation, posttranslational modifications such as SUMOylation, and coregulator recruitment are interconnected. The tissue and context-specific nature of such effects may offer an ideal therapeutic window for activating a receptor and exploit beneficial effects, without causing adverse effects that are common with NR therapeutics (Marciano et al., 2014). In this context, it is important to point out that the biological effects of LRH-1 K289R cannot be compared to those induced by a gain-of-function of LRH-1 or by a potential drug that would enhance the activity of LRH-1 in a broader manner. In fact, the *Lrh-1 K289R* mice show increased activation of selected LRH-1 target genes, whereas other targets are not affected. The *Lrh-1 K289R* mice also seem to display no effects on RCT in the gut, most likely because LRH-1 and PROX-1 are not coexpressed in the same cells of the crypt-villus epithelium (Botrugno et al., 2004) or because of the low abundance of PROX-1 in the intestinal mucosa (Figure 6C). Likewise, no changes on *Scarb1* gene expression could be detected in macrophages (Figure S4E). Such a restriction of the effects of LRH-1

to selected tissues—in this case, the liver—and a subset of target genes, may be the key to drive only antiatherogenic effects of LRH-1. A better understanding into how SUMOylation of LRH-1 and ensuing coregulator recruitment can be modulated will be instrumental and may provide opportunities for pharmacological intervention to combat common diseases, such as atherosclerosis.

EXPERIMENTAL PROCEDURES

Animal Studies

The generation of the *Lrh-1 K289R* mouse model is described in detail in the Supplemental Experimental Procedures. Congenic C57Bl/6J *Lrh-1 WT* or *Lrh-1 K289R* mice were crossbred with congenic C57Bl/6J *Ldlr* knockout mice in order to generate $Ldlr^{-/-}$ *Lrh-1 WT* (LL-WT) or $Ldlr^{-/-}$ *Lrh-1 K289R* (LL-K289R) mice. LL-WT and LL-K289R mice were kept on an HCD (1.25% total cholesterol, Harlan TD.94059) for 14 weeks starting at the age of 8 weeks. Similarly, congenic C57Bl/6J $Lrh\text{-}1^{hep-/-}$ and $Lrh\text{-}1^{hep+/+}$ mice (Oosterveer et al., 2012) were crossbred with $Ldlr^{-/-}$ mice in order to generate $Ldlr^{-/-}$ $Lrh\text{-}1^{hep+/+}$ (Ld-WT) or $Ldlr^{-/-}$ $Lrh\text{-}1^{hep-/-}$ (Ld-LKO) mice and fed a HCD for 12 weeks. All animal procedures were approved by the Swiss authorities (Canton of Vaud, animal protocols ID #2561 and #2768) and performed in accordance with our institutional guidelines.

Site-directed mutagenesis, subcellular fractionation of liver tissue, immunoprecipitation (IP), Coimmunoprecipitation (CoIP), and western blotting are explained in the Supplemental Experimental Procedures.

Protein Alignment

All protein alignments were performed with the standard Geneious (Blosum62 matrix) or ClustalW (BLOSUM matrix) algorithm from the Geneious software (http://www.geneious.com).

Gene Expression and Analysis

RNA was extracted from the livers and jejunums of ad libitum fed Lrh-1 WT (n = 7) and Lrh-1 K289R (n = 7) mice and from liver of ad libitum fed Lrh-$1hep^{+/+}$ (n = 8) and Lrh-$1hep^{-/-}$ (n = 8) mice with TRIZOL (Invitrogen) and purified with the RNeasy Cleanup Kit for Microarray Analysis (QIAGEN). For quantitative RT-PCR (qRT-PCR), cDNA was generated with the QuantiTect Reverse Transcription Kit (QIAGEN) and analyzed by qPCR with a LightCycler 480 Real-Time PCR System (Roche), and the primers are listed in the Table S2. Expression data were normalized to *36B4* or *B2M* mRNA levels. Microarray analysis was performed with the Affymetrix MouseGene 1.0 ST or Affymetrix MouseGene 2.0 ST array and normalized with the robust multiarray average method. A table of reciprocally regulated transcripts is provided in Table S1. Venn diagram analysis and heatmaps were performed with GENE-E (http://www.broadinstitute.org/cancer/software/GENE-E/index.html). For the Venn diagram, the overlap of nominally significantly changed genes ($p < 0.05$ and fold change ≥ 1.5) among the groups was analyzed.

Chromatin Immunoprecipitation

ChIP analysis was performed as described previously with minor modifications (Duggavathi et al., 2008). DNA was purified with the PCR Clean-up extraction kit (Macherey-Nagel), after which qPCR was performed as described previously (Mataki et al., 2007). Data were normalized to the input (fold differences = $2^{-(Ct\ sample\ -\ Ct\ input)}$). ChIP primer sequences are listed in Table S3.

Lipoprotein Separation

Pooled plasma samples were subjected to fast protein liquid chromatography gel filtration with a Superose 6 Column (GE Healthcare). Individual fractions were assayed for cholesterol and triglyceride concentrations with commercially available enzymatic assays (Roche).

Hepatic Lipid Analyses

Hepatic lipids were extracted according to the Bligh and Dyer (1959) protocol. Triglyceride and cholesterol contents in plasma and hepatic lipid fractions were quantified with enzymatic assays (Roche).

Cholesterol Uptake and LPS Stimulation of Peritoneal Macrophages

Thioglycolate-elicited peritoneal macrophages were harvested, cultured, and starved in vitro and then loaded with 50 μg/ml DiI-labeled acetylated LDL for 4 hr in order to assess the cholesterol uptake or 10 ng/ml LPS for 4 hr in order to analyze the expression of inflammatory markers.

Reverse Cholesterol Transport

RCT protocol was adapted from Meissner et al. (2010). In brief, thioglycolate-elicited mouse peritoneal macrophages were harvested, cultured in vitro, loaded with 50 μg/ml acetylated LDL and 3 μCi/ml 3H-cholesterol for 24 hr, and equilibrated in RPMI 1640 medium containing 1% penicillin/streptomycin and 0.2% BSA for 6 hr. For in vivo RCT, two million labeled LL-WT macrophages were injected intraperitoneally into recipient LL-WT or LL-K289R mice. Mice were sacrificed 48 hr postinjection, and plasma, liver, gallbladder, and feces were stored at −80°C until further analysis. Counts within liver were determined after the solubilization of the tissue. Fecal samples were dried, weighed, and thoroughly ground. Then, aliquots were separated into bile acid and neutral sterol fractions prior to liquid scintillation counting.

Bile Flow and Bile Composition

Bile duct cannulation was performed as described previously (Kruit et al., 2005) with LL-WT and LL-K289R mice. In brief, hepatic bile was collected for 30 min from the common bile duct via cannulation of the gallbladder, and bile flow was determined gravimetrically assuming a density of 1 g/ml for bile. Bile composition was analyzed by high performance liquid chromatography (HPLC) tandem mass spectrometry as described previously (Mataki et al., 2007).

Primary Cell Culture

Primary hepatocytes from hepatocyte-specific $Lrh\text{-}1^{hep-/-}$ mice were isolated with Liberase Blendzyme (Roche) perfusion as described previously with minor modifications (Ryu et al., 2011). $Lrh\text{-}1^{hep-/-}$ hepatocytes were plated in Dulbecco's modified Eagle's medium 4.5 g/l glucose with 10% fetal bovine serum. Cells were infected with an adenovirus expressing LRH-1 WT or LRH-1 K289R 4 hr after plating followed by transfection of a Prox1 plasmid with Lipofectamine 2000 (Invitrogen). Cells were lysed 48 hr postinfection and used for subsequent analysis.

Reporter Assays

Transient transfections in HEK293T cells were performed with Lipofectamine 2000 (Invitrogen) or JetPEI (Polyplus) as previously described (Oosterveer et al., 2012). In brief, cells were transfected with pTK-GL3 reporter constructs driven by a heterologous promoter consisting of multiple consensus LRH-1 response elements (pGL3::$(LRHRE)_5$-TK-LUC) in the presence of either pCMX::LRH-1 WT or the KR mutant constructs. Luciferase activities were measured 24 hr posttransfection and normalized to β-galactosidase activities.

Immunohistochemistry

En face plaque analysis was performed on thoraco-abdominal aortae that were fixed with 10% paraformaldehyde overnight and then stained with Oil-Red O (Stein et al., 2010). Aortic sinuses were cut into 5-μm-thick serial cryosections and stained with Sirius Red in order to measure necrotic core size, cap thickness, and collagen content (Stein et al., 2010). Means were taken from n = 6 mice per genotype, and three serial cryosections were evaluated from each mouse.

Statistical Analyses

Data are expressed as means ± SEM. Analysis of en face atherosclerotic plaque content and bile excretion rates was carried out with Mann-Whitney U tests. Comparison of differences between two groups of other experiments was assessed with unpaired two-tailed Student's t tests. Multiple group comparisons were assessed by one-way ANOVA and Bonferonni post hoc tests. $p < 0.05$ was considered statistically significant (*$p < 0.05$, **$p < 0.01$, ***$p < 0.001$).

ACCESSION NUMBERS

All microarray data are accessible at the NCBI Gene Expression Omnibus under number GSE59333.

SUPPLEMENTAL INFORMATION

Supplemental Information contains Supplemental Experimental Procedures, six figures, and three tables and can be found with this article online at http://dx.doi.org/10.1016/j.cmet.2014.07.023.

AUTHOR CONTRIBUTIONS

S.S. carried out most of the experiments, data analysis, and prepared the figures and the manuscript. M.H.O. and R.H. performed lipoprotein analysis and the bile cannulation experiment. C.M. made the initial mutant LRH-1 constructs and carried out reporter assays. P.X. helped with qPCR, stainings, and CoIP experiments. V.L. and A.P. helped with lipid extractions and macrophage isolation. D.R. assisted with the generation of adenoviral constructs. K.J.M. helped with the isolation of primary hepatocytes. X.W. helped with microarray and bioinformatic analyses. C.D. and F.M. helped with SUMOylation assays. S.M.H. performed HPLC analysis of the bile. K.S. designed the experiments and supervised all aspects of the work.

ACKNOWLEDGMENTS

We thank S. Bichet, N. Moullan, and T. Clerc for technical help and Xavier Warot and the Institut Clinique de la Souris for the generation of the LRH-1 K289R mouse. The pcDNA3.1-FLAG::Prox1 plasmid was kindly provided by Panagiotis Politis. This study was supported by EPFL funding and grants from the Swiss Heart Foundation and the Swiss Cancer League (KLS-2809-08-2011). S.S. is supported by a postdoctoral fellowship from the German Academy of Sciences Leopoldina (LPDS 2011-6).

Received: March 4, 2014
Revised: June 12, 2014
Accepted: July 24, 2014
Published: August 28, 2014

REFERENCES

Bernier-Villamor, V., Sampson, D.A., Matunis, M.J., and Lima, C.D. (2002). Structural basis for E2-mediated SUMO conjugation revealed by a complex between ubiquitin-conjugating enzyme Ubc9 and RanGAP1. Cell *108*, 345–356.

Bligh, E.G., and Dyer, W.J. (1959). A rapid method of total lipid extraction and purification. Can. J. Biochem. Physiol. *37*, 911–917.

Botrugno, O.A., Fayard, E., Annicotte, J.S., Haby, C., Brennan, T., Wendling, O., Tanaka, T., Kodama, T., Thomas, W., Auwerx, J., and Schoonjans, K. (2004). Synergy between LRH-1 and beta-catenin induces G1 cyclin-mediated cell proliferation. Mol. Cell *15*, 499–509.

Chalkiadaki, A., and Talianidis, I. (2005). SUMO-dependent compartmentalization in promyelocytic leukemia protein nuclear bodies prevents the access of LRH-1 to chromatin. Mol. Cell. Biol. *25*, 5095–5105.

Coste, A., Dubuquoy, L., Barnouin, R., Annicotte, J.S., Magnier, B., Notti, M., Corazza, N., Antal, M.C., Metzger, D., Desreumaux, P., et al. (2007). LRH-1-mediated glucocorticoid synthesis in enterocytes protects against inflammatory bowel disease. Proc. Natl. Acad. Sci. USA *104*, 13098–13103.

Duggavathi, R., Volle, D.H., Mataki, C., Antal, M.C., Messaddeq, N., Auwerx, J., Murphy, B.D., and Schoonjans, K. (2008). Liver receptor homolog 1 is essential for ovulation. Genes Dev. *22*, 1871–1876.

Fayard, E., Schoonjans, K., Annicotte, J.S., and Auwerx, J. (2003). Liver receptor homolog 1 controls the expression of carboxyl ester lipase. J. Biol. Chem. *278*, 35725–35731.

Fayard, E., Auwerx, J., and Schoonjans, K. (2004). LRH-1: an orphan nuclear receptor involved in development, metabolism and steroidogenesis. Trends Cell Biol. *14*, 250–260.

Fernandez-Marcos, P.J., Auwerx, J., and Schoonjans, K. (2011). Emerging actions of the nuclear receptor LRH-1 in the gut. Biochim. Biophys. Acta *1812*, 947–955.

Freeman, L.A., Kennedy, A., Wu, J., Bark, S., Remaley, A.T., Santamarina-Fojo, S., and Brewer, H.B., Jr. (2004). The orphan nuclear receptor LRH-1 activates the ABCG5/ABCG8 intergenic promoter. J. Lipid Res. *45*, 1197–1206.

Geiss-Friedlander, R., and Melchior, F. (2007). Concepts in sumoylation: a decade on. Nat. Rev. Mol. Cell Biol. *8*, 947–956.

Goodwin, B., Jones, S.A., Price, R.R., Watson, M.A., McKee, D.D., Moore, L.B., Galardi, C., Wilson, J.G., Lewis, M.C., Roth, M.E., et al. (2000). A regulatory cascade of the nuclear receptors FXR, SHP-1, and LRH-1 represses bile acid biosynthesis. Mol. Cell *6*, 517–526.

Hwang, E.J., Lee, J.M., Jeong, J., Park, J.H., Yang, Y., Lim, J.S., Kim, J.H., Baek, S.H., and Kim, K.I. (2009). SUMOylation of RORalpha potentiates transcriptional activation function. Biochem. Biophys. Res. Commun. *378*, 513–517.

Ingraham, H.A., and Redinbo, M.R. (2005). Orphan nuclear receptors adopted by crystallography. Curr. Opin. Struct. Biol. *15*, 708–715.

Jentsch, S., and Psakhye, I. (2013). Control of nuclear activities by substrate-selective and protein-group SUMOylation. Annu. Rev. Genet. *47*, 167–186.

Krasowski, M.D., Reschly, E.J., and Ekins, S. (2008). Intrinsic disorder in nuclear hormone receptors. J. Proteome Res. *7*, 4359–4372.

Kruit, J.K., Plösch, T., Havinga, R., Boverhof, R., Groot, P.H., Groen, A.K., and Kuipers, F. (2005). Increased fecal neutral sterol loss upon liver X receptor activation is independent of biliary sterol secretion in mice. Gastroenterology *128*, 147–156.

Lee, Y.K., and Moore, D.D. (2002). Dual mechanisms for repression of the monomeric orphan receptor liver receptor homologous protein-1 by the orphan small heterodimer partner. J. Biol. Chem. *277*, 2463–2467.

Lee, Y.K., and Moore, D.D. (2008). Liver receptor homolog-1, an emerging metabolic modulator. Front. Biosci. *13*, 5950–5958.

Lee, M.B., Lebedeva, L.A., Suzawa, M., Wadekar, S.A., Desclozeaux, M., and Ingraham, H.A. (2005). The DEAD-box protein DP103 (Ddx20 or Gemin-3) represses orphan nuclear receptor activity via SUMO modification. Mol. Cell. Biol. *25*, 1879–1890.

Lee, F.Y., Faivre, E.J., Suzawa, M., Lontok, E., Ebert, D., Cai, F., Belsham, D.D., and Ingraham, H.A. (2011a). Eliminating SF-1 (NR5A1) sumoylation in vivo results in ectopic hedgehog signaling and disruption of endocrine development. Dev. Cell *21*, 315–327.

Lee, J.M., Lee, Y.K., Mamrosh, J.L., Busby, S.A., Griffin, P.R., Pathak, M.C., Ortlund, E.A., and Moore, D.D. (2011b). A nuclear-receptor-dependent phosphatidylcholine pathway with antidiabetic effects. Nature *474*, 506–510.

Lu, T.T., Makishima, M., Repa, J.J., Schoonjans, K., Kerr, T.A., Auwerx, J., and Mangelsdorf, D.J. (2000). Molecular basis for feedback regulation of bile acid synthesis by nuclear receptors. Mol. Cell *6*, 507–515.

Marciano, D.P., Chang, M.R., Corzo, C.A., Goswami, D., Lam, V.Q., Pascal, B.D., and Griffin, P.R. (2014). The therapeutic potential of nuclear receptor modulators for treatment of metabolic disorders: PPARγ, RORs, and Rev-erbs. Cell Metab. *19*, 193–208.

Mataki, C., Magnier, B.C., Houten, S.M., Annicotte, J.S., Argmann, C., Thomas, C., Overmars, H., Kulik, W., Metzger, D., Auwerx, J., and Schoonjans, K. (2007). Compromised intestinal lipid absorption in mice with a liver-specific deficiency of liver receptor homolog 1. Mol. Cell. Biol. *27*, 8330–8339.

Meissner, M., Nijstad, N., Kuipers, F., and Tietge, U.J. (2010). Voluntary exercise increases cholesterol efflux but not macrophage reverse cholesterol transport in vivo in mice. Nutr. Metab. (Lond) *7*, 54.

Oosterveer, M.H., Mataki, C., Yamamoto, H., Harach, T., Moullan, N., van Dijk, T.H., Ayuso, E., Bosch, F., Postic, C., Groen, A.K., et al. (2012). LRH-1-dependent glucose sensing determines intermediary metabolism in liver. J. Clin. Invest. *122*, 2817–2826.

Out, C., Hageman, J., Bloks, V.W., Gerrits, H., Sollewijn Gelpke, M.D., Bos, T., Havinga, R., Smit, M.J., Kuipers, F., and Groen, A.K. (2011). Liver receptor homolog-1 is critical for adequate up-regulation of Cyp7a1 gene transcription and bile salt synthesis during bile salt sequestration. Hepatology *53*, 2075–2085.

Qin, J., Gao, D.M., Jiang, Q.F., Zhou, Q., Kong, Y.Y., Wang, Y., and Xie, Y.H. (2004). Prospero-related homeobox (Prox1) is a corepressor of human liver

receptor homolog-1 and suppresses the transcription of the cholesterol 7-alpha-hydroxylase gene. Mol. Endocrinol. *18*, 2424–2439.

Rosenson, R.S., Brewer, H.B., Jr., Davidson, W.S., Fayad, Z.A., Fuster, V., Goldstein, J., Hellerstein, M., Jiang, X.C., Phillips, M.C., Rader, D.J., et al. (2012). Cholesterol efflux and atheroprotection: advancing the concept of reverse cholesterol transport. Circulation *125*, 1905–1919.

Ryu, D., Seo, W.Y., Yoon, Y.S., Kim, Y.N., Kim, S.S., Kim, H.J., Park, T.S., Choi, C.S., and Koo, S.H. (2011). Endoplasmic reticulum stress promotes LIPIN2-dependent hepatic insulin resistance. Diabetes *60*, 1072–1081.

Schoonjans, K., Annicotte, J.S., Huby, T., Botrugno, O.A., Fayard, E., Ueda, Y., Chapman, J., and Auwerx, J. (2002). Liver receptor homolog 1 controls the expression of the scavenger receptor class B type I. EMBO Rep. *3*, 1181–1187.

Stein, S., Lohmann, C., Schäfer, N., Hofmann, J., Rohrer, L., Besler, C., Rothgiesser, K.M., Becher, B., Hottiger, M.O., Borén, J., et al. (2010). SIRT1 decreases Lox-1-mediated foam cell formation in atherogenesis. Eur. Heart J. *31*, 2301–2309.

Talamillo, A., Herboso, L., Pirone, L., Pérez, C., González, M., Sánchez, J., Mayor, U., Lopitz-Otsoa, F., Rodriguez, M.S., Sutherland, J.D., and Barrio, R. (2013). Scavenger receptors mediate the role of SUMO and Ftz-f1 in Drosophila steroidogenesis. PLoS Genet. *9*, e1003473.

Treuter, E., and Venteclef, N. (2011). Transcriptional control of metabolic and inflammatory pathways by nuclear receptor SUMOylation. Biochim. Biophys. Acta *1812*, 909–918.

Venteclef, N., Haroniti, A., Tousaint, J.J., Talianidis, I., and Delerive, P. (2008). Regulation of anti-atherogenic apolipoprotein M gene expression by the orphan nuclear receptor LRH-1. J. Biol. Chem. *283*, 3694–3701.

Venteclef, N., Jakobsson, T., Ehrlund, A., Damdimopoulos, A., Mikkonen, L., Ellis, E., Nilsson, L.M., Parini, P., Jänne, O.A., Gustafsson, J.A., et al. (2010). GPS2-dependent corepressor/SUMO pathways govern anti-inflammatory actions of LRH-1 and LXRbeta in the hepatic acute phase response. Genes Dev. *24*, 381–395.

Ward, J.D., Bojanala, N., Bernal, T., Ashrafi, K., Asahina, M., and Yamamoto, K.R. (2013). Sumoylated NHR-25/NR5A regulates cell fate during C. elegans vulval development. PLoS Genet. *9*, e1003992.

Weber, C., and Noels, H. (2011). Atherosclerosis: current pathogenesis and therapeutic options. Nat. Med. *17*, 1410–1422.

Yang, F.M., Pan, C.T., Tsai, H.M., Chiu, T.W., Wu, M.L., and Hu, M.C. (2009). Liver receptor homolog-1 localization in the nuclear body is regulated by sumoylation and cAMP signaling in rat granulosa cells. FEBS J. *276*, 425–436.